THE UNIVERSITY OF MICHIGAN

INDUSTRY PROGRAM OF THE COLLEGE OF ENGINEERING

STABILITY OF CELLULAR COFFERDAMS

Kamal Tawfiq Al-Chalabi

A dissertation submitted in partial fulfillment
of the requirement for the degree of
Doctor of Philosophy in the
University of Michigan
1959

June, 1959

IP-372

Doctoral Committee:

Professor William S. Housel, Chairman
Instructor Robert O. Goetz
Professor John C. Kohl
Professor Lawrence C. Maugh
Professor Earl D. Rainville

ACKNOWLEDGMENT

The writer wishes to express his great gratitude and deep appreciation to Professor W. S. Housel, under whose supervision and direction this present investigation has been carried out. The writer's appreciation is also due to Mr. R. Goetz and the staff of the Engineering Research Institute working with him for their invaluable help. The writer also wishes to express his gratitude to the members of his committee, Professor John C. Kohl, Professor Lawrence C. Maugh and Professor Earl D. Rainville for their guidance and advice in this work.

TABLE OF CONTENTS

TABLE OF CONTENTS (CONT'D)

LIST OF TABLES

LIST OF FIGURES

LIST OF FIGURES (CONT'D)

LIST OF FIGURES (CONT'D)

LIST OF FIGURES (CONT'D)

LIST OF FIGURES (CONT'D)

LIST OF FIGURES (CONT'D)

NOMENCLATURE

A = Area.

b = The equivalent width of the cofferdam.

b' = The actual width of the cofferdam.

c = Constant.

D = The diameter of the circle.

d = The depth of the element of failure below the loading plane.

El. = Elevations USC & GS Datum = -587.5 Plant Datum.

F = Total force.

F_h = Total horizontal force.

F_v = Total vertical force.

fs = Shearing stress.

G_a = The apparent specific gravity.

G_o = The dry bulk specific gravity.

G_b = The wet bulk specific gravity.

GS. = Ground surface. (Natural.)

G_s = The factor of safety.

H = The height of the cofferdam to loading plane.

h_1 = The height of the first soil stratum of soil profile.

h_n = The height of the nth soil stratum of soil profile.

k = Constant

K_1 = The coefficient of settlement ($K_1 = \Delta/n$).

K_2 = The stress reaction coefficient ($K_2 = m/n$).

L = The length of the cofferdam, center to center of cells.

M_a = Overturning moment about the axis a-a.

M_r = Resisting Moment.

m = The perimeter shear.

n = The developed pressure.

P_o = The applied pressure per unit area.

P_h = The horizontal pressure.

P_n = The normal pressure

P_v = The vertical pressure.

q = Bearing capacity.

r = The radius of a circle.

R = The overload ratio.

S = Shearing resistance.

S_c = Shearing resistance due to cohesion.

S_e = Equivalent vertical shearing resistance above loading plane.

S_f = Shearing resistance due to friction.

S_t = Shearing resistance on a horizontal critical sliding plane.

S_{uc} = Shearing resistance as determined by the unconfined compression test.

S_h = Cumulative vertical shearing resistance above loading plane.

T = Tension in interlock.

T_a = Allowable tension in interlock.

V = Volume.

W = Total weight.

NOMENCLATURE (CONT'D)

WS = Water surface.

w = Weight per cubic unit.

w_s = Submerged weight of soil per cubic unit.

w_t = Wet weight of soil per cubic unit.

w_w = Weight of water per cubic foot.

ϕ = The angle of internal friction.

θ = The angle of pressure transmission.

Δ = Settlement.

SYNOPSIS

This dissertation presents a general solution for the stability analysis and design of cellular cofferdams.

A brief resume of the mechanics of soils and a historical review of cellular cofferdams is presented with formulas which are derived accordingly. These formulas covered the various types of soils and the various causes of failure with an emphasis on the mass movement of soils as a criterion of failure.

Then an existing cellular cofferdam of the semi-circular type with arc diaphragms was analyzed. The load capacity of the cofferdam was calculated for various loading areas and various overload ratios. Then a field test was conducted by loading the cofferdam. The field test was done by the Inland Steel Company, Indiana Harbor, Indiana, and the results of the test were made available to the author through the courtesy of the Engineering Research Institute. During the course of the field test, level readings were taken at various stages of loading at different periods of time. These observations were plotted, interpreted and a study of the mass movement of the cofferdam was made. Then a correlation between the results of the field test and the theoretical analysis was made. Finally, conclusions were derived and safe overload ratios (ratios of the stress imposed on the clay soil divided by the yield value as measured by laboratory test) for designing cofferdams were made.

INTRODUCTION

Cellular cofferdams are structures composed of sheet-pile enclosures filled with soil material to stabilize them, and resting on a soil foundation, both acting as one unit.

The design of cofferdams is a matter of some importance in the field of soil mechanics.

Previous methods used to design or analyze cofferdams are based on many incorrect concepts such as the theory of friction as the criterion of stability in the soil and the misinterpretation of the triaxial compression tests on granular mixtures.

In all the previous solutions a clear distinction was not made with regard to cohesive and granular properties of soil, neither in determining lateral pressure nor in determining the internal stability of granular material and the cohesive strength of a cohesive material. Also the stability of the soil mass supporting the cofferdam and surrounding it was not given enough attention in the past. The cofferdam's strength and rigidity depend to a great extent on the subsoil sustaining it, therefore the mass movement of the soil mass supporting and surrounding the cofferdam will be taken as one criterion of failure.

The present investigation deals with methods of designing and analyzing cellular cofferdams taking into consideration the granular property of soil and its stability according to the theory of arching, and the cohesive property of soil and its stability due to the

molecular attraction of the clay particles which gives the cohesive material a certain amound of shearing resistance. Also the cofferdam is dealt with as two units, the structure and the substructure, and their mutual strength as an integral unit is considered.

At the same time methods are set forth to investigate the various causes of failure which have been observed in past experience with cellular cofferdams. On the basis of the new concepts and theories new formulas have been developed and an experimental analysis was carried out on an existing cellular cofferdam. Then a test was conducted according to the analytical results, the cofferdam was loaded and level readings were taken. The results were interpreted and yielded a close correlation between the analysis and the actual results, although it required a modification of the initial solutions, thus giving more accurate procedures for designing and analyzing cellular cofferdams.

CHAPTER I

GENERAL STATEMENTS

Definition of Cellular Cofferdams

A cellular cofferdam is a structure built in place; consisting of a series of cells connected to each other, made of steel sheet-piles, filled with soil to furnish stability, for the purpose of retaining a hydrostatic head of water or to provide a lateral support to the mass of soil behind it. It could be used either as a temporary or a permanent structure.

Description of Cellular Cofferdams

Cellular cofferdams are made of steel sheet-piles driven into the soil in the form of an enclosure of cells. These cells are connected to each other forming a continuous line of cells. The cells are filled with soil material which should be well consolidated.

History

Cofferdams, in their simplest form were found in ancient times. The Mesopotamian rivers, for example, were edged in many places with earth box type of cofferdams to protect the land from the floods. Disregarding the simplicity of the structure they were basically functioning to retain a hydrostatic head of water.

Cellular cofferdams are only fifty years old. The first one was built in the United States of America in 1908-1909 at Black

Rock Harbor, Buffalo, New York. This cofferdam was the rectangular type and it consisted of 70 cells of 30 feet by 30 feet. It was built on rock foundation. The outer and inner walls of this cofferdam bulged.(31) This phenomenon led Major-General Harley B. Ferguson, Corp. of Engineers, U.S. Army (Retired) to the idea of using the circular cells in constructing the cofferdam for raising the battleship Maine.(22)

The first circular cellular cofferdam was built in 1910 for raising the battleship Maine in the harbor of Havana, Cuba.(30) This cofferdam was the circular type. The cells were filled with clay and rested on a stratum of soft silt and clay. Under this stratum was a stratum of medium clay.

The first diaphragm type cellular cofferdam was built in Troy, New York. It was built for constructing Troy's Dam and Lock. In this cofferdam the inner and outer walls of the cofferdam were arcs.

Then more than fourteen cofferdams were built by the Tennessee Valley Authority (TVA) for their various projects. The first of these large projects requiring cellular cofferdams was the Pickwick Landing Dam. In this case a circular type was used. It was successful and economical. Since then the circular type was adopted by the TVA in all the Tennessee River projects.(1)

Other cofferdams have been built. Examples of these are the cofferdams for Gallipolis Dam on the Ohio River(1), Grand Coulee Dam, Kentucky Dam, Bonneville Dam, Jordan Dam in Alabama, Boulder Dam, Hudson

River Bridge, the St. Louis Intake, the Mississippi River at Alton, Illinois, Kensico Reservoir, Valhalla, New York, the entrance to MacArthur and Poe Locks, Sault Ste. Marie, Michigan, the cofferdam for the lock and dam in the Mississippi River, Hastings, Minnesota, the cofferdam for Intake System, Detroit, Michigan, the cofferdam at Kaiser Shipyard, Richmond, California, and the most recent one, the cofferdam for new locks at Markland Dam, Kentucky, on the Ohio River, and many others. These cofferdams are mentioned in Bibliography "B".

Cofferdams have been built to various heights, some reached up to 109 feet in height.(21) As cofferdams are economical and long lasting structures they are used as permanent structures.

The subject of cofferdams from the theoretical aspect has been given very little attention. It has been discussed by Harris Esptein(6), Raymond P. Pennoyer(24), and Karl Terzaghi.(28)

At the University of Michigan, attention has also been given to this problem and a research program was initiated by Professor W. S. Housel to study this problem.

This work is a part of the study toward a more complete and satisfactory solution of cellular cofferdams.

Types of Cellular Cofferdams

Cellular cofferdams can be divided basically into three types, according to the location where they are constructed, and they are as follows:

1. Cofferdams in Water:

This type of cofferdam is used to retain a hydrostatic head of water in order to reach the bottom of the water to allow construction of footings of bridge piers, dams, locks, docking piers and in exposing the bottom of the ocean to salvage ships.

2. Land Cofferdams:

This type of cofferdam is used on land to retain a mass of soil as well as the water table in order to permit construction or exposure of a certain depth of the site, eliminating the danger of mass movement of the soil.

3. Shore Cofferdams:

This type of cofferdam is used mainly at the shoreline to form a dock or at the wings of a dam to retain the shores. This type is now used quite frequently.(29)

Available Solutions and Their Basic Principles and Theories

A solution has been given by Raymond P. Pennoyer under the heading "Gravity Bulkheads and Cellular Cofferdams."(24) This solution was presented in 1934. At that time the orthodox theories of soil mechanics were the basic tools in determining stresses and resistances of soil. Accordingly, these orthodox theories were used in Pennoyer's solution of this problem. One of the misleading concepts is shown in the following statement by Mr. Pennoyer:

> "For lateral earth pressure the Rankine formula is the most satisfactory in all respects, especially in the certainty and simplicity of its application. This formula is based on the theory that the earth is a mass of granular particles

> without cohesion, which admittedly is rarely its actual condition. Unquestionably, the lateral loads thus derived are greater than those generally encountered in practice, as has been proved by numerous tests."(23)

The theory that the earth is a mass of granular particles without cohesion is true only for purely granular soil and it should not be generalized for all soils. Thus this assumption falls short when dealing with cohesive material or granular material mixed with clay. However, he backs the assumption made above by stating:

> "The fact remains that these factors at times do cause the earth to be similar to a cohesionless, granular mass with resulting pressures closely approximating those derived by the Rankine theory."(23)

As far as the solution of the problem of the cofferdam itself, Mr. Pennoyer limited his discussion to cellular cofferdams on rock only, and did not elaborate any further on the cases where cofferdams are constructed on clay or sand foundations. He stated in his discussion of Professor Terzaghi's paper on cellular cofferdams in 1945:

> Cellular Cofferdams in Clay. --"In his former paper(24), the writer did not attempt to discuss cellular cofferdams founded on anything except rock, because he considered there were sufficient intangibles involved in that problem."(25)

Another basic assumption made is that the cofferdam can be ragarded as a simple gravity wall. In this case there was not sufficient explanation of the manner in which the lateral thrust is carried from the outer wall of the cofferdam to the inner wall and of the way the inner wall carries this lateral pressure.

Another solution has been presented by Professor Terzaghi under the heading "Stability and Stiffness of Cellular Cofferdams," in

the Proceedings of the American Society of Civil Engineers, September, 1944.[28] In this paper Professor Terzaghi elaborated further on this subject. His solution, however, falls short from these aspects. In regard to the mechanics of soil as the tools of determining stresses in soils and the resistance of soil masses to these stresses, he abandoned Rankine's formula in determining the lateral pressure in the fill of the cell. Professor Terzaghi favored the use of the semiemperical coefficient, C, which is equal to .4, instead of the term $Tan^2(45-\phi/2)$ in Rankine's formula $P_h = P_v\ Tan^2(45-\phi/2)$. This point is made clear by his conclusion:

> "The lateral earth pressure of the fill in the cell on the sheet-pile enclosure of the cells is not even approximately equal to the Rankine pressure. Therefore, the greatest lock tension can only be estimated on a semiemperical basis."[28]

However he goes farther in advocating against the usage of laboratory test results in determining the properties of the fill material by stating:

> "However, some day an ambitious designer may conceive the idea of determining the soil constants by laboratory tests and using the values furnished by the tests. The results could be fatal for the cofferdam."[28]

In evaluating the bearing capacity of clay stratum underneath the cofferdams he states:

> "Before the cofferdam is acted upon by one-sided water pressure, it presents a continuous uniformly loaded footing whose base ab adheres to the supporting clay. If the upper surface of the clay were at the elevation of the base ab, the failure load (in excess of the pressure which acted on ab before the construction of the cofferdam) would be equal to 5.7 c. The layer of clay above the level of ab in Figure (...) increases the bearing capacity slightly."[28]

However, when he sets up the bearing capacity equation he uses the term 5.7 c only, where c is the average cohesion of the clay per unit area. This is conservative because there are many other factors contributing to the bearing capacity as is shown in Chapter II.

As far as the cofferdam is concerned, Professor Terzaghi has limited his solution to cellular cofferdams filled with sand only. This was one of his first assumptions as he states in the Synopsis:

> "Discussion is specifically limited to cellular cofferdams whose cells are filled with sand or sand and gravel."(28)

Naturally the case of having the cell filled with sand or sand and gravel is not always the case. This point is mentioned by R. P. Pennoyer:

> "It is seldom, however, that a cell entirely filled with sand is encountered in actual practice. Consequently, the paper leaves the reader without a practical basis for analyzing the problem that generally confronts him."(25)

It is true that granular soils are the best material for filling the cell, however clay fill was used in the past in many cases. It was used in the first circular cellular cofferdam which was built for raising the battleship Maine.(30) The cells of this cofferdam were filled with clay soil. Another example is the cofferdam for the new locks at Sault Ste. Marie, Michigan, and many others.

In discussing cellular cofferdams on rock, Professor Terzaghi analyzed a cofferdam built in water on bare rock, with no submerged soil above the rock. This case of having a bare rock foundation is very rare and the driving of the sheet-piles into the desired cellular form represents a major construction problem.

In investigating the tension in the interlock, Professor Terzaghi's solution deals only with one cause for the tension in the interlock. This cause is the lateral pressure of the fill in the cell. The tension in the interlock due to the lateral pressure applied on the cell is not investigated. The lateral pressure transmitted to the inner row of the sheet-pile will be transmitted back to the outer row by means of the diaphragm, causing tension in the interlocks of the diaphragm. This factor of tension in the interlock was pointed out by Greulich when he stated:

> "Because of these phenomena, the diaphragm or cross parts of steel sheet-pile walls are capable of transmitting some direct tension from the inside top of the cell, diagonally down to the outside bottom of the cell. In other words the effect is similar to the introduction of stay rods from the inner top to the outer base of the cell."(5)

Another important point is that there was no alternate solution given to the "middle third" method of approximating the proper width of the cofferdam. Also, in all the preceding solutions the mass stability of the cofferdam has not been given any attention.

In all the previous solutions attention was given to cofferdams built in water, while shore types of cofferdams were not discussed. The shore cofferdam represents a more complex problem which must be discussed.

The Scope of This Investigation

The purpose of this investigation is to establish accurate design principles and stability analysis for cellular cofferdams. This paper will cover the following steps:

1. A clear and definite distinction will be made between granular and cohesive materials. Taking the properties of cohesion and the internal stability due to arching into consideration, the lateral pressure and related functions acting on or within the cofferdam will be determined.
2. An evaluation will be made of the various causes of failure in the light of the more accurate concepts presented in Step 1.
3. A study will be made of the effect of loading and the mass movement of soil as one of the major concepts in cellular cofferdam design and analysis.
4. The behavior of a cellular cofferdam at the storage docks of the Inland Steel Company, Indiana Harbor, Indiana, will be studied under various loading conditions. Recommendations for testing will be concluded.
5. Evaluation of the test results and correlation with the theoretical study will be made.
6. A reliable basis of design and dependable overload ratios for cellular cofferdams will be concluded.

CHAPTER II

MECHANICS OF SOIL

Soil mechanics is a relatively new science. As a new science most of its problems are still under dispute and there is still a considerable amount of controversy about many of its basic principles. Therefore, in this chapter a presentation of the basic theories and concepts of soil mechanics which have been adopted at the University of Michigan is given. These theories and concepts will serve as the bases of the principles of soil mechanics which are used in the analysis presented in the following chapter.

The various rocks of the earth's crust have become disintegrated and decomposed due to various processes of nature forming what is known to us as soil; thus it is a mantle of comparatively loose or unconsolidated material. The rocks forming the soil are of various kinds and are found under various conditions, giving the soil its complex nature. The science of soil mechanics deals with the structural behavior of the soil, and the study of the various physical phenomena affecting the resistance of the soil to stress conditions. To predict the behavior of soil under a set of conditions, the characteristics and properties of the soil are of great importance.

The characteristics of soils are those attributes which serve to identify it and to contribute to a general knowledge of the manner in which it may perform, although not in a measurable sense. These are the texture and gradation, the surface area, the density relations, the color, the chemical composition, the origin, etc.

Texture is a descriptive term referring to the particle size. It indicates the size of the individual soil grains or particles and the proportions of material of each size present in any given case. Texture is determined by mechanical analysis, a laboratory process of separating the soil into groups of grain sizes and establishing the percentages of various sizes in any particular soil material. From these percentages, for any particular soil, the textural classification can be determined according to the Texture Classification Chart shown in Appendix F.(17)

Soil structure is a term used to describe the state in which the particles are held together in the soil mass. It includes the arrangement of the particles and also the type and extent of bonding.

The surface area, or, more properly, the specific surface, which is an important factor in colloidal behavior and adsorption, is defined as surface area per unit volume (absolute volume of the solid). The specific surface of a particle is determined by dividing its surface area by its volume. Fine grained soils have an enormous capacity to adsorb moisture or other material in the film phase. The measurement of specific surface, being dependent on particle size and shape, is extremely hard to accomplish accurately for natural soils. This problem is accentuated by the presence of particles of colloidal size. Hence, indirect methods are most often used for practical purposes.

The density relations of soils are the quantitative evaluations of the proportions of mineral, water and air in the soil mass. Although useful and valuable as indicating potential ability to develop resistance,

these density relations do not constitute direct measures of soil resistance. They are, therefore, classified as characteristics rather than properties.

The specific gravity of a material is the ratio of its weight per unit volume to the weight per unit volume of water. There are a number of definitions of specific gravity which specify the conditions under which it is measured such as absolute specific gravity, specific gravity (G), apparent specific gravity (G_A) and bulk specific gravity.

Soil color is an important soil characteristic in soil classification as it affords a direct clue to the character and extent of the weathering processes to which the soil has been subjected and to some extent identifies the chemical constituents of the soil.

The chemical composition of soils is an important influence in soil behavior and also enters into soil classification. The study of the physical chemistry of soils shows promise of making soil mechanics a more exact science. A further study of the chemical composition of soils may be the most feasible method of stabilizing poor soils. However, problems involving the chemical nature of soil cannot be treated in terms of conventional chemical reactions but must be treated more generally in terms of adsorption, base exchange and similar phenomena.

The origin of soil is important in determining the manner in which the soil was formed and deposited.

The properties of soil are measureable attributes in quantitative terms which control the behavior, and are useful in predicting the manner and extent to which soil acts under a given set of conditions.

They are cohesion, internal stability, compressibility, internal friction, bearing capacity, elasticity, plasticity, viscosity, volume change due to variations in the moisture content, capillarity and permeability.

Cohesion is the property of producing resistance to displacement by mutual attraction between particles of the mass, involving forces of molecular origin.

Internal stability is the mechanical property of granular masses which produces resistance to displacement involving static forces and reaction between particles too large to be appreciably affected by molecular forces.

Compressibility may be defined as that property of material which results in a decrease in volume under applied pressure. Incompressibility, is the inverse property and emphasizes the resistance to volume change. Consolidation in a soil mass subjected to a load is frequently the major source of settlement and must be given equal consideration with settlement due to displacement. Volume change is measured by the coefficient of compressibility which is defined as the volume change per unit volume caused by a unit pressure. Resistance to volume change may be defined by the modulus of incompressibility which is the ratio of developed pressure divided by the volume change per unit volume.

Bearing capacity is the term used to denote the supporting ability of a soil mass without exceeding a specific settlement. It is defined as the average load per unit area for any given size of bearing area which will not cause more than a specified settlement.

Elasticity may be defined as the property of solids which renders them capable of returning to their original shape upon removal of an applied load. A soil mass under an applied load will generally deform. The elastic deformation is generally regarded as temporary strain, while the permanent deformation is regarded as plastic displacement or plastic flow or consolidation.

Plasticity is that property of certain solids by virture of which they may be continuously deformed without rupture by application of shearing stress in excess of a certain limit. In plastic solids a stress less than this limit (the yield value) may be sustained without continued deformation. Thus, plasticity combines the property of rigidity or elasticity characteristic of solids and the property of viscosity characteristic of fluids. In any material the entire range of behavior is apparently related to the degree of cohesion or amount of ultimate shearing resistance. Therefore, plasticity is simply a term indicative of a certain degree of cohesion or lack of cohesion. Generally, plasticity is spoken of in terms of lack of cohesion; the less cohesion a material has the more plastic it is said to be.

Viscosity is the term used when a material suffers a continuous shearing displacement due to the application of any shearing stress. Viscosity in a plastic solid is the term used when a plastic solid is stressed beyond the yield value and the laws of viscous flow control. Frequently the term plastic flow is used instead of viscous flow to show that the material under discussion is a plastic solid rather than a viscous liquid.

Capillarity is visualized as capillary rise which is the result of internal pressure in the liquid in combination with molecular attraction. Certain methods have been developed for measuring capillary rise. The results of such measurements are subject to some question due to experimental difficulties in making such measurements. Direct methods of approach are being developed, one of which is to measure the forces of adhesion between water and various soil material. This still does not eliminate entirely the complications introduced by the complexity of the soil mass.

Permeability is the property of a soil mass which permits the flow of fluid through the mass under the application of hydrostatic pressure. Permeability is measured as the rate of flow. Permeability depends on the porosity of soils, coarse grained soils being more permeable than fine grained soils.

Volume change in a soil mass is a physical property of some importance in engineering. Volume change from the expansion due to adsorption of moisture or shrinkage due to evaporation are volume changes which may be measured directly and are very useful.

A soil profile is a vertical cross-section showing the various horizontal strata including all soil layers. Therefore for any soil investigation or design it is essential to provide a soil profile in which most of the characteristics and properties are recorded.

Cohesive Soils

Cohesive soils are soils in which the particles cohere or stick together because of molecular forces. Soils which possess cohesion usually have small enough particles so that the molecular forces can come into action; the gradation of this type of particles is usually of size 0.005 mm and smaller.

These small particles adsorb a film of water, and this film of water is held in the soil particle as solidified water, cohesive water and capillary water. This film is of great importance. The picture of the mechanism of adsorption is shown in Figure 1.(17) It shows the approximate thickness of the moisture film as compared to the size of the particle. Also it shows the equivalent moisture film thickness at various stages of wetting. The various particles are bounded together by electro-static forces, thus giving the soil a certain resistance to tangential forces which tends to cause a tangential displacement between the particles. This resistance is shearing resistance. Therefore, due to this property, it could be conceived that in purely cohesive soils the shearing resistance is due entirely to cohesion, or in other words, shearing resistance is a measure of cohesion.

Thus cohesion can be defined as that property of a material which produces resistance to displacement by mutual attraction between particles of the same mass, involving forces of molecular origin, characteristic of microscopic and submicroscopic matter. From the

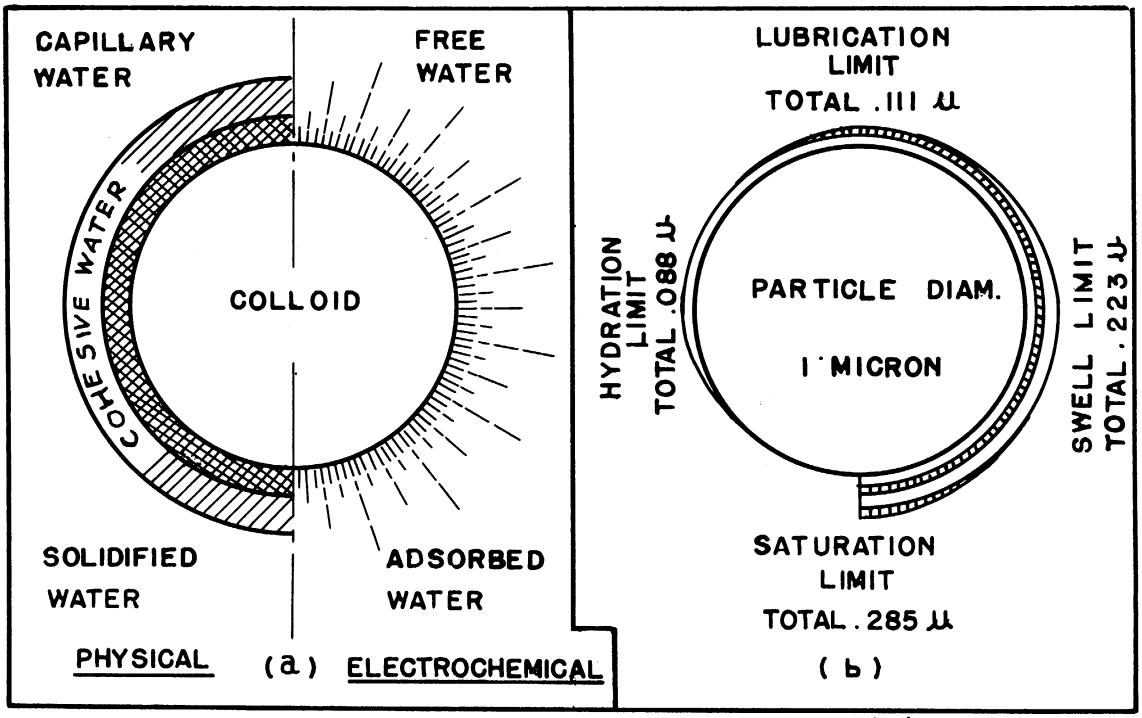

FIGURE 1. ADSORBED MOISTURE FILMS (17)

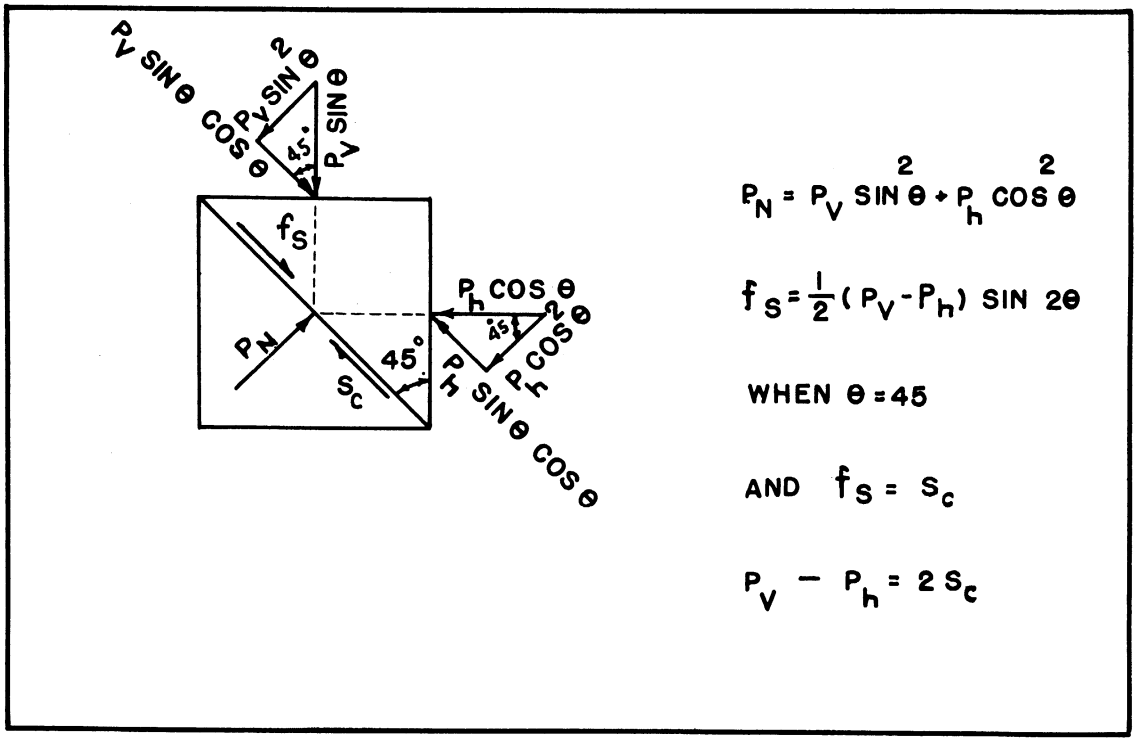

(21)

FIGURE 2. EQUILIBRIUM UNDER COHESION

nature of cohesion it is obvious and logical to conclude that shearing resistance due to cohesion is not affected by normal pressure; thus the resistance to shearing displacement in purely cohesive material is independent of normal pressure and therefore the criterion of failure is given by the relation:

$$P_v - P_h = 2S_c$$

This is derived by taking an element of mass subjected to a loading condition under equilibrium of which P_v is the maximum principal pressure and P_h is the minimum principal pressure. (see Figure 2). The relation between the principal pressures and the shearing stress is:

$$f_s = 1/2\ (P_v - P_h)\ \text{Sin}\ 2\theta$$

It may be shown that the maximum shear stress acts on plane at 45 degrees, according to the theory of elasticity and as it could be demonstrated by the Mohr circle. Therefore, substituting the value of θ as 45 degrees:

$$f_s = 1/2\ (P_v - P_h)$$

When the maximum shearing stress is equal to the shearing resistance the element will fail. Therefore the maximum difference in principal pressure is twice the shearing resistance:

$$S_c = f_s = 1/2\ (P_v - P_h)$$

$$P_v - P_h = 2S_c$$

The shearing resistance of cohesive soil can be determined by the transverse shear test, the unconfined compression test, or the penetration method.(19) The first two methods are more adaptable for

cohesive soils. The measurement of shearing resistance can be reduced to a determination of the yield value of the soil.

The transverse shear test is generally used to measure the shearing resistance of cohesive soils in which case no normal pressure is applied on the shear planes. The core barrel assembly is used to obtain an undisturbed sample of the cohesive soil for the transverse shear test. The steel liner is divided into four sections, a 3-inch piece used for supplementary tests, a 3-inch piece, a 1-inch piece, and a 3-inch piece, in that order. The 3-inch, 1-inch, and 3-inch pieces are used for the test (see Figures 3 and 4). The test is conducted by applying the load on the 1-inch piece while the two 3-inch pieces are supported on a saddle. The vertical displacement of the 1-inch piece is measured by a dial gauge reading to 0.001 inch. The load is applied in increments of static load approximately one-fifth the estimated yield value in order to provide four or five observations below the point of progressive displacement. After each load increment the load is held constant for a period of ten minutes during which deformation readings are taken every two minutes. Enough load increments are added to cause complete failure of the specimen in shear. These data are plotted as deflection against time. The slope of these observations for the last seven minutes are the rates of displacements. Then, by plotting rates of displacement against shearing stress, the yield value can be determined (see Figure 5). A sufficient number of samples must be tested to obtain the shearing resistance of a deposit as a whole.[11]

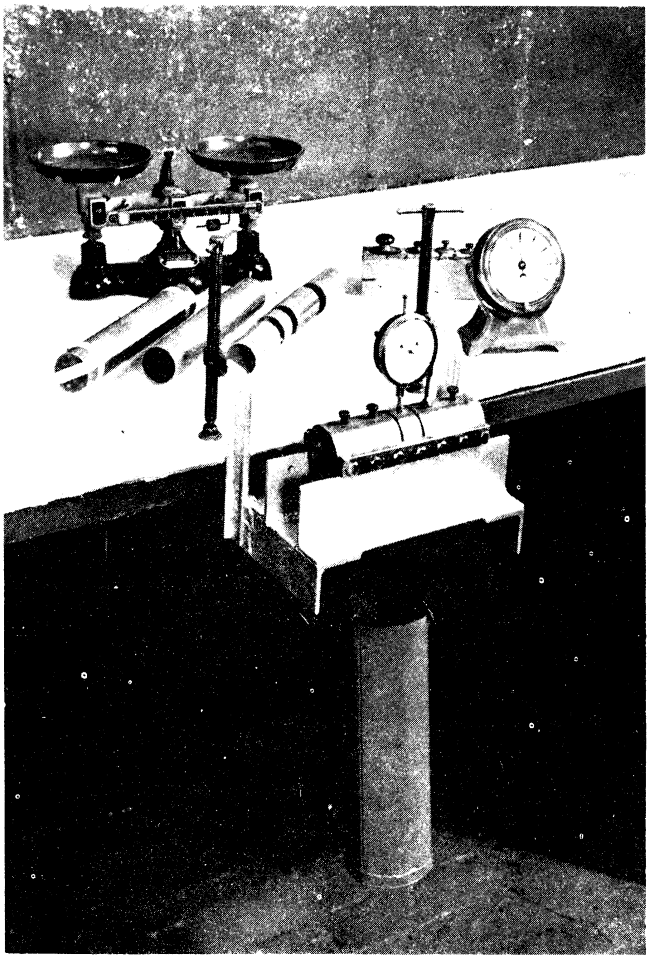

FIGURE 3. EQUIPMENT ASSEMBLY FOR SHEAR TEST OF COHESIVE SOILS (19)

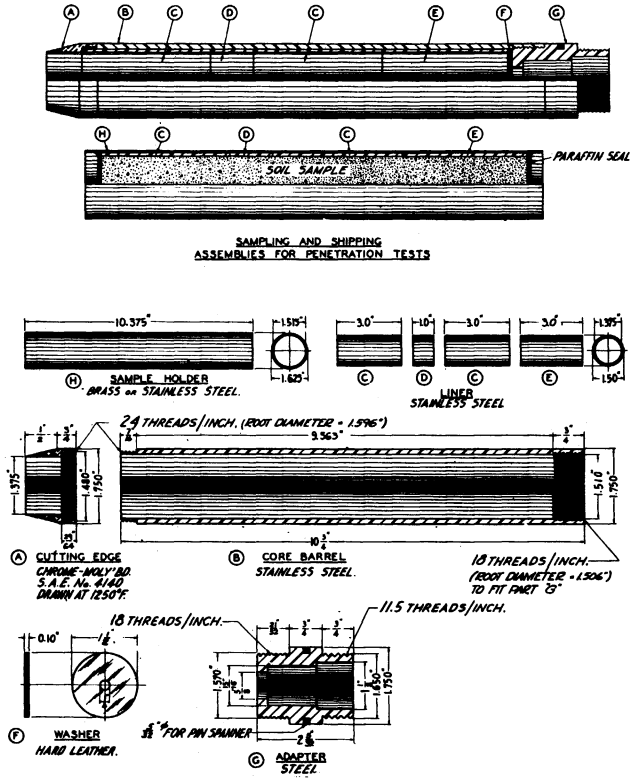

FIGURE 4. CORE BARREL ASSEMBLY FOR UNDISTURBED SAMPLES OF COHESIVE SOILS (19)

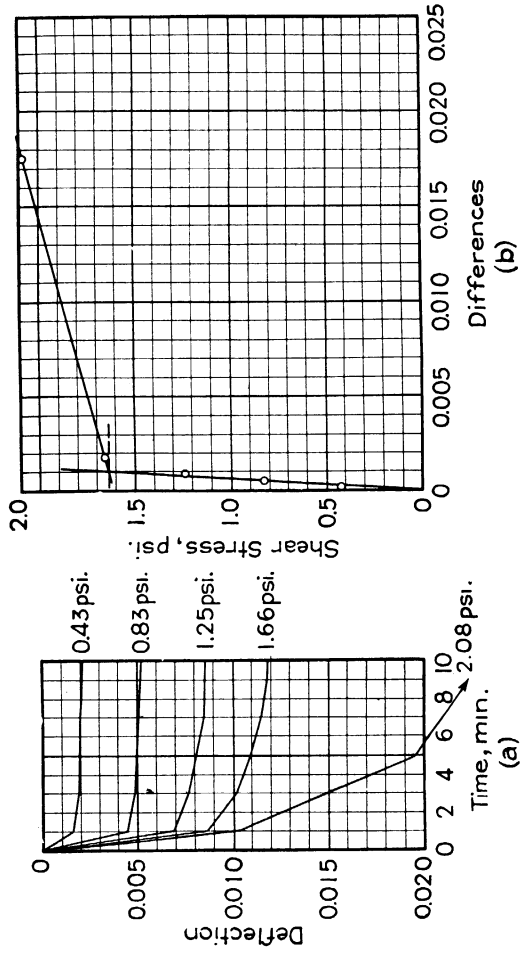

FIGURE 5. TYPICAL RESULTS FROM TRANSVERSE SHEAR TESTS (10)

The unconfined compression test is used to determine the ultimate unconfined compressive strength and ultimate shearing resistance of cohesive clay soil. It is also called a rapid shear test. A three-inch liner section of the sample is used in this test, and it is cut to 2-1/2 inches in length.

The sample is placed in the compression machine in an upright position (see Figure 6). Then loads are added at a constant rate, estimated to cause failure in approximately five minutes. The constant rate of load is obtained by applying selected load increments, and maintaining the load on the sample for thirty seconds. It is desirable that the load increments be unifrom, but they can be varied if necessary. Total deformations are recorded fifteen seconds after each loading. The load increments are added until failure, or until a vertical deformation of 20% is reached. Then the cumulative loads are plotted against the total deformations (see Figure 7). The total load at failure or at 20% deformation is obtained from the plotted results. The unconfined shearing resistance is taken as one-half of the compressive strength.

The penetration method is discussed later as it is usually used for a mass of soil containing mechanical stability.

In a vertical mass of purely cohesive soil the sliding surface is a parabolic surface (see Figure 8a), this fact has been observed, demonstrated experimentally and proven mathematically by D. T. Harroun.(7) Mr. Harroun assumed that the mass of soil was a purely cohesive material and that it possessed no internal stability due to the mechanical support of the particles. The sliding surfaces have been approximated by a

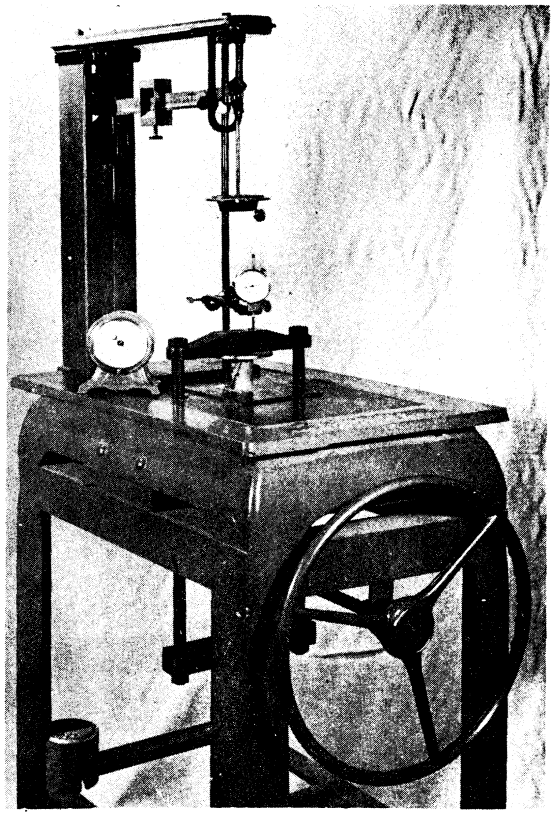

(a) Compression Machine.

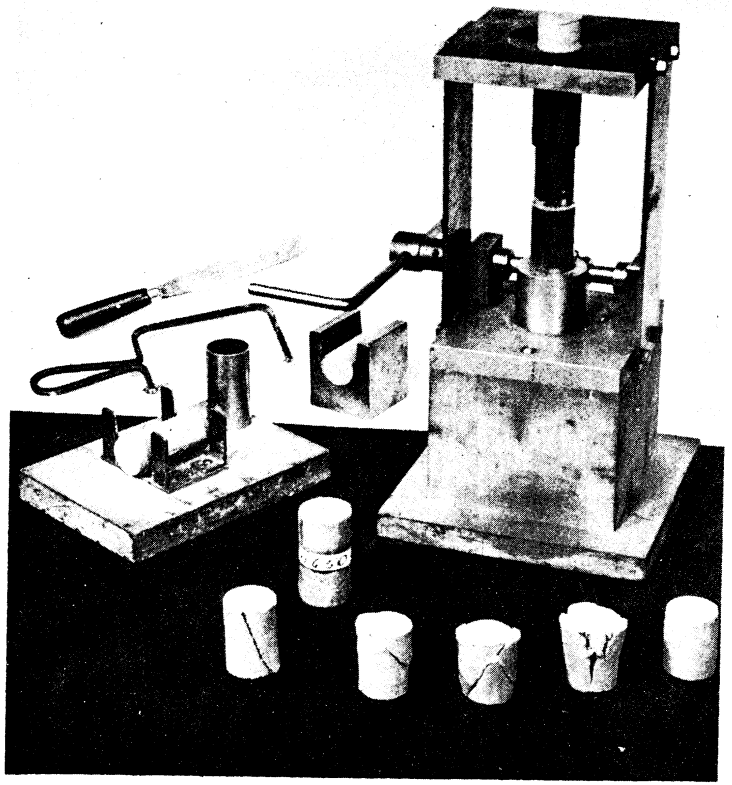

(b) Sample ejector and cutting jig.

FIGURE 6. EQUIPMENTS FOR THE UNCONFINED COMPRESSIVE STRENGTH OF COHESIVE SOILS[19]

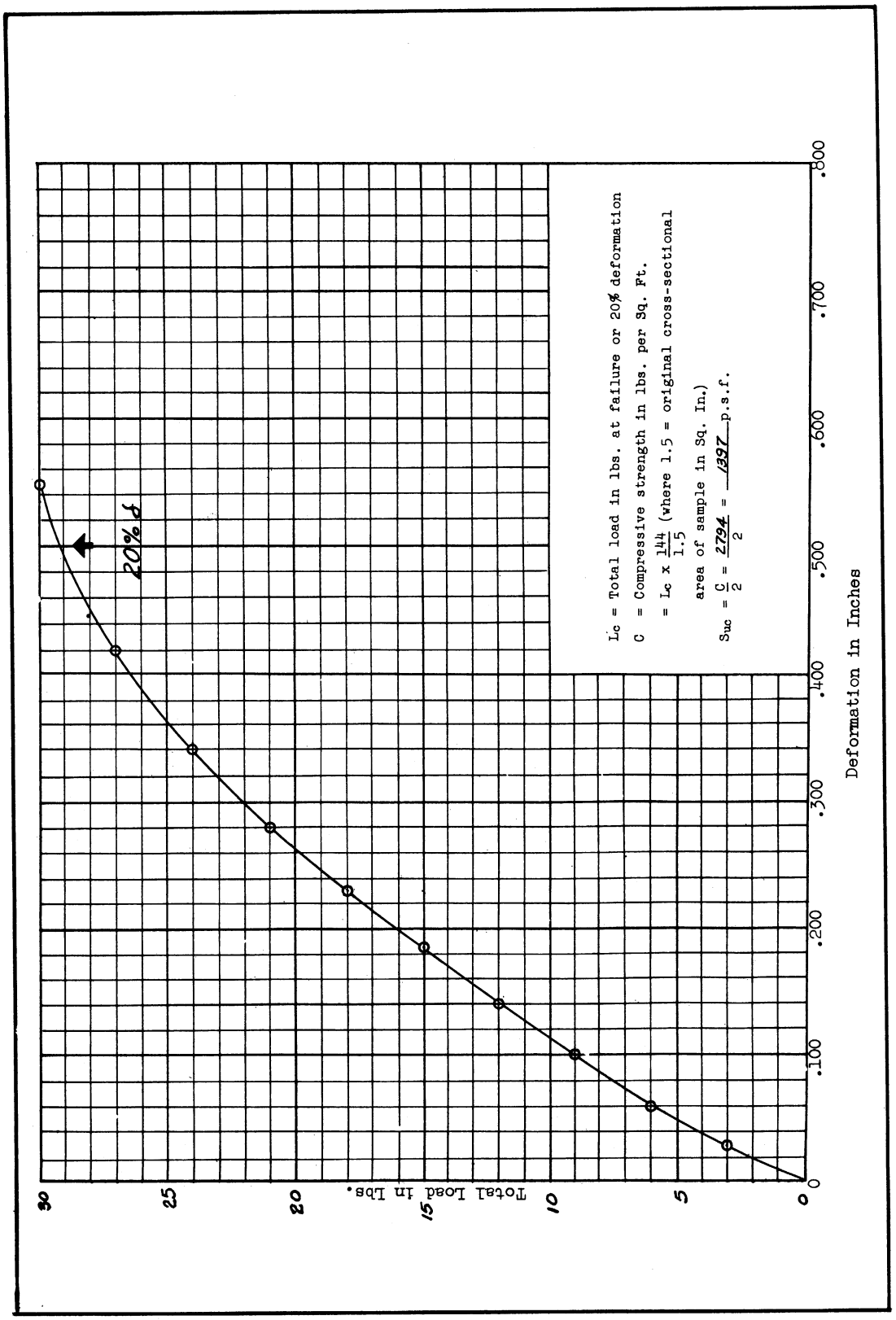

FIGURE 7. TYPICAL RESULT FROM THE UNCONFINED COMPRESSION TEST OF COHESIVE SOILS (19)

straight line and 45 degree line, as shown by Figure 8b. This approximation has been used with considerable success.(12) This approximation is made to simplify the mathematics involved. The parabolic failure surface has been replaced by two straight lines, one representing the 45 degree angle of failure on the lower half of the mass at the toe, the other representing the vertical surface on the upper half of the mass. The error due to this approximation is less than the probable error in evaluating the shearing resistance of the soil and other factors in such a problem. The element of mass at "C" (see Figure 8a) has the maximum shearing stress; the lateral pressure is zero and the vertical pressure on the element is a maximum and equal to wh. Using the relationship between the principal pressure and maximum shearing stress,

$$f = 1/2\ (P_v - P_h).$$

Then $f = 1/2\ wh$, where f is the shearing stress. When the maximum shearing stress is equal to the shearing resistance of the material due to cohesion, the critical depth or the maximum unsupported height is found to be twice the shearing resistance divided by the weight per unit volume of the soil.

$$f = S_c = 1/2\ wh_o$$

$$h_o = \frac{2S_c}{w}$$

To determine the horizontal distance, x, at which such a failure surface would cut the horizontal surface of the unsupported mass, a strip element of mass close to the horizontal surface, where the failure surface is substantially vertical, is selected as a free body. Equating the

forces acting on this element we have,

$$wxdy = fdy$$

$$x = \frac{f}{w} \quad \text{when } f = S_c$$

$$x = \frac{S_c}{w} = \frac{h_o}{2}$$

Thus the distance, x, is equal to half the depth, h_o. This relationship between the controlling dimensions of the primary sliding wedge has been verified many times in connection with construction operations involving subsurface excavations.(20)

The primary sliding wedge is under static equilibrium and this is verified by a study of the sliding wedge as a free body. The stress distribution along the sliding surface at C is equal to the maximum shearing resistance mobilized, S_c, and it is equal to half the static head of earth, when the depth of excavation is equal to or less than h_o, the maximum unsupported height. At D, the shearing stress is only half the maximum shearing resistance of the soil. When the lateral pressure on the vertical face of the triangular element is zero, equality of the horizontal component of the shearing resistance along CD results in the normal pressure being equal to the shearing stress, f_s, which is, in turn, equal to 3/4 S_c.

$$\text{Then } P_n = f_s = 3/8\ wh_o = 3/4\ S_c$$

$$\text{Taking } \Sigma V = 0$$

$$\text{we get } h_o = \frac{2S_c}{w}$$

And by taking the summation of the moment of the forces about C we get $\Sigma M_c = 0$. Therefore the three equilibrium equations are satisfied. As

a result there is no tendency for either vertical shearing stress or tension to be developed on the vertical plane AD.

The bearing capacity of cohesive soils is a function of cohesion or shearing resistance, which controls the resistance to lateral displacement under applied load.

According to the observations of the lateral displacement of the soil under a load greater than the bearing capacity limit, it is obvious that there is a loaded element of mass which is confined by the adjacent elements so that it is capable of developing some concentration of pressure. By establishing the equilibrium of the loaded element and the supporting element, it may be shown that the developed pressure is equal to four times the cohesive shearing resistance (see Figure 9). Other factors which contribute to the bearing capacity are static head and the lateral distribution of the load below the loading plane.

A portion of the load will be distributed away from the loaded Element 1 to the adjacent elements. This reaction originates in the vertical shearing resistance acting on the boundaries of the central column as perimeter shear. In general form, this reaction on Element 1 may be expressed as the vertical shearing resistance multiplied by the perimeter-area ratio of the bearing area and the depth over which this vertical shearing resistance is mobilized. The perimeter ratio for a strip is $\frac{2}{b}$. Therefore the stress reaction due to lateral distribution is $S_c h \times \frac{2}{b} = S_c h \times \frac{2}{h} = 2S_c$. When h is equal to b the lateral distribution is equal to twice the shearing resistance, $2S_c$. The static head

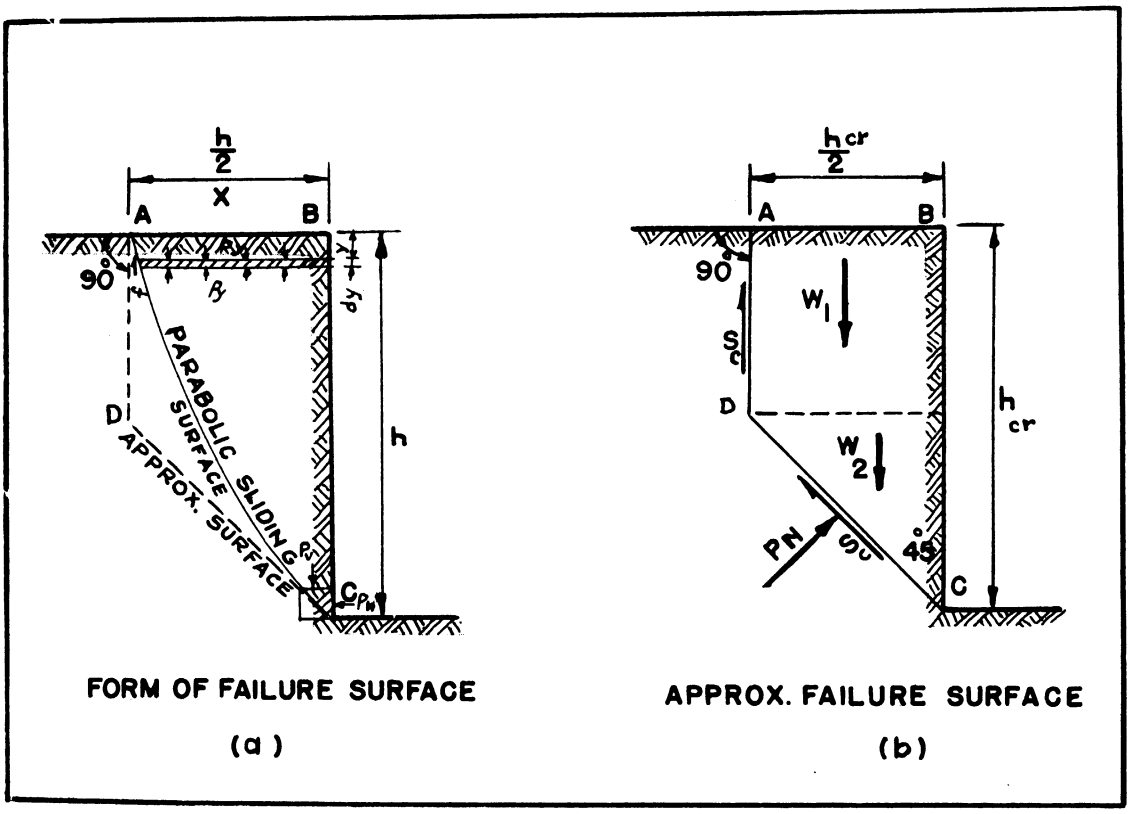

FIGURE 8 . FAILURE SURFACE IN COHESIVE SOILS (12)

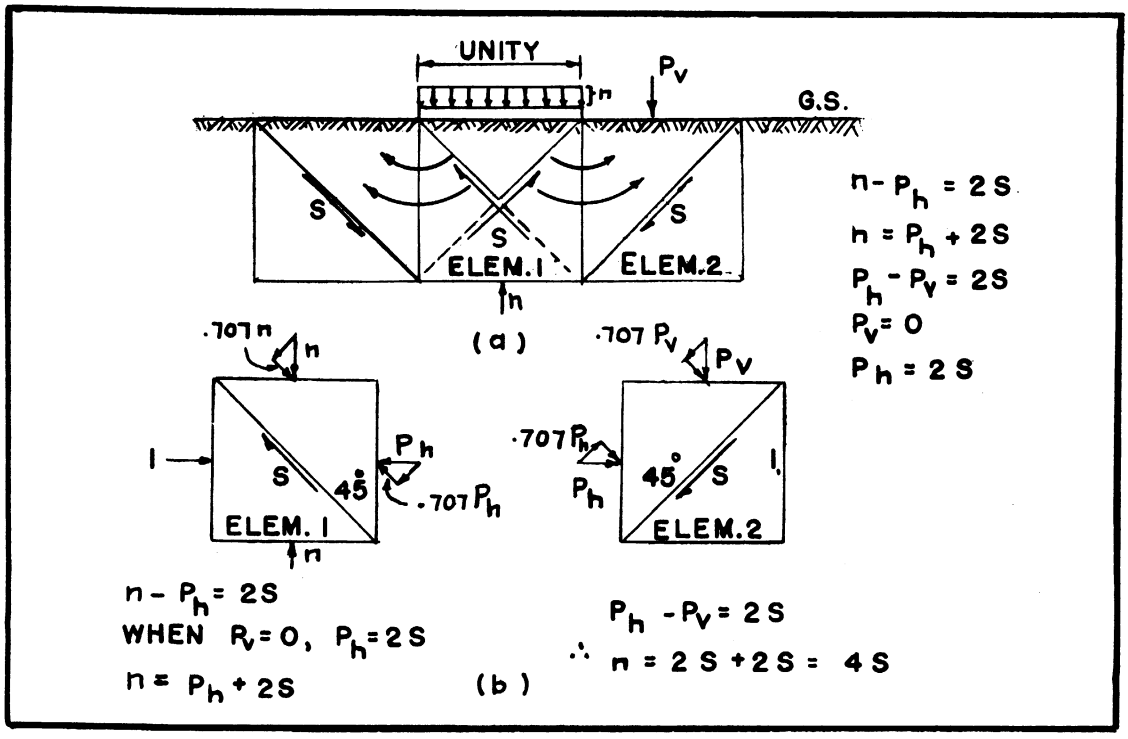

(15)

FIGURE 9 . RESISTANCE TO LATERAL DISPLACEMENT IN COHESIVE MATERIAL

is an overburden pressure and may be regarded as cubical compression transmitted through Elements 1 and 2 to the bottom of the footing. When described as flotation, it is implied that the soil mass is capable of transmitting fluid pressures proportional to the static head with an active pressure or upward reaction on the bearing area. Such a pressure component causes no shearing stresses within the soil mass and being independent of shearing stress plays no part in the lateral distribution of pressure within the central column but merely adds to the concentration of pressure which may be transmitted downward by Element 1. It is equal to the weight of the soil in pounds per cubic foot miltiplied by the depth of overburden, h_o.

Granular Soils

Granular soils are those in which the particles are too large to be noticeably affected by molecular forces of attraction and repulsion. The gradation of this type of particles is usually of the size larger than .05 mm.

Soils of particles larger than .005 mm are divided and named as follows:

TABLE I

NAMES AND SIZES OF SOIL MATERIALS

2	to	1	millimeter, fine gravel
1	to	.5	millimeter, coarse sand
.5	to	.25	millimeter, sand
.25	to	.10	millimeter, fine sand
.10	to	.05	millimeter, very fine sand
.05	to	.005	millimeter, silt

Mixed soils of granular and cohesive properties are discussed later. Silt soil of particles between .005 mm and .05 mm exhibits both cohesive and granular properties.

The particles of granular mass are under various conditions and systems of mechanical arrangement. To simplify the relationship involved in various mechanical arrangements, shape and size, an assumption is made. This assumption is that these particles are spheres of uniform size corresponding to an average shape and size of those particles which actually exist. In order to have the particles of the soil mass resting in stable equilibrium, these particles have to rest on each other in a stable position as shown in Figure 10. In this case any specific grain rests in the depression between several other grains in the layers beneath it. The vertical forces transmitted to any one particle are divided proportionally among the supporting particles which in turn distribute their vertical components in a like manner. The horizontal thrust necessary to maintain stable equilibrium is supplied by the adjacent particles in each layer. To simplify the description of pressure distribution between particles this arching may be represented in two dimensions. The angle of pressure distribution along the arch axis through the center of the primary and the supporting spheres is denoted by angle θ. This angle is known as the angle of pressure transmission.

The relationship between the principal pressures, which is the ratio between the applied vertical pressure and reacting lateral pressure

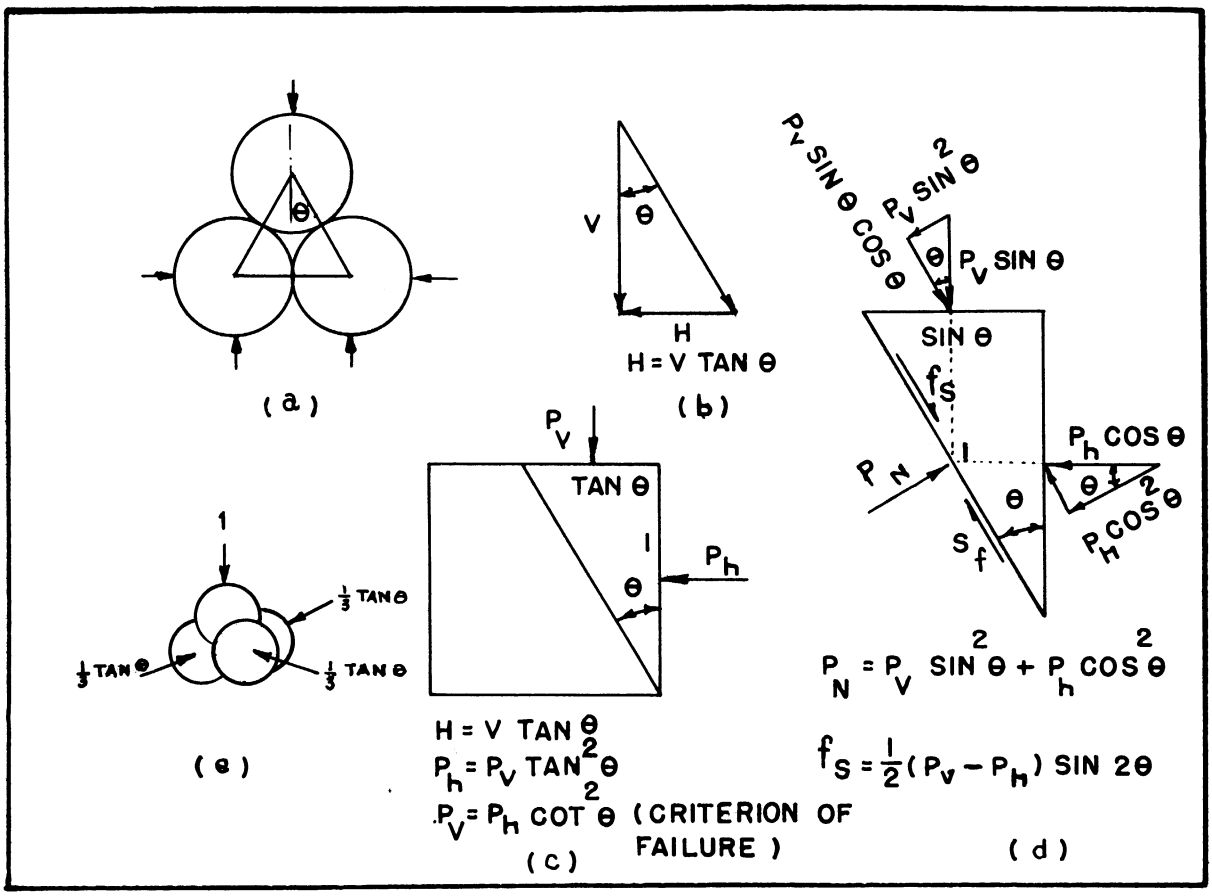

(10)

FIGURE 10. INTERNAL STABILITY BY ARCHING ACTION

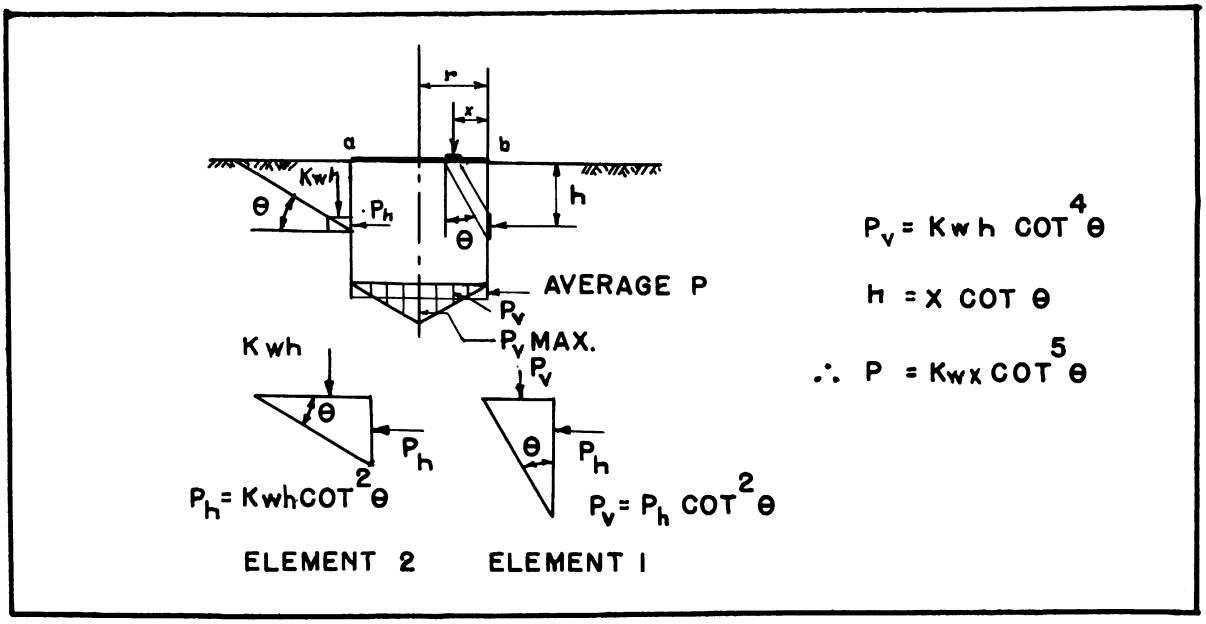

(13)

FIGURE 11. STABILITY UNDER VERTICAL LOAD

or horizontal thrust, may be established by applying the arching theory and introducing the static equilibrium condition as:

$$P_h = P_v \, \text{Tan}^2 \, \theta$$

$$P_v = P_h \, \text{Cot}^2 \, \theta \qquad \text{(See Figure 10).}$$

Thus internal stability in granular mass is described as arching action and independent of shearing resistance, and therefore internal stability in granular material can be defined as the mechanical property of granular masses which produces resistance to displacement by mutual support of adjacent particles in the mass, involving static forces and reactions between particles too large to be noticeably affected by molecular forces.

An important fact which should be mentioned is that the failure in the granular material occurs on the plane of minimum resistance and not on the plane of maximum shearing stress thus violating the assumption of isotropy.

The relationship between the principal pressures as well as the angle of pressure transmission, (θ) for a mass of soil can be determined by the penetration method or the triaxial compression test. The penetration method is used for all types of soils as a field test. This method was presented before The American Society of Testing Materials first in 1935.(9) The method consists of driving a standard core barrel into the soil with a standard blow and measuring the penetration per blow (see Figure 12). The penetration per blow has been correlated with the number of blows for six inches of penetration and this index is used to evaluate the shearing resistance of the soil. Values of shearing resistance obtained by the penetration method have been correlated with

load tests and with a simple transverse shear test carried on the clay core. This index is called the University of Michigan Index; another index is the Raymond Index. A correlation between these two indexes has been made[18] (see Figures 13 and 14).

Another testing method is the triaxial compression test. This test is used to determine the relationship between the principal pressures in a granular soil mass or a soil mixture having granular characteristics. The test is performed by means of the Stabilometer (see Figure 15). The sample is prepared to the proper density at a selected moisture content. The lateral pressure is applied on the sample as an air pressure behind an air tight membrane around the sides. Then the vertical load is applied with the compression machine at a constant rate of deformation. The ultimate vertical pressure sustained by any given lateral pressure is selected directly from the load deformation chart[19] (see Figure 16). In order to obtain the relationship between the principal pressures for any given size of sample, tests at several different lateral pressures varying between 10 and 40 pounds per square inch are required. One test should also be conducted when the lateral pressure is 5 pound per square inch or less, to measure the changing slope of the curve at or near the origin.

The results of each test is plotted. The ultimate vertical pressure, P_v, is plotted against the applied horizontal pressure, P_h, then the best fitted line can be selected. The slope of this line is equal to $\text{Tan}^2\theta$, therefore

$$\theta = \text{Arc Tan } \left(\frac{P_h - P'_h}{P_v - P'_v}\right)^{1/2}$$

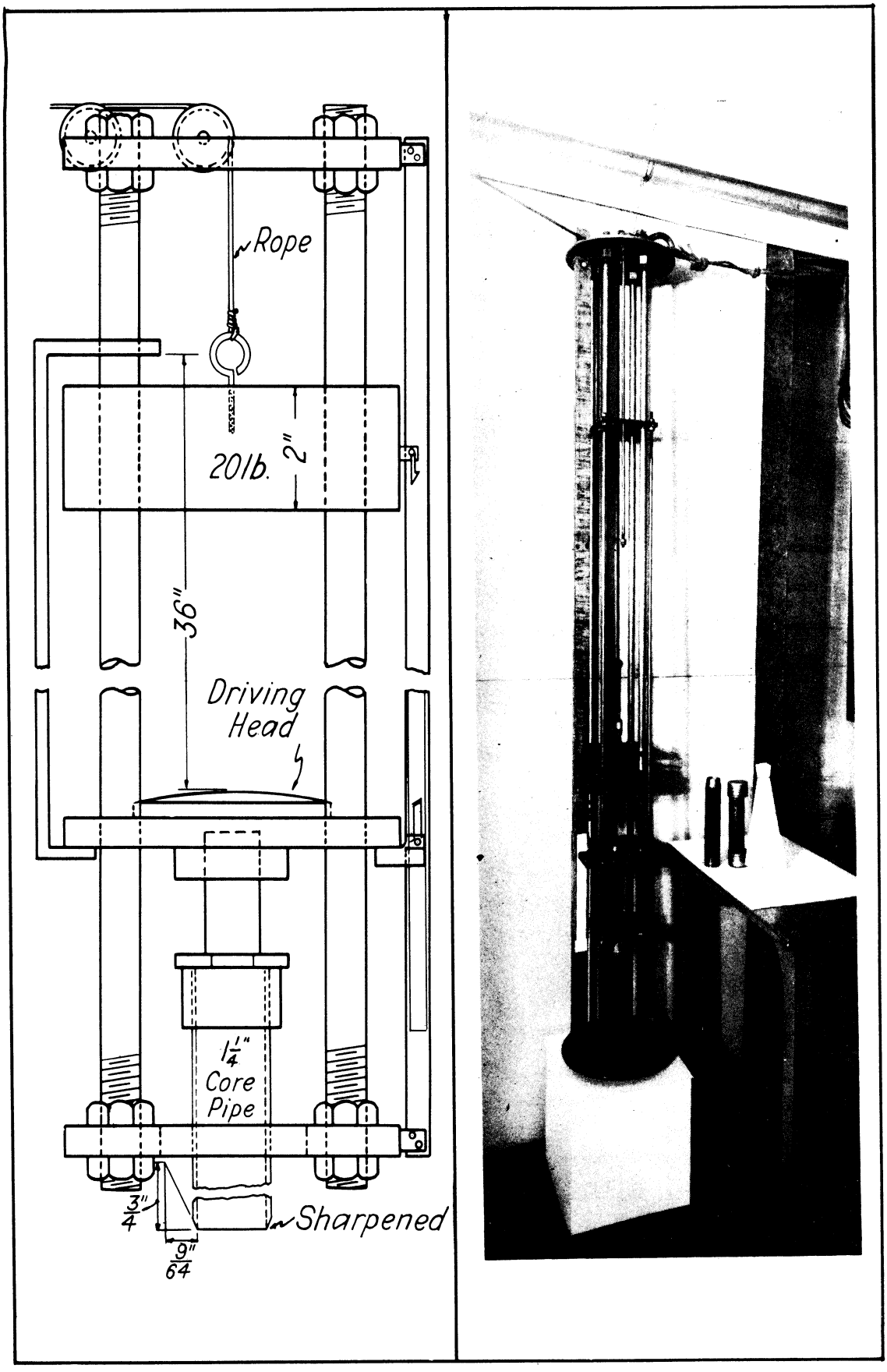

FIGURE 12. STANDARD DRIVING APPARATUS FOR PENETRATION MEASUREMENTS (19)

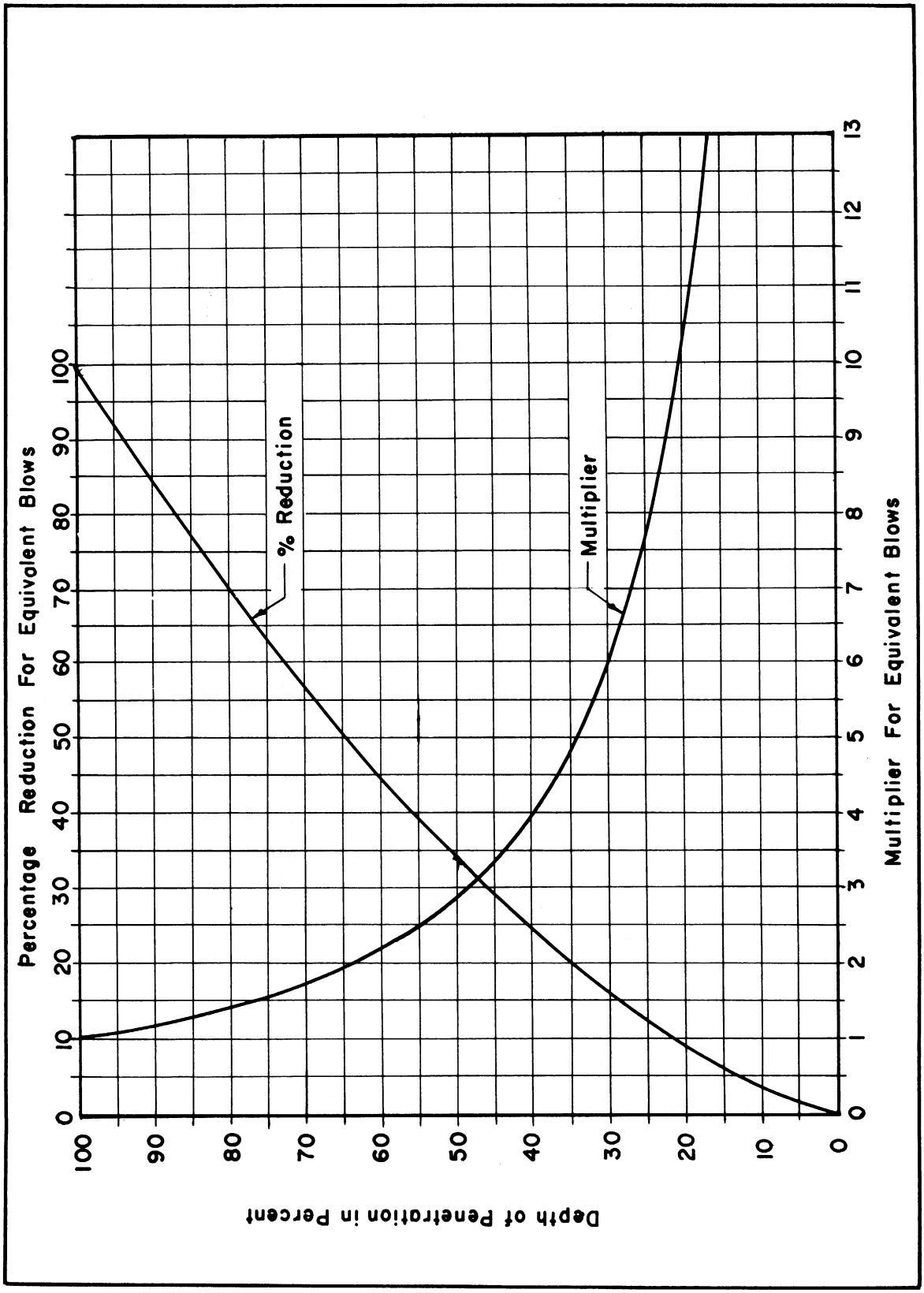

FIGURE 13. CONVERSION FACTORS FOR EQUIVALENT PENETRATION[18]

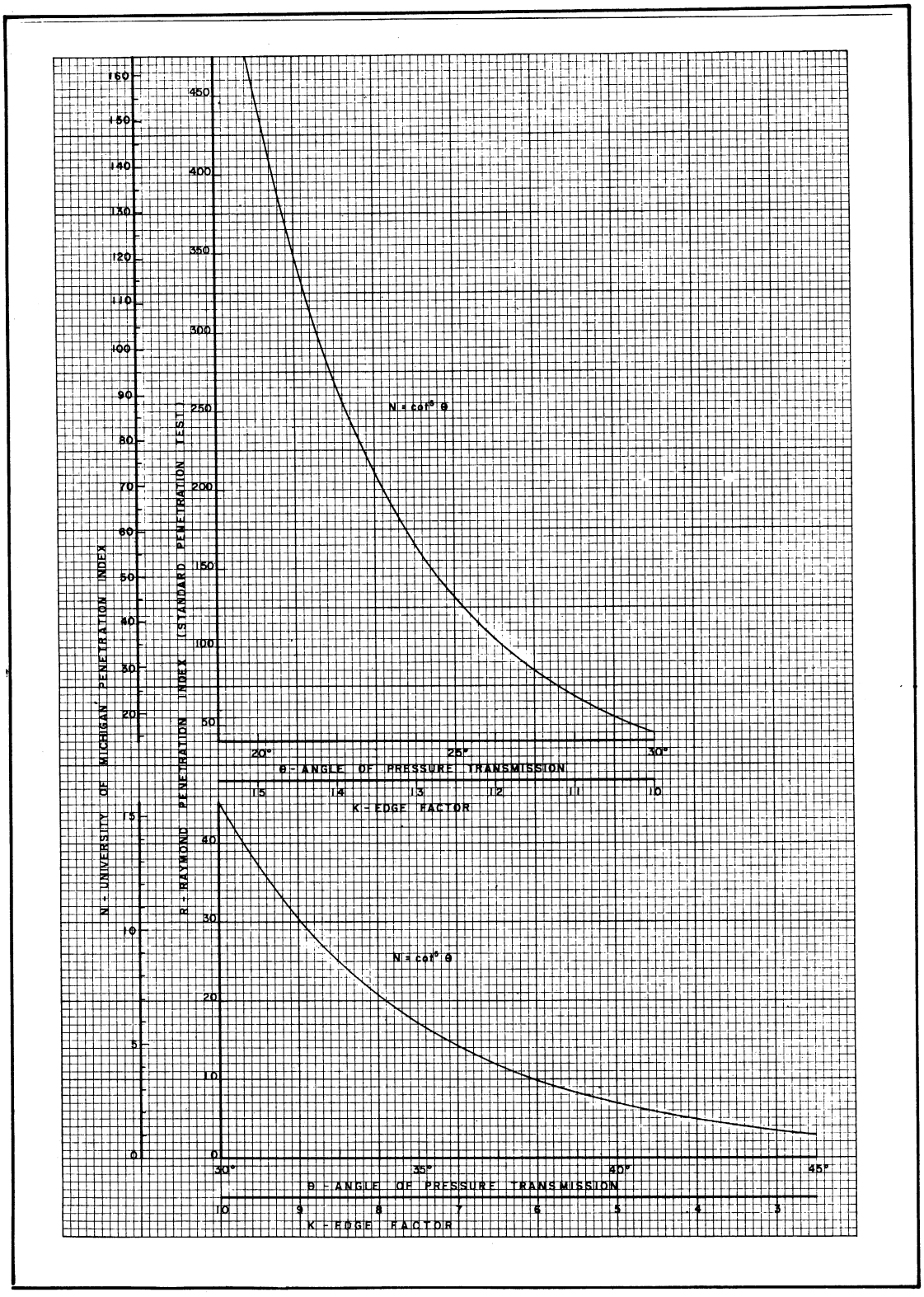

FIGURE 14. INTERNAL STABILITY FACTORS VERSUS PENETRATION INDEXES (18)

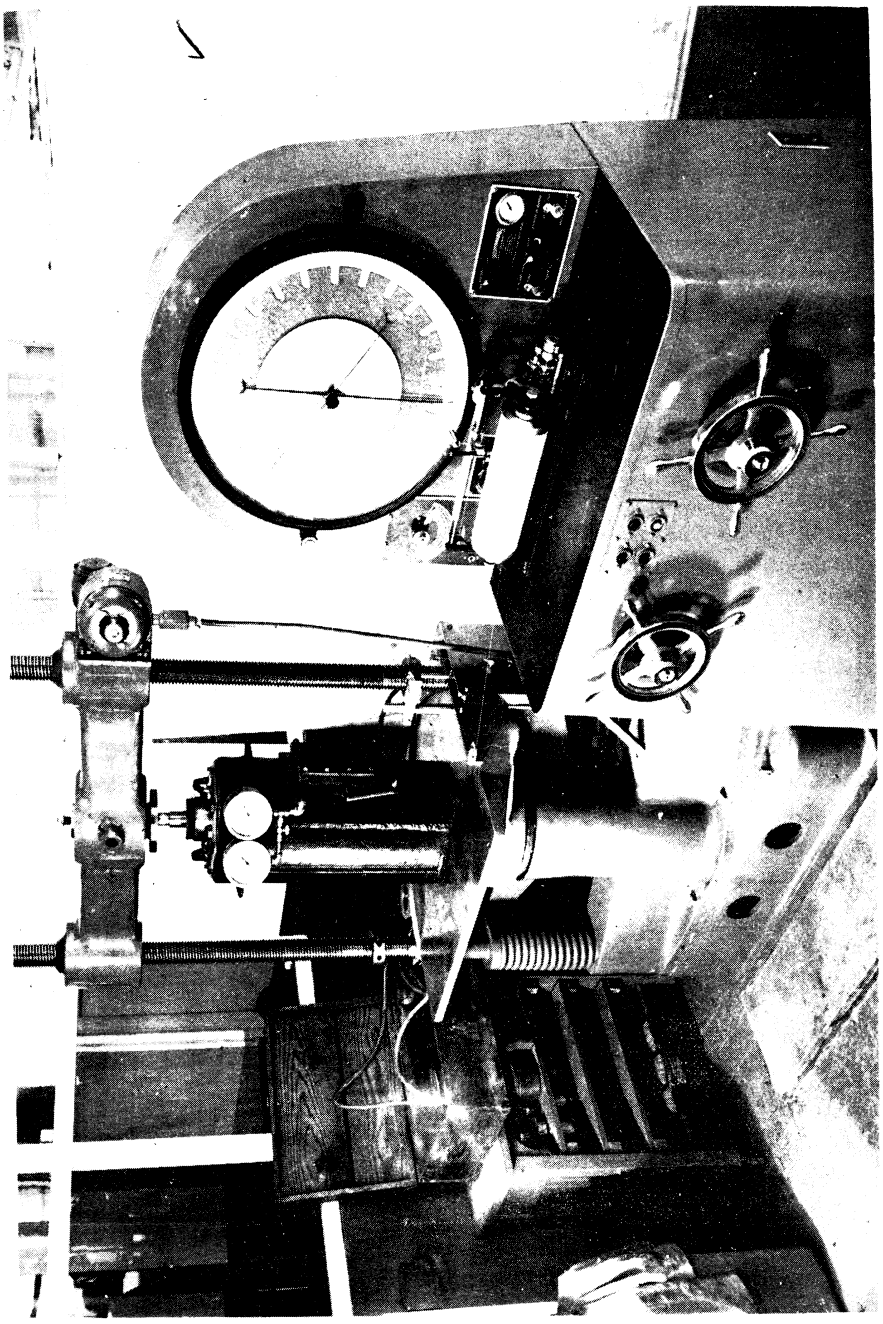

FIGURE 15. STABILOMETER SET-UP IN COMPRESSION MACHINE (19)

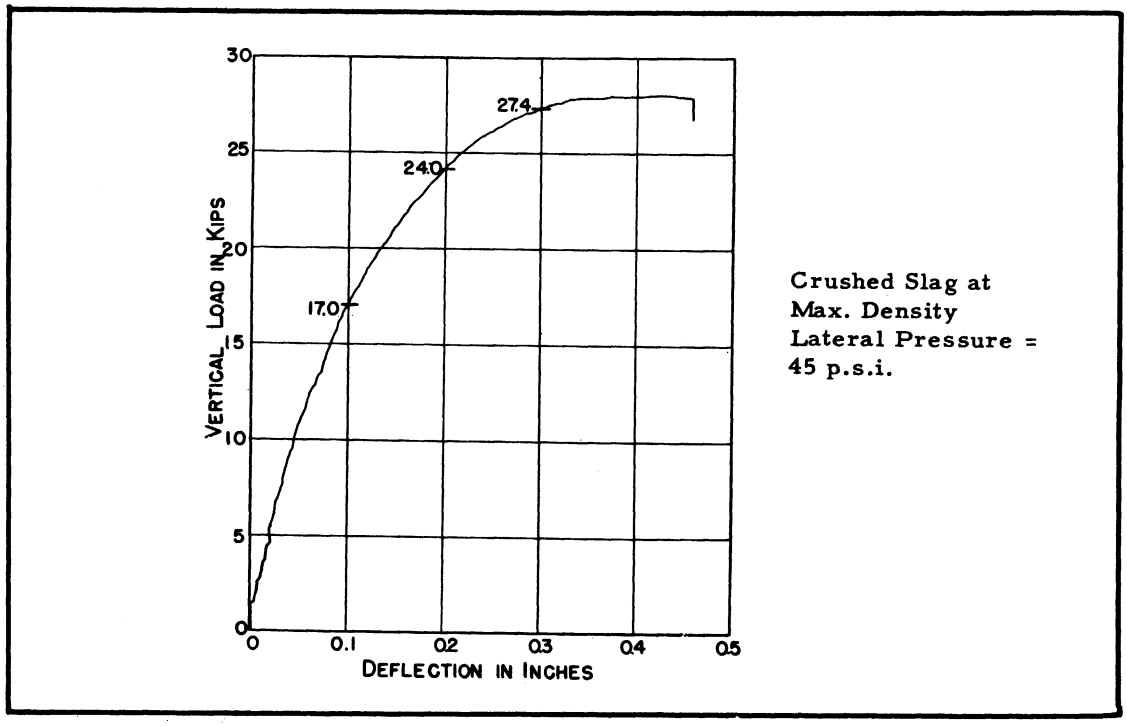

FIGURE 16. TYPICAL LOAD DEFLECTION CURVE (9)

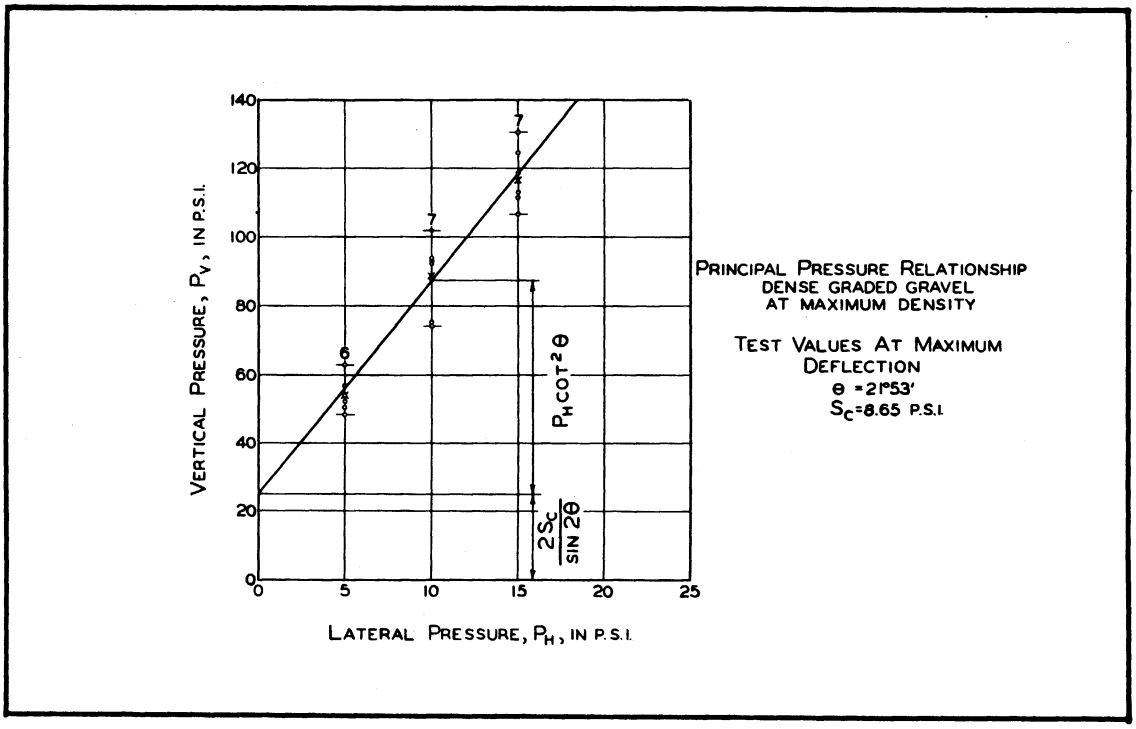

FIGURE 17. TYPICAL RESULTS FROM THE TRIAXIAL COMPRESSION TESTS (9)

The value of P_v at $P_h = 0$ can be determined from the straight line.[13] This value of P_v is equal to $2S_c/\text{Sin } 2\theta$. (see Figure 17).

In a mixed soil where a granular soil contains a cohesive soil the relation between the maximum principal pressure P_v and the minimum principal pressure P_h is determined in such a manner that the shearing resistance of cohesive soil may be introduced as a separate factor to the basic relationship between principal pressures in granular soil, which is based on internal stability due to arching. Taking the plane of failure on a diagonal plane inclined at an angle θ with the vertical principal plane, the shearing resistance due to cohesion on that plane is:

$$S = 1/2\ (P_v - P_h)\ \text{Sin } 2\theta$$

If S is given a certain value of shearing resistance equal to S_c, then:

$$P_v - P_h = 2S_c/\text{Sin } 2\theta$$

These two effects may be added and then will yield:

$$P_v = P_h\ \text{Cot}^2\ \theta + 2S_c/\text{Sin } 2\theta \qquad \text{Passive}$$

$$P_h = (P_v - 2S_c/\text{Sin } 2\theta)\ \text{Tan}^2\ \theta \qquad \text{Active}$$

The arching theory is used as the basis for establishing the bearing capacity of granular soil, thus the relationship between principal pressures will be an essential fundamental. Therefore the bearing capacity will be the limiting load which could be placed on the soil mass before a lateral displacement will take place. The lateral displacement in granular material is usually under the bearing area and surroundings. The particles beneath the bearing area move in a downward

lateral direction and those outside of the central column move in an upward lateral direction. In Figure 11 a diagram is shown illustrating the various factors to be considered in developing the bearing capacity.(10) According to the manner of pressure transmission and the supporting ability of Elements 1 and 2 under equilibrium conditions the following equation is derived:

$$P_v = K\ w\ x\ \mathrm{Cot}^4\ \theta$$

$$P_V = K\ w\ r\ \mathrm{Cot}^5\ \theta \quad \text{for circular areas.}$$

The average pressure $P = 1/3\ K\ w\ r\ \mathrm{Cot}^5\ \theta$.

If surcharge does exist then

$$P_v = 1/3\ K\ w\ r\ \mathrm{Cot}^5\ \theta\ +\ w\ h_1\ \mathrm{Cot}^4\ \theta$$

The factor, K, represents vertical pressure transmitted to the elements outside the central column due to lateral distribution of pressure from the bearing area.

The effect of cohesion introduces the term

$$\left(\frac{2S_c}{\mathrm{Sin}\ 2\theta}\right)\ (1 + \mathrm{Cot}^2\ \theta)$$

Therefore:

$$P_v = 1/3\ K\ w\ r\ \mathrm{Cot}^5\theta + w\ h_1\ \mathrm{Cot}^4\ \theta + (2S_c/\mathrm{Sin}\ 2\theta)(1 + \mathrm{Cot}^2\ \theta)$$

The Element Method

The element method has been applied in determining the stability analysis of soil masses which possess cohesive property and their resistance to lateral displacement or upheaval.

The element is that mass of soil which may be displaced laterally or yield due to the applied pressures. It is formulated in accordance with the possible manners in which the soil mass may fail and be displaced.

Many factors determine the depth of the element and its physical shape. The depth of the element may be equal to the width of the bearing area. This case is usually considered when the stability of the local area under the applied pressure is being investigated. The depth of the element may be determined by the depth of the various soil layers underlying the bearing area. Also the existing structures must be considered in determining the depth of the element whenever these structures are not permitted to take any displacement. This case is considered when the stability of the whole mass of soil is to be investigated. Figure 18 is an illustration showing an example of these elements which are to be taken into consideration.

The critical element is the element which has the highest overload ratio (R). Thus it is the element which has been over stressed more than the other elements. It has become general practice to express the amount of overload as the overload ratio, which is the ratio of the shearing stress imposed on the soil divided by the yield value measured by laboratory test.

Solution of the mass stability problem has been simplified by breaking it into two parts, by selection of a loading plane to separate the superimposed load from the supporting mass. Above the loading plane, the applied forces are the lateral pressure, $\frac{F_h}{d}$, and the static head, wh, less weight transfer. The resisting forces are the lateral pressure, $\frac{F_h'}{d}$,

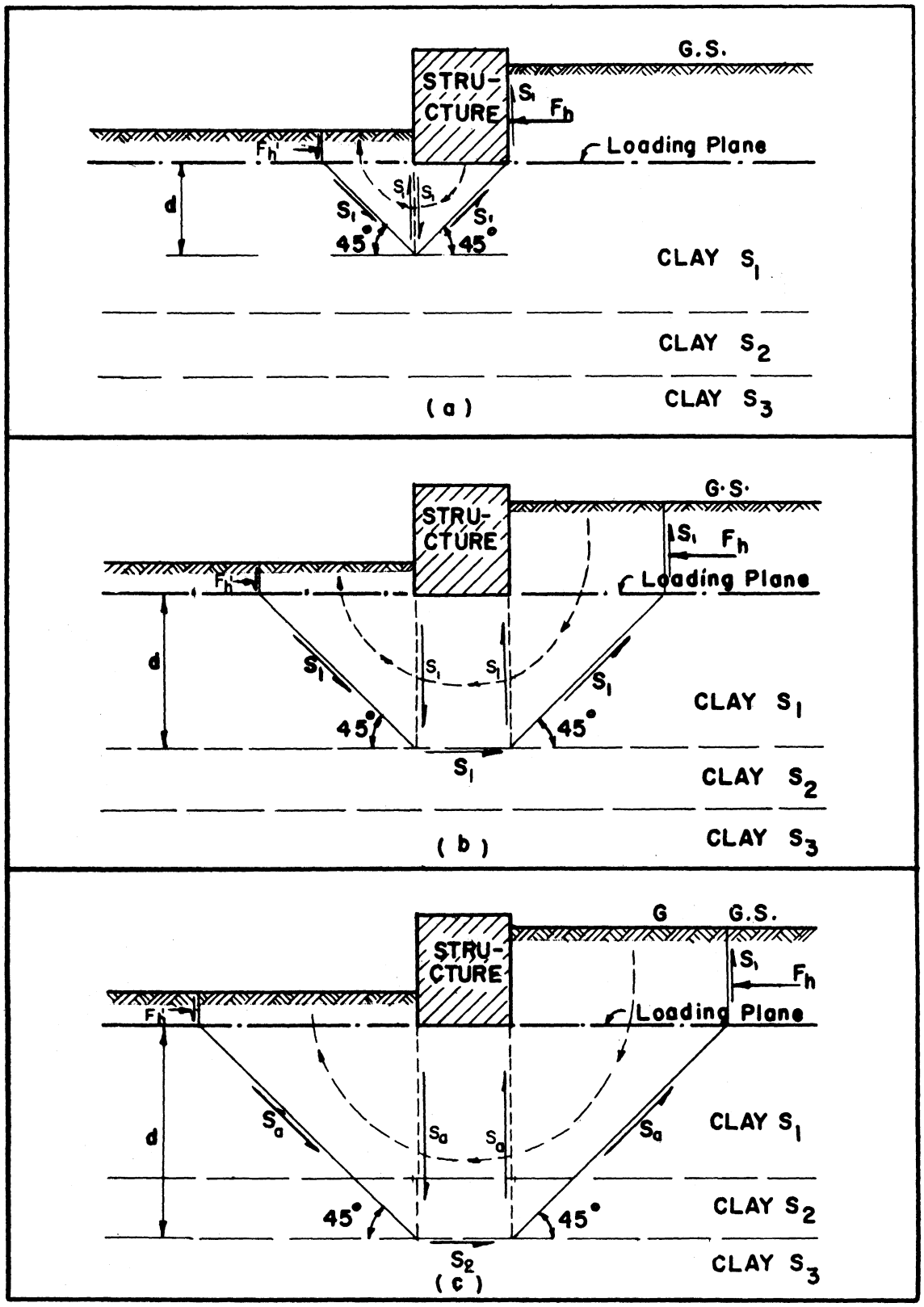

FIGURE 18. UPHEAVAL OF SOIL AND THE ELEMENT

the static head, wh', less weight transfer, resistance to upheaval and parameter shear. Below the loading plane, resistance to displacement is evaluated in terms of developed pressure, lateral distribution of applied load, and resistance to horizontal displacement or sliding. All of these forces and resistances can be combined in a single stability equation, which can be compared to Bernoulli's equation in hydraulics. The loads or driving forces are the static head, w h, and the lateral pressure component $\frac{Fh}{d}$. Such an equation is expressed by including in each shearing resistance term the overload ratio, R, which indicates the amount of overload under the loading condition being considered. Solution of such an equation to obtain the value of the over load ratio, R, and comparison with the limits will determine the degree of hazard involved. Conversely, the allowable load that may be sustained may be calculated from this equation by specifying the permissible overload ratio and solving for the allowable load.

The Equivalent Lateral Pressure

The lateral pressure in cohesive soil is determined according to the relationship $P_h = P_v - 2S_c$. The value of the active lateral pressure will be equal to zero until the vertical pressure becomes more than $2S_c$, then the lateral pressure will be developed.

The lateral pressure in granular soil is determined by the relation $P_h = P_v \text{ Tan}^2 \theta$. If the granular soil contains cohesive soil then $P_h = (P_v - 2S_c/\text{Sin } 2\theta) \text{ Tan}^2 \theta$. Figure 19 illustrates the equivalent active lateral pressure. Figure 20 illustrates the equivalent passive lateral pressure.

$$h_o = \frac{2S}{w} - \frac{P_o}{w}$$

$$P_h = P_o + wh - 2S$$

$$F_h = \frac{1}{2}(P_o + wh - 2S)(h - \frac{2S}{w} + \frac{P_o}{w})$$

$$x = \frac{2}{3}(h + \frac{S}{w} - \frac{P_o}{2w}) \quad \text{When } h_o \geq 0$$

IF $P_o = 0$ THEREFORE $h_o = \frac{2S}{w}$

$$P_h = wh - 2S \qquad F_h = (\frac{wh - 2S}{2})(h - \frac{2S}{w})$$

$$x = \frac{2}{3}(h + \frac{S}{w})$$

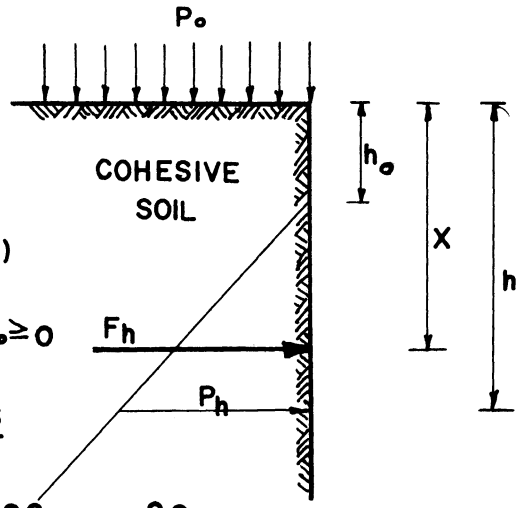

(a)

$$P_h = (wh + P_o)\,TAN^2\theta$$

$$F_h = (P_o h + \frac{wh^2}{2})\,TAN^2\theta$$

$$x = \frac{h(P_o + \frac{2}{3}wh)}{P_o + wh}$$

IF $P_o = 0$ THEREFORE

$$P_h = wh\,TAN^2\theta$$

$$F_h = \frac{1}{2}wh^2\,TAN^2\theta \qquad x = \frac{2}{3}h$$

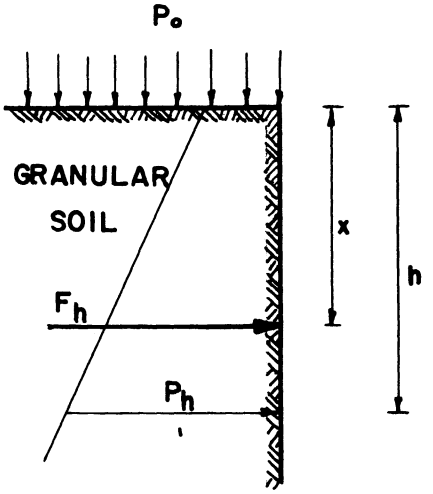

(b)

FIGURE 19. EQUIVALENT ACTIVE LATERAL PRESSURE IN COHESIVE AND GRANULAR SOILS

$$P_h = P_o + wh + 2S$$

$$F_h = P_o h + 2Sh + \frac{1}{2} wh^2$$

$$x = \frac{h}{6}\left(\frac{3P_o + 6S + 2wh}{P_o + 2S + wh/2}\right)$$

IF $P_o = 0$ THEREFORE

$$P_h = wh + 2S$$

$$F_h = h\left(\frac{wh^2 + 4Sh}{2}\right)$$

$$x = \frac{h}{6}\left(\frac{6S + 2wh^2}{2S + wh/2}\right)$$

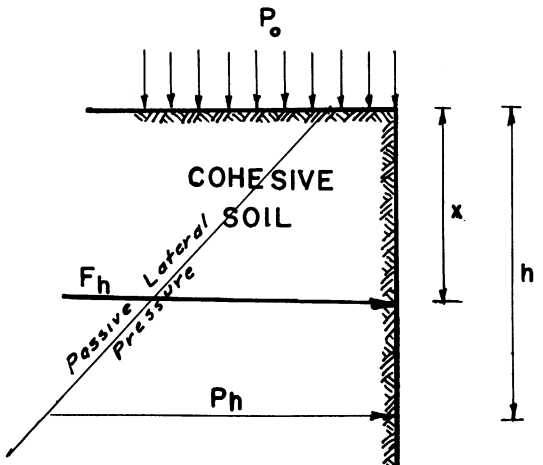

(a)

$$P_h = (wh + P_o)\,COT^2\theta$$

$$F_h = \left(P_o h + \frac{wh^2}{2}\right) COT^2\theta$$

$$x = \frac{h}{6}\left(\frac{3P_o + 2wh}{P_o + wh/2}\right)$$

IF $P_o = 0$ THEREFORE

$$P_h = wh\ COT^2\theta$$

$$F_h = \frac{1}{2} wh^2\ COT^2\theta$$

$$x = \frac{2}{3} h$$

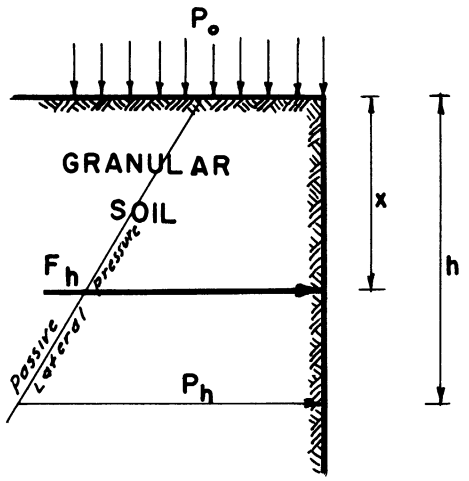

(b)

FIGURE 20. EQUIVALENT PASSIVE LATERAL PRESSURE IN COHESIVE AND GRANULAR SOILS

Whenever a cohesive soil contains an appreciable amount of granular material the values of the shearing resistance determined from the unconfined compression tests, S_{UC} are generally greater than four times the values found from the transverse or ring shear test. The reason is that the granular material controls the angle of rupture which is steeper than the usual 45 degree angle of maximum shear stress in purely cohesive materials. The value of the shearing stress on the plane of minimum resistance, which is causing the failure, is less than the shearing stress on the plane of maximum stress which is at 45 degrees.

The active lateral pressure is

$$P_h = (P_v - \frac{2S_c}{\text{Sin } 2\theta}) \text{ Tan}^2 \theta$$

where

$$S_{uc} = \frac{S_c}{\text{Sin } 2\theta} \quad \text{and} \quad S_{UC} = \frac{kS_c}{\text{Sin } 2\theta}$$

Thus if S_c is determined by the ring shear test and S_{uc} is determined by the unconfined compression test, then the angle of pressure transmission, θ, can be determined as follows:

$$\text{Sin } 2\theta = S_c/S_{uc}, \quad \theta = \text{Arc Sin } S_c/S_{uc}$$

This method theoretically is sound, however, it is not reliable, as the soil in its natural state is confined while the sample used in the unconfined compression test is not confined.

The passive pressure is $P_v = P_h \text{ Cot}^2 \theta + \frac{2S_c}{\text{Sin } 2\theta}$

The shearing resistance on a horizontal or vertical plane or direct shear, is the shearing resistance due to cohesion, S_c, plus the frictional resistance which is a function of the normal pressure, P_n Tan ϕ.

Weight Transfer

Weight transfer is due to the lateral distribution of weight away from the critical element above the loading plane (see Figure 21). The lateral distribution is due to the vertical shearing resistance along any potential failure surface.(15) The weight transfer due to vertical shearing resistance is limited also by the horizontal shearing resistance on the critical sliding plane.

The weight transfer from Element 1 is transmitted as an additional pressure on Element 2 which is capable of carrying such an additional pressure in proportion to the increased horizontal shear on the sliding plane at depth d. It is this increased resistance to sliding on the horizontal plane which sets the limit of static head which may be transferred and from which the equivalent vertical shearing resistance may be determined.

To derive the rules covering the weight transfer a vertical mass of soil is taken as an example (see Figure 21).

When $h > d$, $S_e \, h / h = S_t \, d / d$

Therefore $S_e = S_t \leq S_h$

When $S_e < S_h$ Reduced Static Head = $wh - S_t$

When $S_e \geq S_h$ Reduced Static Head = $wh - S_h$

When $h < d$, $S_e \, h / d = S_t \, d / d$

Therefore $S_e = S_t \, d / h \leq S_h$

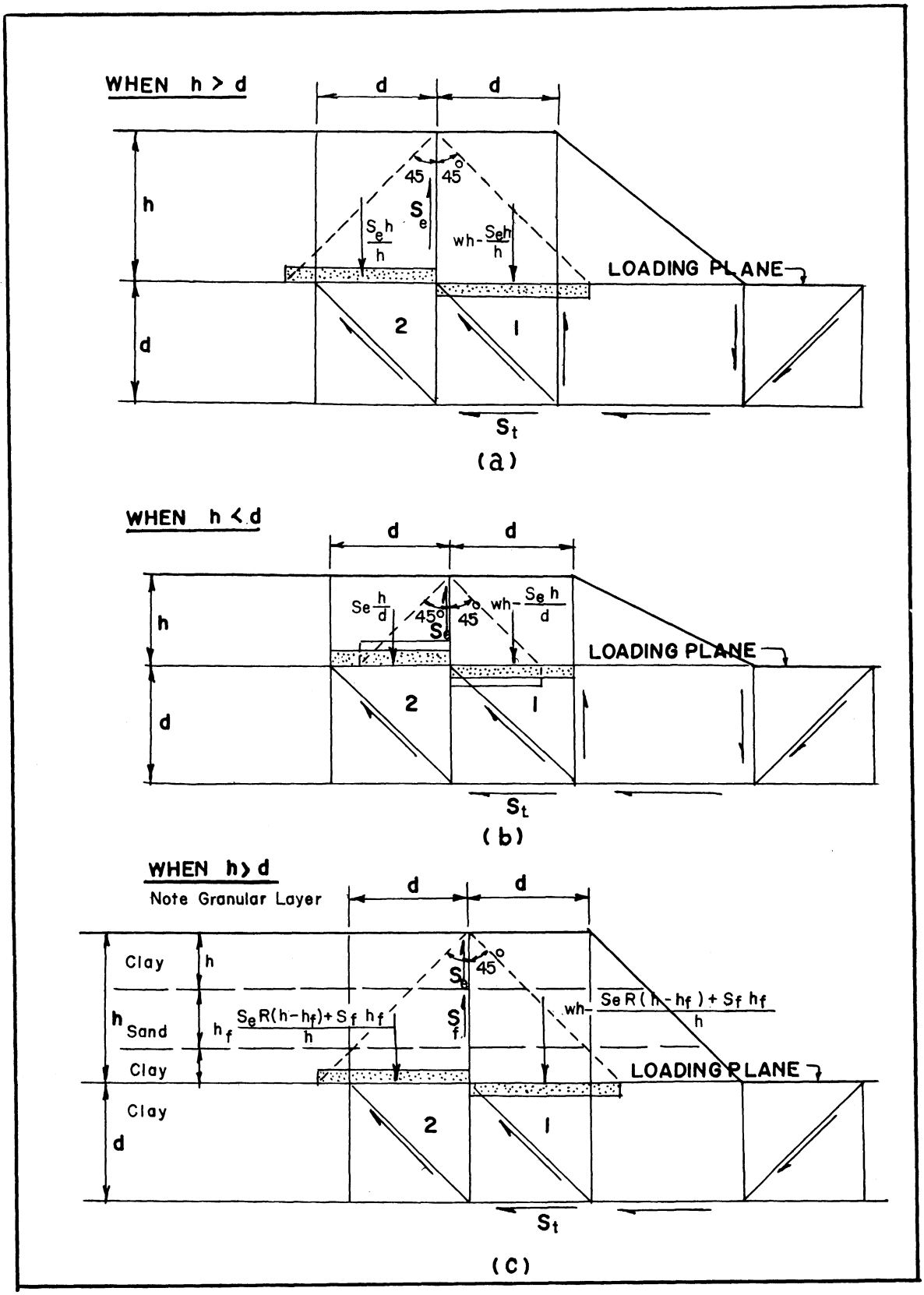

(15)

FIGURE 21. WEIGHT TRANSFER ABOVE THE LOADING PLANE

When $S_e < S_h$ Reduced Static Head = $wh - S_t$

When $S_e \geq S_h$ Reduced Static Head = $wh - S_h(h/d)$

Sometimes a stress distribution must take into consideration a layer of granular material. Figure 21c represents the condition under discussion. The ultimate shearing resistance of the granular material is equal to S_f. And $S_f = P_h \text{ Tan } \phi$; where P_h is the average intergranular lateral pressure and ϕ is the angle of internal friction. The equivalent shear stresses mobilized in the granular layer is S_f' .

$$S_f' = \frac{S_e}{S_h} S_f$$

When $R \leq \frac{S_f}{S_f'}$ Proportionality of shearing resistance in granular layer is valid.

When $R \geq \frac{S_f}{S_f'}$ Shearing resistance in granular layer is constant and equal to S_f .

<u>When $h > d$,</u> and $R > \frac{S_f}{S_f'}$

$$\frac{S_e R(h - h_f) + S_f h_f}{h} = \frac{S_t R d}{d}$$

$$\text{Therefore } S_e R = \frac{S_t R h - S_f h_f}{h - h_f} \leq S_h R$$

Reduced Static Head = $wh - S_t R$

When $S_e < S_h$ Reduced Static Head = $wh - S_t R$

When $S_e \geq S_h$ Reduced Static Head = $wh - \frac{S_h R (h - h_f) + S_f h_f}{h}$

<u>When $h < d$,</u> and $R > \frac{S_f}{S_f'}$

$$\frac{S_e\ R(h - h_f) + S_f\ h_f}{d} = \frac{S_t\ R\ d}{d}$$

$$S_e\ R = \frac{S_t\ R\ d - S_f\ h_f}{h - h_f} \leq S_h\ R$$

Reduced Static Head = $wh - S_t\ R$

When $S_e < S_h$ Reduced Static Head = $wh - S_t\ R$

When $S_e \geq S_h$ Reduced Static Head = $wh - \frac{S_h R(h - h_f) + S_f h_f}{d}$

CHAPTER III

DESIGN AND STABILITY ANALYSIS OF CELLULAR COFFERDAMS

Based on the theories and concepts of soil mechanics presented in the previous chapter, derivations of designing and checking formulas will be presented in this chapter. These formulas will be used in the analysis of the cofferdam which is to be tested.

To simplify this problem the various shapes of cells may be substituted by a rectangular cell of an equivalent width. The cofferdam is then analyzed, first according to the type of soil material used as fill in the cell and then according to the type of foundation it is resting on. This way, any particular cofferdam with any particular type of fill, resting on any type of foundation can be analyzed.

Types of Cells of Cellular Cofferdams

Cellular cofferdams are of various types depending on the shape of the cell. The shapes of the cells have been developed from rectangular shapes to the circular under the influence of desiring to obtain equal tension in the interlock and having the cells independent, in order that a failure in one cell will not be carried on to the other cells. This fact is concluded as the result of study through the literature on cofferdams which is listed in Bibliography B. Thus cofferdams can be classified according to the shape of their cells as follows:

1. The rectangular cellular cofferdam, where the cofferdam is made of straight front row of sheet-piles and a straight

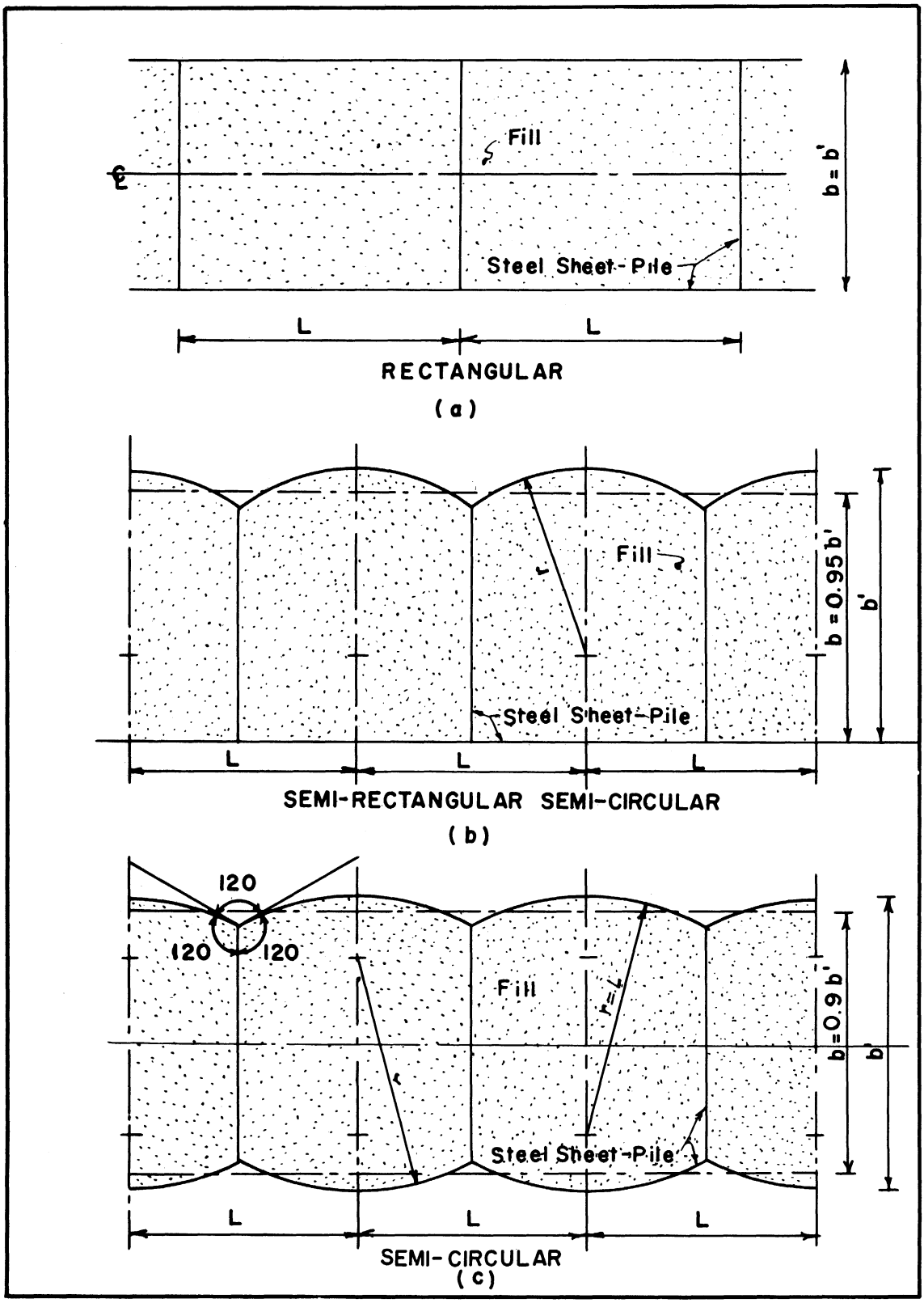

FIGURE 22. TYPES OF CELLS OF CELLULAR COFFERDAMS

back row of sheet-piles with straight diaphragms connecting. This type was one of the early types of cellular cofferdams (see Figure 22a). The first cofferdam of this type is the one built at Black Rock Harbor, Buffalo. It was built to allow the construction of a ship lock. The sides of the cofferdam were made of two walls of steel sheet-piling, the space between the two walls being divided into pockets thirty feet square by diaphragms of the same type of piling as that used in the main walls.(31) Another example of this type of cofferdam is the Breakwater and Sea Wall at Waukegan, Michigan. In this cofferdam the diaphragms were spaced further than the width of the cofferdam. The cells were rectangular in shape.(2)

2. The semi-rectangular semi-circular type of cofferdam, which is the same as the rectangular except that the row of sheet-piles in the front is made of arcs of constant radius between the diaphragms (see Figure 22b). An example of this type of cofferdam is the cellular cofferdam which was used as a foundation and cut-off wall for Dam No. 7, Allegheny River. The front side of the cells was used as a cofferdam. The steel sheet-piling was left in place as part of the permanent structure.(2)

3. The semi-circular cellular cofferdam with straight diaphragm (diaphragm type), where the cofferdam is made of circular arcs with diaphragms connecting them, the radius of the arcs is equal to the length of the cell, thus tending to obtain the

same amount of tension in sheet-pile interlock (see Figure 22c). The radius of the arc is usually made equal to the distance between diaphragms, in which case the interlock tensions in the arcs and cross walls are equal. An example of this type of cofferdam is that used along the east side of the Hudson River in New York City to construct the land section of three large piers, for the city of New York. The length of each typical cell was fifty feet while the radius of the arc diaphragm was forty-six feet.(32) Another example of this type of cofferdam is that used in the construction of a ship pier at the foot of West Forty-sixth Street, New York. The length of the cell was 24 feet and the arc diaphragm was 24 feet in radius also.(1)

4. The semi-circular cofferdam with arc diaphragms, which is the same as the diaphragm type except for the fact that the diaphragms are arcs. This shape gives the cells more independence in case of failure of any one cell (see Figure 23a). An example of this type is the cofferdam used as a Breakwater at Inland Steel Company, Indiana Harbor, Indiana. A full description of this cofferdam will follow. Another example is the cofferdam built across the entrance of MacArthur and Poe Locks, Sault Ste. Marie, Michigan. This cofferdam was made of five cells. The two at the ends were made of circular cells with a radius of 42.5 feet. The other three cells were the semi-circular with arc diaphragms. The radius of the inner and the outer walls was 48.5 feet. The radius of the arc diaphragm was 42.5 feet.(26)

5. The circular cofferdam, where the cells are made of full circular cells connected to each other by short arcs. In this type the cells are very much independent of each other and the tension in the interlock is carried on uniformly (see Figure 23b). An example of this type of cofferdam is the first circular cellular cofferdam which was built in the harbor of Havana, Cuba, for raising the battleship Maine.(30) Another example of this type is the cellular cofferdam used for the Kensico Reservoir, New York. This cofferdam consisted of thirteen circular cells of fifty feet radius connected with short arcs of ten feet radius.(26)

6. The cloverleaf type, where the cells are made of four arcs connected by two cross diaphragms. This one is used whenever the size of the cell is large and extra stability is needed for sheet pile enclosure (see Figure 23c). An example of this type of cofferdam is the cofferdam designed for Kentucky Dam of the TVA. This type of cells is usually used at the end of the cofferdam where extra stability is needed.(1)

If the actual width of the cofferdam is b', then the equivalent width which is to be used for design purposes is b, where b is a certain ratio of b'. This ratio is based on an equivalent area of a rectangular cell to the area of the actual cell.

In Figures 22 and 23 these ratios are shown for the various types of cells according to the standard dimensions used in practice.

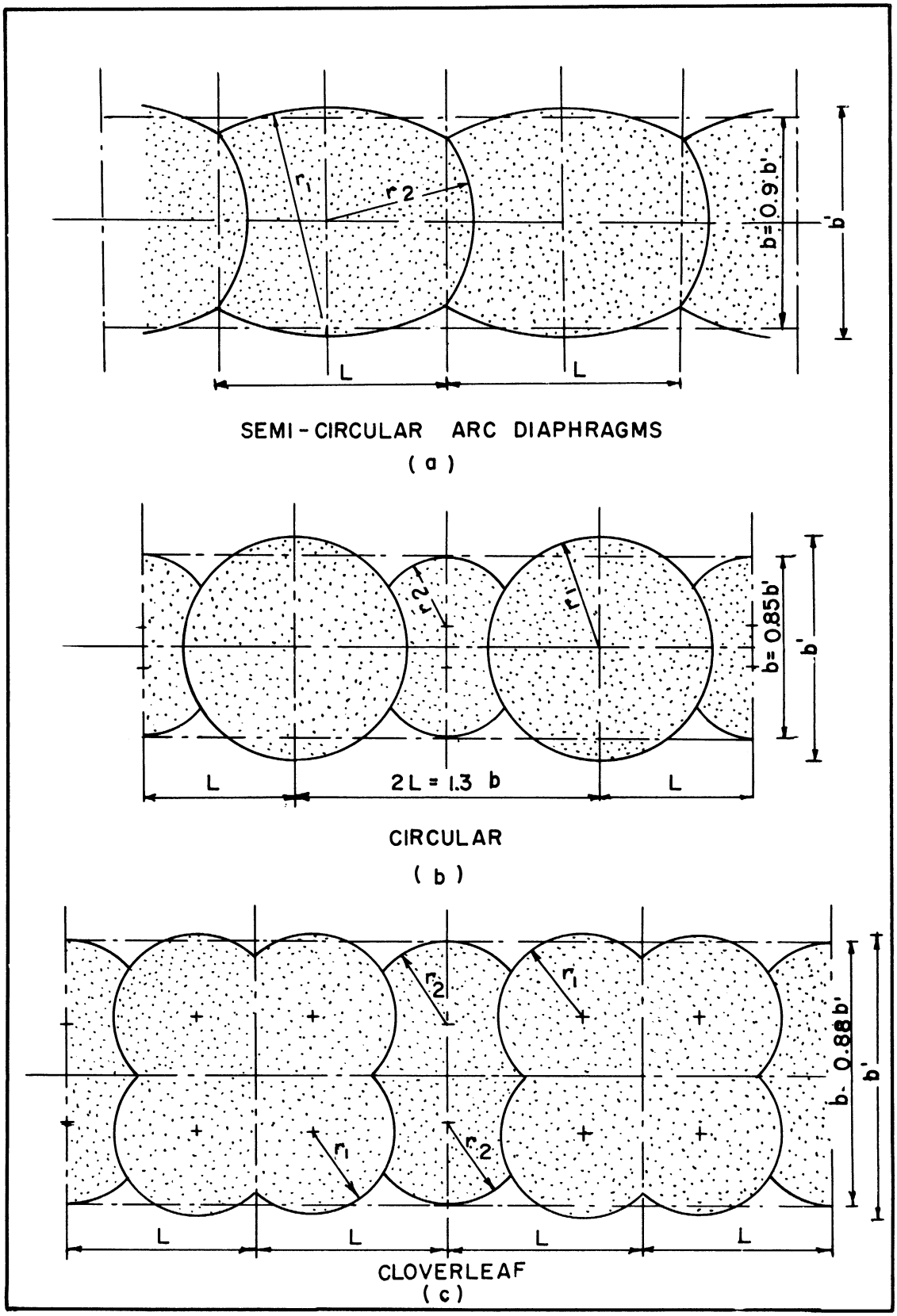

FIGURE 23 .TYPES OF CELLS OF CELLULAR COFFERDAMS

Causes of Failure

From past experience in cellular cofferdam construction and the result of study, the cellular cofferdam may fail by bursting of the cell, by overturning, by sliding on its base, by shearing along its vertical plane, by local failure of the soil underneath the cofferdam or by loss of mass stability of the soil mass which provides stability to the cofferdam and its foundation. The following is a discussion of each of these.

Tension in Interlocks and Bursting of the Cells

Bursting of the cell is due to failure of interlocks. The interlocks may fail because of faulty construction when the sheet-piles are driven. This happens usually during the driving process or immediately after placing the fill material in the cell. Another reason for failure of the interlocks is exceeding the allowable stresses for the interlock. These stresses are due to the tension in the cell which is in turn due to either the lateral pressure of the submerged fill in the cell or to the lateral pressure applied on the cell. The lateral pressure is retained by the cofferdam and transmitted to the lower strata. This lateral thrust will be transmitted through the fill of the cell to the front wall of the cell where there is no resistance, above the bottom, except that of the sheet-pile. The resistance of the sheet-pile is not very great, thus the sheet-pile will yield, and accordingly a stress will be developed at the diaphragm, throwing the thrust back to the back wall which, in turn, will carry the thrust back to the lower strata.

Overturning

Usually the cofferdam is subject to unbalanced lateral forces acting at different heights. These unbalanced forces will tend to produce a resultant moment which tends to overturn the cofferdam. Failure may occur due to this reason whenever the static moment of the acting lateral forces on the cofferdam exceeds that of the resisting forces. This factor is very important in high cofferdams; it becomes more critical the higher the cofferdam.

Sliding

The cofferdam may slide on its base due to the unbalanced lateral forces acting on each side of the cofferdam whenever the shearing stress at the base exceeds the shearing resistance. This cause of failure is more critical in clay soil than in other types of soils. The active forces acting on one side of the cofferdam will be resisted by the passive forces on the other side and the excess would be transmitted to the foundation of the cofferdam through the base providing the cofferdam is strong enough in other aspects. Thus this sliding stress is developed in the base of the cofferdam.

Shearing Along the Vertical Plane

Cellular cofferdams may fail due to the shearing stress along the vertical plane which passes through the neutral axis of the base (see Figure 26). This shearing stress is due to the bending moment resulting from the unbalanced lateral pressure. This shearing stress will be resisted by the combined resistance of the fill and the frictional resistance in the interlock at the plane of failure.

For this reason whenever the shearing stress exceeds the resistance of these two factors the cofferdam will fail.

Local Failure of the Soil Underneath the Cofferdam

This is due to overstressing the soil mass laying underneath the cofferdam because of the weight of the cofferdam and the stress variation due to the applied overturning moment. In other words, the bearing capacity of the soil mass is inadequate underneath the cofferdam.

The Mass Movement of the Soil Mass Providing Stability to the Cofferdam and Its Foundation

The problem of mass stability of soil is of great importance in soil investigation. Whenever a soil mass is subjected to loading and a progressive settlement is taking place, it implies that the clay mass is overstressed. The mass stability is a major factor when designing large excavations, embankments, footings and mass storage areas.

Whenever a cofferdam is to be investigated this problem should be given consideration. In case of shore cofferdams in which a great thrust is to be resisted and transmitted to the lower strata, this problem may become a controlling factor.

The cellular cofferdam and its foundation as one unit may fail. This type of failure is concerned with the overall stability of the cofferdam where the whole mass of soil is providing and contributing to the strength of the cofferdam and to its foundation. The entire mass of soil surrounding the cofferdam must be stable in order for the cofferdam to be stable.

In investigating the literature published on cofferdams the writer has not found evidence of consideration of this cause of failure. One of the objectives of the present study is to investigate this problem.

Design and Analysis of Cellular Cofferdams Considering the Fills

The fill in the cells of the cellular cofferdams acts as a stabilizing material. Thus the strength of the cofferdam is dependent on the fill material to a certain extent. Several important factors determine the mechanical behavior of the fill. These factors are the type of the soil material used in filling the cell, the process by which the fill is placed and consolidated in the cell and the saturation line in the fill. The consolidation depends on the actual field practice used in filling the cell and it could not be limited by any set of rules. Therefore the only definite aid is knowing what type of soil is to be used for the fill and the characteristics and properties of this soil. When the cell is filled, but before allowing the various forces acting on the cofferdam to be developed, an undisturbed sample of the fill may furnish further data in determining the full strength of the cofferdam for loading.

Soil material used as fill can be of three types, cohesive soils such as clay, granular soils such as sand and gravel, or a mixture of these soils. To know the type of fill used in any cofferdam, the fill properties must be determined. The type of soil will be determined as explained in Chapter II. Therefore the fill in the cells will be studied

according to these types of fills. From the viewpoint of soil mechanics, the granular fill is the most suitable and trouble free. The saturation line is also the lowest. However from the point of view of boils and piping it is not as suitable. Cells filled with clay will have insignificant seepage and therefore the saturation line will be high. Thus the clay makes a poor fill.

Cells Filled With Clay Fill

Sliding: The lateral pressure which tends to cause the cofferdam to slide is the resultant of the active pressures on both sides. The lateral pressures are determined by formulas given in Chapter II, see Page 46 for determining the lateral pressures. This resultant force must be carried through the base of the cofferdam by the resisting force which has the value of ($b\ LRS_c$), where S_c is the shearing resistance at the base of the cofferdam at the plane of loading, L is one unit length and b is the equivalent width of the cofferdam. The value of S_c is independent of the normal pressure. R is the overload ratio. For zero rate of displacement R = 1. Therefore, when R = 1, as a design formula

$$b = \frac{F_H\ (\text{Active}) - F_{h_1}(\text{Passive})}{S_c} .$$

As a checking formula, introducing R in the equation above

$$F_H\ (\text{Active}) - F_{h_1}(\text{Active}) - b\ S_c\ R = 0$$

and then solving for R, which is the overload ratio in the clay soil.

If the soil strata on either side of the cofferdam have cohesion, the overload ratio, R, will be present in some of the terms of the applied forces.

If the obtained overload ratio, R, is greater than one, then the passive pressure on the resisting side must be considered, because the shear at the base is fully developed. Thus the passive pressure on the resisting side will be developed.

This factor, sliding at the base, does not have a direct relationship with the depth of penetration. However the depth of penetration could be chosen to meet a stratum where the value of the shearing resistance is higher, for design purposes.

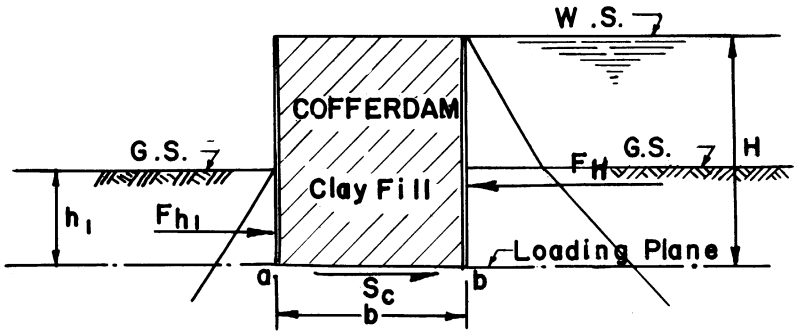

Figure 24. Sliding at the Base, Clay Fill

Tension in Interlock and Bursting of the Cells: Two cases are to be considered when investigating the tension in the interlocks. The first case is during construction of the cell and filling it, before the unbalanced lateral forces are applied on the cofferdam. This case could be the only case when the cofferdam under investigation is used as breakwater. The tension in the interlock is due to the lateral pressure of the submerged fill inside the cell (see Figure 25a). The lateral pressure inside the cell is $P_h = w_s h - 2S_c$ where w_s is the submerged weight of the clay fill per cubic foot and S_c is the shearing resistance of the clay fill.

The total force in the fill per foot,

$$F_h = 1/2\ (w_s H - 2S_c)(H - \frac{2S_c}{w_s})$$

The total force in the interlock is

$$T\ H = 1/2\ L\ (w_s H - 2S_c)(H - \frac{2S_c}{w_s})$$

$$L = 2\ T\ H\ /\ (w_s H - 2S_c)(H - \frac{2S_c}{w_s}) \quad \text{(see Figure 25a)}$$

If T is taken in pounds per inch as given in the various steel sheet-pile manuals:

$$L = \frac{12\ T}{1/2\ w_s H - 2S_c + (2\ S_c^2/\ w_s H)}$$

L obtained from this equation is the maximum spacing of the diaphragm without exceeding the maximum allowable interlock tension. The basic assumption made here is that the tension is equal along the entire interlock. This assumption is an approximation made to simplify the problem.

As a checking formula:

$$T = \frac{L}{12}\ (1/2\ w_s H - 2S_c\ R + \frac{2S_c^2\ R^2}{w_s\ H})$$

The allowable tension in the interlock is given by various steel sheet-pile manufacturers. It is usually given in pounds per inch of the interlock.

The second case to be investigated is when the lateral pressures are applied on the cofferdam. This case is critical with shore cofferdams because shore cofferdams are usually subjected to greater lateral thrust than cofferdams built in water for the purpose of retaining it.

The active lateral pressure applied on the back wall of the cofferdam will be transmitted through the fill to the front wall. A portion of this thrust will be resisted by the lateral pressure which is acting on the outer face of the front wall. It is then the function of the diaphragms to carry the excess lateral pressure by interlock tension from the front wall to the back wall and deliver it to lower strata at the base of the cofferdam (see Figure 25b). The active lateral pressure applied on the back of the cofferdam as well as the active lateral pressure applied on the front of the cofferdam are determined according to types of soil strata and the effect of surcharge by the formulas for determining the lateral pressures given in Chapter II. The lateral pressure which is to be transmitted through the fill must not be greater than the passive lateral pressure of the soil mass inside the cell.

If the net lateral pressure per foot run is designated as F'', then the total force on one diaphragm will be $F'' L$. This force will be carried by a diaphragm over a length of the interlock equal to b Tan θ at the bottom, where θ is the angle of pressure transmission in the fill soil. This is based on the fact that the resistance of the back wall is obtained from the resistance to sliding at the base of the cofferdam. This resisting force is providing the support for the sheet-pile, and therefore the tension in the interlock due to the lateral pressures is equal to $F'' \frac{L}{b \text{ Tan } \theta}$ where F'' is the net unbalanced force acting on the outer wall of the cofferdam.

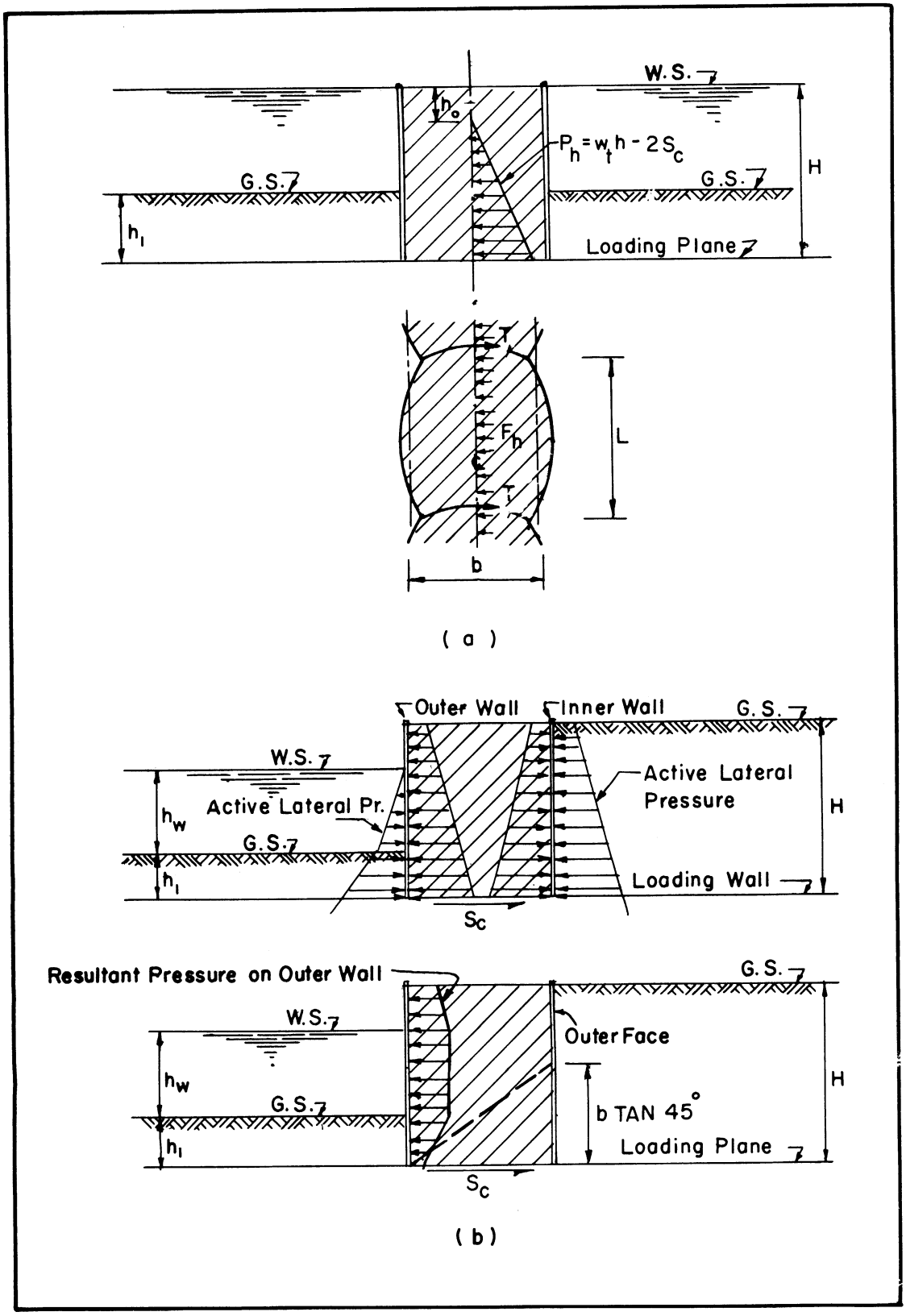

FIGURE 25. TENSION IN INTERLOCK CLAY FILL

If a stratum of relatively higher strength is at the bottom of the cofferdam and the sheet-piles have been driven to a depth d' into this stratum, then the length of the interlock which will carry the tension will be equal to the depth d'.

Shear on the Vertical Plane y-y: The shearing stress inside the fill on section y-y must be investigated (see Figure 26). The resultant overturning moment will be designated as M_a. M_a is the resultant moment of the active lateral pressures on both sides of the cofferdam above the loading plane per foot run. The moments are taken about the neutral axis at the base of the cofferdam.

This applied moment will be resisted by two factors. A part of it will be resisted by the cofferdam by transmitting the stresses to the base of the cofferdam at the loading plane and this is designated as M_{a1}. The other portion of the applied moment will be resisted above the loading plane due to the lateral distribution caused by the shearing forces at the outer faces of the cofferdam and this portion of the moment is designated as M_{a2}.

A plane x-x will be considered at the bottom of the cofferdam at an infinitesimal distance below the sheet-pile as shown by Figure 26. The stress at that plane will be discussed. The moment resisted at the base of the cofferdam causes an approximate parabolic stress distribution at plane x-x as shown in Figure 26a. This stress distribution will cause a shear stress in the section with maximum value at the neutral axis of the section, thus the soil is acting as shear transmitting medium. This shear at the neutral axis is all along the vertical plane.

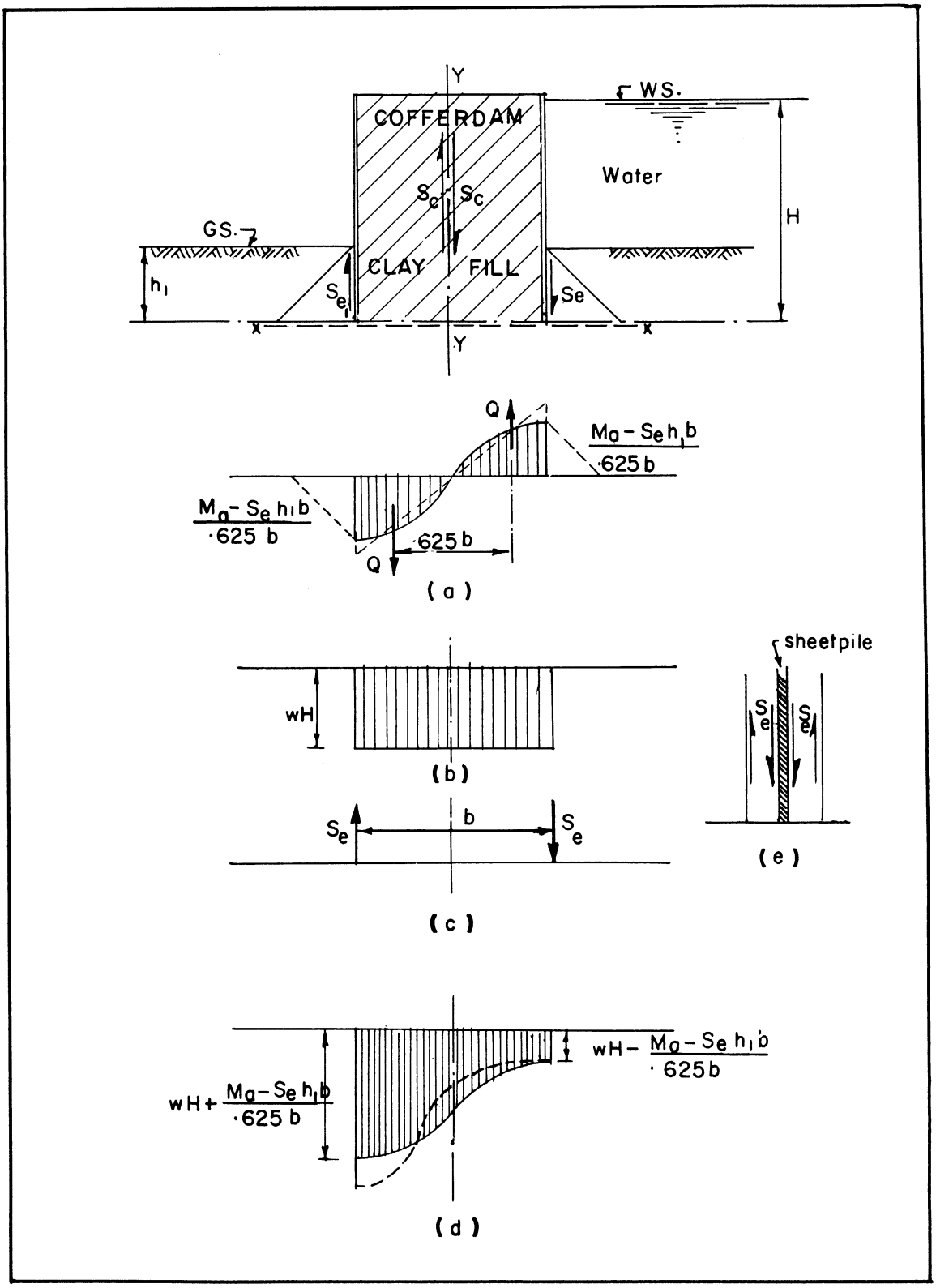

FIGURE 26. SHEAR ALONG VERTICAL PLANE Y-Y
CLAY FILL

The weight of the cofferdam causes a stress distribution as shown in Figure 26b. The shearing forces at the outer face of the cofferdam will be represented by two equal forces having a moment arm equal to b/2, the width of the cofferdam, acting about the assumed neutral axis at the center line of the section. The difference in the values of these two vertical shear forces is compensated for by varying the stress distribution of the soil resistance due to bending, thus not violating the laws of static equilibrium. However, when calculating, either the minimum shear must be used in both sides or the stress distribution must be modified to satisfy equilibrium. The first assumption is to be used and it remains on the safe side. The value of the shear S_e will be equal to the average shearing resistance of the soil or the frictional stress between the soil and the sheet-pile, whichever is smaller. The stress diagram due to M_{a1} and the stress diagram due to the weight of the cofferdam add to the stress diagram shown in Figure 26d. In this diagram it is shown that the soil is under compression, and tension does not develop. When designing a cofferdam this condition must be satisfied if there are no shearing forces available on the outer faces of the cofferdam.

The moment M_{a1} is the portion of the moment which causes the vertical shear and it is computed as follows:

$$M_a = M_{a1} + M_{a2}$$

$$M_{a1} = \frac{5}{8} Q\, b$$ where Q is the undetermined force causing the vertical shear.

$M_{a2} = \frac{b}{2}(S_{e1} h_1 + S_e h)$ where S_{e1} is the equivalent vertical shearing resistance on the dredged side and S_e is equivalent vertical shearing resistance on the back side.

$S_e h$ is greater than the developed shear force on the other side $S_{e1} h_1$, therefore $S_{e1} h_1$ is to be used instead of $S_e h$, therefore

$$M_{a2} = b(S_{e1} h_1)$$

$$M_a = b S_{e1} h_1 + \frac{5}{8} Q B$$

$$Q = \frac{8}{5b}(M_a - b S_{e1} h_1)$$

The force along the width of one cell will be QL, therefore

$$QL = 1.6 \frac{L}{b}(M_a - b S_{e1} h_1).$$

This force has to be resisted by the vertical shearing resistance in the cell and is equal to

$$Q_f L = S_c R H L + c T H$$

where T is the tension stress in the interlock as determined previously and c is the coefficient of friction for the sheet-pile interlock which is given by various steel sheet-pile manufacturers.

Cells Filled with Sand Fill

Sliding: The resultant lateral pressure acting against the cofferdam per unit length will be transmitted to the foundation through the base at the plane of loading. The shearing resistance at the sliding surface is a frictional resistance depending on the normal pressure at the surface of sliding. The total sliding resistance per foot

run is:

$$S_f\ b = b\ P_n\ \text{Tan}\ \phi$$

$$P_n = P_v = w_t\ H$$

$$S_f\ b = b\ w_t\ H\ \text{Tan}\ \phi\ .$$

When overturning moment is applied the normal stress distribution will vary, however the total will stay the same. Assuming a factor of safty, $G_s = 1$, and an overload ratio of 1 then:

$$F_H\ (\text{active}) - F_{h1}\ (\text{passive}) = b\ w_t\ H\ \text{Tan}\ \phi$$

$$b = \frac{F_H\ (\text{active}) - F_{h1}\ (\text{passive})}{w_t\ H\ \text{Tan}\ \phi}$$

As a checking formula:

$$G_s = \frac{w_t\ b\ H\ \text{Tan}\ \phi}{F_H\ (\text{active}) - F_{h1}\ (\text{active})}$$

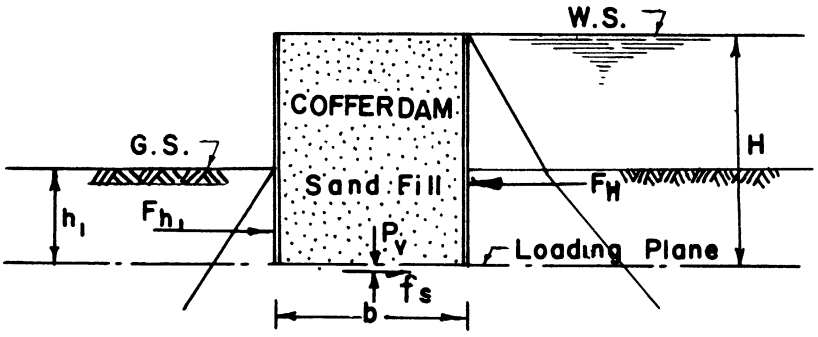

Figure 27. Sliding at the Base, Sand Fill

If the factor of safety is less than one, then the passive lateral pressure on the resisting side must be considered, because the shearing

resistance at the base of the cofferdam is fully mobilized thus the passive lateral pressure on the resisting side is developed.

Tension in Interlocks and Bursting of the Cell: The first case to be investigated is during the construction of the cell, before the unbalanced lateral forces are applied. The lateral pressure of the fill inside the cell is:

$$P_h = w_s \, H \, \mathrm{Tan}^2\theta$$

Total force in the fill per foot run = $1/2 \, w_s \, H^2 \, \mathrm{Tan}^2\theta$, where θ is the angle of pressure transmission, w_s is the submerged weight of sand per cubic feet. Total force which can be carried across the vertical interlock of the steel sheet-pile is:

$$T \, H = 1/2 \, L \, w_s \, H^2 \, \mathrm{Tan}^2 \, \theta$$

where T is the tension in the interlock, and

$$T = 1/2 \, L \, w_s \, H \, \mathrm{Tan}^2 \, \theta \, .$$

The maximum diaphragm spacing without exceeding the maximum allowable interlock tension is:

$$L = \frac{12 \, T}{1/2 \, w_s \, H \, \mathrm{Tan}^2 \, \theta}$$

where T is given in pounds per inch of the interlock.

As in the previous solution an assumption is made that the tension stress in the interlock is equal along the entire height of the interlock.

The second case to be investigated is when the lateral pressures are applied on the cofferdam. The tension in the interlock is determined as discussed previously in the case of cells filled with clay. The

tension in the interlock due to the lateral pressures is equal to $F'' \frac{L}{b \text{ Tan } \theta}$, where F'' is the net unbalanced force acting on the front wall of the cofferdam and θ is the angle of pressure transmission in the sand. If a stratum of relatively higher strength is at the bottom of the cofferdam and the sheet-piles have been driven to a depth d' into this stratum, then the length of the interlock which will carry the tension will be equal to the depth d' (see Figure 28b).

Shear on the Vertical Plane y-y: The applied moment on the cofferdam is M_a, which is discussed on Page 69, and it will be resisted in the same manner as described there. The force causing the vertical shear is:

$Q\ L = 1.6 \frac{L}{b} (M_a - b\ S_{el}\ h_1)$ where S_{el} is the equivalent vertical shearing resistance above the loading plane on the outer face, and h_1 is the height from the loading plane to the ground surface on the outer side of the cofferdam.

The resisting force in the vertical plane of failure y-y is the frictional shearing resistance in the fill plus the frictional force in the interlock of the diaphragm, and these are equal to:

$Q_f\ L = 1/2\ w_t\ H^2\ \text{Tan}^2\ \theta\ L\ \text{Tan}\ \phi + c\ T\ H$ where T is the tension stress in the interlock as determined previously and c is the coefficient of friction for the sheet-pile interlock which is given by various steel sheet-pile manufacturers.

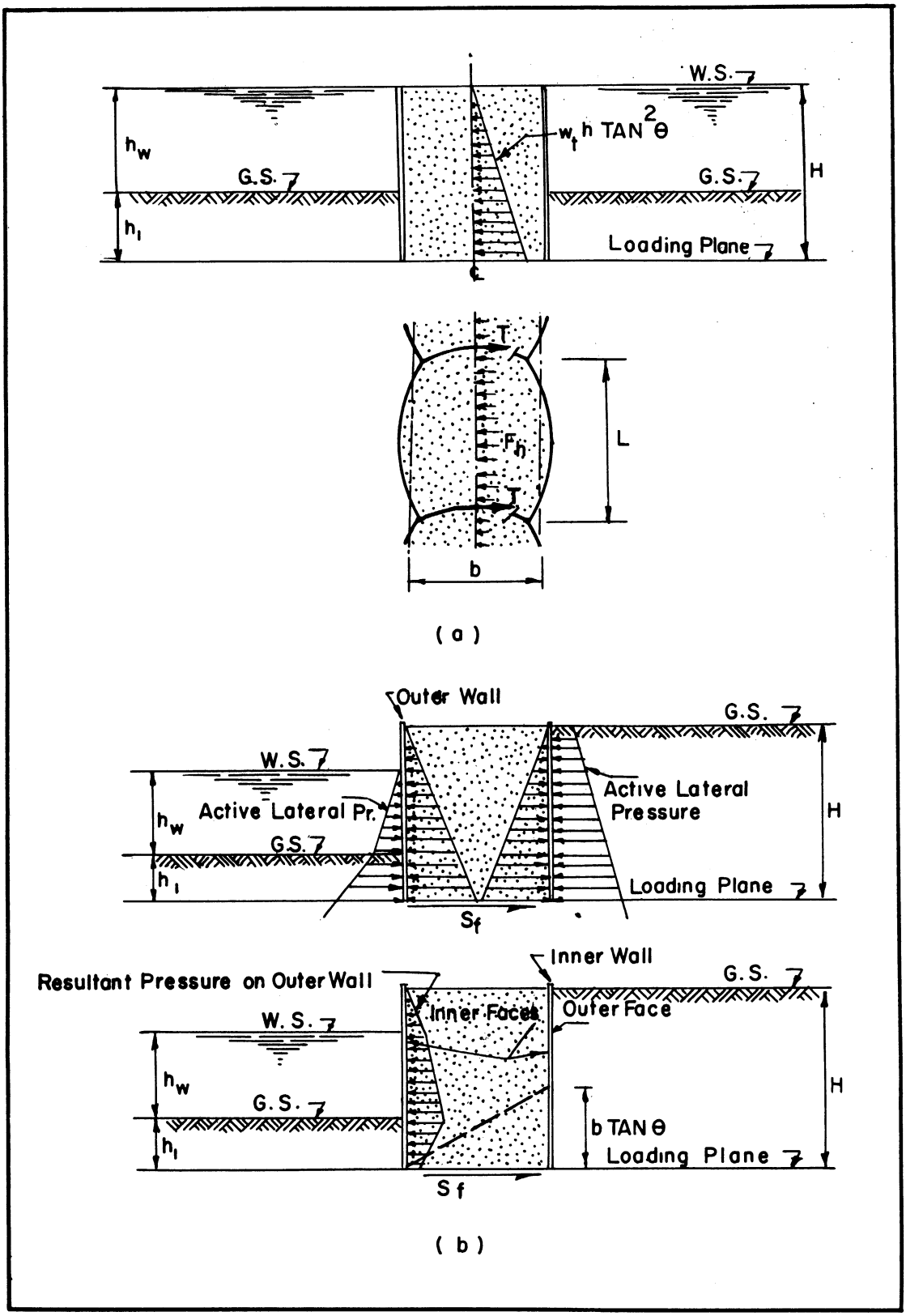

FIGURE 28. TENSION IN INTERLOCK GRANULAR FILL

Cells Filled with Mixed Granular and Cohesive Soils

Sliding: The lateral pressure which tends to cause the cofferdam to slide is the resultant of the active pressures on both sides. The lateral pressures are determined by formulas given in Chapter II, see page 46 for determining the lateral pressures. This resultant force must be transmitted to the foundation by the resisting force at the base of the cofferdam. This resisting force is the combination of the shearing resistance due to cohesion and the shearing resistance due to internal friction. Therefore for mixed soils it is necessary to determine the shearing resistance due to cohesion, S_c, and the angle of internal friction, ϕ.

Therefore the width of the cofferdam is determined by the formula

$$b = \frac{F_H \text{ (active)} - F_{hl} \text{ (passive)}}{b\ (S_c + w_t\ H\ \text{Tan}\ \phi)} \quad .$$

In the above equation, for a zero rate of displacement, the overload ratio, R, is taken as one.

As a checking formula, introducing R in the equation above, we get:

$$F_H \text{ (active)} - F_{hl} \text{ (active)} - b\ (S_c R + w_t H\ \text{Tan}\ \phi) = 0$$

If the soil strata on either side of the cofferdam have cohesion, R will be present in some of the terms of the applied forces.

If the obtained overload ratio, R, is greater than one, then the passive pressure on the resisting side must be considered, because the shear at the base is fully developed. Thus the passive pressure on the resisting side will be developed.

Tension in the Interlocks and Bursting of the Cell: Here again two cases are to be investigated. The first case is during the construction, before the unbalanced lateral forces are applied on the cofferdam. The lateral pressure of the fill inside the cell is:

$$P_h = (w_s h - \frac{2S_c}{\text{Sin } 2\theta}) \text{ Tan}^2 \theta .$$

The total lateral force in the fill per foot run equals

$$1/2 \ (w_s H - \frac{2S_c}{w_s \text{ Sin } 2\theta}) \ (H - \frac{2S_c}{w_s \text{ Sin } 2\theta}) \text{ Tan}^2 \theta .$$

The total force in the interlock is:

$$T = \frac{L}{12} [1/2 \ w_s H - \frac{2S_c}{\text{Sin } 2\theta} + (\frac{2S_c 2}{w_s H \text{ Sin}^2 2\theta})] \text{Tan}^2 \theta \text{ where}$$

T is the tension in the interlock in pounds per inch and L is the diaphragm spacing.

The maximum diaphragm spacing without exceeding the allowable tension in the interlock is:

$$L = \frac{12 \ T}{[1/2 \ w_s H - \frac{2S_c}{\text{Sin } 2\theta} + (2S_c^2 \ / \ w_s H \text{ Sin}^2 2C)] \text{Tan}^2 \theta}$$

The basic assumption made here is that the tension is equal along the entire length of the interlock. This assumption is an approximation made to simplify the problem.

The second case to be investigated is when the lateral pressures are applied on the cofferdam. The lateral thrust applied on the cofferdam is the same as given previously when cells with clay fill were discussed. The resultant force on the outer wall of sheet-pile will be F", which will be transmitted to the back wall over a length of b Tan θ;

therefore the tension in the interlock due to the lateral pressure is:

$T = F'' \frac{L}{b \text{ Tan } \theta}$ where F'' is the net unbalanced lateral force acting on the front wall of the cofferdam.

Shear on the Vertical Plane y-y: The force causing the shear on the vertical plane y-y is the same as given previously when cells filled with clay were discussed. It is equal to:

$$QL = 1.6 \frac{L}{b} (M_a - S_{el} h_1) .$$

The resisting force on the vertical plane of failure y-y is:

$$Q_f L = S_c H L + 1/2 w_t H^2 L \text{ Tan}^2\theta \text{ Tan } \phi + c T H$$

where T is the tension stress in the interlock as determined previously and c is the coefficient of friction for the sheet-pile interlock which is given by various steel sheet-pile manufacturers.

Design and Analysis of Cellular Cofferdams on Various Foundations

Cellular cofferdams are built on foundations of either rock, sand, clay or strata of sand and clay. The foundation of a cellular cofferdam is an important factor and the soil mass sustaining it has a great effect on the cofferdam's behavior, as the strength of the cofferdam is a function of the strength and rigidity of the soil sustaining it. A foundation which does not react rigidly will allow displacements which in turn will allow excess stresses to be developed in the cofferdam. This point is well substantiated by the fact that there is no case of failure of a cellular cofferdam built on a rock foundation.(28) On the other hand there are many failures of cofferdams on foundations other than rock.

the shearing resistances on the outer faces of the cells will be developed. Thus the resisting moment due to the stress distribution at the base of the cofferdam could be neglected.

Past experience, as revealed by the literature on cellular cofferdams, has indicated that most failures have been in sandy soils where boils were formed and the sand lost its stability, which caused the cofferdams to overturn. Examples of this type of failure are two cofferdams on the Mississippi River[26] and the cofferdam in Grand Coulee.[3]

There have also been difficulties with cofferdams built on a clay foundation. Examples of such cofferdams are the cofferdam for raising the battleship Maine and the cofferdam for the Jones-Laughlin ore yard. In the case of the cofferdam for raising the battleship Maine, the cofferdam served its purpose, however, there was a progressive displacement of the clay beneath the base of the cofferdam and an inward tilt of the cofferdam which necessitated that the stability of the structure be increased by adding an inner berm. During the last stage of excavation and pumping it was necessary to brace the cofferdam against the ship to provide lateral support for the cofferdam.[30] The cofferdam for the Jones-Laughlin ore yard suffered an unanticipated progressive settlement. Such a settlement defeats the purpose for which this type of cofferdam is built.

The cofferdam used for the field test in this investigation is also built on a plastic clay foundation. Although the problem of a cofferdam on a clay foundation is of especial interest in this study, all types of foundation are discussed in order to cover the subject thoroughly.

Cellular Cofferdams on Rock

Cellular cofferdams built on rock foundations must be designed to stand the three causes of failure mentioned in discussing the fill in the cell. Another cause of failure to be considered is the lack of stability of the cofferdam to resist overturning.

The forces causing the cofferdam to overturn are the unbalanced lateral pressures applied on the cofferdam. The resistance to this overturning moment is provided by the weight of the cofferdam and the shearing forces acting against the outer faces of the sheet-pile enclosure.

The resisting moment due to the stress distribution at the base of the cofferdam is neglected for two reasons. The first reason is that the resisting moment of the stress distribution at the base of the cofferdam decreases as the cofferdam's tendency to overturn increases. This is because when the cofferdam tends to overturn the stress ordinate of the stress distribution at the heel decreases, approaching the value zero, which is the tension stress in the soil. The greater the tendency of the cofferdam to overturn, the closer the stress concentration will be to the toe, thus minimizing the resisting moment (about the toe) of the stress distribution at the base. The second reason is that the magnitude of the resisting moment due to the shearing resistance at the outer faces of the cells is much greater than the resisting moment of the stress distribution at the base. When the cofferdam tends to overturn the shearing resistances on the outer faces of the cells will be developed. Thus the resisting moment due to the stress distribution at the base of the cofferdam could be neglected.

Therefore the criterion of failure due to overturning is when the applied moment on the cofferdam exceeds the resisting moment.

The lateral pressures are determined as shown in Chapter II. The lateral forces at each stratum are calculated as well as the moment arm about the toe of the cofferdam, point O (see Figure 29a). The applied moment is calculated, as is the resisting moment. The weight of the cofferdam contributes to the resisting moment with the value

$$w\ H\ \frac{b^2}{2}$$

Therefore the applied moment is the moment of the lateral forces on the active side of the cofferdam, and the resisting moment is the moment of the lateral forces on the resisting side plus the resisting moment due to the weight of the cofferdam. If the applied moment is greater than the resisting moment then there will be a tendency for the cofferdam to overturn developing the shearing resistance along the back of the cofferdam. This additional resisting moment will be equal to $S_a\ b$, where S_a is the average shearing resistance developed on the outer face of the back wall (see Figure 29a).

In order for the cofferdam to act as one unit the weight of the confined fill must not exceed the shearing force between the confined fill and the steel shell.

In the previous discussion it is assumed that the steel shell of the cellular cofferdam and the enclosed soil are considered to act as a unit.

If this assumption is to be abandoned then another approach could be used to investigate the overturning of the cellular cofferdam,

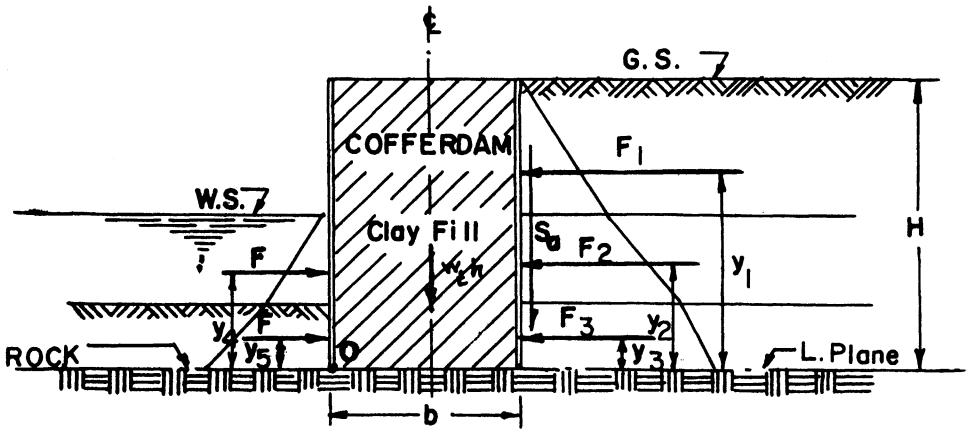

(a)*

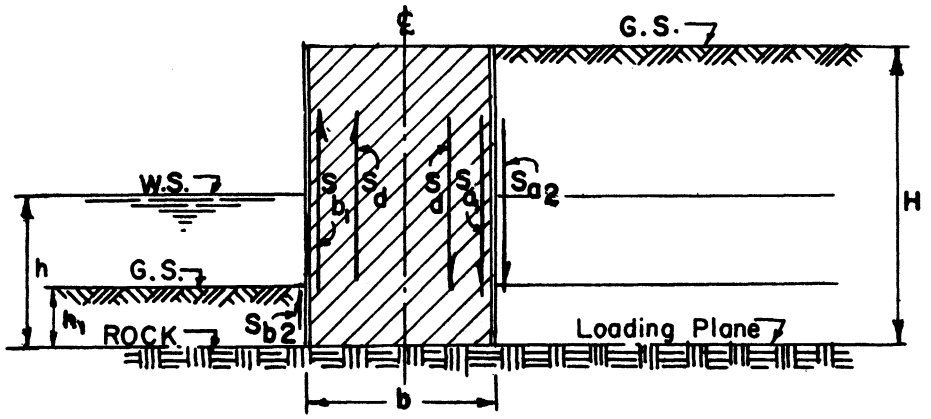

(b)

---

* Applied Moment = $F_1 y_1 + F_2 y_2 + F_3 y_3$

Resisting Moment = $F_4 y_4 + F_5 y_5 + w_t H.b.\frac{b}{2}$ OR,

$= F_4 y_4 + F_5 y_5 + w_t H \cdot b \cdot \frac{b}{2} + S_a \cdot b H$ When S_a is developed

FIGURE 29. OVERTURNING MOMENT OF CELLULAR COFFERDAM ON ROCK FOUNDATIONS

assuming the steel shell of the cellular cofferdam acts as a free body. In this case the overturning moment is resisted by the moment of the active lateral pressure on the resisting side, plus the resisting moment of the shearing forces at the faces of the sheet-pile enclosure (see Figure 29b).

The frictional shearing resistance at the outer face of the back wall of the cofferdam is S_{a2} which is the average frictional shearing resistance between the outer face of the sheet-pile and the soil mass. The shearing resistance at the inner face of the back wall is S_{a1} which is the average frictional shearing resistance between the inner face of the sheet-pile and the soil mass of the fill. The lateral pressure in the fill equals the active lateral pressure on the outer face of the back wall, but it does not exceed the available passive pressure in the fill. The frictional shearing resistance at this face will not be fully developed. This is assumed in order to justify the static equation $\Sigma V = 0$ on the sheet-pile enclosure. The frictional shearing resistance at the inner face of the front wall is S_{b1} which is the average shearing resistance between the soil mass of the fill and the sheet-pile. The frictional shearing resistance at the outer face of the front wall is S_{b2} which is the average shearing resistance between the sheet-pile and the mass of soil in the resisting side, the front side, of the cofferdam. The average frictional shearing resistance at the diaphragms is S_d. Assuming the frictional shearing resistance varies over one half the width of the diaphragm from zero at the center to the maximum at the ends, then:

$S_d H = 1/2\ S_m \frac{H}{2} \frac{2}{L} b$ where S_m is the maximum frictional

shearing resistance at the ends of the diaphragm. The amount of S'_{a1} which will be developed is:

$$S'_{a1} = S_{a2} + S_d - S_d - S_{b1} - S_{b2} \frac{h_1}{H} , \Sigma V = 0$$

The resisting moment is therefore equal to:

$$M_r = F_4Y_4 + F_5Y_5 + \frac{bH}{2} (S_{a2} + S'_{a1} + S_{b1} + \frac{h_1}{H} S_{b2} + \frac{4}{3} S_d)$$

while the applied moment is equal to:

$$M_a = F_1Y_1 + F_2Y_2 + F_3Y_3 .$$

Cellular Cofferdams on Sand

Granular soil such as sand provides a stable foundation as far as strength is concerned. Its great weakness lies in loss of stability due to piping. The percolating water through the sand may form boils. When boils are formed the sandy soil becomes quicksand, which is an unstable soil. Experience with cofferdams indicates that the major problem in designing a cofferdam on a sandy soil is piping and the problem of stability due to strength is of secondary importance. The problem of piping is covered very well in the text on cofferdams by White and Prentis.(26)

The following paragraphs are a brief review on the mechanics of boil formation and its prevention.

The basic principles of flow through soils are the only satisfactory approach in determining the laws governing the nature of flow through soils. Darcy's law of flow of water through porous media is that the rate of flow varies directly with the hydraulic gradient and

with a coefficient of permeability.

$v = k \frac{h}{\ell}$ where v is the velocity of flow, $\frac{h}{\ell} = i$ is the hydraulic gradient, and k is a coefficient of permeability.

Taking a prismatic element of a mass of sand with a volume, V, and a length, ℓ, the percolated water through the sand in the direction of ℓ will have a head loss equal to h. This loss of head reduces the pressure per unit area by $w_w h$. This causes an unbalanced force

$F_s = w_w \frac{h}{\ell} = i\, w_w$ per unit of area and unit of length (see Figure 30a). When the water flows in an upward direction this unbalanced force will be in an opposite direction to that of gravity. When this force, F_s, is equal to or greater than the submerged weight of the sand, w_s, then the sand becomes a quicksand because the resultant of the hydrostatic pressures counterbalances the force of gravity, and the sand behaves like a liquid

$$F_s = i_1 w_w = w_s \; ; \quad \text{therefore} \quad i_1 = \frac{w_s}{w_w} \quad .$$

In order to investigate the formation of boils it is necessary to study the flow of water through the subsoil of the cofferdam. Figure 30b shows the flow lines. They are drawn in such a manner that the quantity of percolating water, v_d, between two flow lines is the same for every pair of flow lines. The spacing, d, between the flow lines indicates the distribution of the seepage force, F_s. The methods of constructing the flow lines have been discussed by White and Prentis.[26]

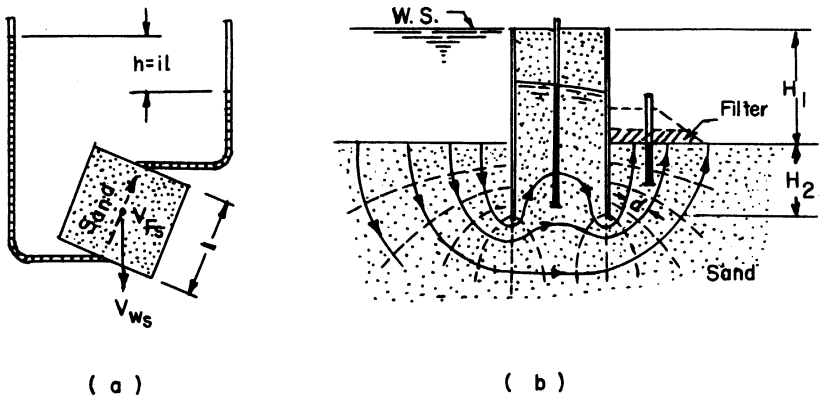

Figure 30. Cellular Cofferdam on Sand, Hydrodynamic of Cofferdam, Flow Lines.(28)

The quantity of water percolating between two adjoining flow lines per unit of the distance between these flow lines is $\frac{v_d}{d}$ which is the velocity of percolation. Therefore, according to Darcy's law

$$\frac{v_d}{d} = k\ i$$

$$F_s = i\ w_w = \frac{v_d}{d}\frac{w_w}{k} = \frac{c}{d} \quad \text{where c is a constant.}$$

The equation above shows that the seepage force, F_s, is inversely proportional to the spacing of the flow lines. The seepage force, F_s, acts at every point in a direction as that of the tangent to the flow line through this point.

To prevent the formation of boils, either an inverted filter should cover the danger zone on the front side or the steel sheet-pile should be driven deeper.

Although the problem of boil formation is of primary importance in designing a cofferdam on granular soil, the three causes of failure mentioned previously where the fill in the cell was discussed must be considered. The following causes of failure should be discussed also:

Overturning: The cofferdam will be subjected to unbalanced lateral pressures. The resulting overturning moment will be resisted in the same manner as mentioned before where cofferdams on rock are discussed. The shearing forces at the sheet-piles will be the frictional forces of the granular soils and these could be calculated on the basis of formulas given in Chapter II for determining the lateral pressures and the frictional shearing resistance of granular soils. This factor is seldom critical as the greater danger in cofferdams on sandy soils lies in the problem of boil formation.

The Local Failure of the Soil Underneath the Cofferdam: The applied load on the foundation of the cofferdam per square foot is $w_t H$, assuming that the cell is well drained.

$$q = 1/3 \; K \; w_t \; r \; \mathrm{Cot}^5\theta + w_t \; h \; \mathrm{Cot}^4\theta \;, \text{ where } r = \frac{b}{2}$$

The first term of the equation is the ultimate bearing capacity developed by arching action. The second term is due to surcharge. The effect of cohesion can be introduced by adding the term $\frac{2S_c}{\mathrm{Sin}\ 2\theta} (1 + \mathrm{Cot}^2\theta)$ into the bearing capacity equation above. The factor of safety will be:

$$G = \frac{1}{w \; H} (1/3 \; K \; w_t \; r \; \mathrm{Cot}^5\theta + w_t \; h \; \mathrm{Cot}^4\theta)$$

Cellular Cofferdams on Clay

Cofferdams built on clay strata present greater problems as far as the mechanics of soil stability is concerned. In addition to the three causes of failure mentioned under fill in the cell, the cofferdam must be adequate to satisfy the following causes of failure.

Overturning: The stability analysis, with respect to overturning, of cellular cofferdams built on clay is the same as given previously where cofferdams built on rock are discussed with the exception that the frictional shearing forces at the faces of the sheet-pile do not exceed the shearing resistance of the clay in which the sheet-pile is embedded.

Local Failure of the Soil Underneath the Cofferdam: The soil underneath the cofferdam must be strong enough to sustain the weight of the cofferdam. In order to determine the bearing capacity of the soil mass underneath the cofferdam it is necessary to investigate the various fashions in which the soil strata may react to the applied pressure. The fashions in which the strata may react depends upon both the depth and the shearing resistance of each stratum.

If a homogeneous soil stratum underneath the cofferdam extends to a depth greater than the width of the cofferdam, then the depth of the failing element will be equal to the width of the cofferdam. To evaluate the bearing capacity at the base of the cofferdam for this case, all the forces and resistances can be combined in a single stability equation. This stability equation can be compared to Bernoulli's equation in hydraulics. The applied load is the static head due to the weight of the cofferdam. The resistances above the loading plane are the static head on the resisting side and the resistance to upheaval due to the shearing resistance above the loading plane. The resistances below the loading plane are the developed pressure, the perimeter shear

and the lateral distribution of the applied load below the loading plane (see Figure 31). Thus the stability equation will be written as:

$$w_t H - w_t h_1 - 4S_c - 2S_c - 2S_e \frac{h_1}{d} - 2S_e \frac{h_1}{d} = 0 \quad .$$

Introducing the overload ratio, R, in each shearing resistance term in the above equation, the checking formula will be

$$R = \frac{w_t H - w_t h_1}{6S_c + 4S_c \frac{h_1}{d}}$$

The overload ratio, R, obtained above, indicates the amount of overload under the loading condition being considered.

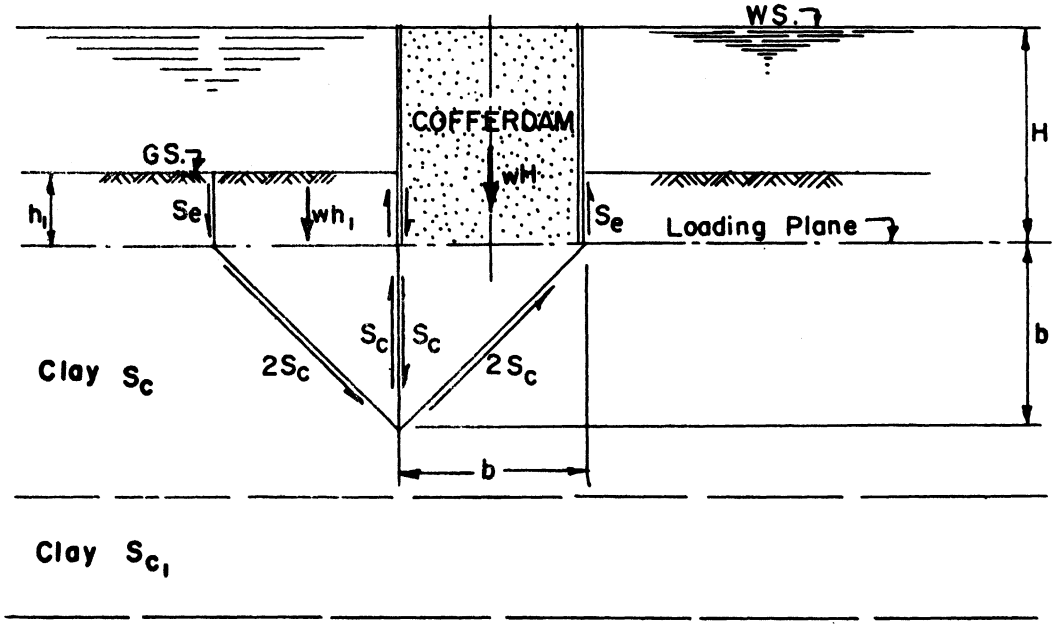

Figure 31. Stability of the Element Underneath the Cofferdam.

If a homogeneous soil stratum underneath the cofferdam extends to a depth less than the width of the cofferdam, then the depth of the failing element will be equal to the depth of the stratum, assuming the shearing resistance of this stratum is less than the shearing resistance of the stratum below it.

If the shearing resistance of the upper stratum is greater than the shearing resistance of the stratum below it, then the depth of the failing element will be equal to the thickness of the soft stratum or to the width of the cofferdam, whichever is smaller. The upper stratum will tend to distribute the load, thus increasing the resistance due to the lateral distribution below the loading plane.

The types of soil stratum given above illustrate the basic principles of analysis for this type of problem. However, it is a matter of judgement in each particular case to see which elements should be investigated. The critical element is the element with the highest overload ratio.

When designing, the previous method enables the designer to design for various rates of settlements, depending upon whether the cofferdam is to be used as a permanent structure or as a temporary structure, by selecting a suitable overload ratio.

The Mass Movement of the Soil Mass Providing Stability to the Cofferdam and Its Foundation: This cause of failure has not been discussed previously in the literature on cofferdams. The expanding uses of cofferdams make it essential to consider this cause of failure.

Shore cofferdams, used frequently in recent years, are an example of the type of cofferdams where this cause of failure is of major concern.

The depth of the failing elements is governed by the depth and strength of the various clay strata. Every natural strata is different from every other and each must be analyzed and judged for itself. Each case will present certain conditions and a number of elements that may fail. It is a matter of judgement in each particular case to see which elements should be checked and which one is the most likely to be the critical element with the highest overload ratio.

To simplify the discussion it is assumed that the cofferdam is resting on a homogeneous clay stratum of a depth, d. Therefore, the failing element has the depth, d, as one possible case to be investigated. The mass stability is evaluated by setting a stability equation in which the applied loads are the surcharge (P_o), the static head (w H), the lateral pressure on the active side which must be transmitted to the underlying mass ($\frac{F_H}{d}$), less some load transfer due to the vertical shear above the loading plane. The resistances above the loading plane are the static head on the other side, the lateral pressure ($\frac{F_h}{d}$), and the resistance to upheaval above the loading plane on the resisting side. The resistances below the loading plane are the developed pressure, the lateral distribution below the loading plane and resistance to horizontal displacement or sliding. Therefore the stability equation is written as:

$$P_o + wH + \frac{F_H}{d} - S_e\frac{H}{d} - (wh_1 + w_w h_w) = 4S_c - 2S_c - S_t \frac{b}{d} - S_{el} \frac{h_1}{d} = 0$$

The overload ratio, R, may be introduced into each shearing resistance term in order to indicate the amount of overload under loading condition.

The term, $S_e \frac{H}{d}$, in this stability equation is the weight transfer to the mass of soil adjacent to the failing element and it is governed by the rules of weight transfer as discussed in Chapter II. In the example shown here it is assumed that the stratum at the bottom has a higher shearing resistance than the one above. Thus the element has the shape shown in Figure 32.

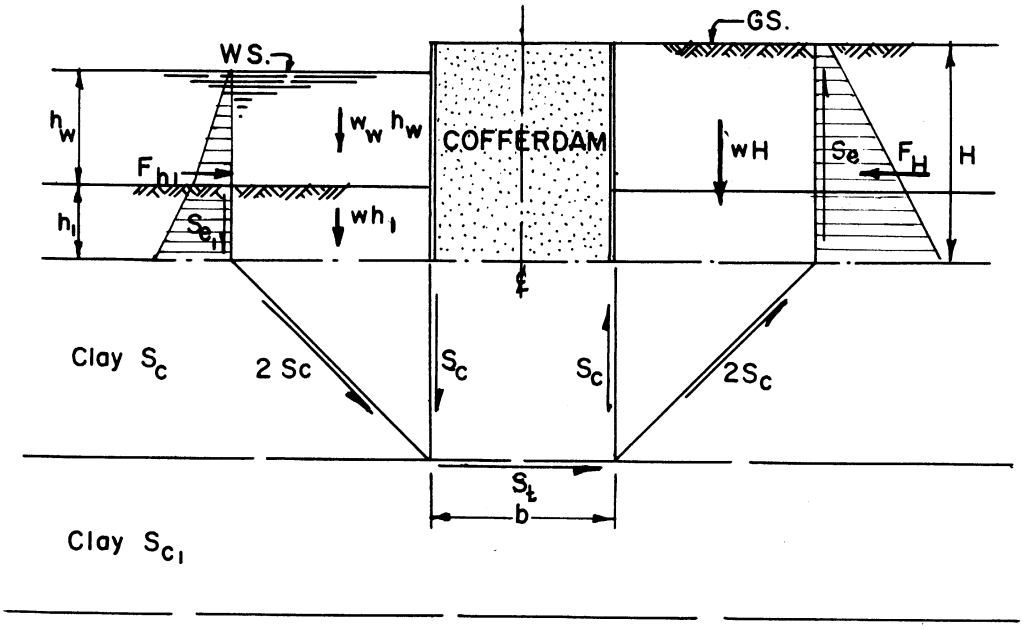

Figure 32. Stability of the Soil Mass Sustaining the Cofferdam.

Cellular Cofferdams on Mixed Strata

Cofferdams built on strata of cohesive and granular material should be treated the same as the previous case, where cofferdams built on clay soils are discussed, with the exception of the evaluation of the shearing resistance of the granular stratum.

There are many practical examples in which a layer of granular material occurs as a part of the natural soil deposits. In such a granular material not having the characteristics of a plastic solid the overload ratio can not be used to express the increase in shearing resistance due to increasing rates of deformation or rate of loading. The shearing resistance in the granular material is a function of the normal pressure and it has a specific limiting value. The effect of such a sand stratum is to be considered on a rational basis. The developed shearing resistance of the sand is assumed to be proportional to the overload ratio in the clay up to the limiting shearing resistance in the sand due to internal friction. If the shearing resistance in the clay stratum times the overload ratio exceeds the internal friction value in the granular soil, the limiting value will control and the shearing resistance in the sand will remain at a constant value.

The soil mass below the loading plane could react in the fashion shown in Figure 33. Therefore the stability equation for equilibrium condition will be set as follows:

$$P_o + wH + \frac{F_H}{d} - \frac{F_h}{d} - (wh_1 + w_w h_w) - 4S_a - 2S_a - S_t \frac{b}{d} - S_{el} \frac{h_1}{d} - S_e \frac{H}{d} = 0$$

where S_a is the average shearing resistance below the loading plane as illustrated in Figure 33.

However, the soil mass below the loading plane could also react in another fashion which is more probable. This depends on the soil strata below the loading plane and the strength of these strata.. Although it is more probable that the sand stratum will contribute to the lateral distribution and the failing element will be below it, this element is here chosen to react in this fashion in order to demonstrate the evaluation of the granular layer as part of the failing element. The various elements must be investigated and the corresponding overload ratios determined. The critical element will be the one with the highest overload ratio.

The other causes of failure which were mentioned in discussing the fill of the soil must also be considered.

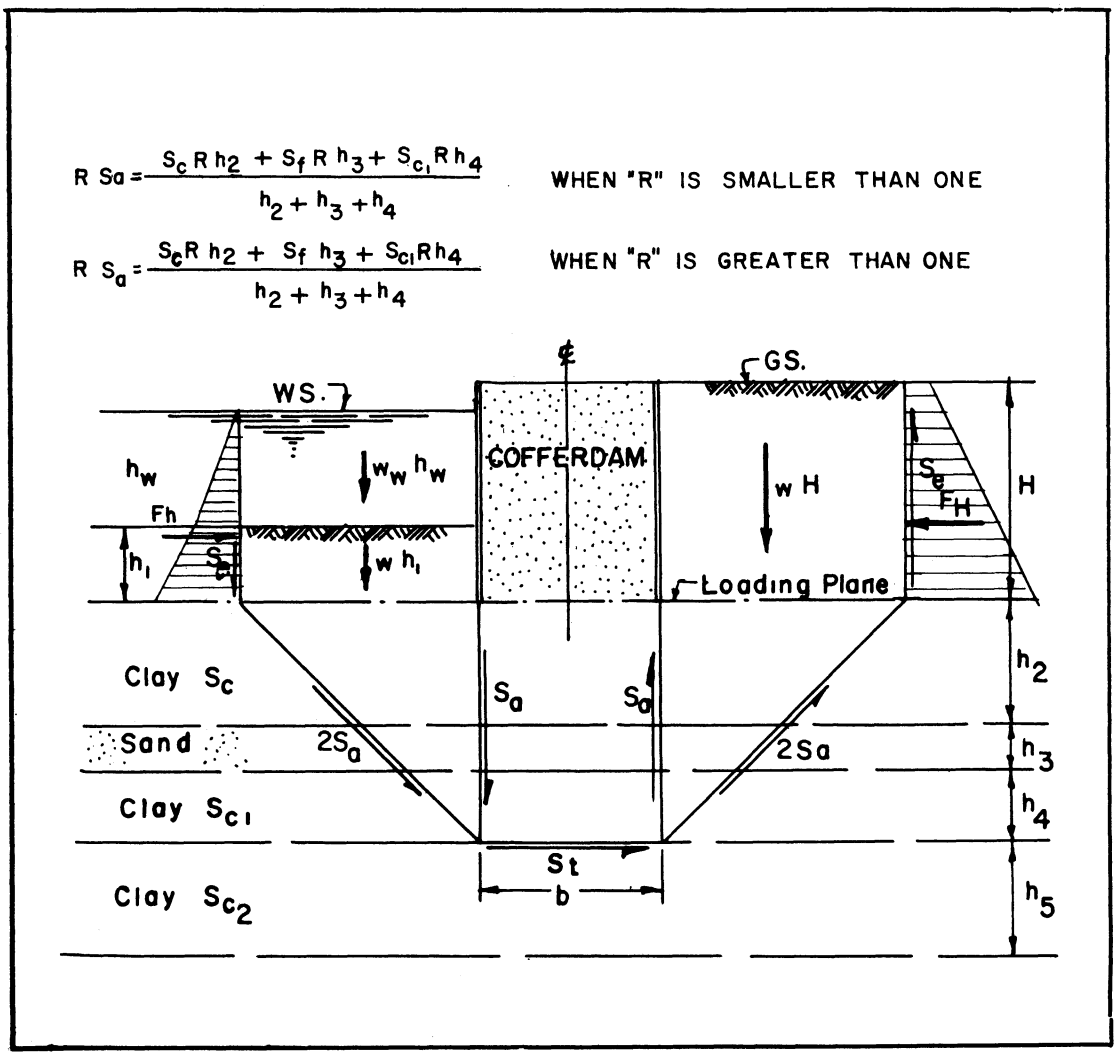

FIGURE 33. STABILITY OF THE SOIL MASS SUSTAINING THE COFFERDAM WHEN A STRATUM OF GRANULAR MATERIAL IS INVOLVED

where S_a is the average shearing resistance below the loading plane as illustrated in Figure 33.

CHAPTER IV

STABILITY ANALYSIS OF CELLULAR COFFERDAM AT INDIANA HARBOR, INDIANA, FOR TESTING

In order to provide experimental corroboration for the theoretical analysis presented in the previous chapter it was necessary to conduct a field test. In order to run this field test it was essential to analyze an existing cofferdam which was made available for testing by Inland Steel Company. In this analysis it was found that the test cofferdam is critical in regard to its stability with respect to mass movement, thus verifying one of the major concepts in this dissertation, the importance of the mass stability of the cofferdam as a critical factor in designing cofferdams and in evaluating cofferdam stability.

This chapter presents a description of the cellular cofferdam and its cells, data on the mass of soil on which this cofferdam is built, and the mathematical analysis for evaluating the cofferdam's stability with respect to mass movement, sliding, overturning, vertical shear and tension in the interlock. Finally, recommendations for testing this cofferdam are given. The recommendations concern the manner in which the cofferdam should be loaded, the area to be loaded, the amounts and stages of loading, and the manner in which the effect of this loading is to be measured.

Description of the Cellular Cofferdam

The cellular cofferdam under investigation is located at the shore of Lake Michigan, on the property of Inland Steel Company, East Chicago, Indiana. This cofferdam was built as part of the Company's

harbor development, about the year 1934. At a later date the land behind the cofferdam was filled, forming a dock. The cofferdam on line "A" consists of 143 cells. The portion of the cofferdam which was tested, is at the west end near the breakwater. For the location plans of the cofferdam and the test area see Figures 34 and 35.

The cells of this cofferdam are the semi-circular type with arc diaphragms. The radius of the outer wall of each cell is 25 feet as is the radius of each cell of the inner wall. The arc diaphragms have a radius of 30 feet except for some cells, built at a later date, which have a radius of 15 feet. The outer row, as well as the inner row, of each cell is made of 23 sheet-piles. The arc diaphragm is made of 11 sheet-piles. The length of each sheet-pile is 41 feet. Figure 36 shows a typical cell and the end cell for this portion of the cofferdam.

Data of Soil Borings and Fill Soil

In order to carry out the analysis for testing this cofferdam it is necessary to present a soil profile for the soil mass on which this cofferdam was built.

Sixteen soil borings were taken by Inland Steel Company for the proposed dock area shown previously in Figure 34. A comparison of the borings indicates that soil conditions within the area covered are quite uniform and the shearing resistance profiles from the sixteen borings can be successfully combined to obtain a composite profile from which average design values may be selected. Since there were no soil borings taken at the test area the composite soil profile of the sixteen borings is assumed to represent the soil profile at the test area, because of the uniformity of the soil strata.

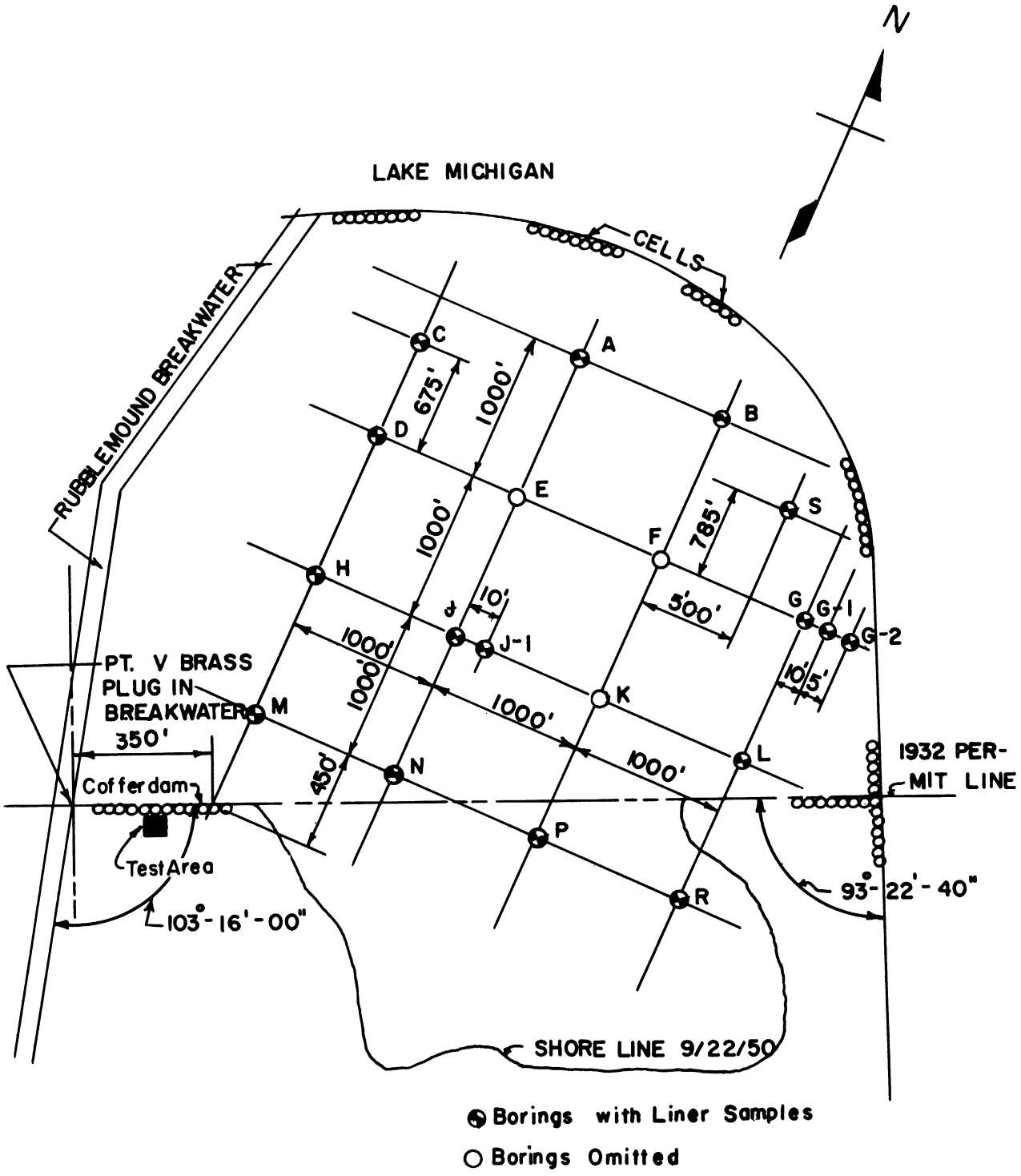

FIGURE 34. BORING LOCATION PLAN

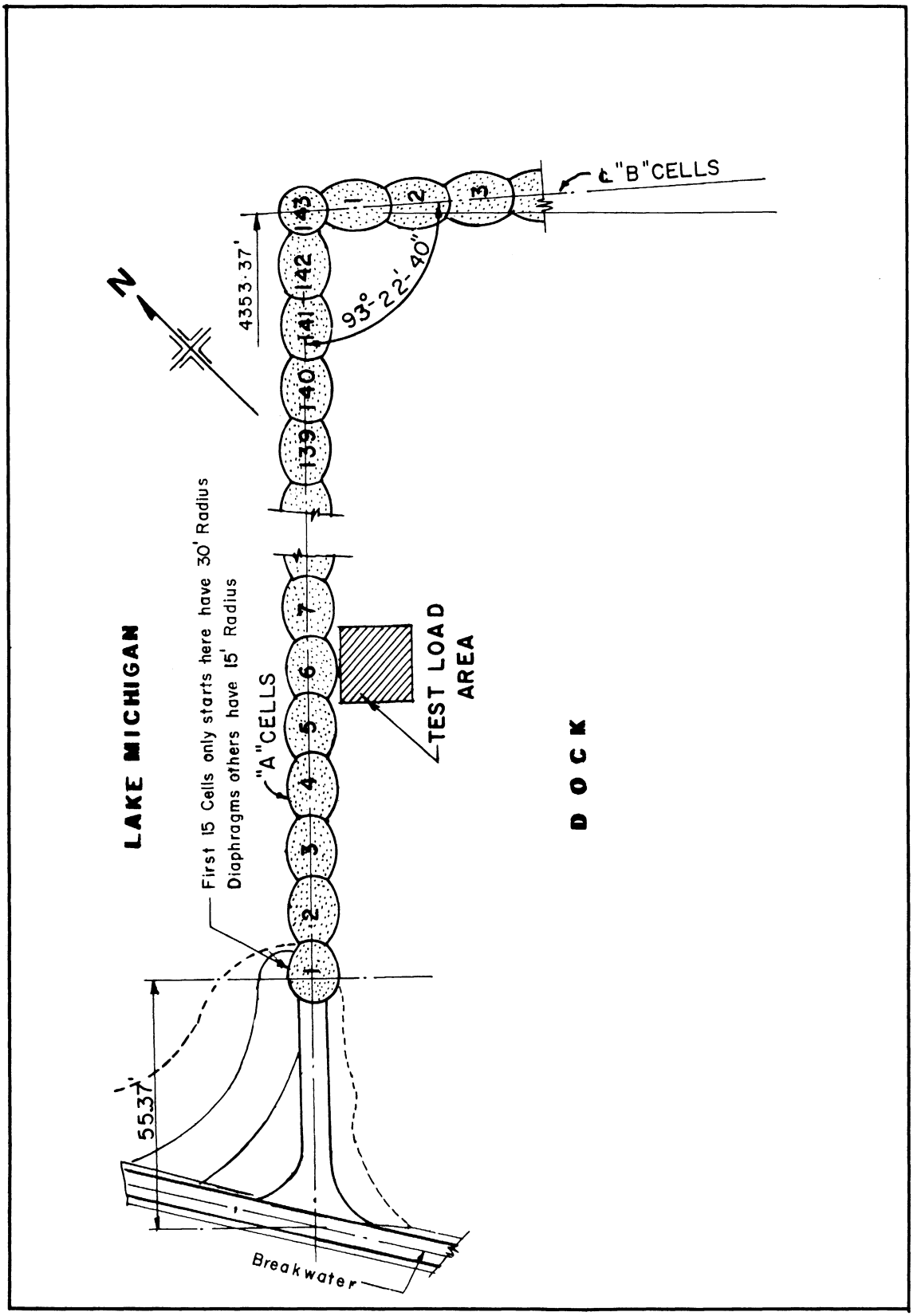

FIGURE 35. LOCATION PLAN OF TEST LOAD AREA

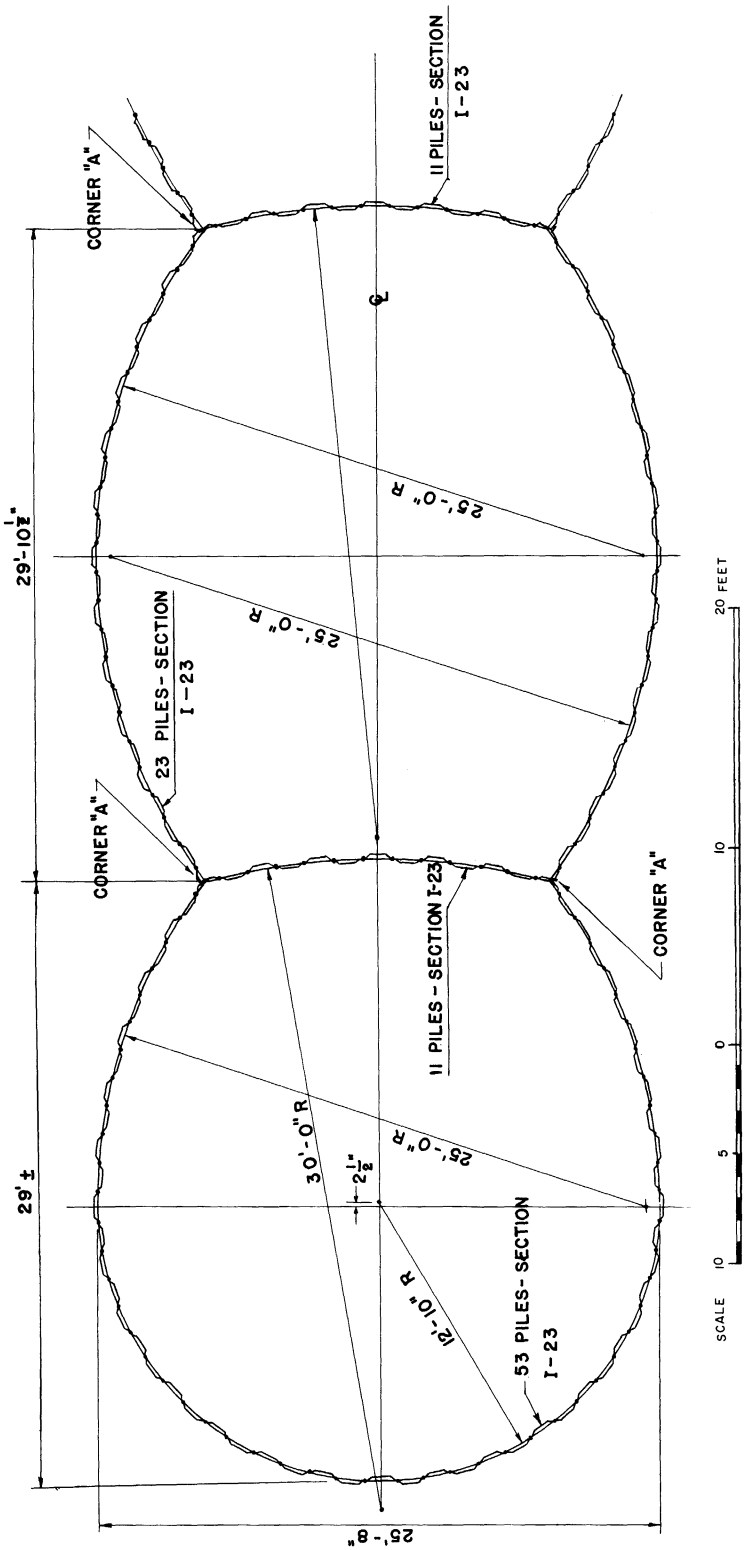

FIGURE 36. DETAILS OF TYPICAL CELL AND THE END CELL

From the sixteen borings, samples were obtained to conduct both types of shear tests, the unconfined compression test and the transverse shear test, in order to determine the shearing resistance of the soil.

The ring shear test is a measure of what may be called the static yield value or shear stress greater than which the soil will suffer progressive deformation. In these tests observations are made of the rate of shearing deformation for each load increment applied. From this may be determined by extrapolation the actual load at which progressive deformation occurs. The final results as shown are thus independent of dynamic resistance and represent that applied stress which may be sustained in static equilibrium.

The shearing resistance, as determined by the unconfined compression test conducted in accordance with generally accepted procedures, has not been corrected for dynamic effects, so the test may be termed a rapid shear test. The load is applied at a continuous rate until failure is produced and in a much shorter period of time (five minute loading period).

The composite shear profile from the transverse shear values and the combined test results are shown in the Composite Subsoil Analysis, Figure 37, and is so designated. The composite shear profile from the equivalent shear values from unconfined compression is shown on the Composite Subsoil Analysis, Figure 38, and is so designated. The average shear values selected are indicated by heavy dashed lines.

Figures 39 and 40 show two borings adjacent to the test load area. For the location of these borings see Figure 34.

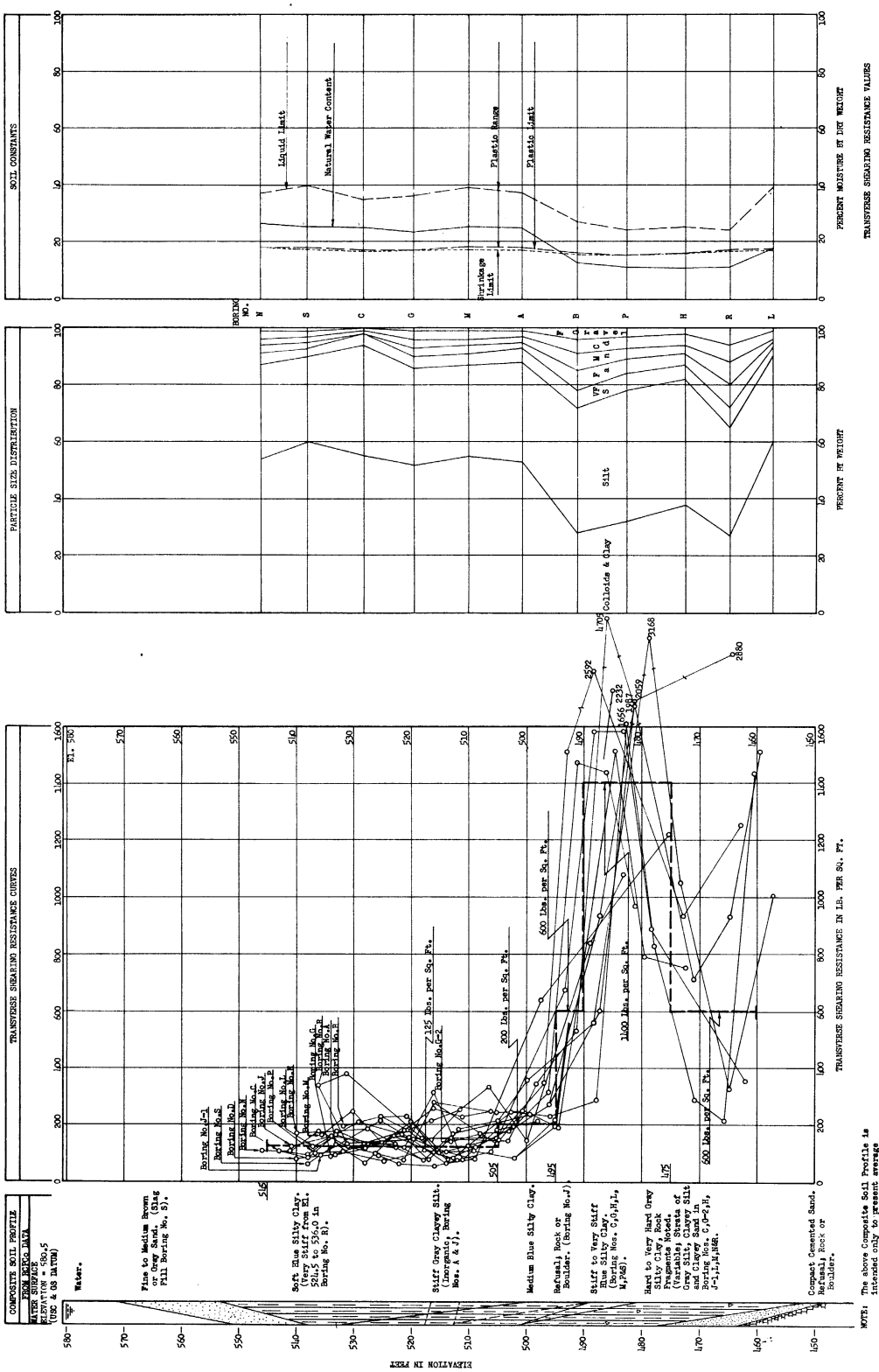

FIGURE 37. COMPOSITE SUBSOIL ANALYSIS OF BORINGS NO. A, B, C, D, G, G-2, H, J, J-1, L, M, N, P, R & S TRANSVERSE SHEARING RESISTANCE VALUES

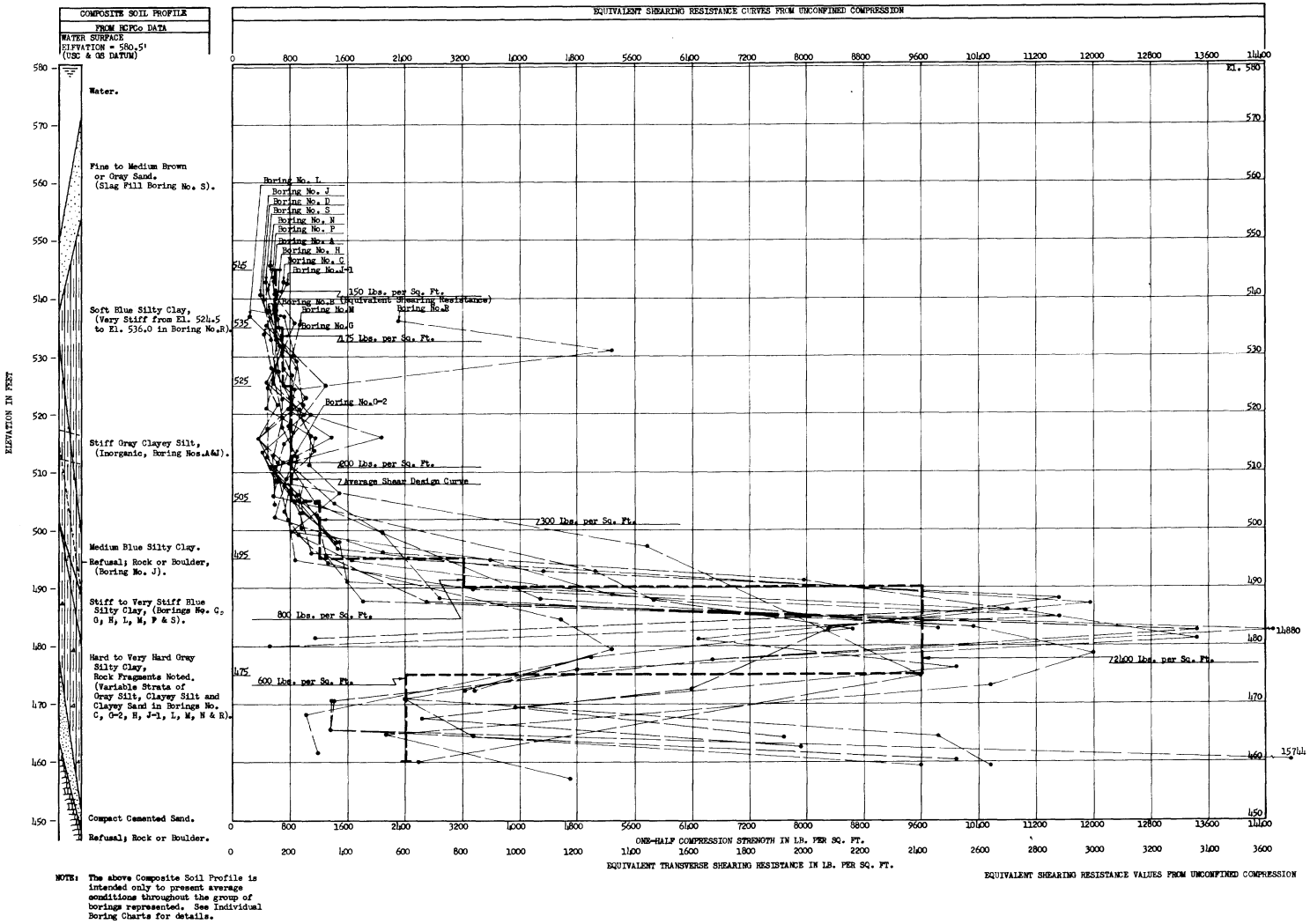

NOTE: The above Composite Soil Profile is intended only to present average conditions throughout the group of borings represented. See Individual Boring Charts for details.

FIGURE 38. COMPOSITE SUBSOIL ANALYSIS OF BORINGS NO. A,B,C,D,G,G-2,N,J,J-1,L,M,N,P,R & S EQUIVALENT S_{uc} VALUES FROM UNCONFINED COMPRESSION

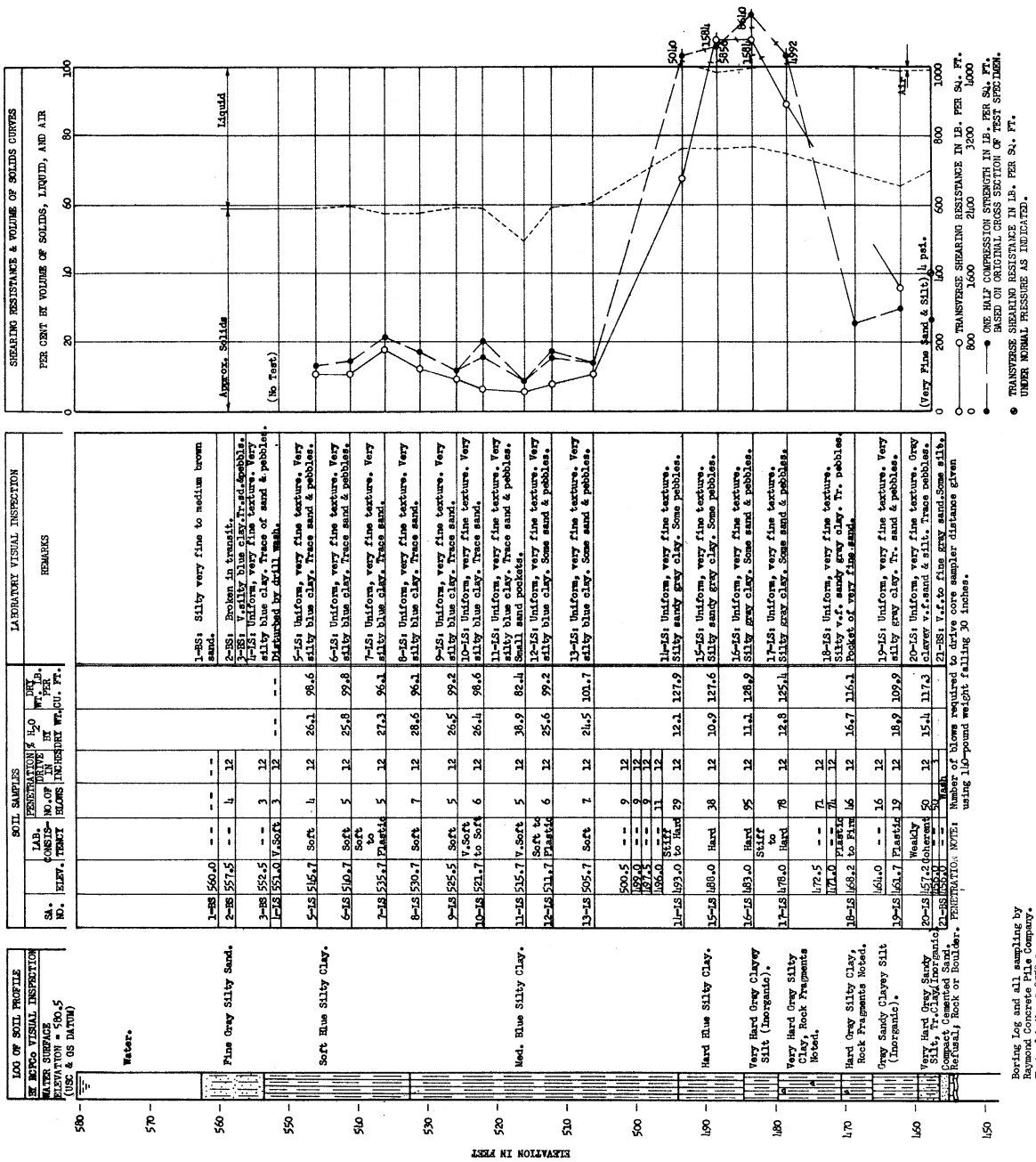

Boring Log and all sampling by Raymond Concrete Pile Company. Their Job No. 1-P-750-C.

FIGURE 39. SUBSOIL ANALYSIS OF BORING NO. N

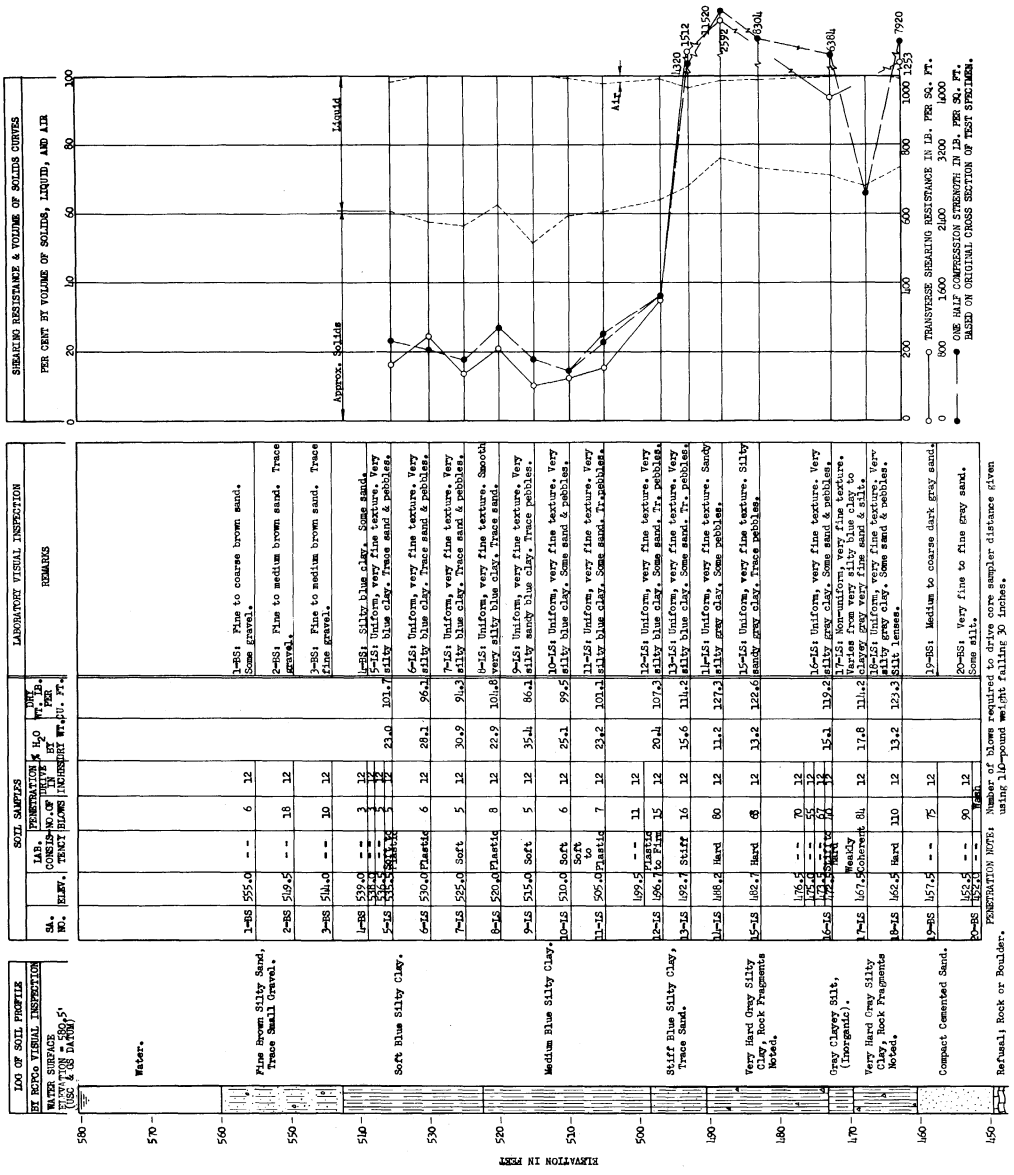

FIGURE 40. SUBSOIL ANALYSIS OF BORING NO. M

A typical soil profile for the test area is concluded from these data and it consists of the top stratum, which is made of a fill material of crushed slag. The properties of the crushed slag are assumed according to past experience with this material in the same locality in other jobs. The properties of the slag are assumed as follows:

Dry Weight (estimated)	= 95 lb./cu.ft.
Wet Weight (5 $\pm$ percent moisture)	= 100 lb./cu.ft.
Voids in Slag (estimated)	= 42%
Submerged Weight (95 - .58 x 62.4)	= 58.8 lb./cu.ft.
Angle of Pressure Transmission θ	= 27.5 degrees (assumed)
Angle of Internal Friction ϕ	= 45 degress (assumed)

This stratum extends from El. 556.0 to the top of the soil at El. 583.5. Under this stratum lays a stratum of fine to medium brown or gray sand to El. 546.5. The properties of this stratum are as follows:

Dry Weight (estimated)	= 110 lb./cu.ft.
Wet Weight (5 $\pm$ percent moisture)	= 115 lb./cu.ft.
Voids in Sand (estimated)	= 33%
Submerged Weight (110 - .67 x 62.4)	= 68.2 lb./cu.ft.
Angle of Pressure Transmission θ	= 27.5 degrees (assumed)
Angle of Internal Friction ϕ	= 45 degrees (assumed)

Beneath this stratum is a stratum of a soft blue clay which extends 41.5 feet to El. 505.0. The soft clay weight 130 pounds per cubic foot. Its shearing resistance is 125 pounds per square foot as determined by the Transverse Shear Test and an average of 180 pounds per

square foot as determined by the Unconfined Compression Test; this average shearing resistance is computed from the actual shearing resistances of the stratum which are 150 pounds per square foot in the top 11.5 feet, 175 pounds per square foot in the next 10 feet below it and 200 pounds per square foot in the remaining 20 feet of the stratum. Then below this stratum is a stratum of a medium blue clay which extends about 10 feet to El. 495.0. The medium blue clay in this stratum weights 130 pounds per cubic foot. Its shearing resistance is 200 pounds per square foot as determined by the Transverse Shear Test and 300 pounds per square foot as determined by the Unconfined Compression Test. Below the medium clay lays a stratum of very stiff blue clay which extends five feet to El. 590.0. Its shearing resistance is 600 pounds per square foot as determined by the Transverse Shear Test and 800 pounds per square foot as determined by the Unconfined Compression Test.

The water surface of the lake is El. 578.5 USGS which is the mean low water surface. The depth on the front side is 22.5 feet. Therefore the elevation of the lake bottom is El. 556.0.

The fill in the cell is made of granular fill having the same properties as that of the sand.

Theoretical Analysis

From the information presented previously a typical profile showing the properties and dimensional data is illustrated in Figure 41. This profile is used in the theoretical analysis of the cofferdam as the basic soil data.

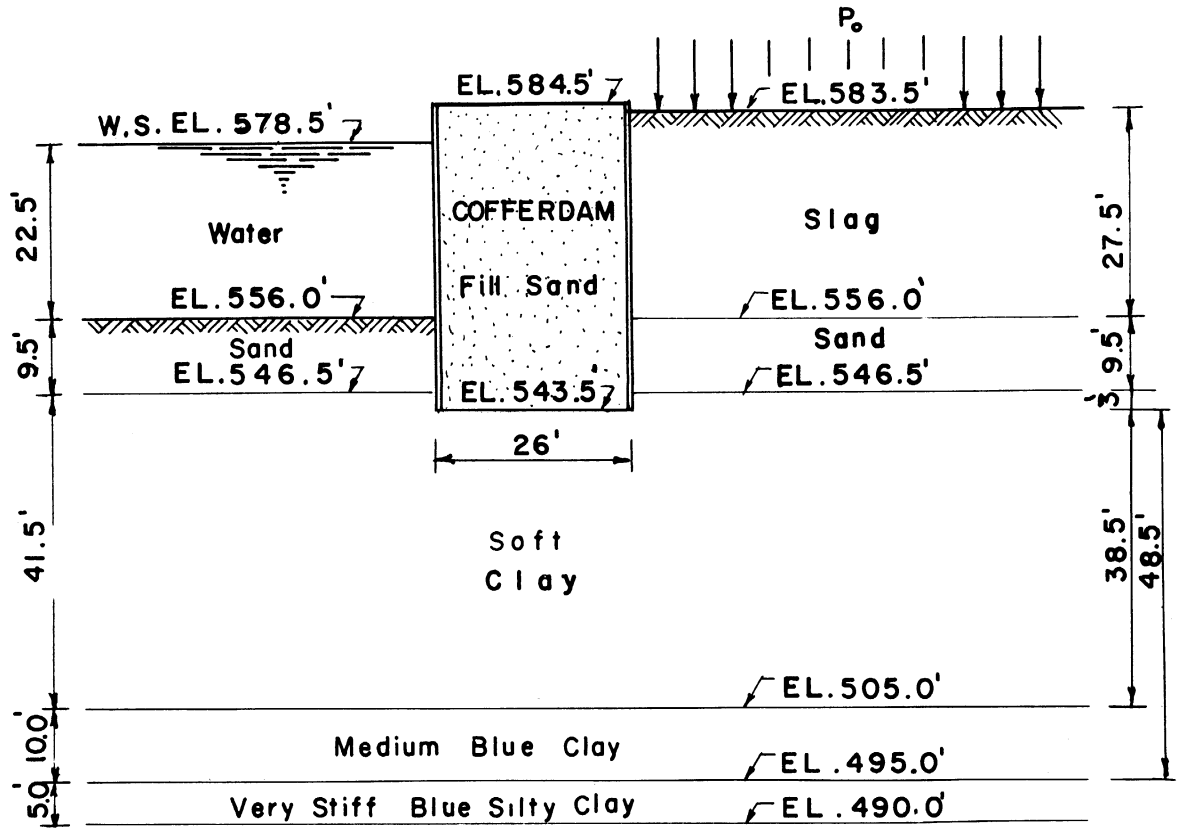

SOIL PROPERTIES:

Slag :	Submerged Weight		=	58.8	lb / Cu. ft.
	Wet Weight		=	100·0	lb / Cu. ft.
	θ = 27·5° ,	ø	=	45°	
Sand :	Submerged Weight		=	68.2	lb/ Cu .ft.
	θ = 27·5° ,	ø	=	45°	
Clay :	Weight		=	130	lb / Cu .ft.
	Soft Clay	S_{c_1}	=	125	lb/ Sq.ft.
		S_{uc_4}	=	180	lb / Sq. ft. (ave.)
	Medium Clay	S_{c_2}	=	200	lb / Sq . ft.
		S_{uc_5}	=	300	lb/S q . ft.

FIGURE 41. DETAILS OF TEST COFFERDAM

In order to test the existing cofferdam it is necessary to apply some forces on it. This could be accomplished by placing loads behind the cofferdam. These loads would produce a lateral thrust acting on the cofferdam, which would increase the tendency of the cofferdam to overturn, slide, develop higher tension in the interlock, and lose its mass stability.

Thus the following analysis is made to determine the area to be loaded, the amount of load to be placed, and the reaction of the cofferdam to this loading.

Under a loading condition the resultant applied thrust on the cofferdam will be transmitted through the cofferdam to the mass of soil underneath it. Therefore both the soft clay stratum between El. 543.5 and 505 and the soft clay with the medium blue clay between 505.0 and 495 should be strong enough to carry this thrust. Therefore in regard to the mass stability of the cofferdam with respect to upheaval, the elements of d = 38.5 feet and d = 48.5 feet are considered. At the stiff clay strata the possibility of a failing element which will include the stiff clay is remote due to the stiffness of the strata. Therefore the analysis is made for these two cases taking into consideration the following loading conditions:

a. When all the area behind the cofferdam is loaded and the critical element has a depth of either 48.5 feet or 38.5 feet.

b. When a square area behind the cofferdam with dimensions equal to the depth of the failing element is loaded.

c. When a square area of 48.5 feet times 48.5 feet behind the cofferdam is loaded and the depth of the failing element is equal to 38.5 feet.

For the loading conditions mentioned above, the overload ratio is calculated when the load is assumed to be zero. Then the allowable loads are calculated for the overload ratios of 2.0, 2.5, 3.0, and 3.5.

The allowable loads to be placed behind the cofferdam, for the various overload ratios, are also calculated as controlled by sliding, overturning, tension in interlock and vertical shear in the cell.

From the analysis made following all the steps mentioned previously it was found that the mass stability of the cofferdam is critical. The critical loading condition, excluding the case when all the area is loaded, is when a square area "O" of 48.5 feet by 48.5 feet is loaded and the failing element depth is 38.5 feet. The following pages contain a brief summary of the calculations illustrating the stability analysis which was made prior to the test. The full mathematical calculations are shown in Appendix A.

This analysis is revised in Chapter VI as a result of new data obtained during the test period.

Total static head above the loading plane at the back side,

$$wh_b = P_o + 4858 \text{ lb./sq.ft.}$$ (see Page 206)

Total static head above the loading plane at the dredged side,

$$whd = 3035 \text{ lb./sq.ft.}$$ (see Page 206)

Total active lateral force at the back side,

$$F_{hb} = 13.03\ P_o + 58940 - 900\ R \text{ lb./ft. run}$$

(see Page 208)

Total active lateral force at the dredged side,

F_{hd} (active) = 41320 - 900 R lb./ft. run (see Page 208)

Total passive lateral force at the dredged side,

F'_{hd} (passive) = 51880 + 900 R lb./ft. run (see Page 208)

Total vertical shearing resistance at the dredged side,

S_{hd} = 836 + 375 R lb./ft. (see Page 208)

Total vertical shearing resistance at the back side,

S_{hb} = 10.03 P_o + 12960 + 375 R lb./ft. (see Page 209)

Average vertical shearing resistance at the dredged side,

S_{ad} = 66.88 + 30 R lb./sq.ft. (see Page 208)

Average vertical shearing resistance at the back side,

S_{ab} = 0.251 P_o + 324 + 9.4 R lb./sq.ft. (see Page 209)

Average shearing resistance in the clay strata below the loading plane, between El. 543.5 and 495.0,

S_c (Ave.) = 140 lb./sq.ft. (see Page 209)

S_{uc} (Ave.) = 205 lb./sq.ft. (see Page 209)

Stability Analysis with Respect to Mass Movement of the Soil Mass (Upheaval)

When All the Area Behind the Cofferdam is Loaded and the Depth of the Failing Element is 48.5 Feet.--This case is illustrated in Figure 42. The applied forces are the active lateral force on the back side, F_{hb}/d, and the static head on the back side, wh_b. The resisting forces are the active lateral pressure on the dredged side, F_{hd}/d, the static head on the dredged side, wh_d, the lateral distribution below the loading plane, 2 $S_{c(Ave.)}$, the developed pressure, 4 $S_{uc(Ave.)}$, the

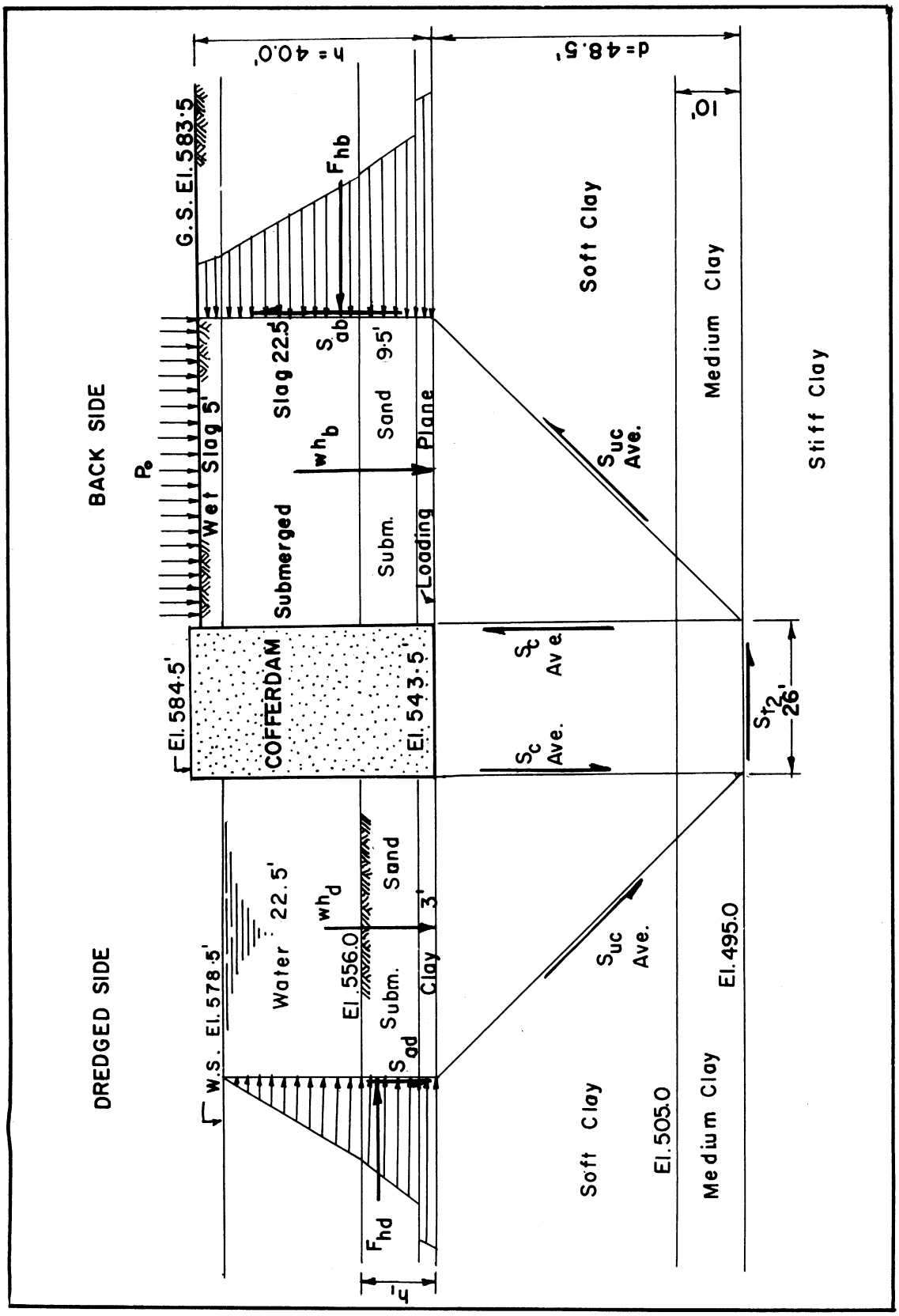

FIGURE 42. APPLIED AND RESISTING FORCES ACTING ON TEST COFFERDAM, FAILING ELEMENT DEPTH IS 48·5 FEET.

resistance to horizontal displacement, $S_{t_2}b/d$, the weight transfer above the loading plane at the dredged side, S_{hd}/d (see Page 212), and the weight transfer above the loading plane at the back side which is equal to either S_{hb}/d or S_{t_2} whichever will control (see Page 212). The values of S_{hb}/d depend upon the values of R and P_o (which is indeterminate). Therefore, the stability equation is set using either S_{hb}/d or S_{t_2} and then the values of P_o are determined and controlling values are selected (see Page 213).

Therefore, the stability equation, using S_{hb}/d for weight transfer at the back side, is:

$$wh_b + F_{hb}/d - wh_d - F_{hd}/d - S_{hd}/d - 4\ S_{uc(Ave.)}R$$

$$- 2\ S_{c(Ave.)}R - S_{t_2}\ R\ b/d - S_{hb}/d = 0$$

$$(P_o + 4858) + (13.03P_o + 58940 - 900R)/48.5 - (3035)$$

$$- (41320 - 900R)/48.5 - (836 + 375R)/48.5 - (4 \times 205R)$$

$$- (2 \times 140R) - (26 \times 200R)/48.5$$

$$- (10.03P_o + 12960 + 375R)/48.5 = 0$$

$$1.062P_o + 1902 - 1223R = 0$$

For $P_o = 0$ $\quad R = 1.55$, and $(h/d)S_{ab} = 279 < 200\ R$

For $R = 2.0$, $P_o = 510$, and $(h/d)S_{ab} = 388 < 200\ R$

For $R = 2.5$, $P_o = 1090$, and $(h/d)S_{ab} = 512 > 200\ R$*

For $R = 3.0$, $P_o = 1665$, and $(h/d)S_{ab} = 635 > 200\ R$*

For $R = 3.5$, $P_o = 2240$, and $(h/d)S_{ab} = 758 > 200\ R$*

$h/d = 40/48.5 = .825$, and $S_{ab} = 0.251\ P_o + 324 + 9.4\ R$

When $(h/d)S_{ab}$ is greater than 200 R (where marked with *), the stability equation using S_{hb} is not valid because the weight transfer is limited by $S_{t_2}R$. Therefore the stability equation using S_{t_2} as the weight transfer will control.

The stability equation, with weight transfer using S_{t_2}, is:

$$wh_b + F_{hb}/d - wh_d - F_{hd}/d - S_{hd}/d - 4\ S_{uc(Ave.)}R$$

$$- 2\ S_{c(Ave.)}R - S_{t_2}R\ b/d - S_{t_2}R = 0$$

$$(P_o + 4858) + (13.03P_o + 58940 - 900R)/48.5 - (3035)$$

$$- (41320 - 900R)/48.5 - (836 + 375R)/48.5$$

$$- (4 \times 205R) - (2 \times 140R) - (26 \times 200R)/48.5 - 200R = 0$$

$$1.269\ P_o + 2169 - 1415\ R = 0 \qquad \text{(see Page 213)}$$

For $P_o = 0$, $R = 1.53$, and $(h/d)S_{ab} = 279 < 200\ R$*

For $R = 2.0$, $P_o = 520$, and $(h/d)S_{ab} = 390 < 200\ R$*

For $R = 2.5$, $P_o = 1080$, and $(h/d)S_{ab} = 509 > 200\ R$

For $R = 3.0$, $P_o = 1635$, and $(h/d)S_{ab} = 628 > 200\ R$

For $R = 3.5$, $P_o = 2190$, and $(h/d)S_{ab} = 747 > 200\ R$

When $(h/d)S_{ab}$ is smaller than 200 R in the above cases (where marked with * above) the shearing resistance S_{ab} controls and the stability equation using S_{t_2} is not valid.

Summary of the results when all the area behind the cofferdam is loaded; depth of the failing element, d, is equal to 48.5 feet:

For R = 1.55, P_o = 0

For R = 2.00, P_o = 510 lb./sq.ft.

For R = 2.50, P_o = 1080 lb./sq.ft.

For R = 3.00, P_o = 1635 lb./sq.ft.

For R = 3.50, P_o = 2190 lb./sq.ft.

When Area "0" of 48.5 Feet Times 48.5 Feet is Loaded and the Depth of the Failing Element is 48.5 Feet.--The allowable loads for various overload ratios, to be placed behind the cofferdam when all the area is loaded, were calculated above, in which the problem was considered two dimensional.

To find the allowable loads on area "0" (see Figure 43), the problem will become three dimensional. The approach in this case is based on the assumption that the load capacity of areas 0, 1, 2, 3, 4, and 5 could be concentrated on area "0", providing there is sufficient shear in the vertical planes A-B, B-C, and C-D, in excess of what has already been mobilized for weight transfer, to distribute the concentration back to the five adjacent elements at the loading plane. This assumption is abandoned later as shown in the revised solution in Chapter IV.

Average shearing resistance on planes A-B, B-C, and C-D due to active lateral pressure is:

$$S_{ab} = 0.251\ P_o + 324 + 9.4\ R$$ (see Page 209)

The shearing resistance mobilized along plane B-C when S_{t_2} controls is:

$$S_{t_2}\ x(d/h)x\ R = 200\ \ R\ x\ 48.5/40 = 243\ R\ lb./sq.ft.$$

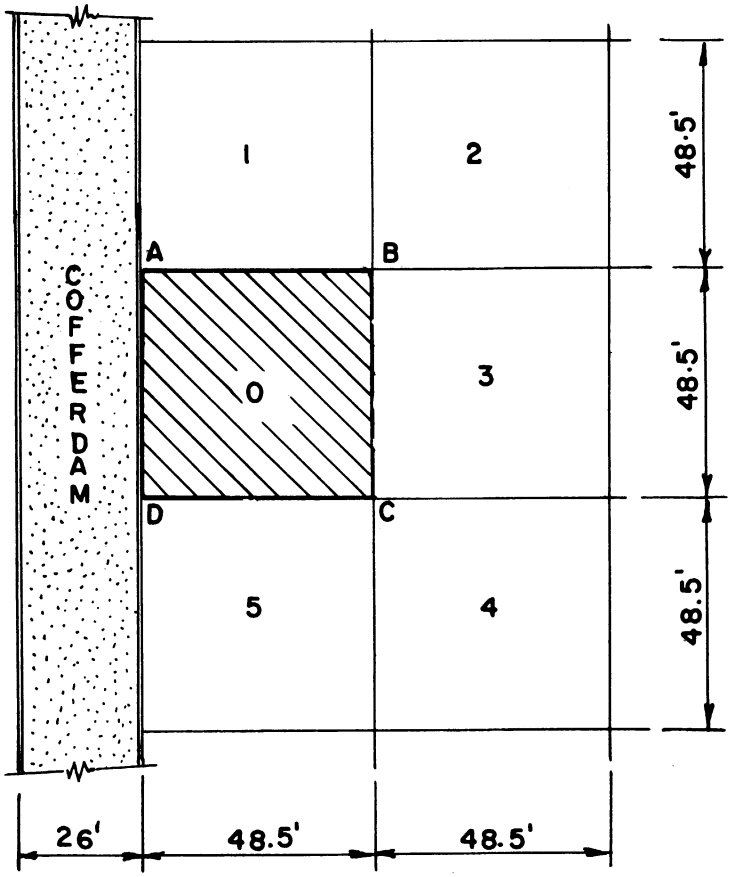

FIGURE 43 . AREA "O" OF 48·5' BY 48·5' AND ADJACENT AREAS 1, 2, 3, 4 AND 5, DEPTH OF ELEMENT D = 48·5'

Therefore, assuming the allowable load when all the area is loaded equal to P_o and the allowable load when area "0" is loaded only equal to P'_o,

$P'_o = 6 \times P_o$ or, as controlled by vertical shear,

$P'_o = P_o + (3\ S_{ab} - S_{ab}) \frac{hxd}{dxd} = P_o + 2\ S_{ab} \frac{h}{d}$ when S_{ab} controls or,

$P'_o = P_o + (3\ S_{ab} - S_{t_2} R \frac{d}{h}) \frac{hxd}{dxd} = P_o + (3 S_{ab} \frac{h}{d} - S_{t_2} R)$ when S_{t_2} controls.

By introducing the values of R and the corresponding values of P_o, the values of S_{ab}, S_{t_2}, h and d, the allowable loads for various overload ratios are:

For R = 2.0, P'_o = 1830 lb./sq.ft. (see Page 217)

For R = 2.5, P'_o = 3760 lb./sq.ft.

For R = 3.0, P'_o = 5040 lb./sq.ft.

For R = 3.5, P'_o = 6250 lb./sq.ft.

When All the Area Behind the Cofferdam is Loaded and the Depth of the Failing Element is 38.5 Feet.--This case is illustrated in Figure 44. The applied forces are the active lateral force on the back side, F_{hb}/d, and the static head on the back side, wh_b. The resisting forces are the active lateral force on the dredged side, F_{hd}/d, the static head on the dredged side, wh_d, the lateral distribution below the loading plane, $2\ S_{c_1}$, the developed pressure, $4\ S_{uc_4}$, the resistance to horizontal displacement, $S_{t_1} b/d$, the weight transfer above the loading plane at the dredged side, S_{hd}/d (see Page 219), and the weight transfer above the loading plane at the back side which is equal to either S_{hb}/d or $S_{t_1} R$, depending upon which one will control.

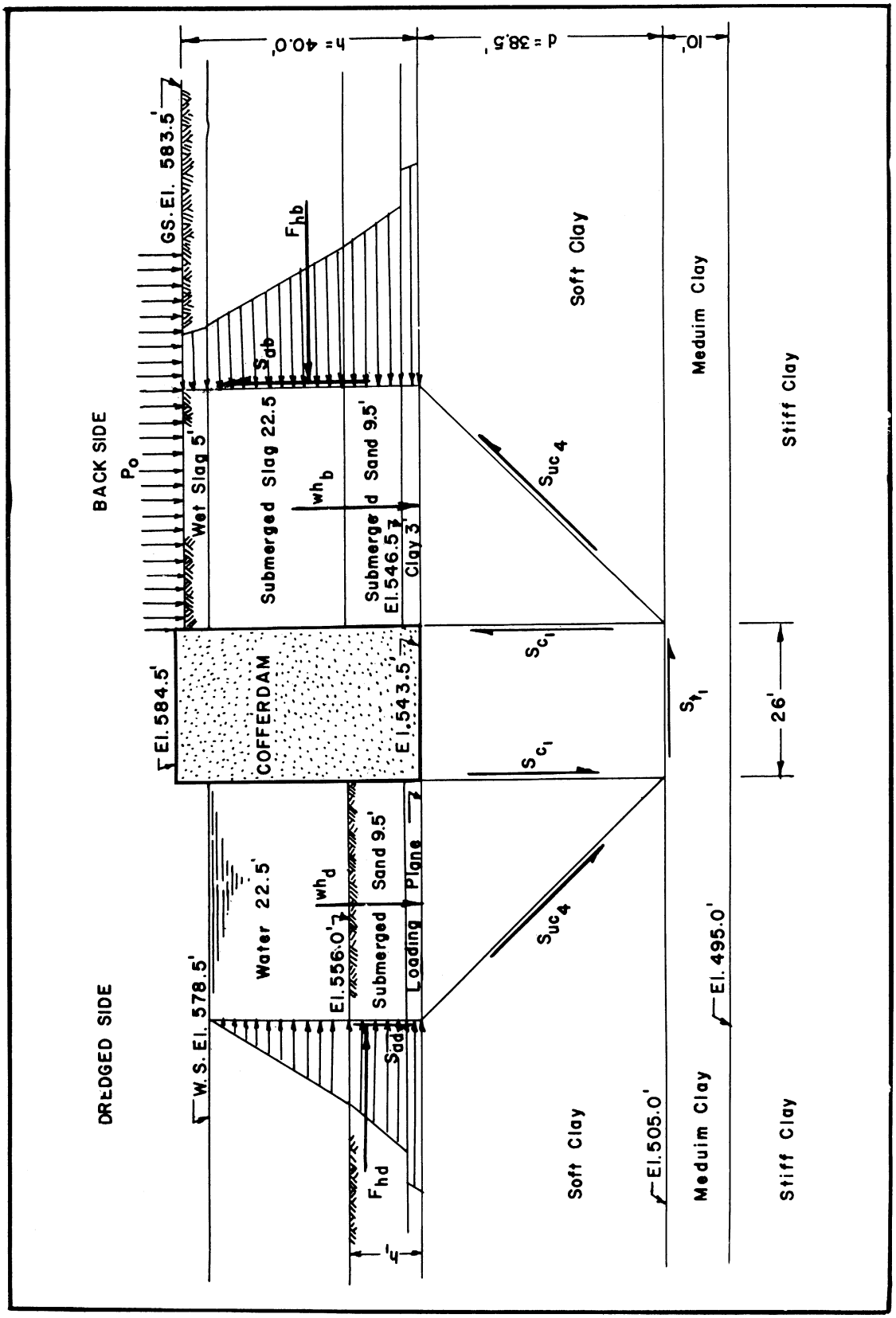

FIGURE 44. APPLIED AND RESISTING FORCES ACTING ON TEST COFFERDAM, FAILING ELEMENT DEPTH 38.5 FEET.

The stability equation will be set with the assumption that $S_{t_1}R$ will control. This will be verified later. Therefore, the stability equation will be:

$$wh_b + F_{hb}/d - wh_d - F_{hd}/d - S_{hd}/d - 4\,S_{uc_4}R - 2\,S_{c_1}R - S_{t_1}R\,b/d - S_{t_1}R = 0$$

$$(P_o + 4858) + (13.03P_o + 58940 - 900R)/38.5 - (3035) - (41320 - 900R)/38.5 - (836 + 375R)/38.5 - (4 \times 180R) - (2 \times 125R) - (26 \times 125R)/38.5 - 125R = 0$$

$$1.338\,P_o + 2258 - 1189\,R = 0 \qquad \text{(see Page 220)}$$

For $P_o = 0$, $R = 1.9$ and $S_{ab} = 342 > 125R$

For $R = 2.0$, $P_o = 90$ and $S_{ab} = 365 > 125R$

For $R = 2.5$, $P_o = 535$ and $S_{ab} = 482 > 125R$

For $R = 3.0$, $P_o = 980$ and $S_{ab} = 598 > 125R$

For $R = 3.5$, $P_o = 1420$ and $S_{ab} = 712 > 125R$

The values of S_{ab} as shown above, for the various overload ratios, R, and the corresponding P_o, are always greater than 125R. Thus the assumption that S_{t_1} will control is valid and therefore the weight transfer at the back side is controlled by $S_{t_1}R$.

When Area "0" of 38.5 Feet Times 38.5 Feet is Loaded and the Depth of the Failing Element is 38.5 Feet.--The allowable loads for various overload ratios, to be placed behind the cofferdam when all the area is loaded, were calculated previously. To find the allowable loads on area "0" (see Figure 45), the assumption is made that the load capacity of areas 0, 1, 2, 3, 4, and 5 could be concentrated on area "0", providing there is sufficient shear in the vertical planes A-B, B-C, and C-D, in excess

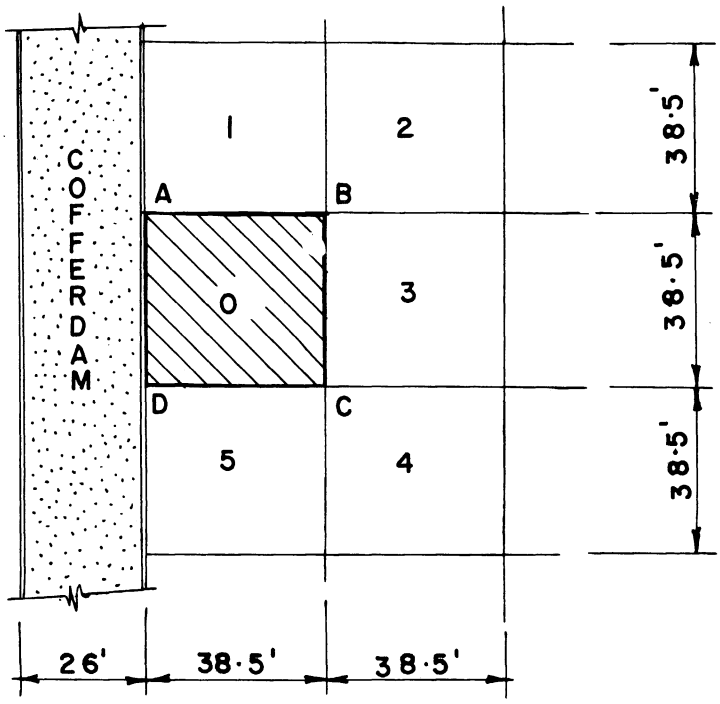

Figure 45. Area "O" of 38.5' by 38.5' and Adjacent Areas 1, 2, 3, 4, and 5, Depth of Element D = 38.5'.

of what has already been mobilized for weight transfer, to distribute the concentration back to the five adjacent elements at the loading plane. This assumption has been abandoned as shown in Chapter VI.

The average shearing resistance on planes A-B, B-C, and C-D due to the active lateral pressure is:

$$S_{ab} = 0.251\ P_o + 324 + 9.4\ R \qquad \text{(see Page 209)}$$

The shearing resistance mobilized for weight transfer along plane B-C is S_{t_1} and is equal to 125 R. (see Page 220)

Using the symbol P_o for the allowable load when all the area is loaded and the symbol P'_o for the allowable load when area "O", of

38.5 feet by 38.5 feet is loaded only, then the load P'_o will be determined as follows:

$$P'_o = 6 \times P_o \quad \text{or, as controlled by vertical shear,}$$

$$P'_o = P_o + (3S_{ab} - S_{t_1}R)\frac{hxd}{dxd} = P_o + 3S_{ab}\frac{h}{d} - S_{t_1}R\frac{h}{d}$$

By introducing the values of R and the corresponding values of P_o, the values of S_{ab}, S_{t_1}, h and d, the allowable loads for various overload ratios are:

For R = 2.00, P'_o = 540 lb./sq.ft. (see Page 222)

For R = 2.50, P'_o = 3210 lb./sq.ft.

For R = 3.00, P'_o = 5880 lb./sq.ft.

For R = 3.50, P'_o = 8520 lb./sq.ft.

When the Area "0" of 48.5 Feet Times 48.5 Feet is Loaded and the Depth of the Failing Element is 38.5 Feet.--The allowable loads for various overload ratios, to be placed behind the cofferdam when all the area is loaded, are calculated on Page 220.

To find the allowable loads for area "0" (see Figure 46), the assumption is made that the load capacity of areas 0, 1, 2, 3, 4, and 5 could be concentrated on area "0" of 48.5 feet by 48.5 feet, providing there is sufficient shear in the vertical planes A-B, B-C, and C-D, in excess of what has already been mobilized for weight transfer, to distribute the concentration back to the five adjacent elements at the loading plane. This assumption has been abandoned as shown in Chapter VI.

The average shearing resistance on planes A-B, B-C, and C-D due to the active lateral pressure is:

$$S_{ab} = 0.251\ P_o + 324 + 9.4\ R \qquad \text{(see Page 209)}$$

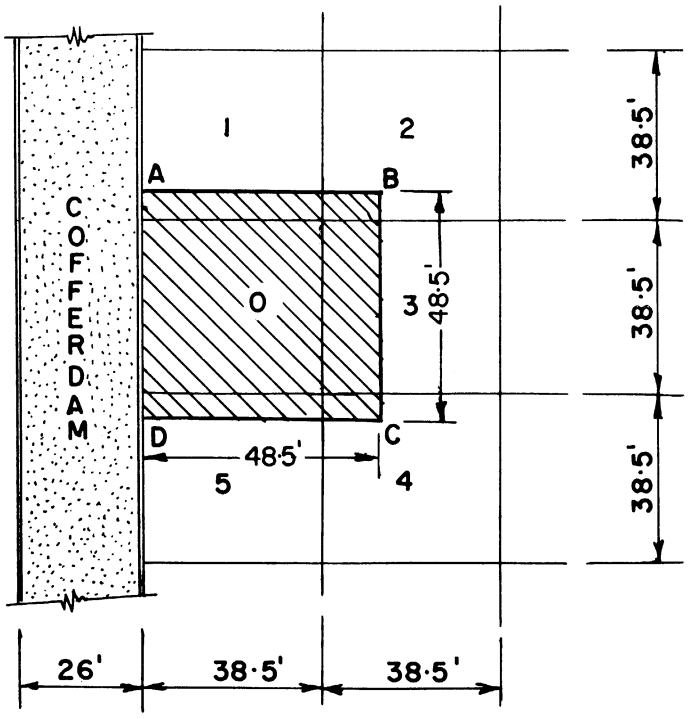

Figure 46. Area "O" of 48.5' by 48.5' and Adjacent Areas 1, 2, 3, 4, and 5, Depth of Element D = 38.5'.

The shearing resistance mobilized for weight transfer along plane B-C is S_{t_1} and is equal to 125 R. (see Page 220)

Using the symbol P_o for the allowable load when all the area is loaded and the symbol P'_o for the allowable load when area "O" of 48.5 feet by 48.5 feet is loaded only, then the load P'_o will be determined as follows:

$$P'_o = P_o \times 6 \times (38.5 \times 38.5)/(48.5 \times 48.5)$$

$$P'_o = 3.78\ P_o \quad \text{or, as controlled by vertical shear,}$$

$$P'_o = P_o + (3\ S_{ab} - S_{t_1}R)\ \frac{hxd}{dxd}$$

$$P'_o = P_o + .825(3\ S_{ab} - S_{t_1}R)$$

By introducing the values of R and the corresponding values of P_o, the values of S_{ab} and S_{t_1}, the allowable loads for various overload ratios are calculated as follows:

For R = 2.00, P'_o = 340 lb./sq.ft. (see Page 225)

For R = 2.50, P'_o = 2022 lb./sq.ft.

For R = 3.00, P'_o = 3702 lb./sq.ft.

For R = 3.50, P'_o = 5125 lb./sq.ft.

Summary of stability analysis with respect to mass movement of the underlying soil strata (upheaval):

Overload Ratio, R,	When All Area is Loaded		When Area "O" of 38.5 x 38.5 is Loaded	When Area "O" of 48.5x 48.5 is Loaded	
	d=38.5	d=48.5	d=38.5	d=38.5	d=48.5
2.00	90	510	540	340	1830
2.50	535	1080	3210	2022	3760
3.00	980	1635	5880	3702	5040
3.50	1420	2190	8520	5125	6250

Stability Analysis with Respect to Sliding

Two cases are considered; the first is when all the area behind the cofferdam is loaded and the second case is when the square area of 48.5 feet by 48.5 feet is loaded only.

When All the Area is Loaded.--The active lateral pressure on the back side will be resisted by the passive lateral pressure on the dredged side and the shearing resistance at the base of the cofferdam (see Figure 47).

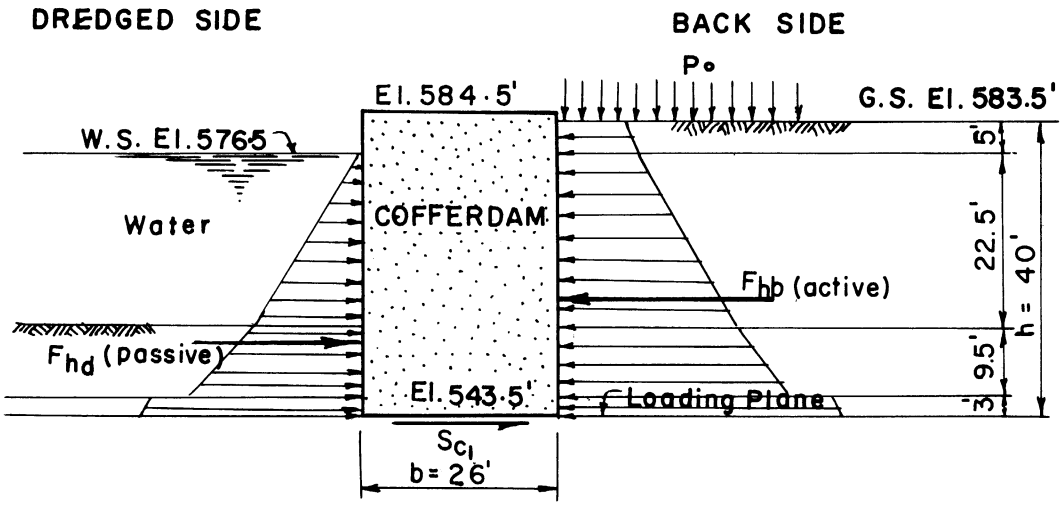

Figure 47. Forces Acting on Test Cofferdam with Respect to Sliding.

Therefore, the stability equation will be:

$$F_{hb} \text{ (active)} - F'_{hd} \text{ (passive)} - S_{c_1} R \; b = 0$$

$$(13.03\ P_o + 58940 - 900\ R) - (51880 + 900\ R)$$

$$- (26 \times 125\ R) = 0$$

$$P_o = 388\ R - 538 \quad \text{(see Page 227)}$$

For $P_o = 0$, $R = 1.38$

For $R = 2.00$, $P_o = 232$ lb./sq.ft.

For $R = 2.50$, $P_o = 430$ lb./sq.ft.

For $R = 3.00$, $P_o = 624$ lb./sq.ft.

For $R = 3.50$, $P_o = 818$ lb./sq.ft.

When Area "O" is Loaded Only.--The stability equation is set taking into consideration the continuity effect of the cofferdam's structure.

The applied force on the cofferdam is the active lateral force on the back side, F_{hb}, and is equal to:

$$(13.03\ P_o + 58940 - 900\ R)\ \text{lb./ft.} \quad \text{(see Page 208)}$$

The resisting forces are the passive lateral force on the dredged side, the resistance to sliding at the base of the cofferdam and the resistance due to the continuity effect of the unloaded portion of the cofferdam. The lateral passive force on the dredged side is equal to:

$$F'_{hd} = (51880 + 900\ R)\ \text{lb./ft.} \quad \text{(see Page 208)}$$

The resistance to sliding at the base of the cofferdam is equal to:

$$S_{c_1} \times R \times b = 125 \times 26\ R = 3250\ R\ \text{lb./ft.}$$

The resistance due to the effect of the continuity will be the total resistance of the unloaded portion of the cofferdam in excess of what has been mobilized for the stability of the unloaded portion of the cofferdam. For any value of R greater than 1.38, which is the overload ratio for P_o equal to zero, the increase in the value of R will affect the clay strata. This increase in the resistance will be equal to:

$$41337\ (R - 1.38)\ \text{lb./ft.} \quad \text{(see Page 228)}$$

Therefore the stability equation with respect to sliding will be set as follows:

$$F_{hb} - F'_{hd} - S_{c_1} R\ b - 41338\ (R - 1.38) = 0$$

$$(13.03\ P_o + 58940 - 900\ R) - (51880 + 900\ R)$$

$$- (3250\ R) - (41337\ R - 57045) = 0$$

Therefore $13.03\ P_o + 64105 - 46387\ R = 0$ (see Page 228)

$$P_o = 3560\ R - 4915$$

For R = 2.00, P_o = 2205 lb./sq.ft.

For R = 2.50, P_o = 3985 lb./sq.ft.

For R = 3.00, P_o = 5765 lb./sq.ft.

For R = 3.50, P_o = 7545 lb./sq.ft.

Tension in the Interlock

The active lateral pressure acting on the back wall of the cofferdam will be transmitted to the front wall provided that there is sufficient passive lateral pressure in the fill of the cell. This pressure will be resisted by the passive lateral pressure on the dredged side. The resultant pressure will be transmitted to the back wall through the diaphragm causing a tension in the interlock. (see Figure 48)

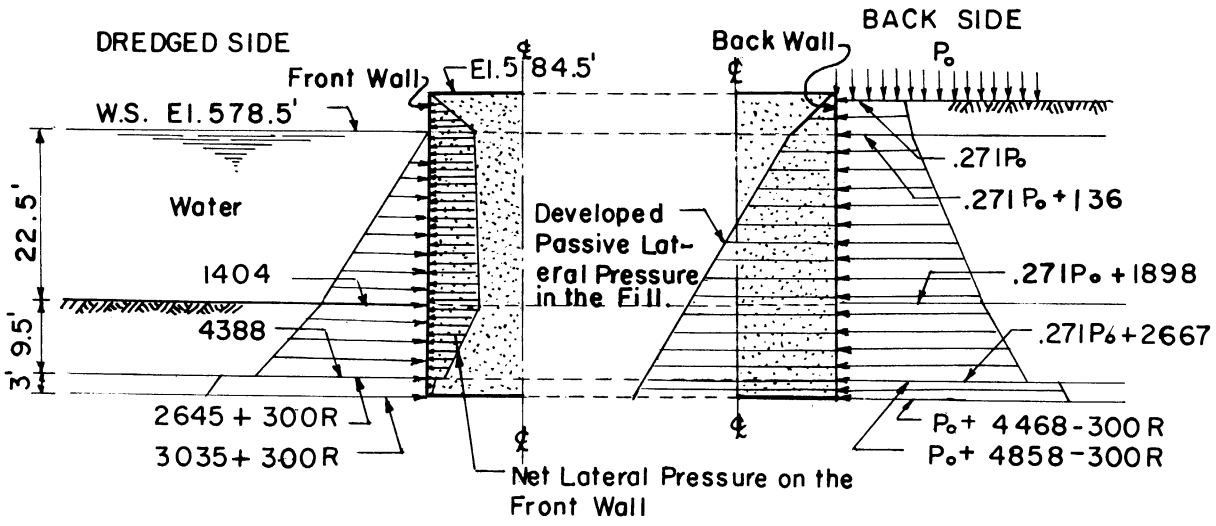

Figure 48. Forces Acting On Test Cofferdam with Respect to Tension in the Interlock.

The total active force on the back side is:

$F_{hb} = 13.03\ P_o + 58940 - 900\ R$ lb./ft. run of the cofferdam.

The total passive force on the dredged side is F'_{hd},

$F'_{hd} = 51880 + 1080\ R$ lb./ft. run of the cofferdam.

The net pressure on the front wall is:

$$F_{hb} - F'_{hd} = (13.03\ P_o + 58940 - 900\ R) - (51880 + 900\ R)$$
$$= 13.03\ P_o + 7060 - 1800\ R$$

This net pressure will be carried to the back wall by the diaphragm causing the tension in the interlock. The tension in the interlock is:

$$T = \frac{(F_{hb} - F'_{hd}) \times 3L}{4b \text{ Tan } \theta \times 12} = (13.03\ P_o + 7060 - 1800\ R)/7.255$$

(see Page 230)

If the allowable tension in the interlock is 10,000 pounds per inch of the interlock then the allowable loads to be placed behind the cofferdam without exceeding the allowable tension in the interlock is:

$P_o = 138\ R + 4990$ lb./sq.ft. (see Page 230)

Therefore for various assumed overload ratios P_o is:

When R = 2.00, $P_o = 5262$ lb./sq.ft.

When R = 2.50, $P_o = 5331$ lb./sq.ft.

When R = 3.00, $P_o = 5400$ lb./sq.ft.

When R = 3.50, $P_o = 5469$ lb./sq.ft. (see Page 230)

The above equation for the tension in the interlock is based on the assumption that the total active lateral force on the back side will be transmitted to the front wall. The maximum force that could be transmitted through the fill is limited by the passive lateral pressure of the fill in the cell.

The passive lateral force of the fill in the cell is calculated on Page 209 and is equal to 250888 pounds per foot which is greater than, F_{hb}, 127051 pounds per foot. Therefore there is sufficient passive lateral force in the cell to transfer the applied lateral force, F_{hb}, from the back wall to the front wall of the cofferdam. (See Page 231)

Allowable Load, P_o, with Respect to Overturning When All Area is Loaded

The applied moment due to the active lateral pressure on the back side is M_a and is equal to: (see Page 231)

$$M_a = 220.3\ P_o + 539400 - 1350\ R \text{ lb.ft./ft. run of cofferdam.}$$

The resisting moment due to the passive lateral pressure on the dredged side is M'_{rd} and is equal to:

$$M'_{rd} = 519500 + 1350\ R \text{ lb.ft./ft. run of cofferdam}$$

(see Page 233)

The resisting moment due to the weight of the cofferdam, about the toe (point O, see Figure 89, Appendix A), is equal to:

$$M_{rw} = 80000 \times 26/2 = 1040000 \text{ lb.ft./ft.}$$ (see Page 233)

The resisting moment due to the shearing force at the outer face of the back wall:

$$M_{rs} = 78.234\ P_o + 101088 + 2925\ R$$ (see Page 234)

The total resisting moment is designated as M_r and is equal to $M'_{rd} + M_{rw} + M_{rs}$ which are calculated above.

$$M_r = 78.234\ P_o + 1660588 + 4275\ R$$ (see Page 234)

Equating the applied moment, M_a, to the resisting moment, M_r, the stability equation with respect to overturning will be:

$$P_o = 7895 + 40\ R$$ (see Page 234)

For R = 1.00, P_o = 7935

For R = 1.50, P_o = 7955

For R = 2.00, P_o = 7975

For R = 2.50, P_o = 7995

For R = 3.00, P_o = 8015

For R = 3.50, P_o = 8035

In the stability equation above the mobilized shearing resistance at the outer face of the back wall must not exceed the passive shearing resistance in the fill of the cell, S'_{hf}. The shearing resistance, S_{hb}, will be equal to S'_{hf} when the load, P_o, placed behind the cofferdam reaches the value 23346 pounds per square foot (see Page 235). This value of P_o is very high. Therefore the shearing resistance on the outer face of the back wall, S_{ab}, will control.

The previous solution is made on the assumption that all the area behind the cofferdam is loaded. Therefore, if an area "O" is loaded, the cofferdam will maintain its stability as if all the area is loaded and then a portion of the area is unloaded. This makes it unnecessary to investigate the case when area "O" is loaded.

Allowable Load, P_o, with Respect to Vertical Shear, When All Area is Loaded

The total applied moment due to the active lateral pressure acting against the cofferdam on the back side equals: (see Page 231)

$$M_a = 220.3\ P_o + 539400 - 1350\ R \text{ lb.ft./ft. run of cofferdam.}$$

The total resisting moment due to the passive lateral pressure acting against the cofferdam on the dredged side equals:

$$M'_{rd} = 519500 + 1350\ R \text{ lb.ft./ft. run of cofferdam}$$

(see Page 233)

The resisting moment due to the shearing resistances on the outer faces of the cofferdam walls is:

$$M_{rsd} = 0.3\ S'_{hd}\ b = 26(2391 + 375\ R) \times 0.3$$

The net moment causing the vertical shear in the cofferdam is M_{rv} and is equal to:

$M_{rv} = M_a - M'_{rd} - 0.3\ S'_{hd}\ b$ (moments are about center line of cofferdam)

$$M_{rv} = 220.3\ P_o + 1250 - 5625\ R \qquad \text{(see Page 236)}$$

This resultant moment will cause the vertical shear in the cell which is symbolized by Q and is equal to:

$$220.3\ P_o + 1250 - 5625\ R = \frac{5}{8} \times 26 \times Q$$

The shearing resistance in the fill of the cell is equal to the lateral pressure of the fill times Tan ϕ. The lateral pressure in the fill is greater than the active lateral pressure of the fill of the cell due to the applied lateral pressure on the back side. However, the lateral pressure in the fill must not exceed the passive lateral pressure in the fill. The shearing resistance of the fill in the cell is:

$$S_v = F_{hb} \times \text{Tan}\ \phi$$

$$S_v = 13.03\ P_o + 58940 - 900\ R$$

The stability criterion with respect to vertical shear is that the shearing stress, Q, must not exceed the shearing resistance, S_v. Thus, substituting S_v in the equation for Q above, the stability equation with respect to vertical shear in the cell is:

$$220.3\ P_o + 1250 - 5625\ R = \frac{5}{8} \times 26(13.03\ P_o + 58940 - 900\ R)$$

P_o = 110176 lb./sq.ft. (see Page 237) which is a very

high value. Thus the vertical shear in the cell is not a critical factor in the stability of this cofferdam.

An examination of the allowable loads to be placed on area "O", with respect to mass stability (upheaval), sliding, tension in the interlock and overturning, indicates that the mass stability is the controlling factor. Thus the cofferdam is critical with respect to mass movement and the critical loading is when area "O" of 48.5 feet by 48.5 feet is loaded and the depth of the failing element is 38.5 feet.

Final Recommendations for Testing

From the theoretical analysis of the test cofferdam and based on the assumptions discussed in the preceding analysis, the following conclusions and recommendations for testing were drawn:

a. If the dock behind the cofferdam is loaded, the failing element may have a depth of 38.5 feet or 48.5 feet. Thus either the square area 38.5 feet by 38.5 feet or 48.5 feet by 48.5 feet was suggested. As shown in the summary of stability analysis with respect to mass movement (upheaval) on Page 124 , the critical loading condition is when the square area "O" of 48.5 feet by 48.5 feet is loaded. In this case the critical depth is 38.5 feet. Although the case when all the area is loaded is more critical, loading the entire area is not advisable as it is costly and not possible for purposes of testing. Thus, the area "O" of 48.5 feet by 48.5 feet is chosen.

b. As shown in the analysis, the allowable load to be placed behind the cofferdam on the test area is 3702 pounds per square foot when the overload ratio is 3.0. The overload ratio 3.0 is anticipated to be the critical overload ratio, thus this load was suggested as the first step of loading. This load will total to 4350 tons which will be approximated to 4500 tons which is to be placed over the entire 48.5 foot by 48.5 foot area. This load was to be placed on the test area as long as permitted by the Company.

c. For an overload ratio of 3.5, a progressive settlement representing loss of stability and failure is anticipated. Such an overload ratio would ensure that a progressive settlement of a high range would occur, leading to loss of some of the resistances and failure. To reach an overload ratio of 3.5, a load of 5125 pounds per square foot as obtained from the analysis should be placed behind the cofferdam, which is equivalent to 6010 tons over the entire area. The load suggested for the second stage of loading was, however, 5500 tons, which represents the ore load that the Company intends to place on their ore yard if a cofferdam of this type is feasible to be used for a shore dock.

d. Monuments were proposed to be placed around the test area at distances of 25 feet from the cofferdam in both directions. For an illustration, see Figure 49, showing the location of these monuments. Also, points at a distance of 25 feet on the lake side in both directions were proposed in order to measure the upheaval of the soil in the dredged side. Points on the

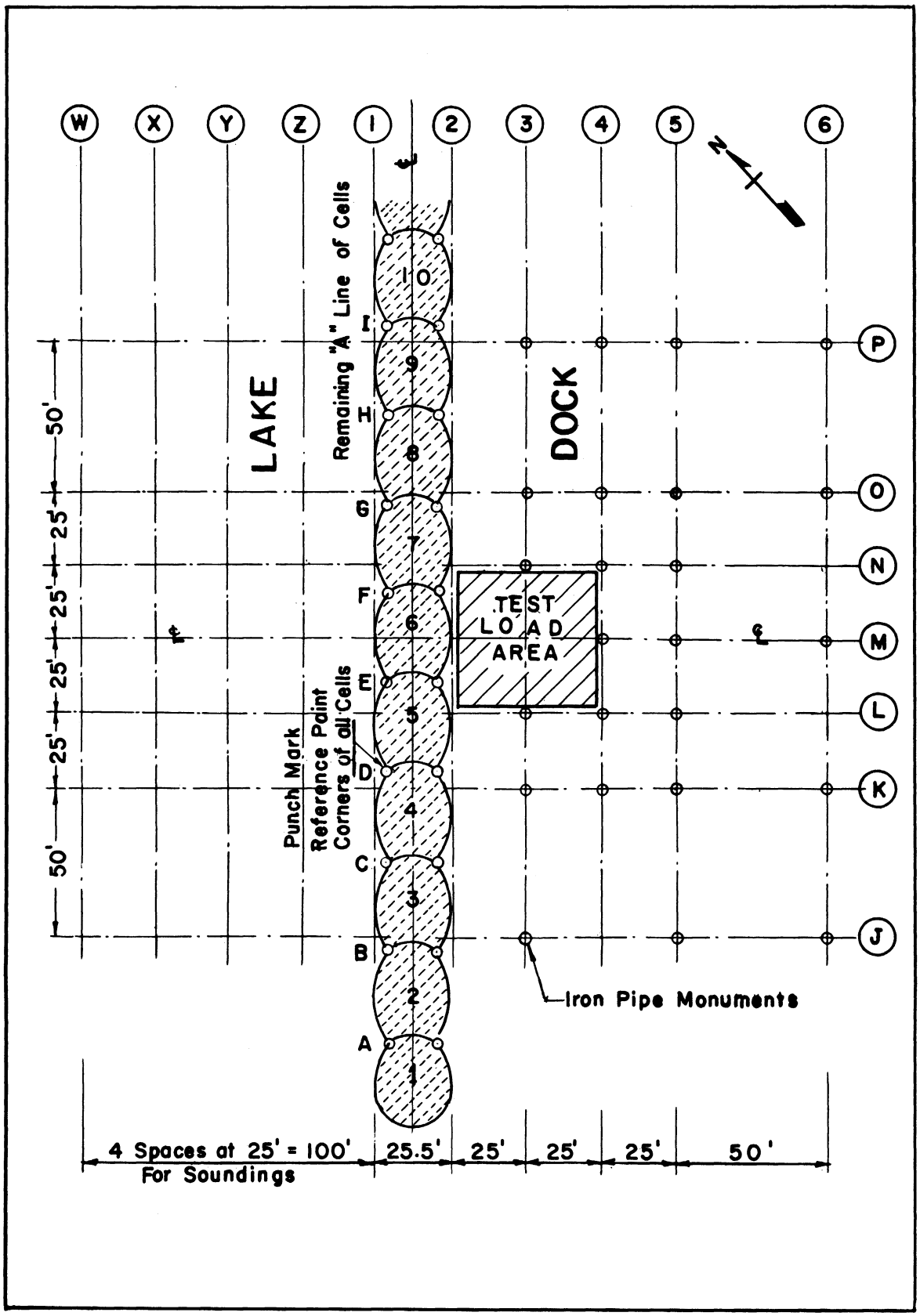

FIGURE 49. LOCATION PLAN OF MONUMENTS AT TEST SITE

corner of each cell were suggested to be marked to measure the vertical and horizontal displacements of the cofferdam.

e. Exact horizontal measurements were suggested to be taken between the points to observe specifically the deflection of the cofferdam.

f. The third step of the testing operation was to unload the test area and take a final reading of the displacements.

CHAPTER V

TESTING

Loading

Based on the recommendations made previously, Inland Steel Company prepared the site for the test. Monuments were placed as recommended. These monuments were made of concrete cylinders with an iron pipe inside them. The pipe was marked at a definite point for setting the leveling rod when the levels were to be taken. These monuments were set to a sufficient depth to prevent their disturbance from outside effects. See Figure 50 for a photograph showing a typical monument. Later, on November 28, 1956, the monuments were marked more definitely with a welded spot, and a level reading was taken to get a correction factor. The welded spot was made in order to obtain a fixed point on the monument for more accurate level readings.

After placing the monuments, the test area was framed to contain the loads and support them laterally (see Figures 51 to 54). The loading was started and the capacity of 4500 tons was reached on September 22, 1956. On that date, a level reading was taken. The load was left on the cofferdam for 124 days, until January 24, 1957, during which time seven readings were taken, including the first one. One check was made on October 10, 1956, and a correction for the welded spots on November 28, 1956.

Then a loading increase was started on January 24, 1957, continuing until March 21, 1957, a total of 56 days. During this period three readings were taken, one for all the points and two for the points surrounding the test load. The load on the area reached a total of 5500 tons on March 21, 1957.

FIGURE 50. TYPICAL MONUMENT

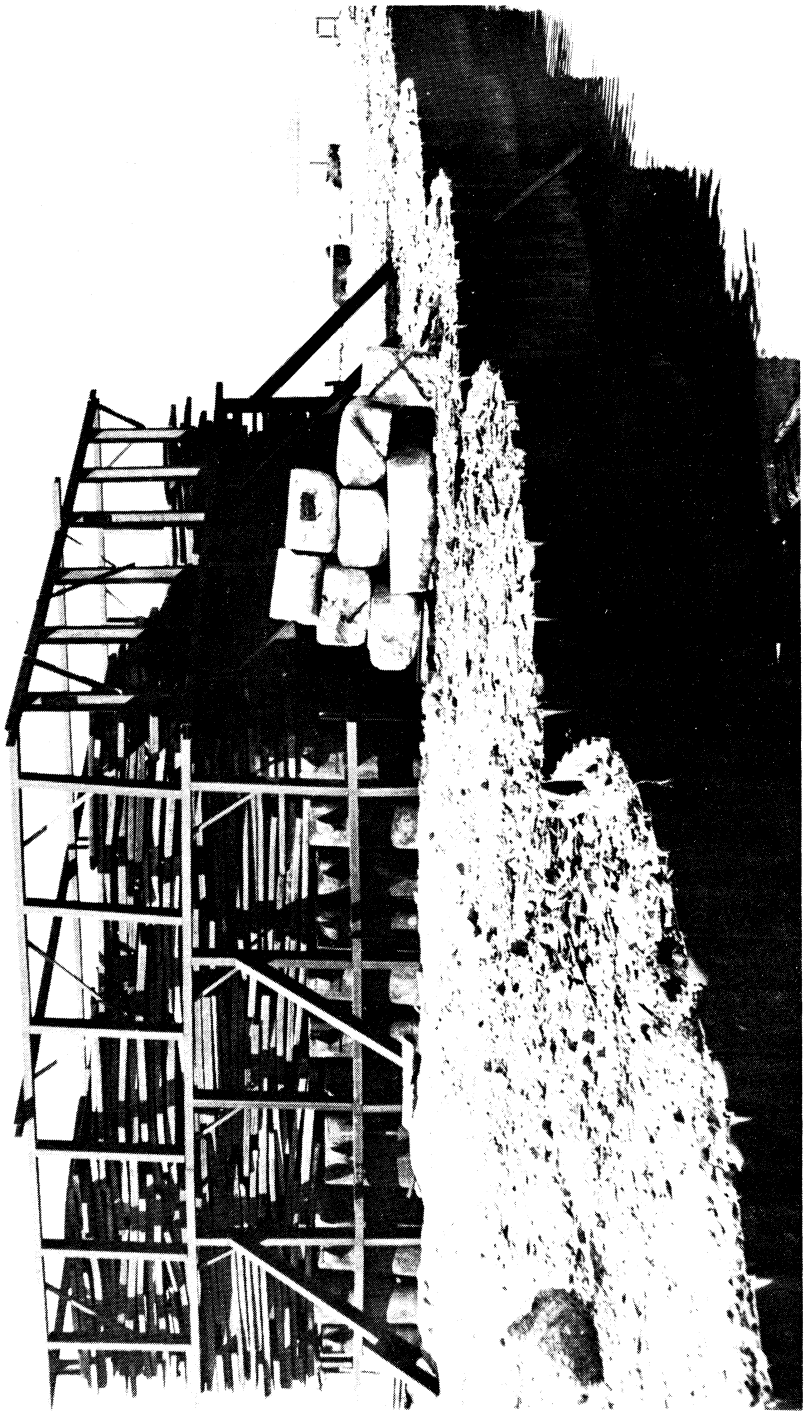

FIGURE 51. FRONT VIEW OF THE COFFERDAM LOADED

FIGURE 52. LOADS AND LOADED AREA BEHIND THE COFFERDAM

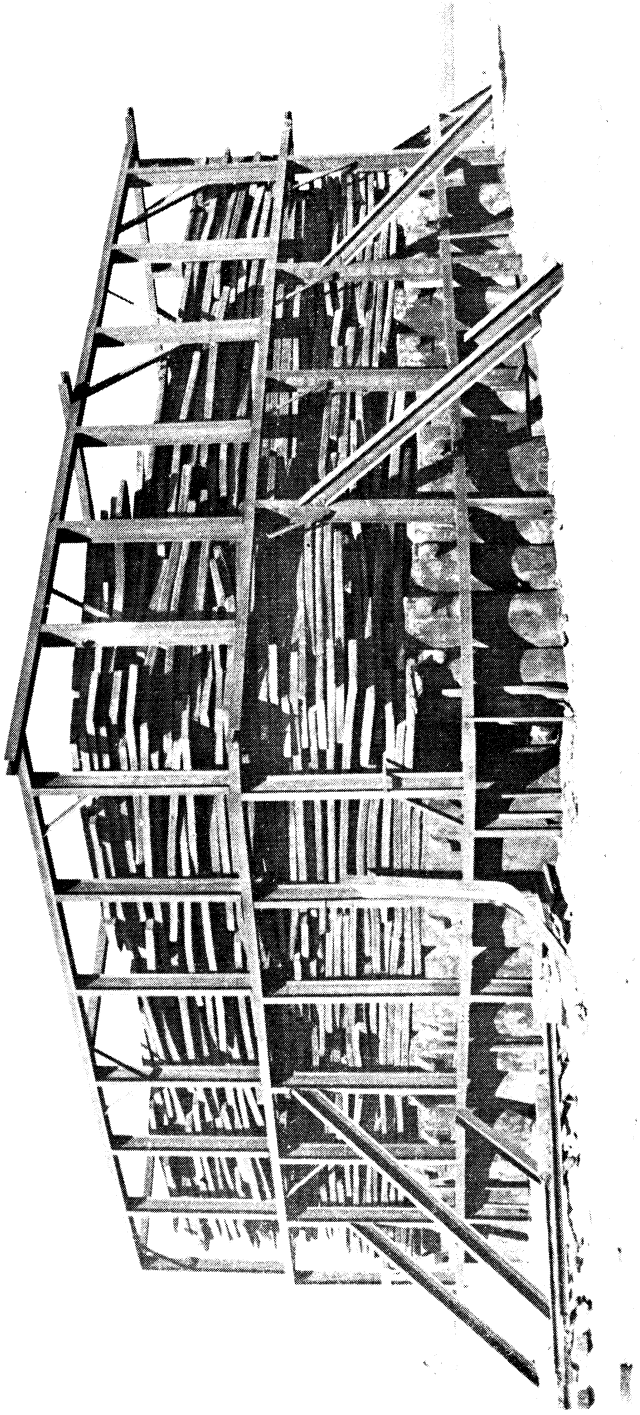

FIGURE 53. EAST CORNER OF LOADS & LOADED TEST AREA

FIGURE 54. NORTH CORNER OF LOADS & LOADED TEST AREA

The load of 5500 tons was left on the area for 64 days. During this period four readings were taken, on March 21, April 14, April 26, and May 24, 1957.

Then the unloading operation was started on May 24, 1957, continuing until August 3, 1957. At that date the unloading operation was stopped due to the breakage of the unloading crane. Thus the load was brought down to 3319 tons and was left for 29 days during which time three readings were taken, on August 3, August 17, and August 30, 1957.

Field Data on Test

The valuable data which were obtained from the field test were the vertical displacements of the monuments behind the cofferdam around the test area. The horizontal movement and the soundings were not taken except at the beginning, and then they were dropped out. In obtaining the level readings, a party of three members, instrument, rod and recording, were used. Each reading was taken twice. The instrument used for leveling has an accuracy of 0.001 feet.

The manner in which the readings were taken was by approaching from the bench mark, setting the instrument between P-3 and O-3 and sighting certain points, then closing with the first point sighted. By using point M-5 as a turn point, the second instrument setting was between K-5 and K-6. Then another set of points was sighted. The first point sighted in this setting was also sighted last for closing. By using point K-3 as a turn point, the third setting of the instrument was between D-2 and C-2. Then the remaining points were sighted (see Figure 55 for an illustration of this). This manner was kept fairly the same every time the readings were taken except once on January 24, 1957, when the

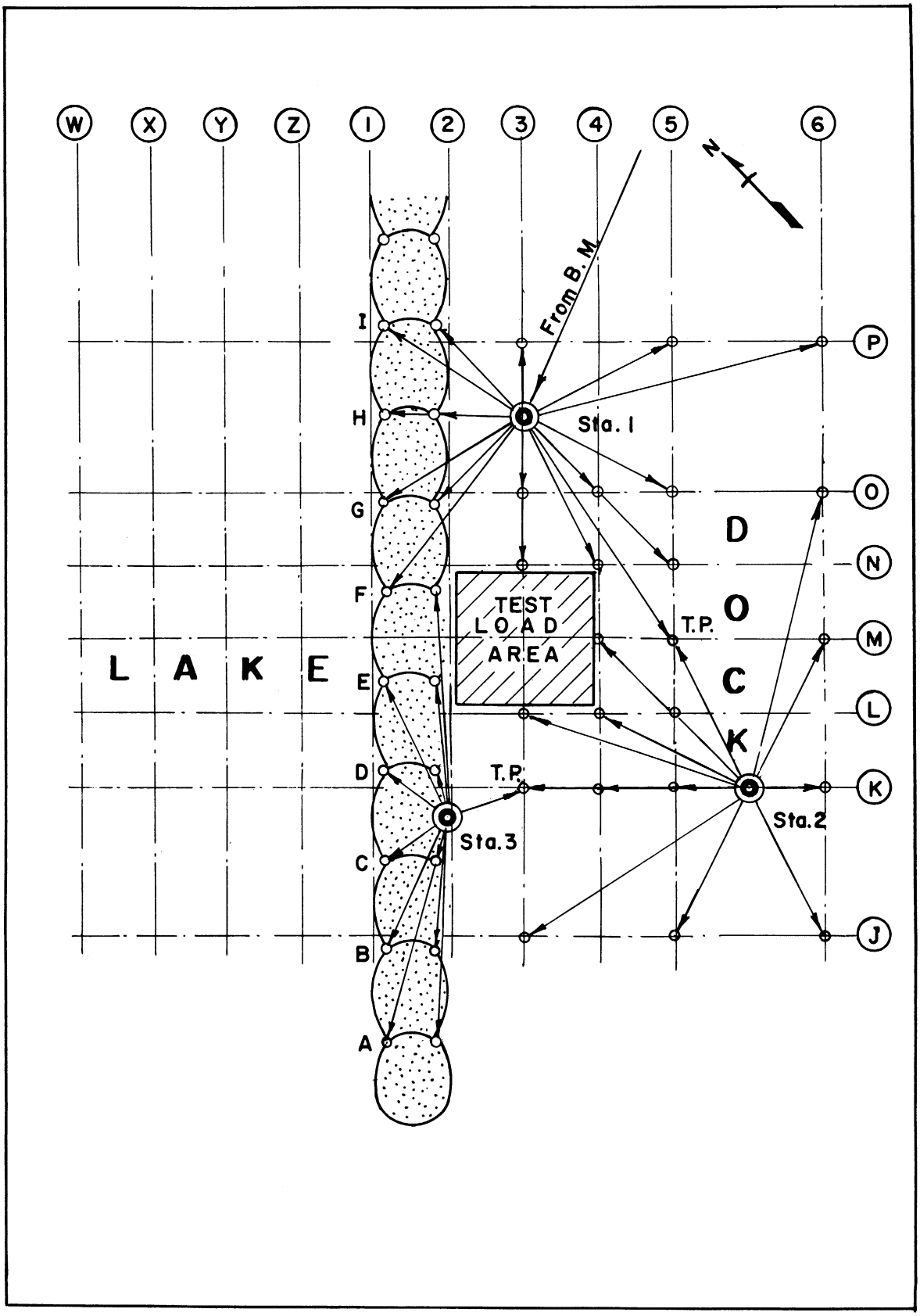

FIGURE 55.TYPICAL SETTINGS OF INSTRUMENT

same settings were used but some points which should have been sighted in the first setting were sighted in the third setting. Photo-static copies of the field notes were received from Inland Steel Company showing the manner of surveying, which aided in correcting some errors in the readings.

Appendix D lists a tabulation of the level readings during the various time intervals of the test period, starting on September 22, 1956 and ending on August 30, 1957.

Level Readings and Settlements

The settlements were obtained from the readings of the elevations of the monuments; these readings of the elevations, as received from Inland Steel Company, are shown in Appendix D.

The first reading, which was taken September 22, 1956, was considered as the basic reading of zero displacement. The settlement of each point at any time was taken as the difference between the reading at that time and the reading of September 22, 1956. This was true for readings taken before November 28, 1956. For readings taken after that date an adjustment was made. This adjustment is due to the welded spot on the monument. The adjustment factor was calculated as the difference between the first and second readings of November 28, 1956.

The settlements of each point are drawn on a settlement chart covering the period of time in which the readings were taken. In the settlement charts the settlements are drawn on the vertical axis with a scale of one inch equal to .025 feet against the time on the horizontal axis with a scale of one inch equal to fifty days. The settlement charts

are shown in Figures 56 to 71 and Figures 91 to 115. Figures 91 to 115 are in Appendix C. In the settlement charts the graph indicated by "Actual Settlement" represents the settlement ordinate based on the actual readings as discussed above. In the level readings there were a very few mistaken readings of the rods, which were easy to detect, as they were much greater than the range of the displacement; that is the error was in terms of feet and not in thousandths of a foot.

A careful examination of the settlement charts shows that in a group of points, at a certain date, the settlement ordinates increased or decreased by a constant value which is greater than the range of settlement taking place. This change in the settlement ordinates is approximately constant throughout certain groups of points. Clear examples of this are the settlement ordinates on October 2, 1956, for the points A-1, A-2, B-1, B-2, C-1, C-2, D-2, E-1, E-2, and F-2; the settlement ordinates on December 27, 1956, for the points F-1, G-1, G-2, H-1, H-2, I-1, I-2, P-3, P-5, P-6, O-3, O-4, O-5, N-3, and N-4; and the settlement ordinates on April 26, 1957, for the points K-3, K-4, K-5, K-6, M-4, M-5, M-6, O-6, L-5, J-5, and J-6. The points in each example are sighted in one particular setting of the instrument on that particular date. The points in the first example are those points sighted from the third setting of the instrument, from the third station, on October 2, 1956; the points in the second example are those points sighted from the first setting of the instrument, from the first station, on December 27, 1956; and the points in the third example are those points sighted from the second

setting of the instrument, from the second station, on April 26, 1957. The fact that there was a constant error in each setting of the instrument shows that this error is due to the height of the instrument. Thus, a correction factor was introduced in order to compensate for this error.

The correction method was based on the following two assumptions. The first assumption is that the outer points, those on rows P, J, 6, and 1, which are at a distance greater than 48.5 feet from the boundary of the test load area, will not be affected by the loading; therefore, they will have no vertical displacement. This assumption is based on the fact that, if an upheaval will take place, the failing element will have a depth not greater than 48.5 feet, due to the stiff clay stratum below elevation 495.0. Thus the outer points are outside the failing element. The only load which is affecting these points is the weight transfer above the loading plane. In order to have the effect of weight transfer developed, the resistances above and below the loading plane must be fully mobilized. This in turn will take a long period of time because of the size of the test load area.

The second assumption is that, in determining the correction factor for each setting, the settlements to be considered must be within a reasonable range, usually .010 foot, which is the range of the possible error.

The correction factor for each setting of the instrument, which is to compensate for the error in the height of the instrument, was determined by taking the algebraic summation of the settlements of those outer points which were within a reasonable range and any other

point which had a settlement of less than .010 foot. Then this summation was divided by the number of points which had the same algebraic sign as that of the summation. This method of correction indicated a reasonable correction when the corrected settlements were plotted on the settlement charts. The corrected settlements are indicated by dotted lines on the settlement charts and called "Corrected Values."

However, there were a few cases where a correction factor was not applied to a particular settlement of a particular point, and the actual reading was left as it was. This was done whenever a particular point which was sighted in a particular setting of the instrument, due to other compensating errors, did not have the same deviation possessed by the rest of the points which were sighted in the same instrument setting. Several examples of this can be shown for the examples given on page 145. In the first example, point D-1 did not possess the same error as the rest of the points sighted in the same setting of the instrument, and thus the correction factor was not applied to it. In the second example, point N-5 did not possess the same error as the rest of the points sighted in the same setting of the instrument, and thus, the correction factor was not applied to it. Finally, in the third example, the points J-3, L-3, and L-4 did not possess the same error as the rest of the points sighted in the same setting of the instruments, and thus, the correction factor was not applied to them. Also, the correction factor was not applied in a few other cases where the application of the correction factor led to greater error as indicated by the pattern of the prior and subsequent settlements of that point.

The points on the boundary of the test load area and those within 48.5 feet of the boundary of the test load area had a measurable displacement greater than the possible error (See Figures 56 to 71), and they were used in determining the rates of settlement. The outer points, those on rows P, J, 6, and 1, which were assumed to have a zero displacement, are shown in Figures 91 to 115 in Appendix C. These points were used in determining the correction factor but were not used in determining the rates of settlement because the settlement ordinates of these points fell within the range of error as shown in the settlement charts.

Figure 72 shows the contours of the total vertical displacement up to January 24, 1957. Figure 73 shows the contours of the total vertical displacements up to May 24, 1957, and Figure 74 shows the contours of the total vertical settlements up to August 30, 1957. The contour lines indicate an interval of .25 inch displacement. The dotted contours are estimated to be in the manner they are shown.

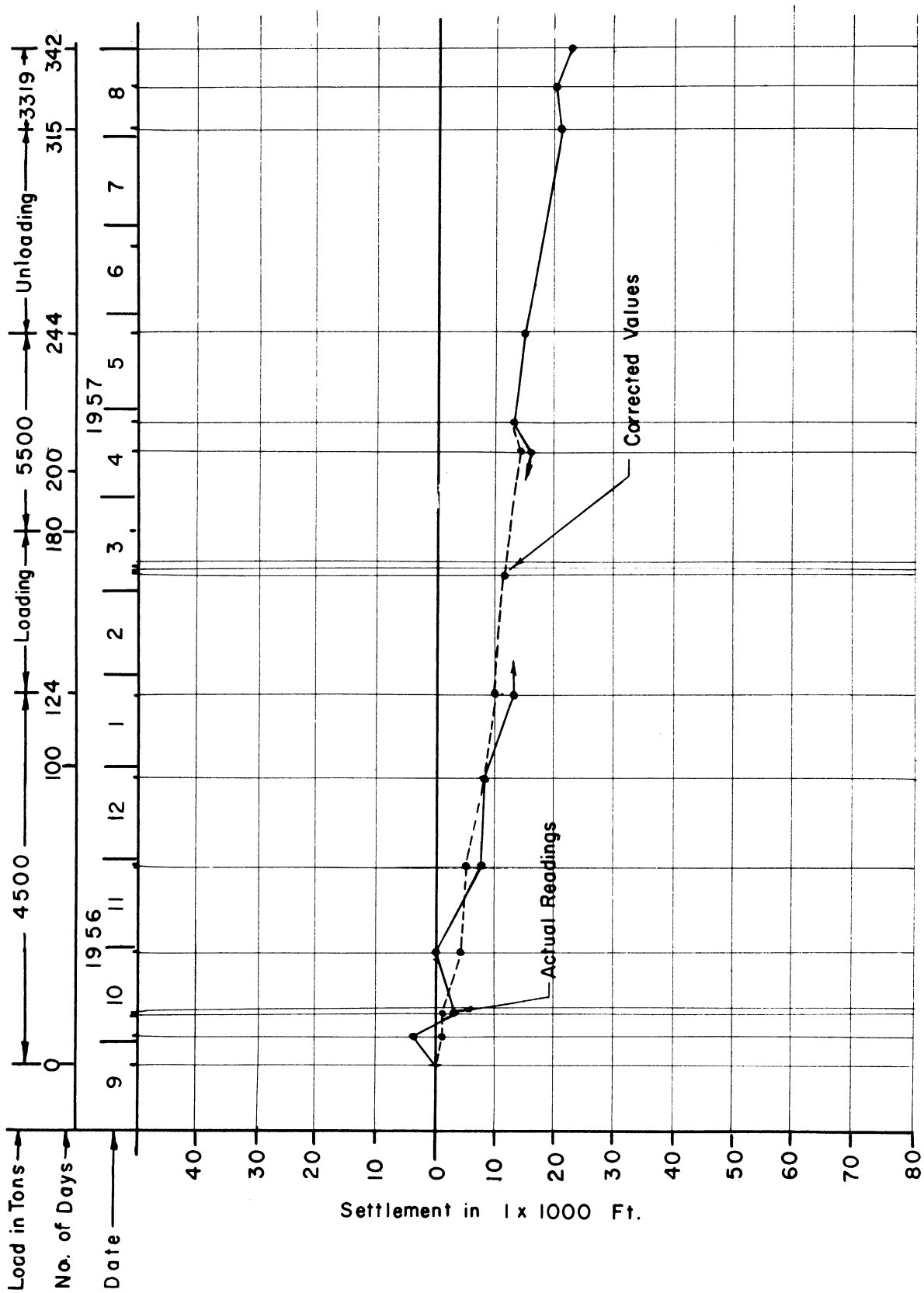

FIGURE 56. SETTLEMENT OF POINT E-2

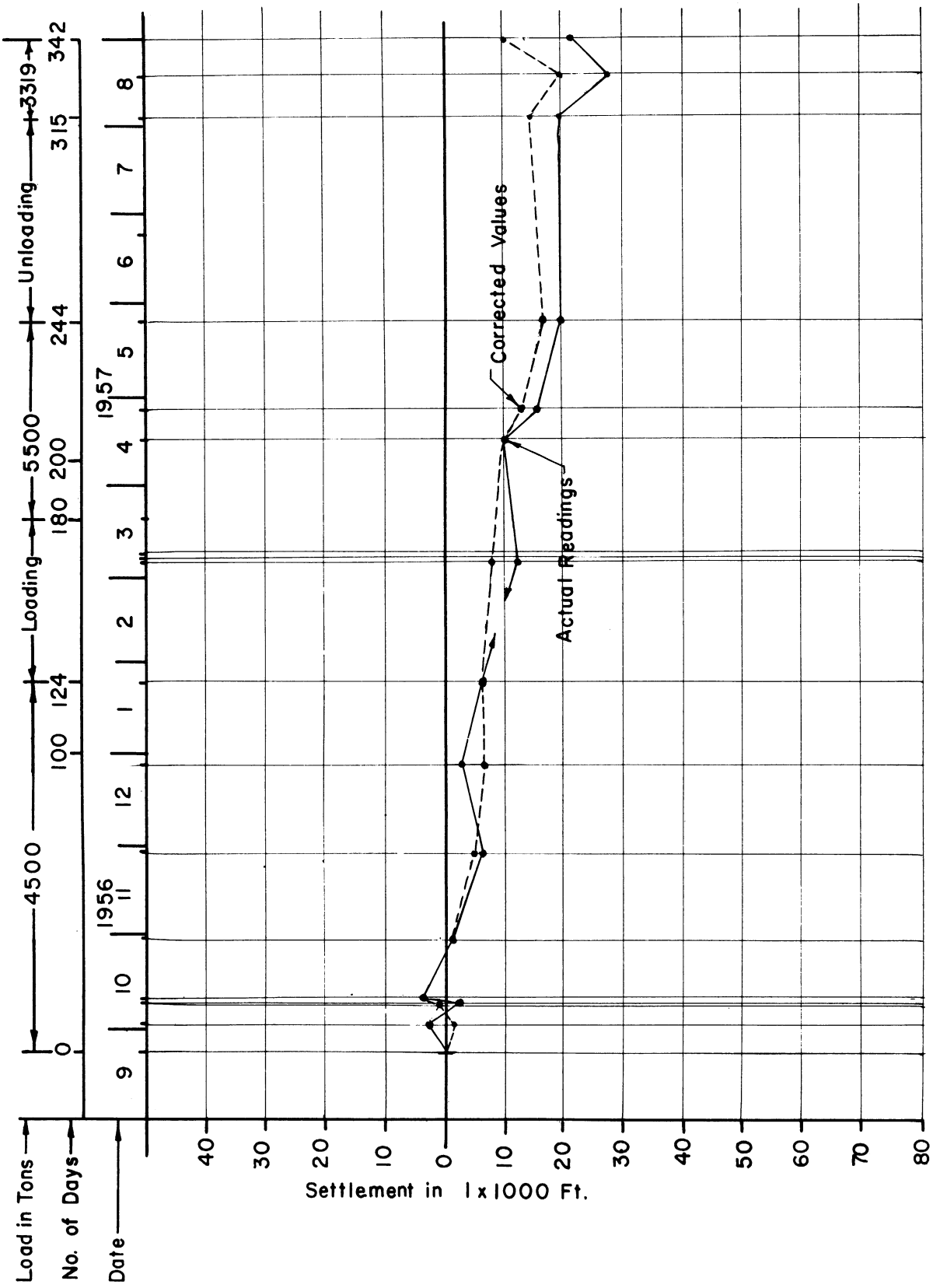

FIGURE 57. SETTLEMENT OF POINT F-2

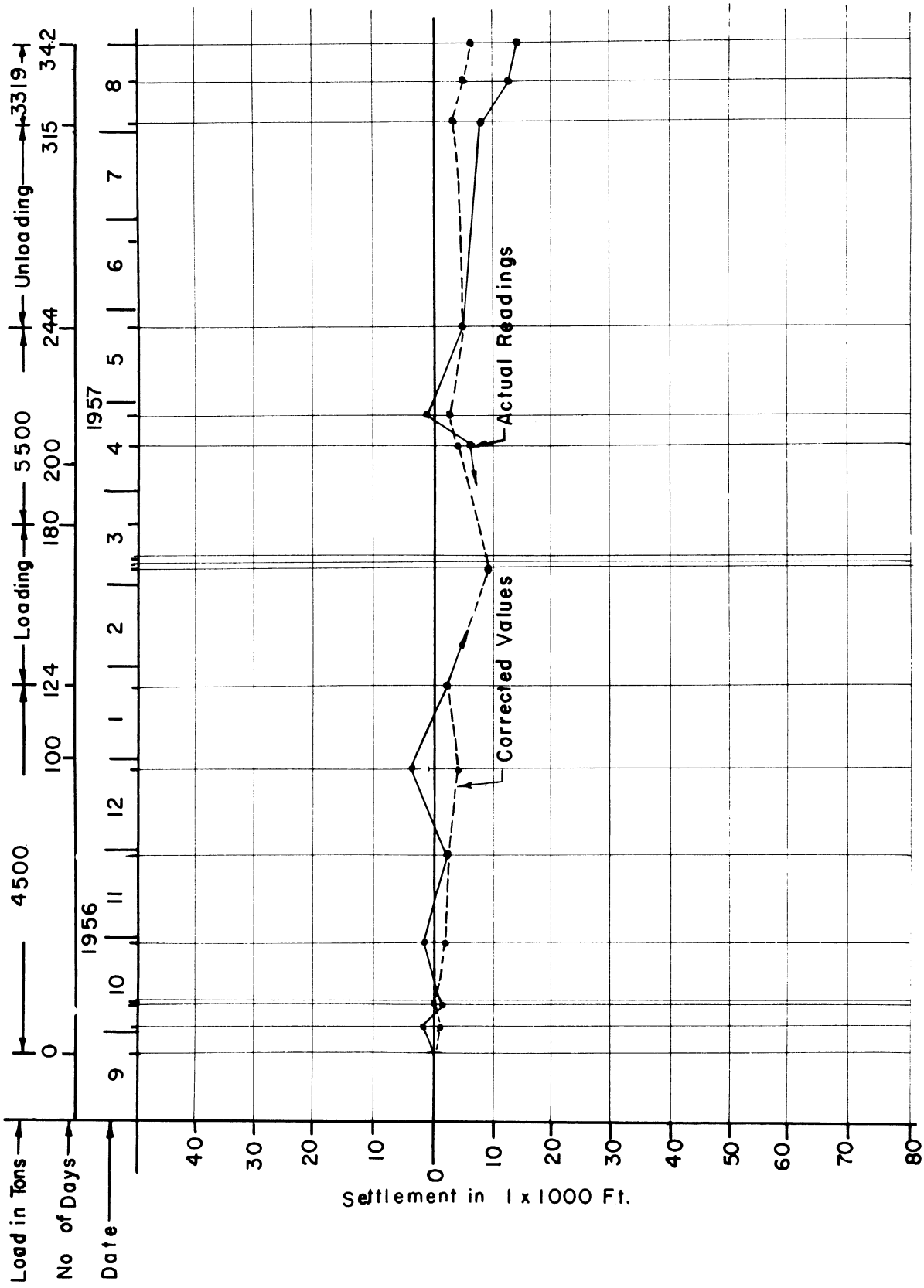

FIGURE 58. SETTLEMENT OF POINT K - 3

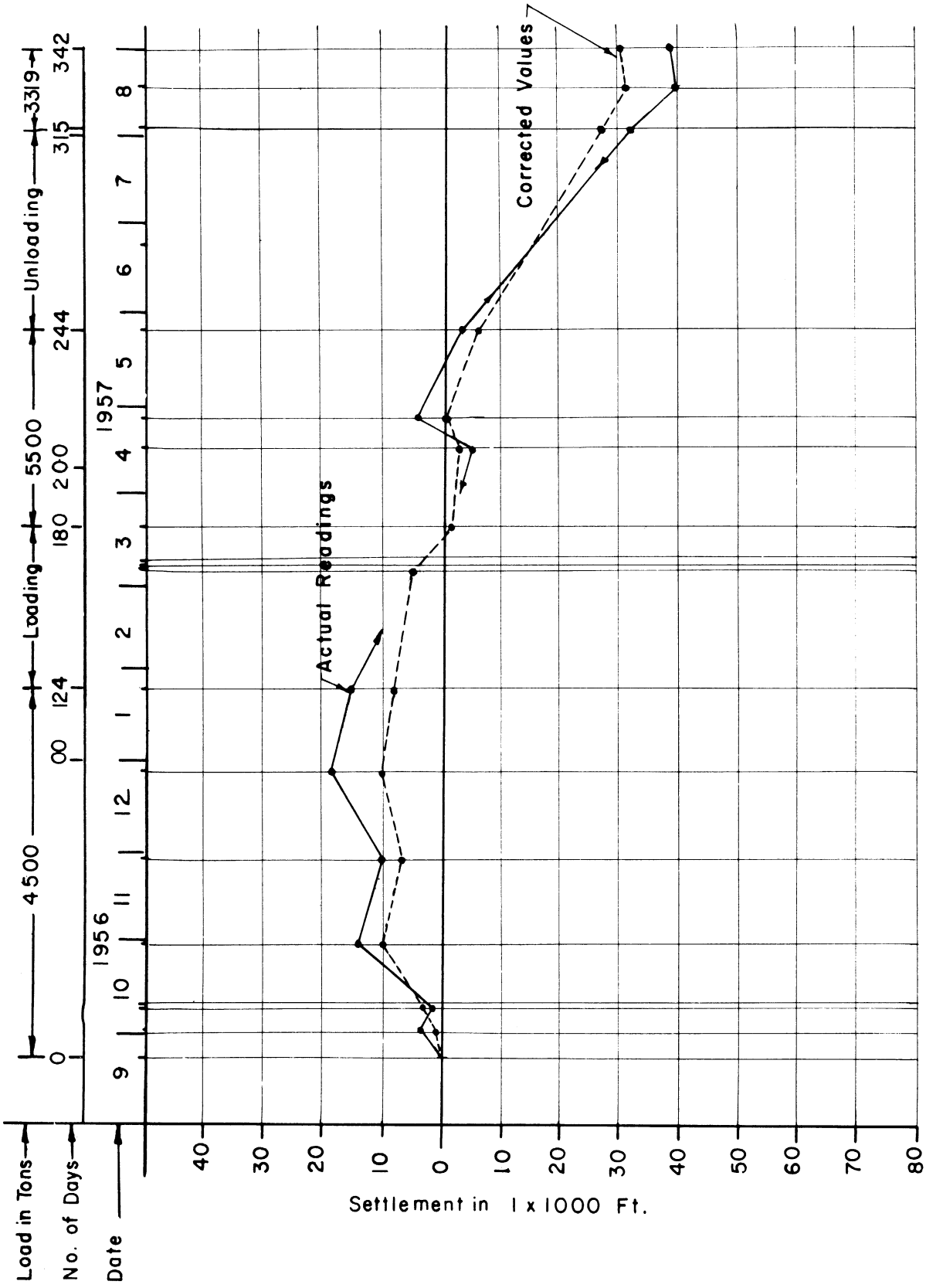

FIGURE 59. SETTLEMENT OF POINT K-4

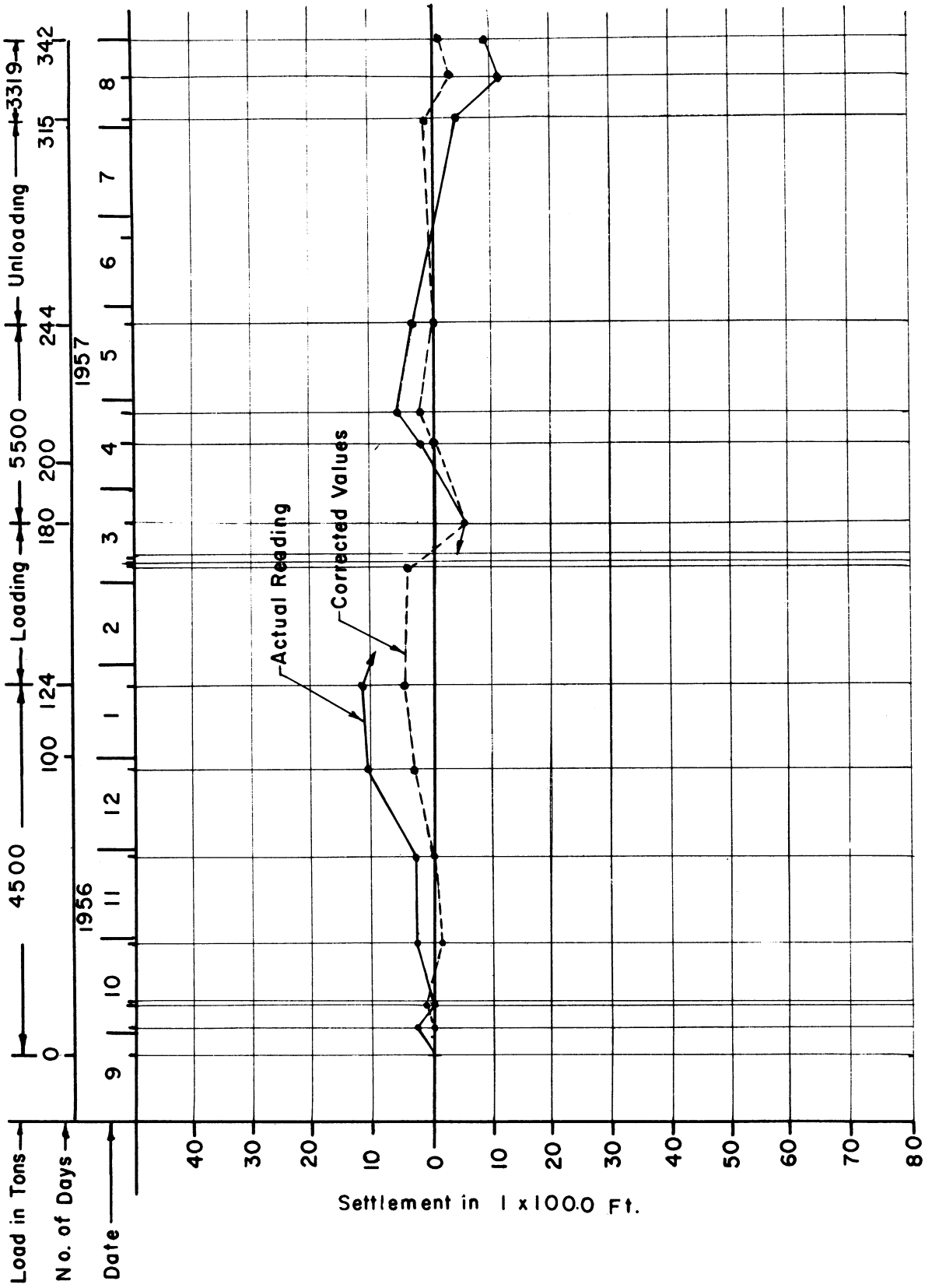

FIGURE 60. SETTLEMENT OF POINT K-5

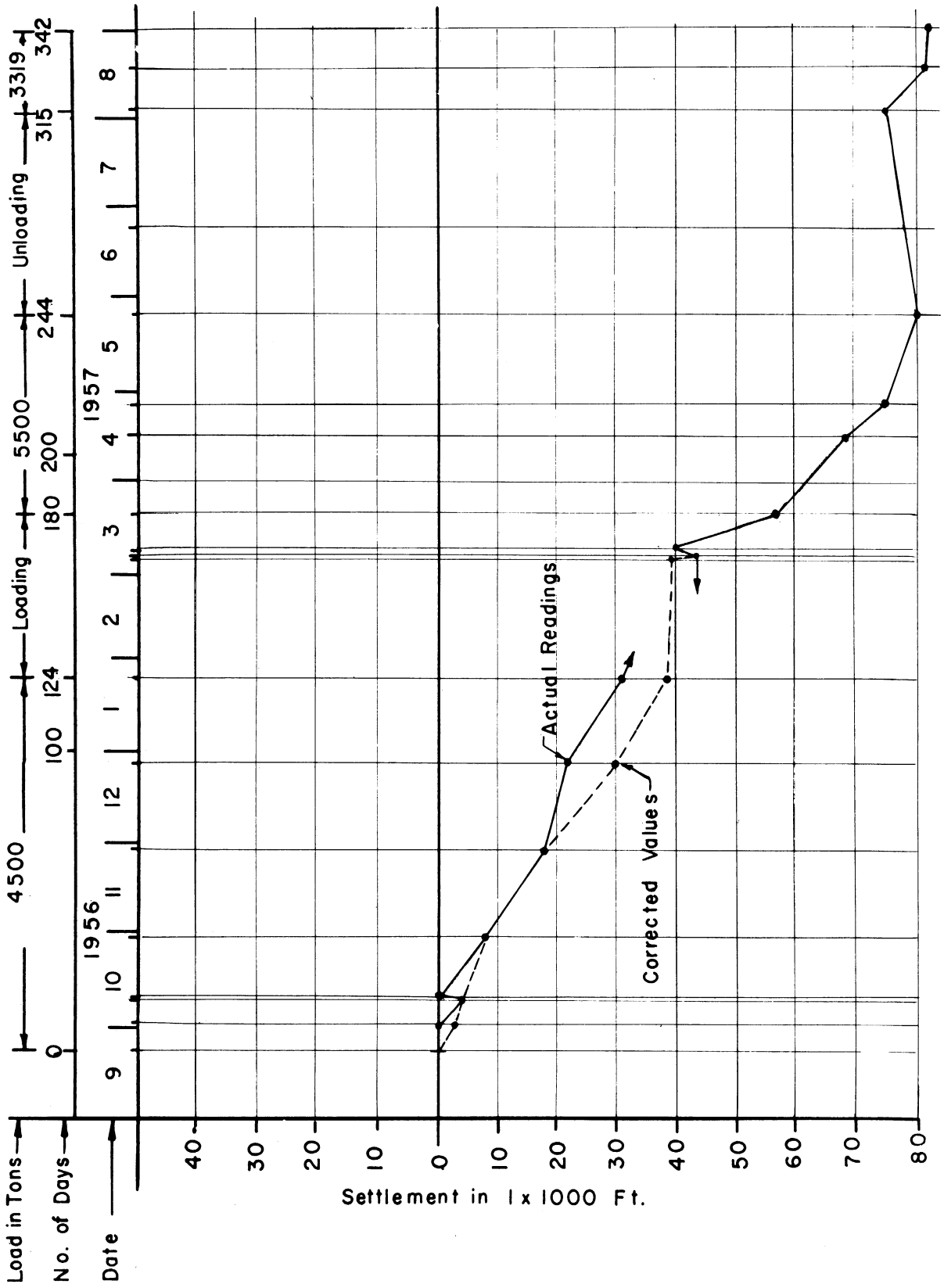

FIGURE 61. SETTLEMENT OF POINT L-3

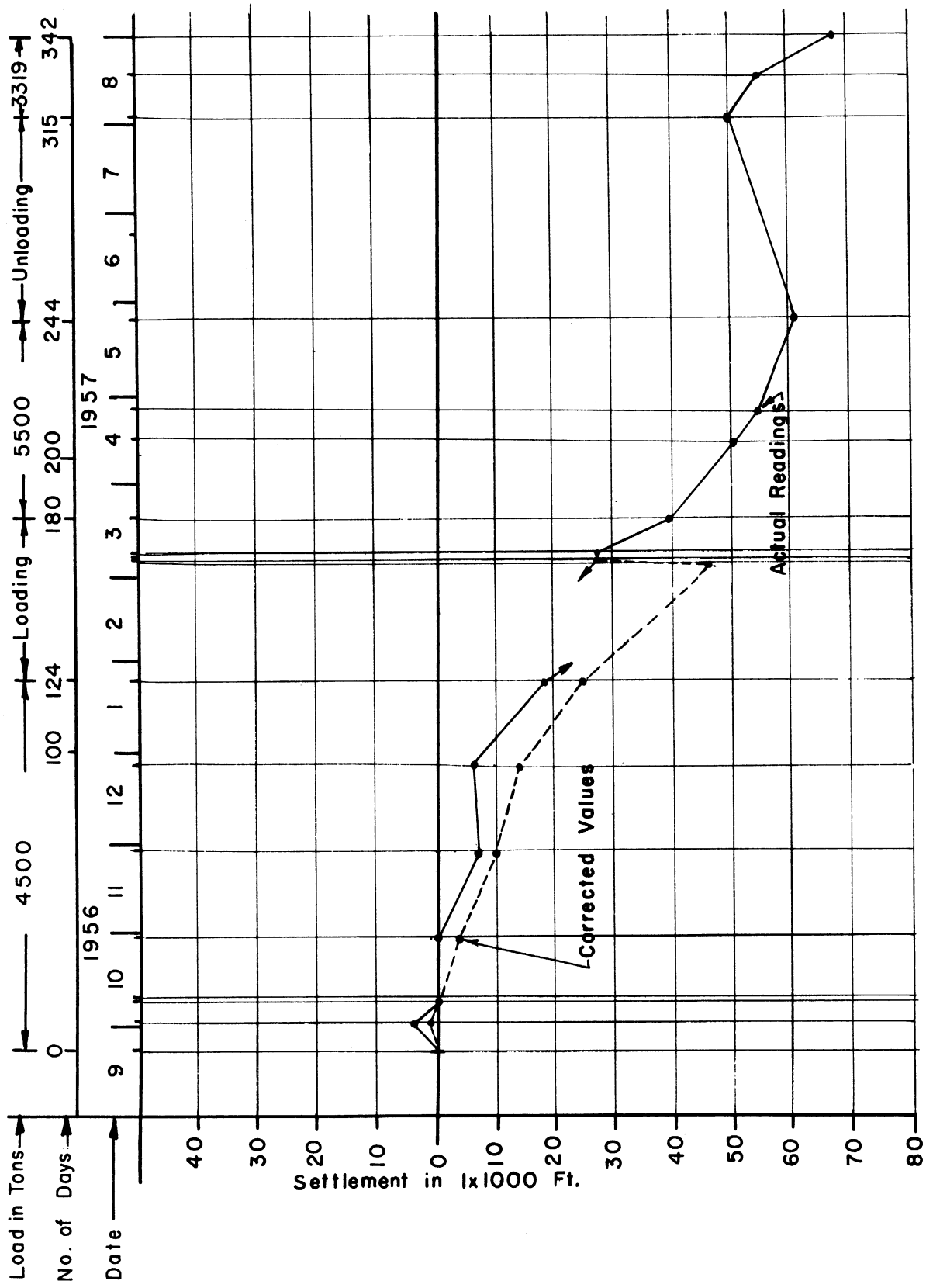

FIGURE 62. SETTLEMENT OF POINT L-4

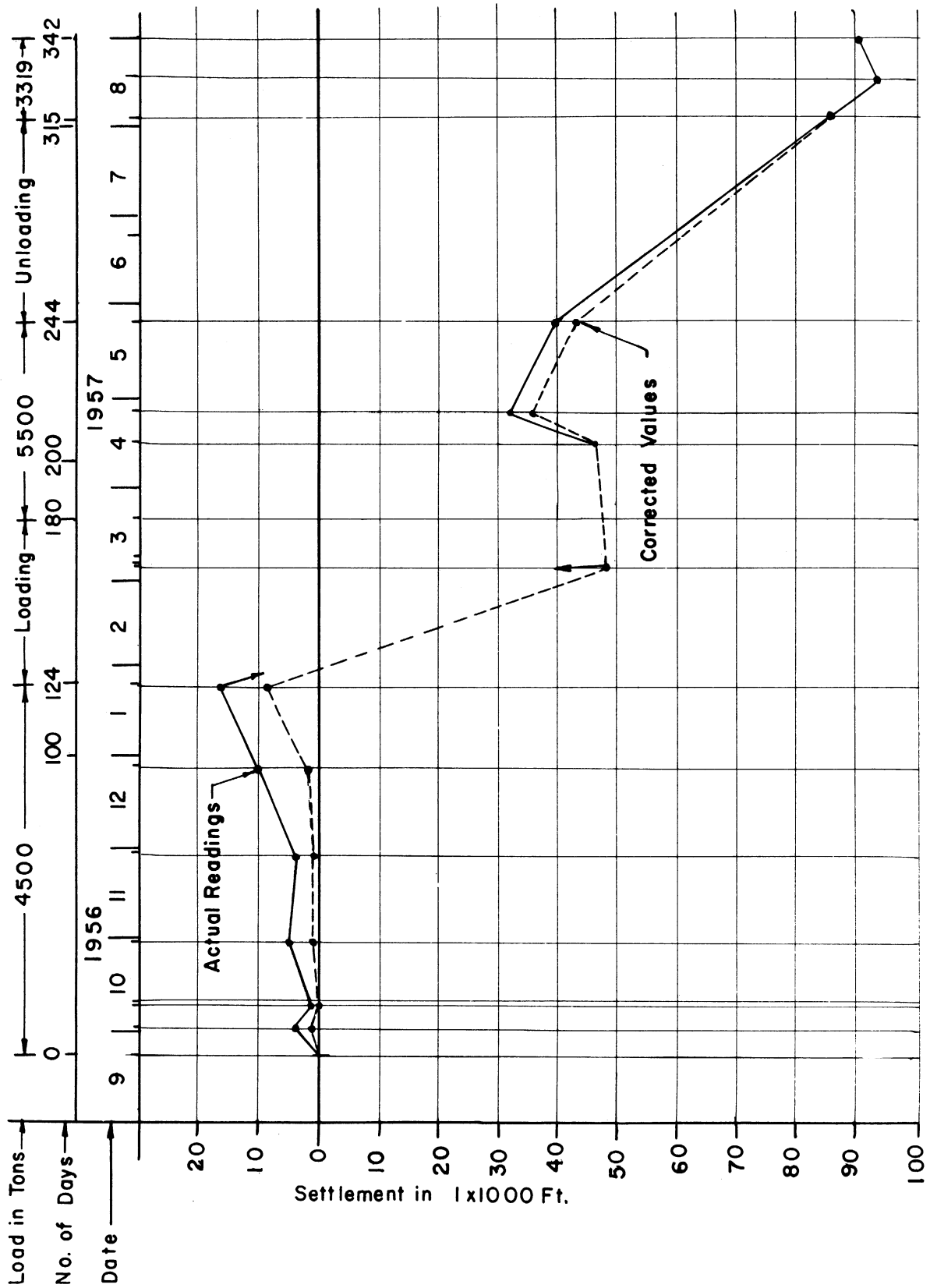

FIGURE 63. SETTLEMENT OF POINT L-5

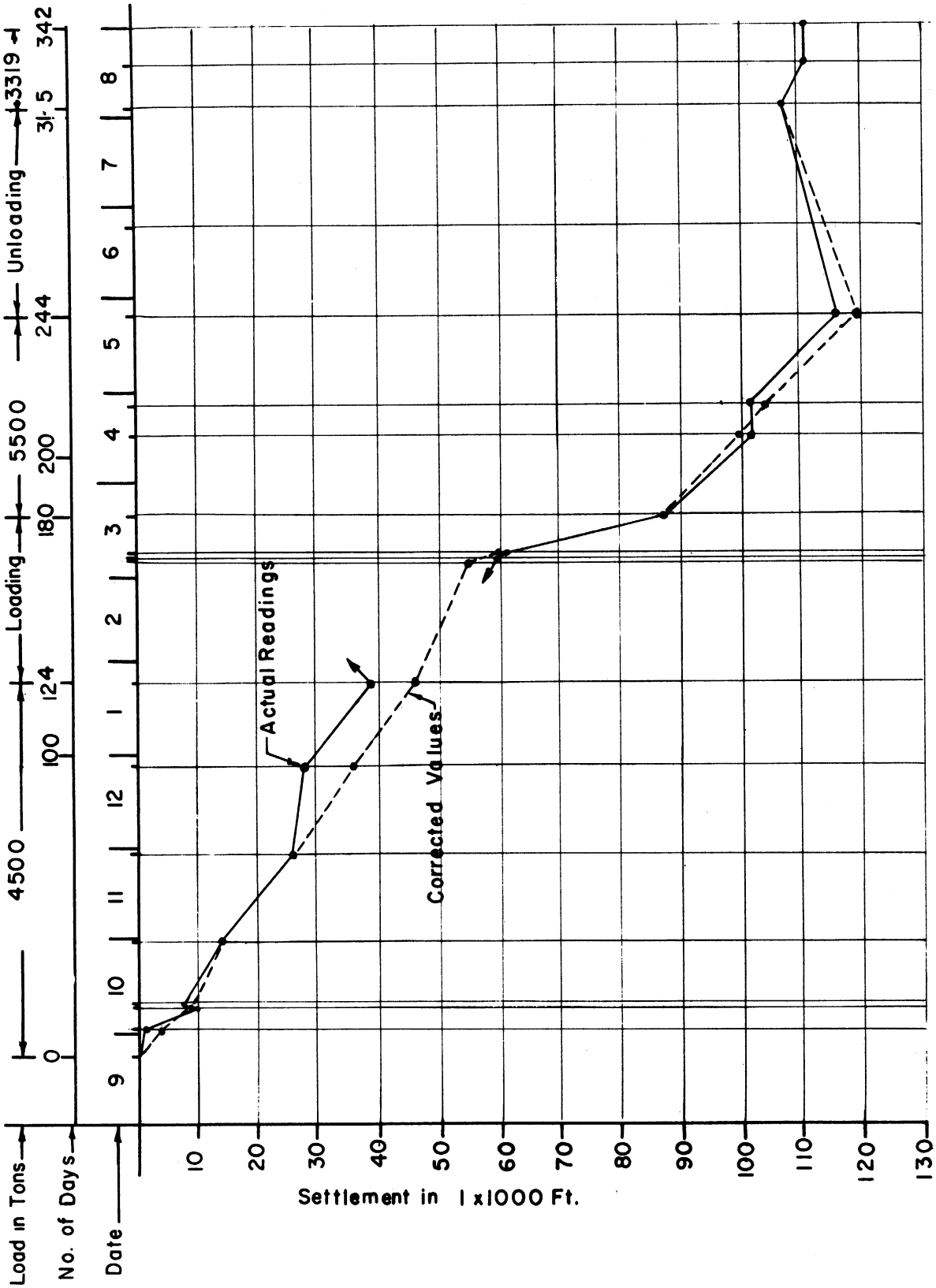

FIGURE 64. SETTLEMENT OF POINT M-4

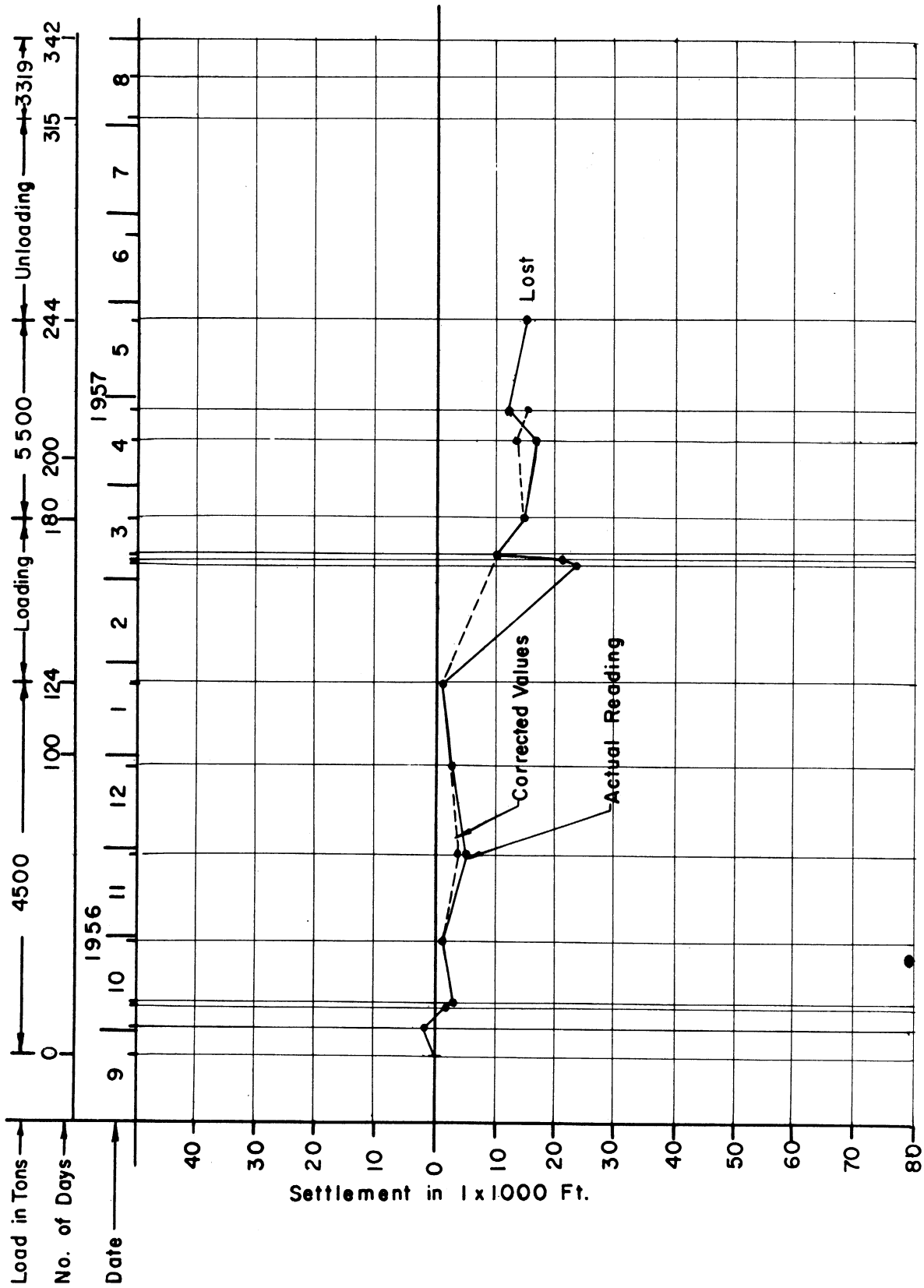

FIGURE 65. SETTLEMENT OF POINT M-5

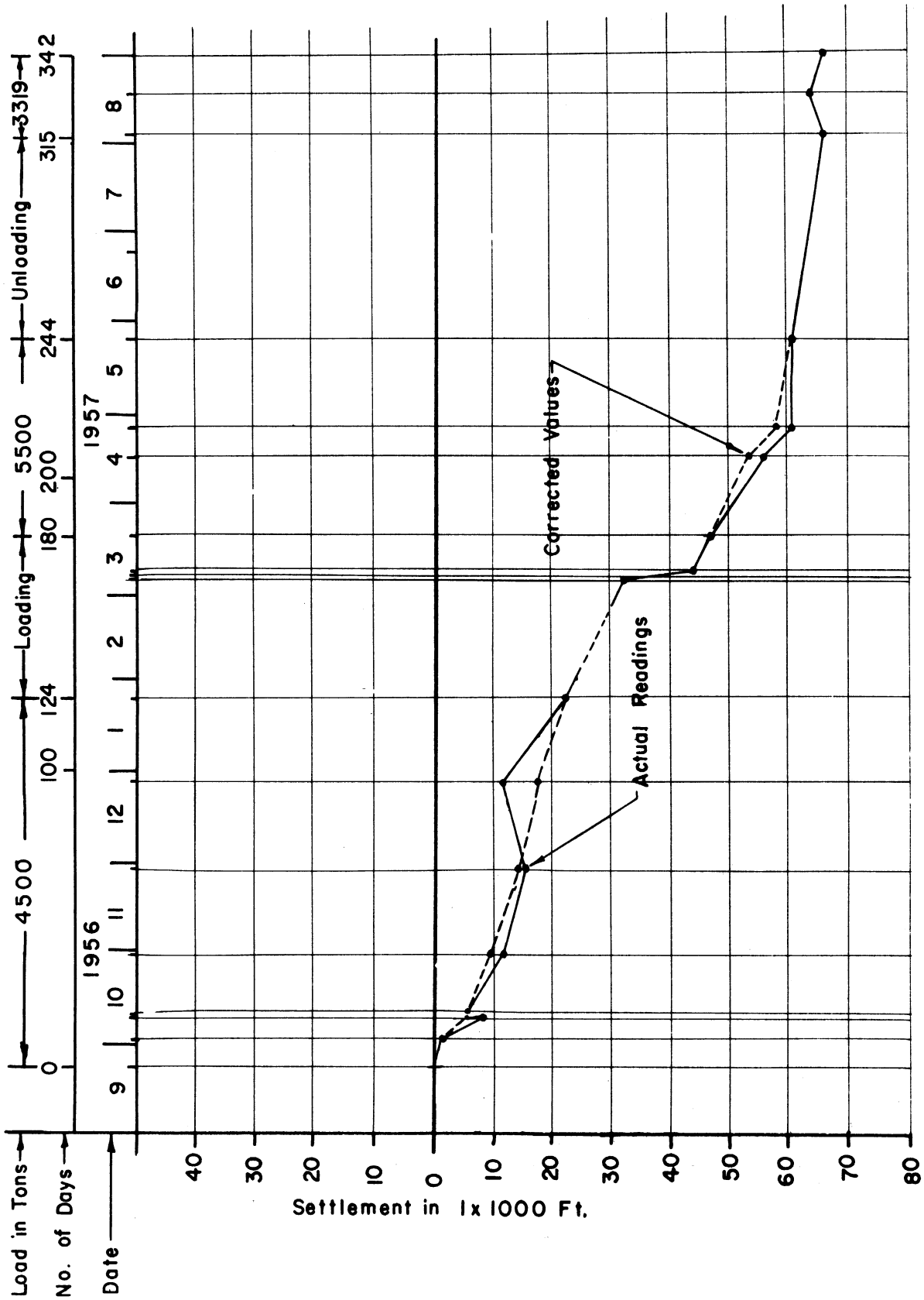

FIGURE 66. SETTLEMENT OF POINT N-3

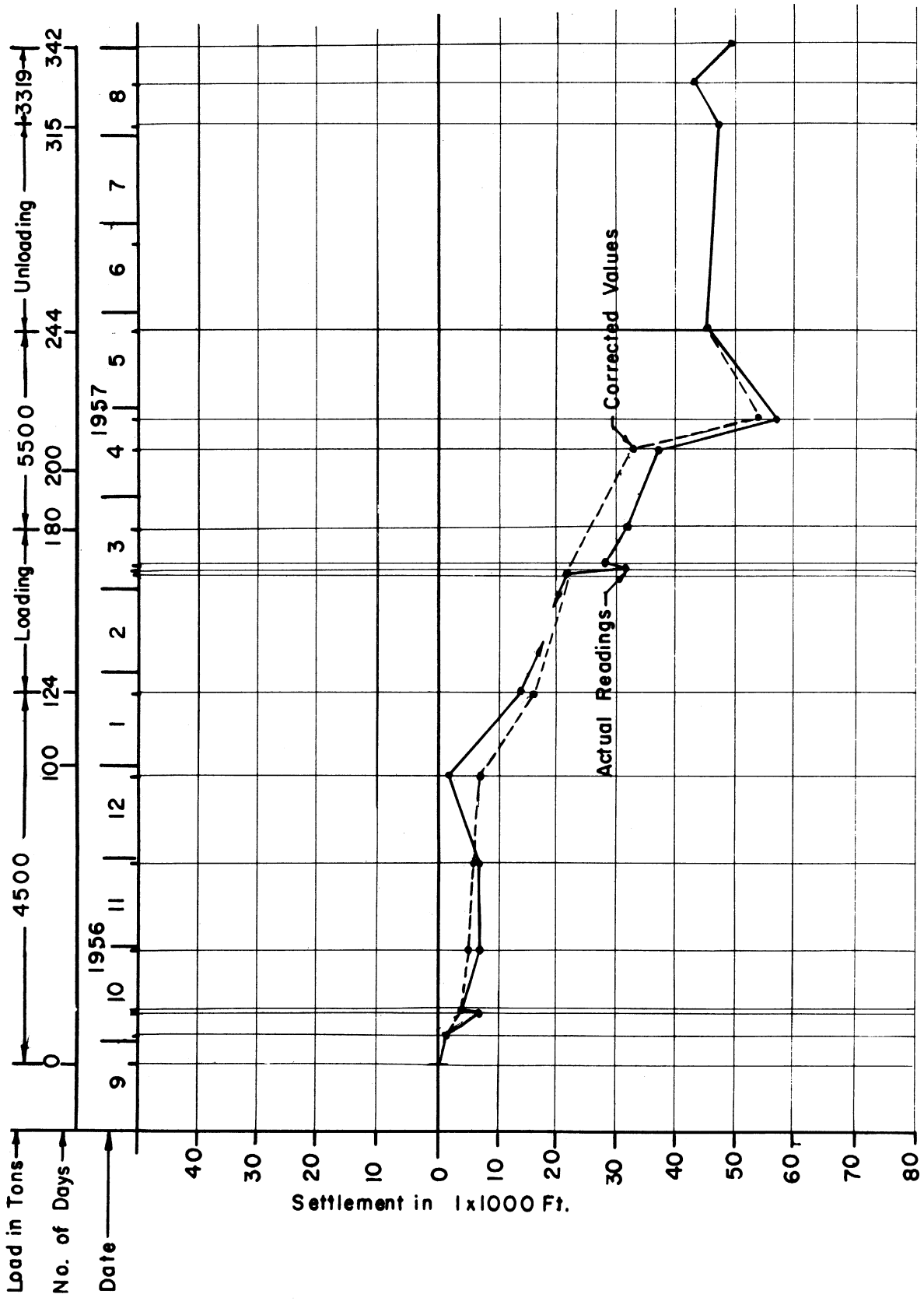

FIGURE 67. SETTLEMENT OF POINT N-4

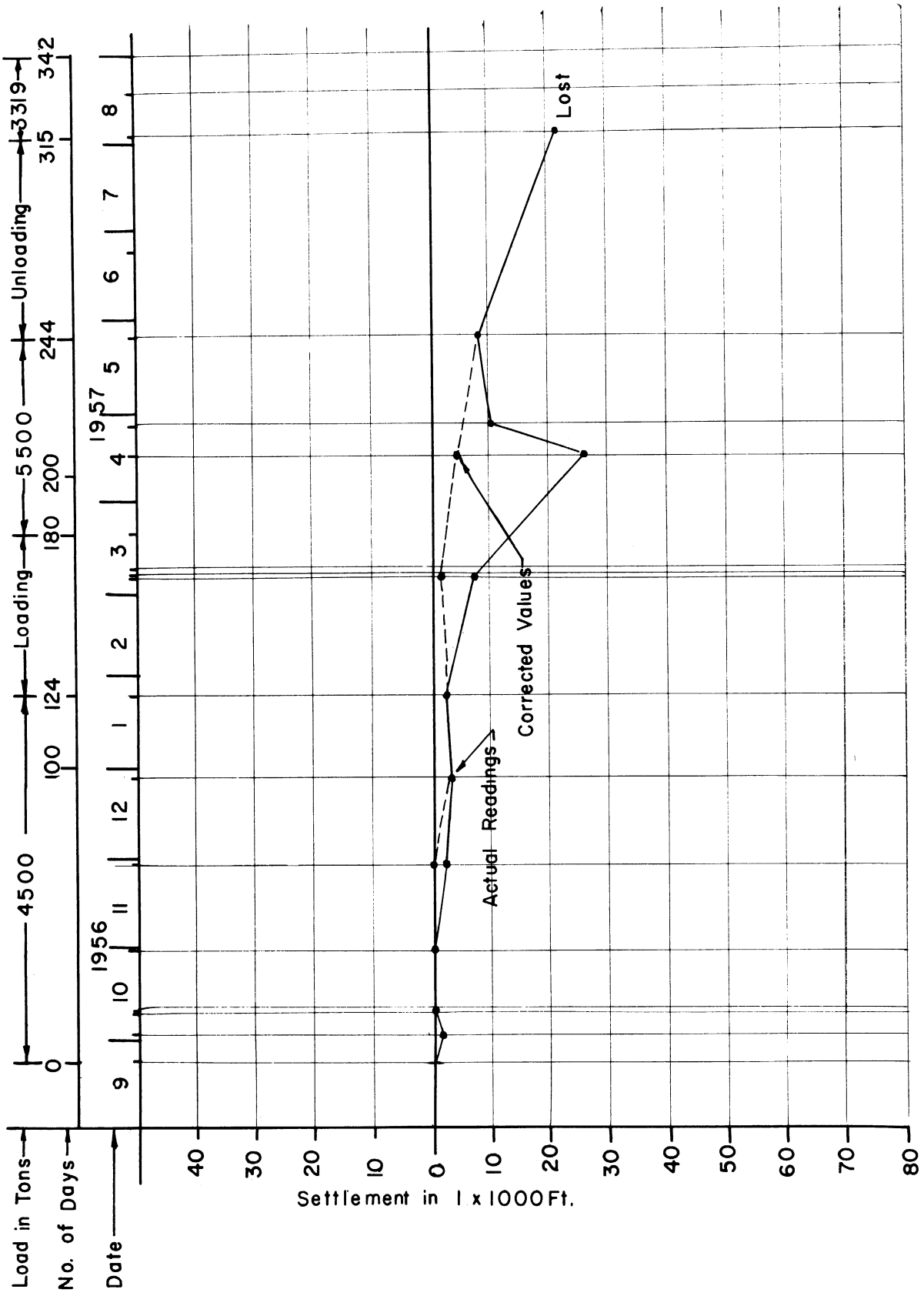

FIGURE 68. SETTLEMENT OF POINT N-5

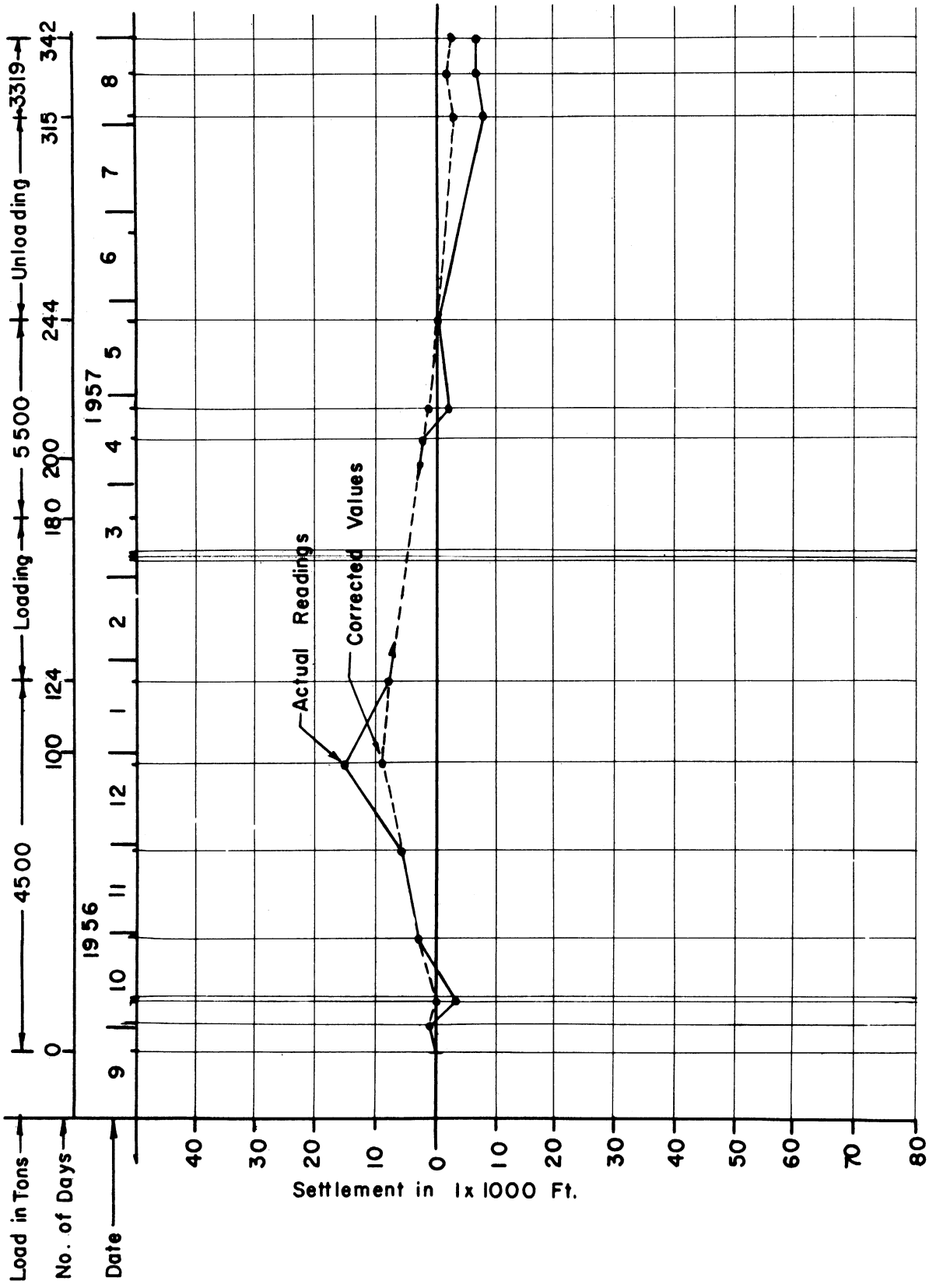

FIGURE 69. SETTLEMENT OF POINT O-3

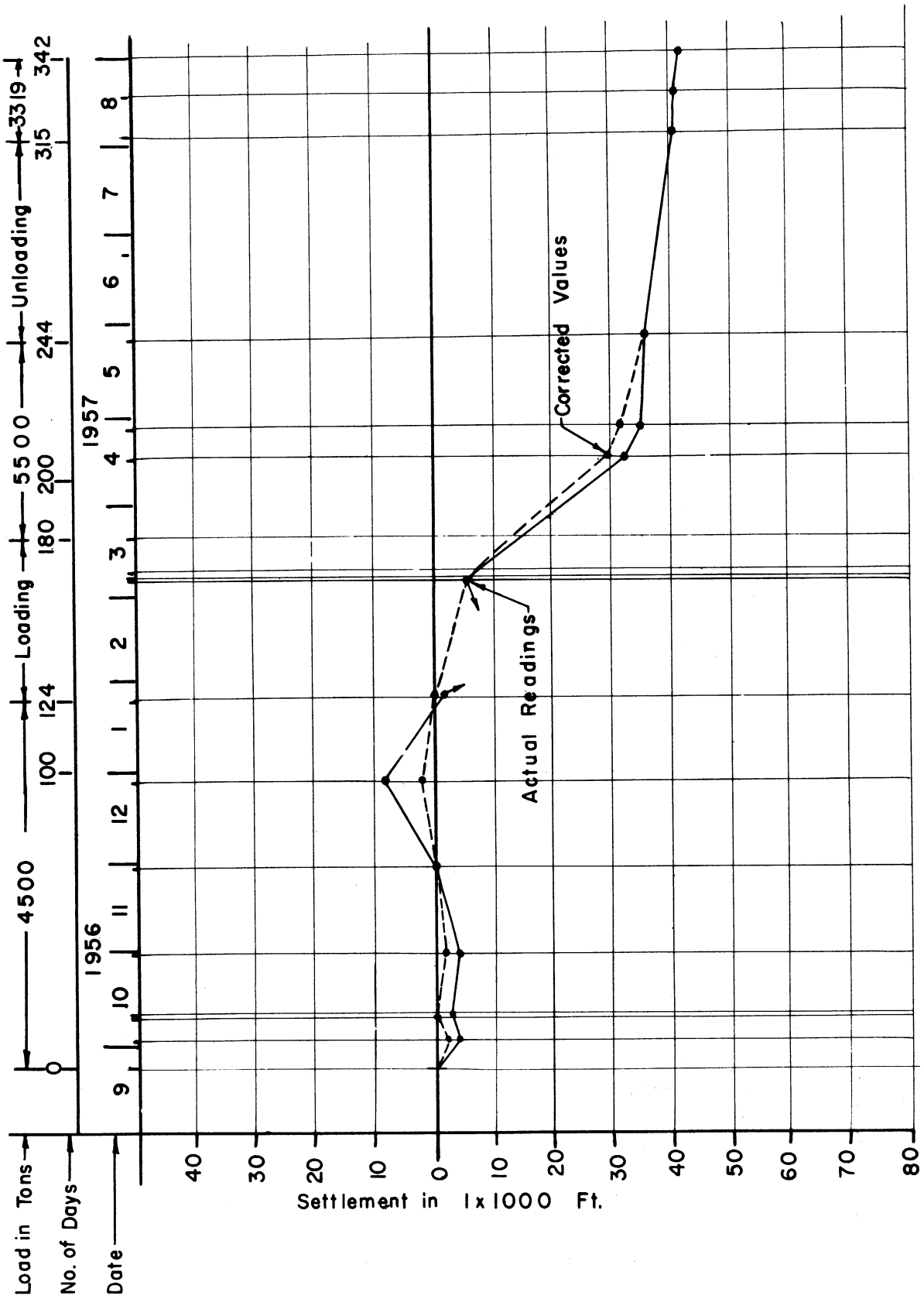

FIGURE 70 . SETTLEMENT OF POINT 0-4

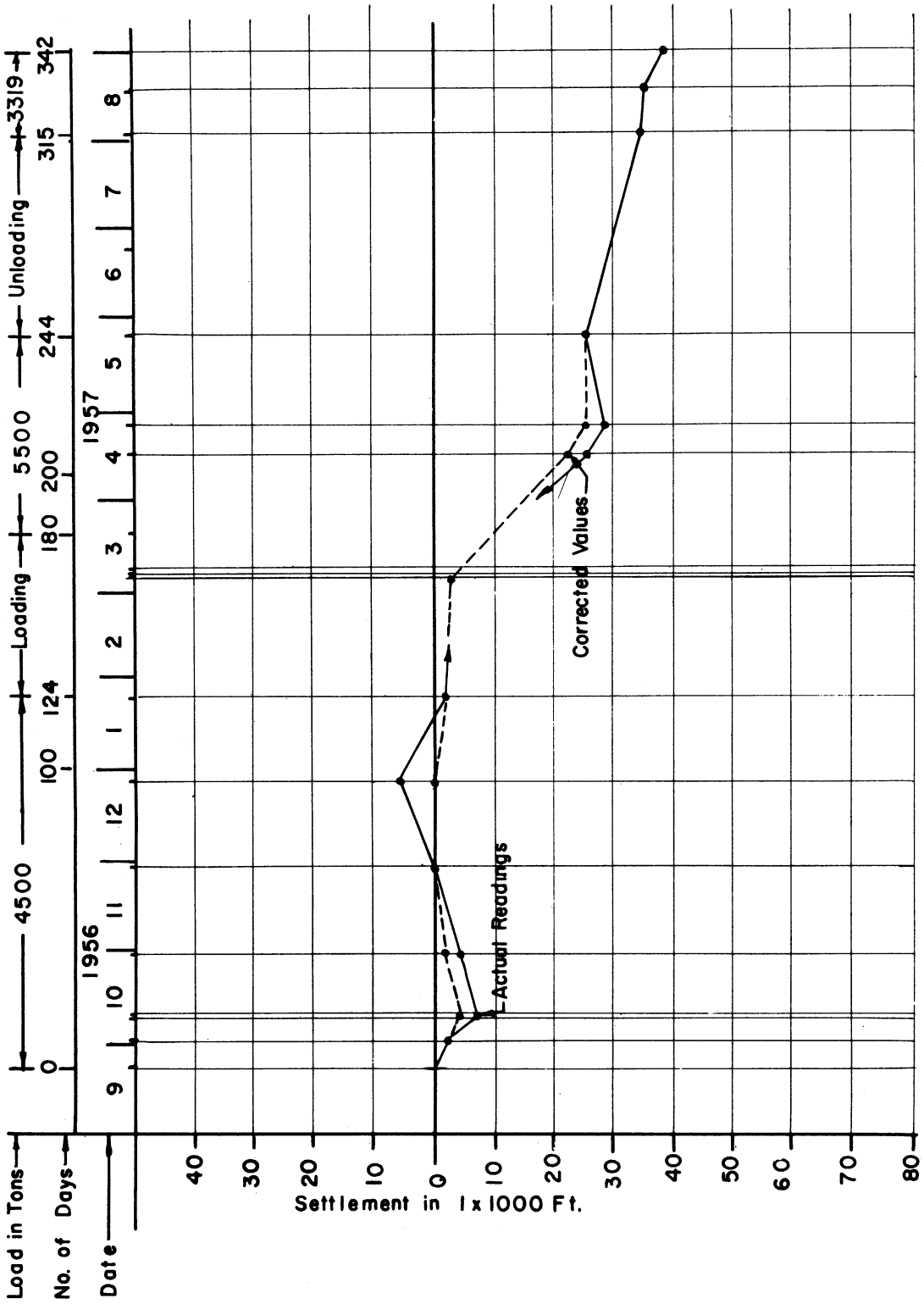

FIGURE 71 . SETTLEMENT OF POINT O-5

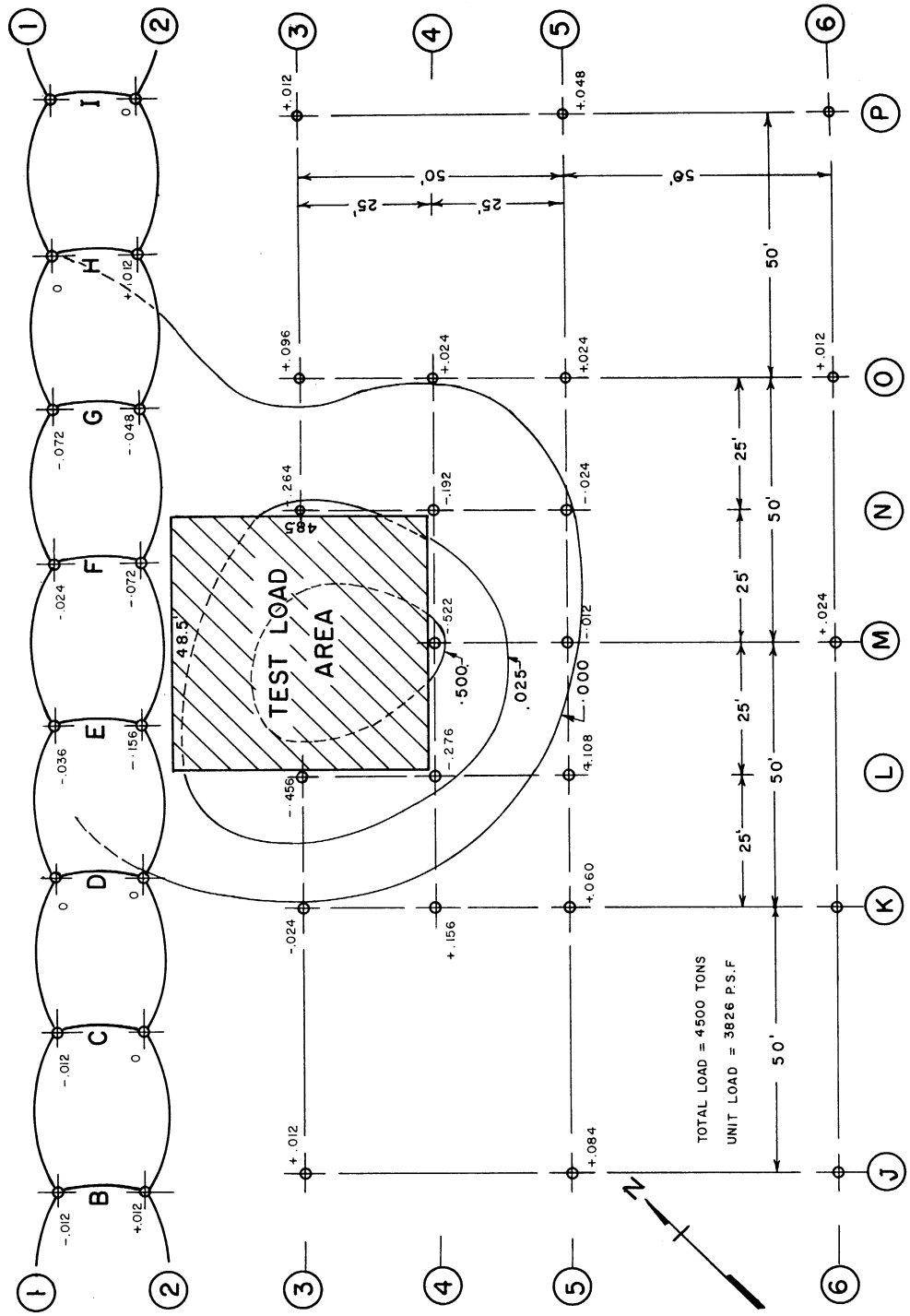

FIGURE 72. TOTAL SETTLEMENTS CONTOURS FROM 9-22-1956 TO 1-24-1957

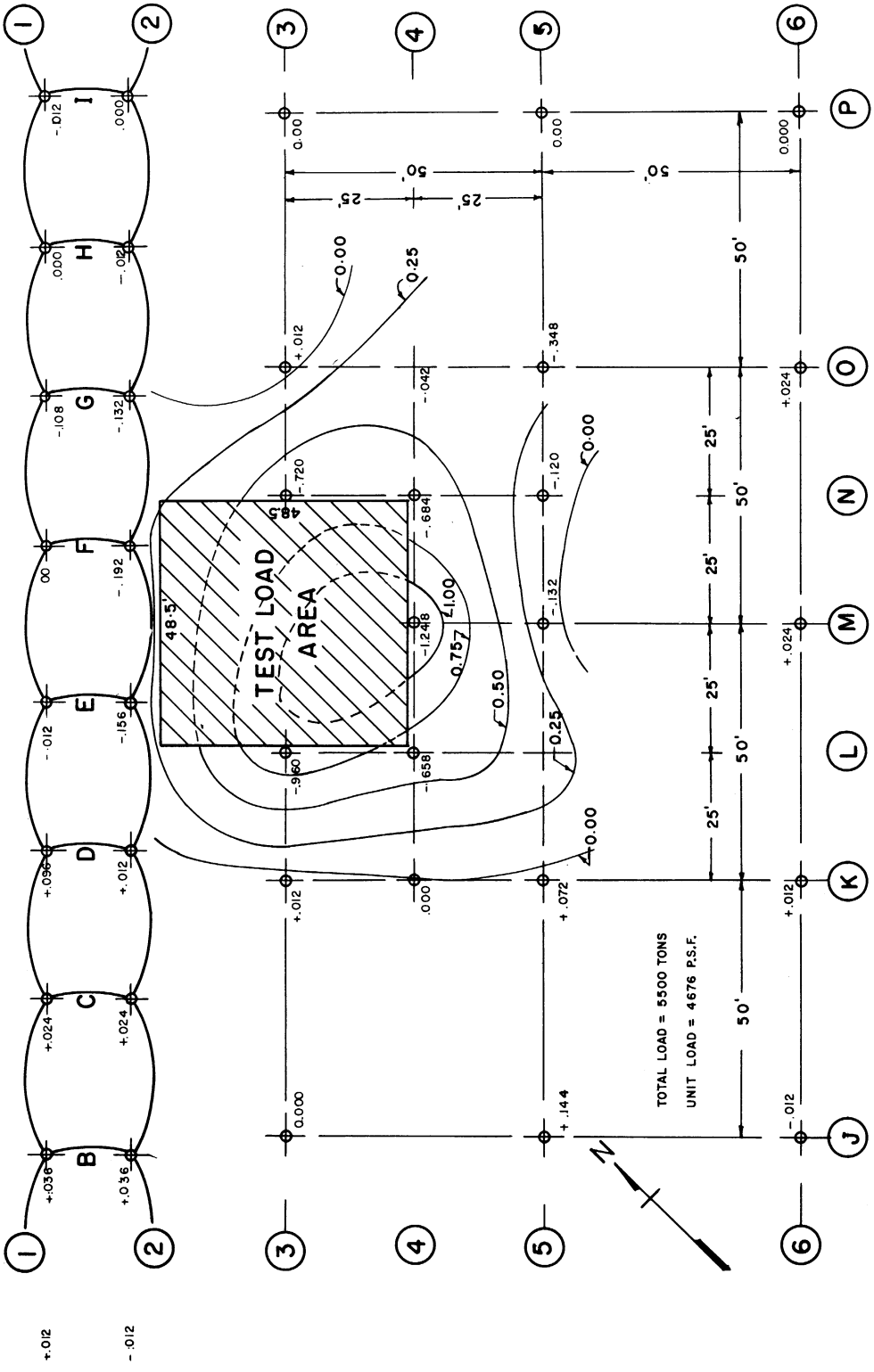

FIGURE 73. TOTAL SETTLEMENTS CONTOURS FROM 9-22-1956 TO 5-24-1957

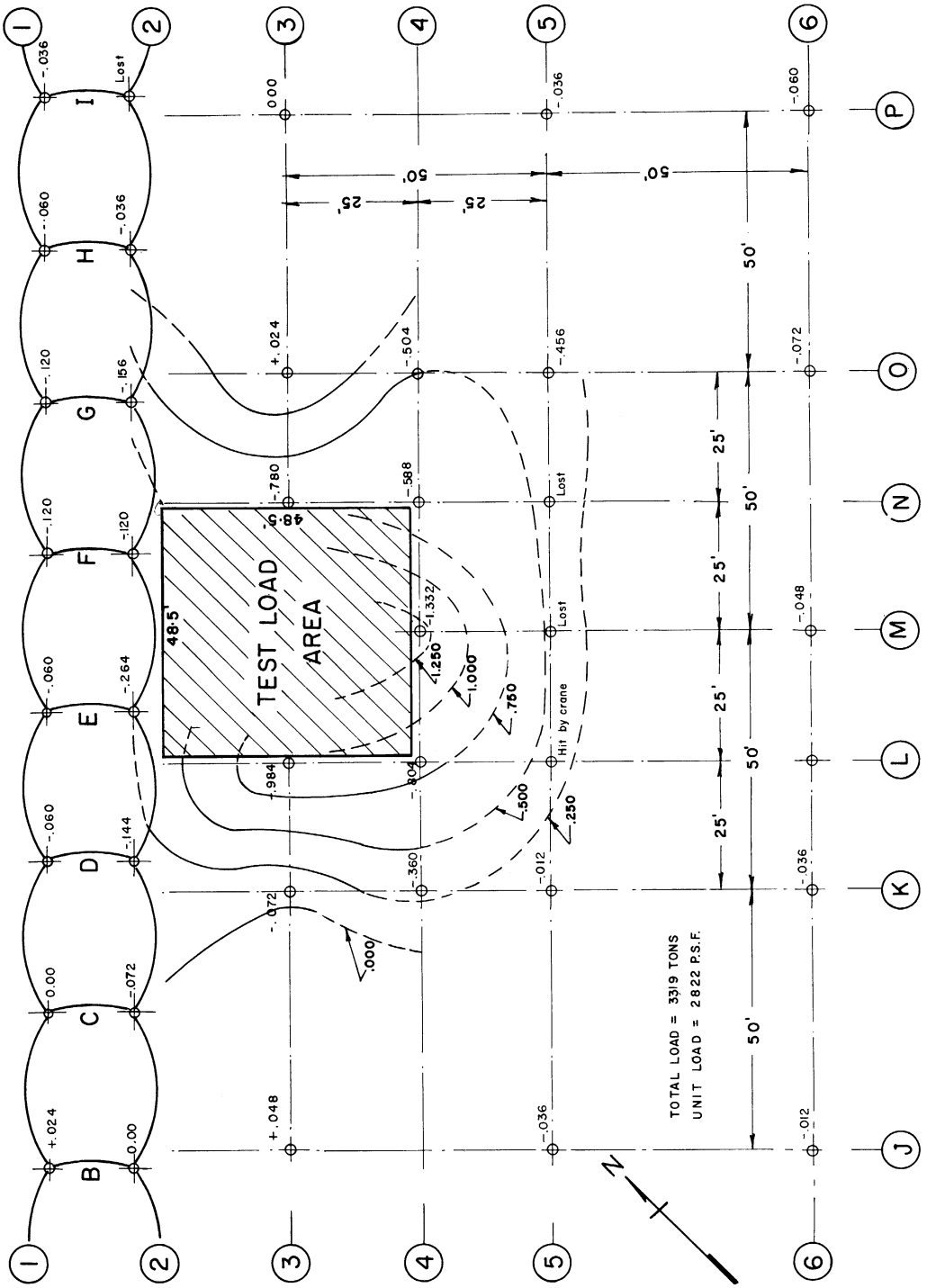

FIGURE 74. TOTAL SETTLEMENTS CONTOURS FROM 9-22-1956 TO 8-30-1957

CHAPTER VI

REVISION OF STABILITY ANALYSIS BASED ON DATA OBTAINED DURING THE TIME OF TESTING

During the test period, data were obtained concerning the dredged side. These data were soundings taken at the beginning of the test. The soundings indicated different elevations for the bottom of the lake next to the cofferdam than that previously available. According to this, the stability analysis is revised. This revision did not affect the recommendations made previously or the progress of testing.

The elevation of the bottom of the lake next to the cofferdam was assumed to be at El. 556.0. The data obtained from the soundings show the ground elevation at the dredged side as illustrated in Figure 75. An approximation is made by taking the average ground level at row "z" and is found to be 572.5. Also the average ground level at row "y" is found to be 562.5. Therefore, the ground surface at the dredged side is assumed to have a profile as shown in Figure 76.

Based on these data, a revision of the stability analysis is made. The full mathematical steps and details are shown in Appendix B.

The revised stability analysis with respect to the mass movement of the soil mass (upheaval) is made taking into consideration the following four cases:

a) When the depth of the failing element, d, equals 48.5 feet and the failing element is at the dredged side next to the cofferdam directly.

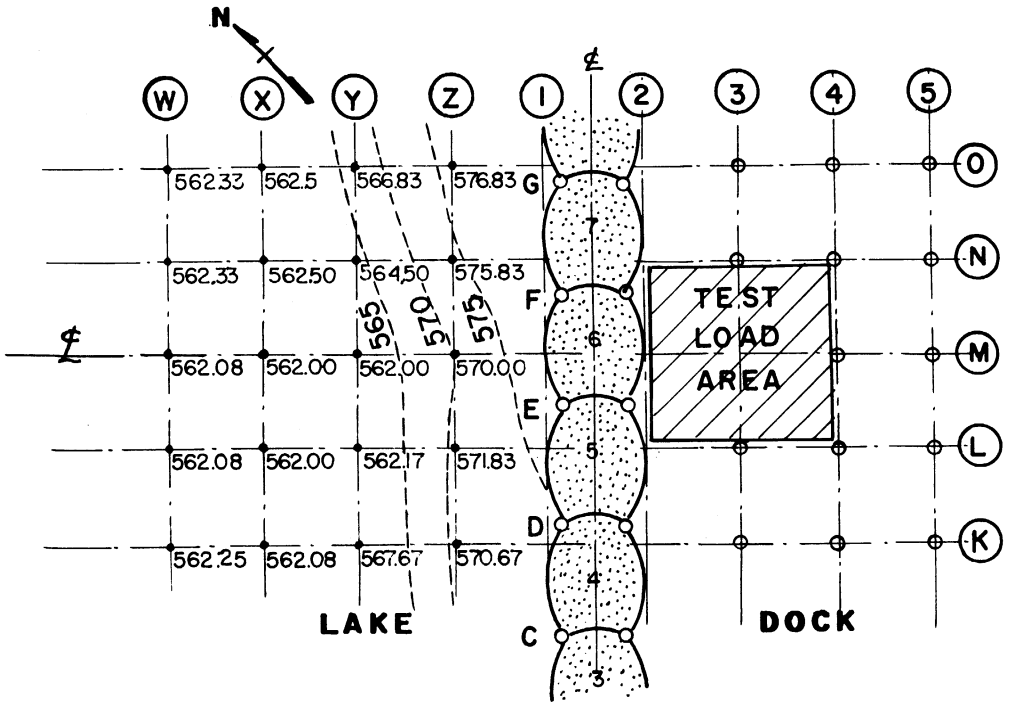

Figure 75. Ground Elevations on the Lake Side.

b) When the depth of the failing element, d, equals 48.5 feet and the failing element is at the dredged side at the toe of the berm.

c) When the depth of the failing element, d, equals 38.5 feet and the failing element is at the dredged side next to the cofferdam directly.

d) When the depth of the failing element, d, equals 38.5 feet and the failing element is at the dredged side at the toe of the berm.

These four cases are illustrated in Figures 76 and 77. The revised stability analysis with respect to sliding is made taking into consideration the following two cases:

a) When either the active or the passive lateral pressure at the dredged side acting against the cofferdam directly is used.

b) When either the active or the passive lateral pressure at the dredged side at the toe of the berm is used.

These two cases are illustrated in Figure 78.

The following is a summary of this analysis.

Soil Properties:

Soil Properties are as shown in Chapter IV. The berm above El. 556.0 at the dredged side is assumed to be sand of the same type as in the sand stratum between El. 546.5 and 556.0.

Static Heads:

The static head above the loading plane at the back side, wh_{bo}, is equal to:

$$wh_{bo} = .2068\ P_o + 4858 \text{ lb./sq.ft.} \quad \text{(see Page 239)}$$

The load placed behind the cofferdam, P_o, is assumed to be distributed above the loading plane within the limit of load distribution of 1:1.

The static head at the dredged side, above the loading plane, assuming the failing element has a depth, d, equal to 48.5 feet and failure is occurring next to the cofferdam directly, is wh_{dl}, and is equal to:

$$wh_{dl} = 4004 \text{ lb./sq.ft.} \quad \text{(see Page 239)}$$

The static head at the dredged side above the loading plane, assuming the failing element has a depth, d, equal to 38.5 feet and failure is occurring next to the cofferdam directly, is wh_{d2}, and is equal to:

$$wh_{d2} = 4128 \text{ lb./sq.ft.} \quad \text{(see Page 240)}$$

The static head at the dredged side above the loading plane, assuming the failure is occurring beyond the toe of the berm, is wh_{d3}, and is equal to:

$$wh_{d3} = 3478 \text{ lb./sq.ft.} \quad \text{(see Page 240)}$$

Lateral Forces and Shearing Resistances:

The active lateral force on the back side, F_{hb}, is equal to:

$$F_{hb} = 13.03 P_o + 58940 - 900 R \text{ lb./ft. run} \quad \text{(see Page 208)}$$

The active lateral force on the dredged side, at section X-X (see Figure 90, Appendix B) is equal to: (see Page 242)

$$F_{hdx} = 50094 + 1.48 X^2 - 274.18 X - 900 R \text{ lb./ft. run}$$

For X = 23.5', $F_{hd1} = (44468 - 900 R)$ lb./ft. run.

For X = 13.5', $F_{hd2} = (46663 - 900 R)$ lb./ft. run.

For X = 25.0', $F_{hd3} = (44164 - 900 R)$ lb./ft. run.

For X = 0, $F_{hd4} = (50094 - 900 R)$ lb./ft. run.

The passive lateral force on the dredged side at section X-X is equal to: (see Page 243)

$$F'_{hdx} = 128905 + 20.132 X^2 - 2699.06 X + 900 R \text{ lb./ft. run.}$$

For X = 23.5', $F'_{hd1} = (76595 + 900 R)$ lb./ft. run.

For X = 13.5', $F'_{hd2} = (96137 + 900 R)$ lb./ft. run.

For X = 25.0', $F'_{hd3} = (74011 + 900 R)$ lb./ft. run.

For X = 0, $F'_{hd4} = (128905 + 900 R)$ lb./ft. run.

The active shearing resistance at the dredged side at section X-X is equal to: (see Page 243)

$$S_{hdx} = 6247 - 192.2\ X + 1.479\ X^2 + 375\ R \text{ lb./ft. run.}$$

For X = 23.5', $S_{hd1} = (2447 + 375\ R)$ lb./ft. run.

For X = 13.5', $S_{hd2} = (3922 + 375\ R)$ lb./ft. run.

For X = 25.0', $S_{hd3} = (2366 + 375\ R)$ lb./ft. run.

For X = 0, $S_{hd4} = (6247 + 375\ R)$ lb./ft. run.

The passive shearing resistance at the dredged side at section X-X is equal to: (see Page 244)

$$S'_{hdx} = 85058 - 2617.24\ X + 20.133\ X^2 + 375\ R \text{ lb./ft. run.}$$

For X = 23.5', $S'_{hd1} = (35472 + 375\ R)$ lb./ft. run.

For X = 13.5', $S'_{hd2} = (53390 + 375\ R)$ lb./ft. run.

For X = 25.0', $S'_{hd3} = (32191 + 375\ R)$ lb./ft. run.

For X = 0, $S'_{hd4} = (85058 + 375\ R)$ lb./ft. run.

Stability Analysis with Respect to the Mass Movement of the Soil Mass (Upheaval)

a) When the depth of the failing element, d, equals 48.5 feet and the failing element is at the dredged side next to the cofferdam:

This case is illustrated in Figure 76. The applied forces and the resisting forces are equated resulting in the following stability equation, in which the active lateral pressure on the dredged side is used:

$$.4755\ P_o + 1102 - 1415\ R = 0 \quad \text{(see Page 245)}$$

For P_o equal to zero the overload ratio will be equal to:

$$R = 1102/1415 = 0.78$$

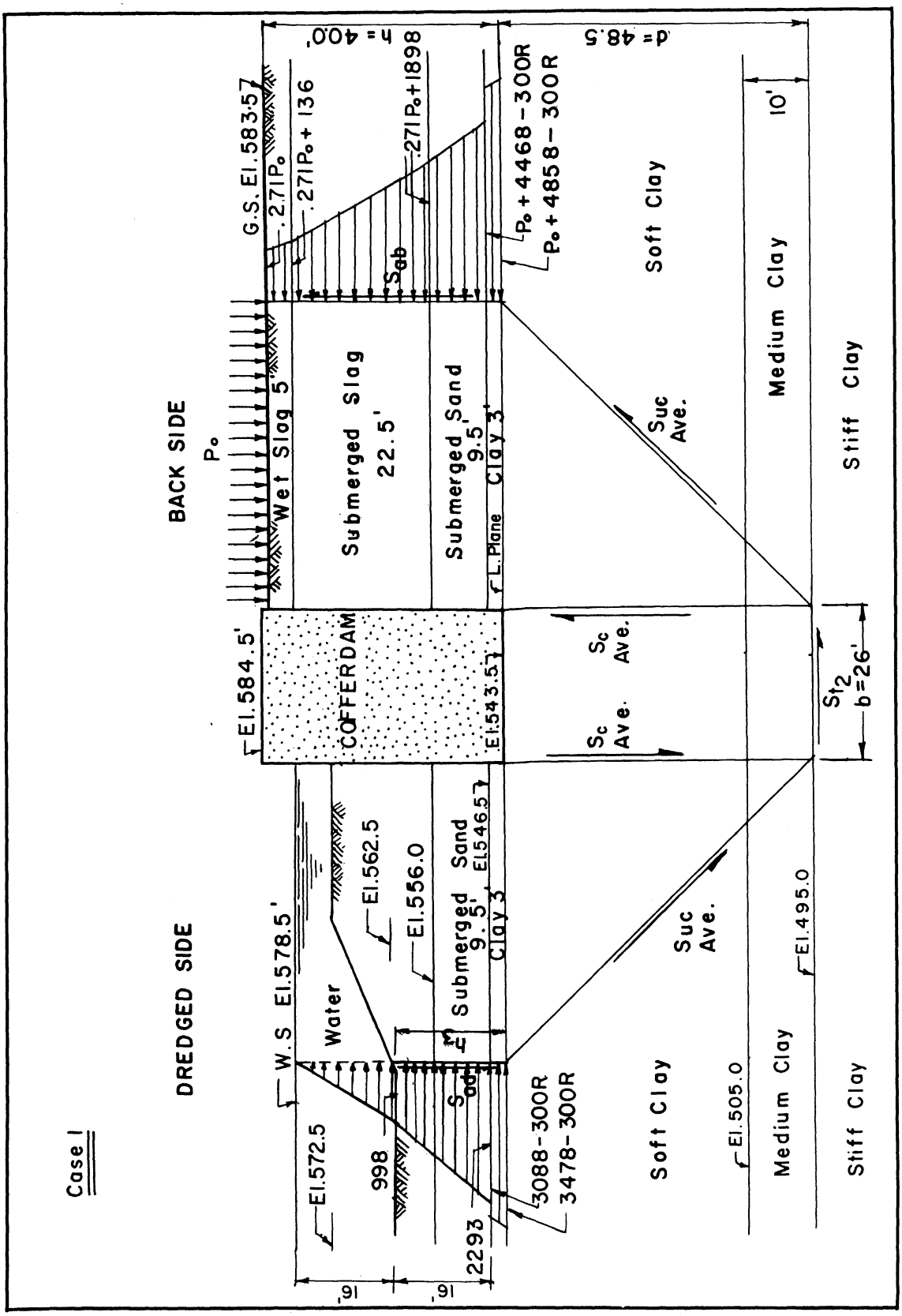

FIGURE 76. APPLIED AND RESISTING FORCES ACTING ON TEST COFFERDAM, FAILING ELEMENT DEPTH IS 48.5' FEET. (DATA HAS BEEN REVISED HERE.)

When the load, P_o, will be increased the overload ratio will exceed one, thus the passive lateral pressure on the dredged side will be developed. Therefore, the stability equation, using the passive lateral pressure for the dredged side, will be:

$$(.2068\ P_o + 4858) + (13.03\ P_o + 58940 - 900\ R)/48.5 - (4004) - (76595 + 900\ R)/48.5 - (4 \times 205\ R) - (2 \times 140\ R) - (26 \times 200\ R)/48.5 - (2447 + 375R)/48.5 - (200\ R) = 0$$

$P_o = 3056\ R + 118$ (see Page 246)

For R = 1.00, P_o = 3174 lb./sq.ft.

For R = 1.50, P_o = 4702 lb./sq.ft.

For R = 2.00, P_o = 6230 lb./sq.ft.

For R = 2.50, P_o = 7758 lb./sq.ft.

For R = 3.00, P_o = 9286 lb./sq.ft.

For R = 3.50, P_o = 10814 lb./sq.ft.

b) When the depth of the element, d, equals 48.5 and the failing element is at the dredged side at the toe of the berm:

This case is illustrated in Figure 77b. The applied forces and the resisting forces are equated, resulting in the following stability equation, in which the active lateral pressure on the dredged side is used:

$$wh_{bo} + F_{hb}/d - wh_{d3} - F_{hd3}/d - 4\ S_{uc(Ave.)}R - 2\ S_{c(Ave.)}\ R - S_{t_2}R(50 + b)/d - 2\ S_{hd3}/d - S_{t_2}\ R - .3\ S_{hb}/d = 0$$

$$(.2068\ P_o + 4858) + (13.03\ P_o + 58940 - 900\ R)/48.5 - (3478) - (44164 - 900\ R)/48.5 - (4 \times 205\ R) - (2 \times 140\ R) - (76 \times 200\ R)/48.5 - 2(2366 + 375\ R)/48.5 - (200\ R) - (.062\ P_o + 80 + 2.3\ R) = 0$$

$.4135\ P_o + 1506 - 1631.2\ R = 0$ (see Page 249)

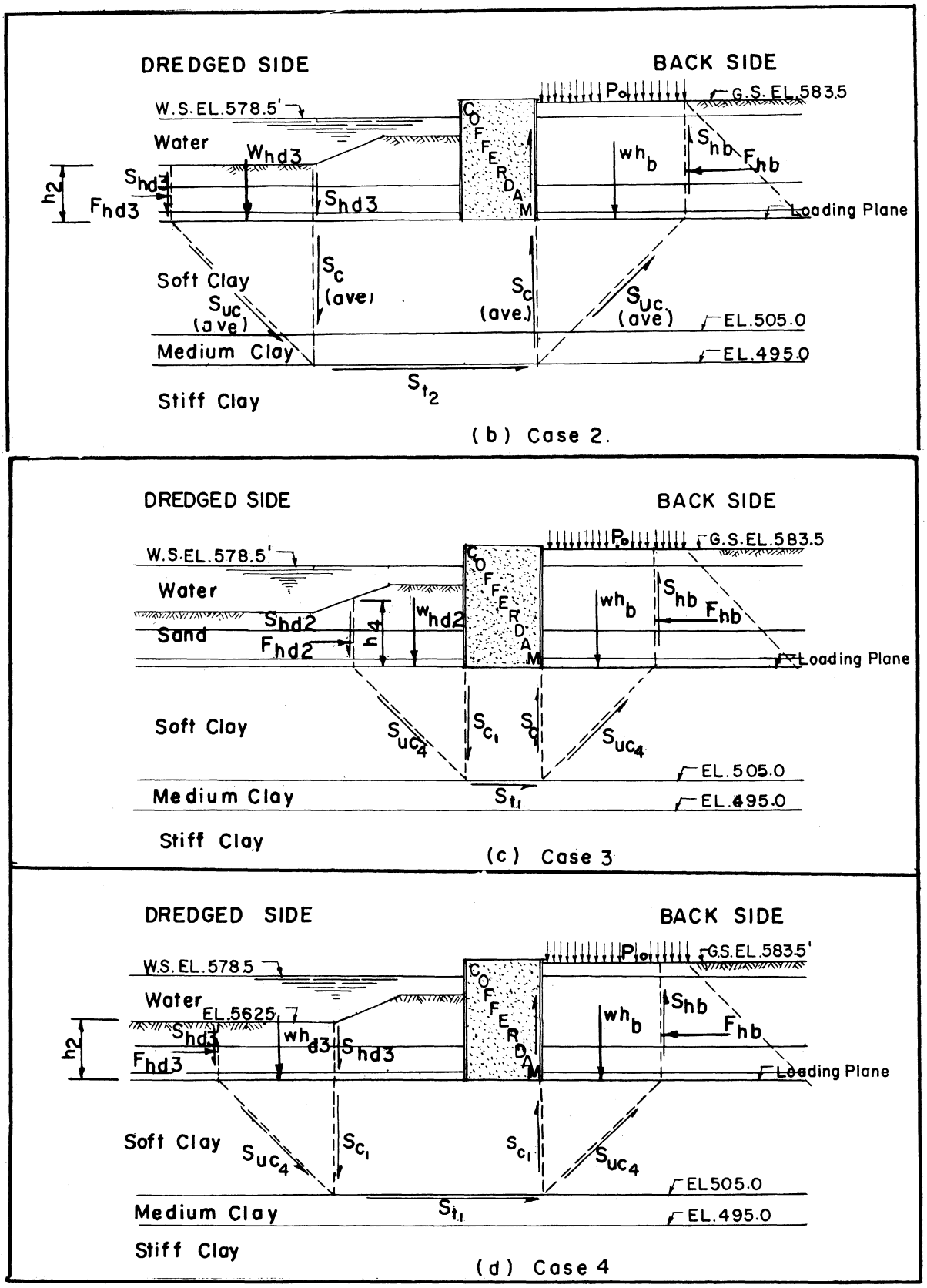

FIGURE 77 . APPLIED AND RESISTING FORCES ACTING ON COFFERDAM, (DATA HAS BEEN REVISED HERE)

For P_o equal to zero the overload ratio is:

$$R = 1506/1631.2 = .924$$

When the load, P_o, will be increased, the overload ratio will exceed one, thus the passive lateral pressure on the dredged side will be developed. Therefore the stability equation, using the passive lateral pressure on the dredged side, will be:

$$wh_{bo} + F_{hb}/d - wh_{d3} - F'_{hd3}/d - 4\ S_{uc(Ave.)}R - 2\ S_{c(Ave.)}\ R$$
$$- S_{t_2}\ R(50 + b)/d - 2\ S_{hd3}/d - S_{t_2}\ R - 3\ S_{hb}/d = 0$$
$$(.2068\ P_o + 4858) + (13.03\ P_o + 58940 - 900\ R)/48.5$$
$$- (3478) - (74011 + 900\ R)/48.5 - (4 \times 205R)$$
$$- (2 \times 140R) - (76 \times 200R)/48.5 - 2(2366 + 375R)/48.5$$
$$- (200R) - (.062P_o + 80 + 2.3R) = 0$$
$$P_o = 4034\ R - 2157 \text{ for values of R less than 2.2}$$
$$P_o = 4014\ R - 2137 \text{ for values of R greater than 2.2}$$

(see Page 250)

For R = 1.00, P_o = 1877 lb./sq.ft.

For R = 1.50, P_o = 3894 lb./sq.ft.

For R = 2.00, P_o = 5911 lb./sq.ft.

For R = 2.50, P_o = 7884 lb./sq.ft.

For R = 3.00, P_o = 9891 lb./sq.ft.

For R = 3.50, P_o = 11898 lb./sq.ft.

c) When the depth of the element, d, equals 38.5 feet and the failing element is at the dredged side next to the cofferdam:

This case is illustrated in Figure 77c. The applied forces and the resisting forces are equated, resulting in the following stability equation, in which the active lateral pressure on the dredged side is

used: (see Page 252)

$$wh_{bo} + F_{hb}/d - wh_{d2} - F_{hd2}/d - 4\ S_{uc_4}R - 2\ S_{c_1}\ R$$
$$- S_{t_1}\ R\ b/d - S_{hd2}/d - S_{t_1}\ R = 0$$
$$(.2068\ P_o + 4858) + (13.03\ P_o + 58940 - 900\ R)/38.5$$
$$- (4128) - (4663 - 900\ R)/38.5 - (4 \times 180R)$$
$$- (2 \times 125R) - (125 \times 26R)/38.5 - (3922 + 375R)/38.5$$
$$- 125\ R = 0$$
$$.5450\ P_o + 944 - 1189.2\ R = 0$$

For P_o equal to zero, the overload ratio is:

$$R = 944/1189.2 = 0.79$$

When the load, P_o, will be increased the overload ratio will exceed one, thus the passive lateral pressure on the dredged side will be developed. Therefore, the stability equation, using the passive lateral pressure for the dredged side will be:

$$wh_{bo} + F_{hb}/d - wh_{d2} - F'_{hd2}/d - 4\ S_{uc_4}\ R - 2\ S_{c_1}\ R$$
$$- S_{t_1}\ R\ b/d - S_{hd2}/d - S_{t_1}\ R = 0$$
$$(.2068\ P_o + 4858) + (13.03\ P_o + 58940 - 900\ R)/38.5$$
$$- (4128) - (96137 + 900\ R)/38.5 - (4 \times 180\ R)$$
$$- (2 \times 125\ R) - (125 \times 26\ R)/38.5$$
$$- (3922 + 375\ R)/38.5 - (125\ R) = 0$$
$$P_o = 2268\ R + 626 \qquad \text{(see Page 253)}$$

For R = 1.00, P_o = 2894 lb./sq.ft.

For R = 1.50, P_o = 4028 lb./sq.ft.

For R = 2.00, P_o = 5162 lb./sq.ft.

For R = 2.50, P_o = 6296 lb./sq.ft.

For R = 3.00, P_o = 7430 lb./sq.ft.

For R = 3.50, P_o = 8564 lb./sq.ft.

d) When the depth of the element, d, equals 38.5 feet and the failing element is at the dredged side at the toe of the berm:

This case is illustrated in Figure 77d. The applied and the resisting forces are equated, resulting in the following stability equation, in which the active lateral pressure on the dredged side is used:

$$wh_{bo} + F_{hb}/d - wd_{d3} - F_{hd3}/d - 4\ S_{uc_4}\ R - 2\ S_{c_1}\ R - S_{t_1}\ R(50 + b)/d - 2\ S_{hd3}/d - S_{t_1}\ R - .3\ S_{hb}/d = 0$$

$$(.2068\ P_o + 4858) + (13.03\ P_o + 58940 - 900\ R)/38.5 - (3748) - (44164 - 900\ R)/38.5 - (4 \times 180\ R) - (2 \times 125\ R) - (76 \times 125\ R)/38.5 - 2(2366 + 375\ R)/38.5 - 125\ R - (.0781\ P_o + 101 + 2.9\ R) = 0$$

$$.4669\ P_o + 1542 - 1512.2\ R = 0$$ (see Page 256)

For P_o equal to zero, the overload ratio is:

$$R = 1542/1512.2 = 1.02$$

When the load, P_o, will be increased the overload ratio will exceed one, thus the passive lateral pressure on the dredged side will be developed. Therefore, the stability equation, using the passive lateral pressure for the dredged side, will be:

$$wh_{bo} + F_{hb}/d - wh_{d3} - F_{hd3}/d - 4\ S_{uc_4}\ R - 2\ S_{c_1}\ R - S_{t_1}\ R(50 + b)/d - 2\ S_{hd3}/d - S_{t_1}\ R - .3\ S_{hb}/d = 0$$

$$(.2068\ P_o + 4858) + (13.03\ P_o + 58940 - 900\ R)/38.5 - (3478) - (74011 + 900\ R)/38.5 - (4 \times 180\ R) - (2 \times 125\ R) - (76 \times 125\ R)/38.5 - 2(2366 + 375\ R)/38.5 - (125\ R) - (.0781\ P_o + 101 + 2.9\ R) = 0$$

$$P_o = 3339\ R - 1638 \quad \text{for values of R less than } 4.3$$

(see Page 257)

For R = 1.00, P_o = 1701 lb./sq.ft.

For R = 1.50, P_o = 3371 lb./sq.ft.

For R = 2.00, P_o = 5040 lb./sq.ft.

For R = 2.50, P_o = 6710 lb./sq.ft.

For R = 3.00, P_o = 8379 lb./sq.ft.

For R = 3.50, P_o = 10049 lb./sq.ft.

Stability Analysis with Respect to Sliding

To determine the allowable load, P_o, for the various overload ratios with respect to sliding, two cases are considered. These two cases are illustrated in Figure 78. In the first case the lateral pressures acting on the cofferdam directly are considered. In the second case the lateral pressure on the back side directly and the lateral pressure on the dredged side at the toe of the berm, which is less than the lateral pressure on the cofferdam directly, are considered. Also, in both cases the active or the passive lateral pressures on the dredged side are used.

Case One, Using the Active Lateral Pressure on the Dredged Side.--The applied force and the resisting forces are equated resulting in the following stability equation with respect to sliding:

$$F_{hb} - F_{hd4} - 19810 - S_{c_1}\, b\, R = 0 \qquad \text{(see Page 258)}$$

$$(13.03\, P_o + 58940 - 900\, R) - (50094 - 900\, R) - (19810) - (3250\, R) = 0$$

$$P_o = 841 + 249\, R$$

For R = 1.0, P_o = 1090 lb./sq.ft.

when exceeded, the passive lateral pressure will be developed.

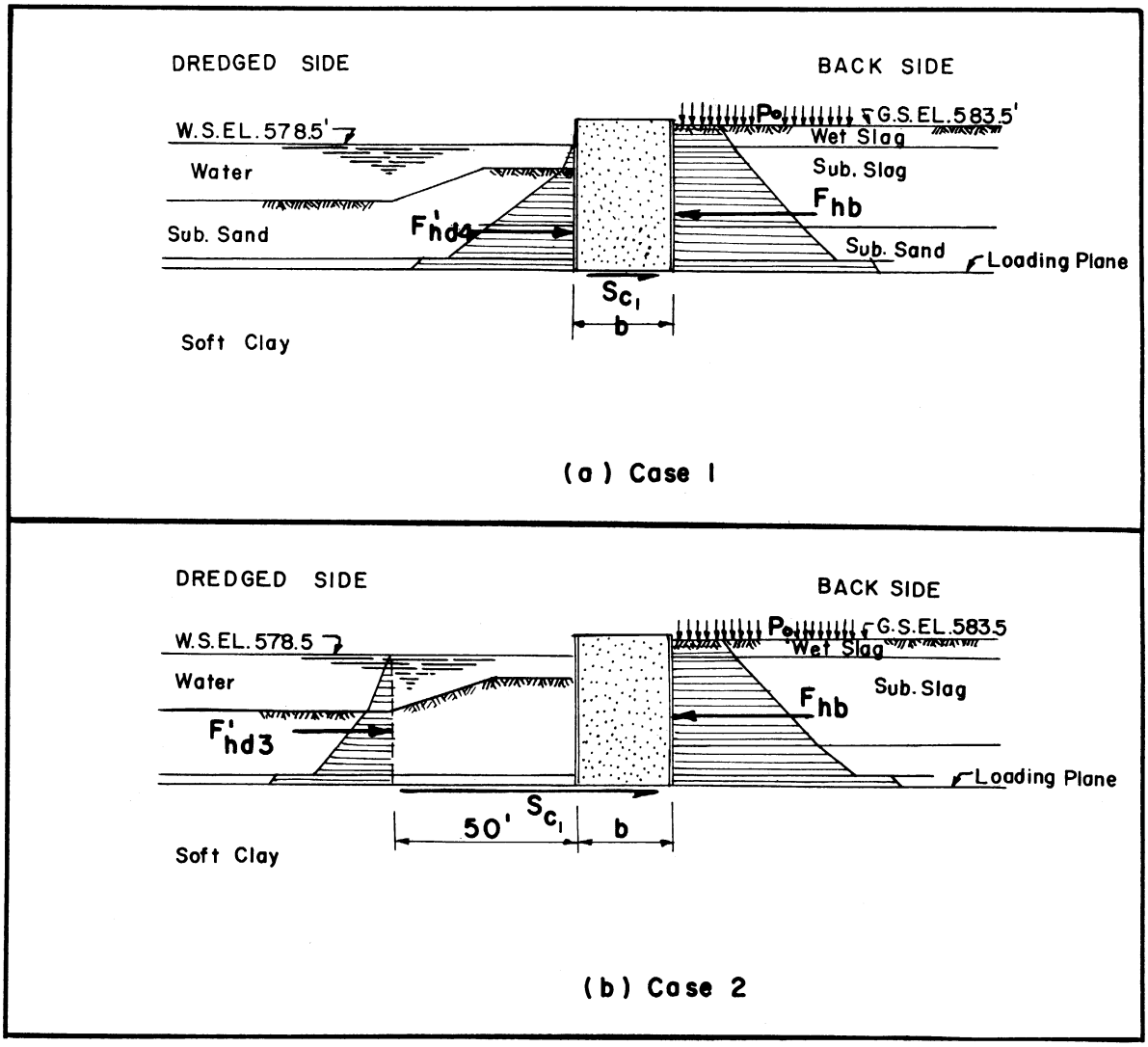

FIGURE 78 APPLIED AND RESISTING FORCES ACTING ON TEST COFFER-DAM WITH RESPECT TO SLIDING (DATA HAS BEEN REVISED HERE)

Case One, Using the Passive Lateral Pressure on the Dredged Side.--The applied force and the resisting forces are equated resulting in the following stability equation:

$$F_{hb} - F'_{hd4} - 19810 - 3250\ R = 0 \qquad \text{(see Page 259)}$$

$$(13.03\ P_o + 58940 - 900\ R) - (128905 + 900\ R)$$

$$- (19810) - (3250\ R) = 0$$

$$P_o = 6889 + 387\ R$$

For R = 1.00, P_o = 7276 lb./sq.ft.

For R = 1.50, P_o = 7469 lb./sq.ft.

For R = 2.00, P_o = 7662 lb./sq.ft.

For R = 2.50, P_o = 7855 lb./sq.ft.

For R = 3.00, P_o = 8049 lb./sq.ft.

For R = 3.50, P_o = 8232 lb./sq.ft.

Case Two, Using the Active Lateral Pressure at the Toe of the Berm on the Dredged Side.--The applied force and the resisting forces are equated resulting in the following stability equation with respect to sliding:
(see Page 260)

$$F_{hb} - F_{hd3} - 19810 - 125 \times (50 + b)\ R = 0$$

$$(13.03\ P_o + 58940 - 900\ R) - (44164 - 900\ R)$$

$$- (19810) - (9500\ R) = 0$$

$$P_o = 386 + 728\ R$$

For R = 1.00, P_o = 1114 lb./sq.ft.

when the load, P_o, exceeds 1114 pounds per square foot the passive lateral pressure will be developed.

Case Two, Using the Passive Lateral Pressure at the Toe of the Berm on the Dredged Side.--The applied force and the resisting forces are equated, resulting in the following stability equation:

$$F_{hb} - F'_{hd3} - 19810 - 9500\ R = 0 \qquad \text{(see Page 261)}$$

$$(13.03\ P_o + 58940 - 900\ R) - (74011 + 900\ R)$$

$$- (19810) - (9500\ R) = 0$$

$$P_o = 2677 + 867\ R$$

For R = 1.00, P_o = 3544 lb./sq.ft.

For R = 1.50, P_o = 3977 lb./sq.ft.

For R = 2.00, P_o = 4411 lb./sq.ft.

For R = 2.50, P_o = 4844 lb./sq.ft.

For R = 3.00, P_o = 5278 lb./sq.ft.

For R = 3.50, P_o = 5706 lb./sq.ft.

The other causes of failure are not controlling as was shown in Chapter IV. The change in the elevations in the dredged side favors these causes and permits greater allowable loads for various overload ratios and therefore they are not revised.

The results of the foregoing analysis are plotted on Figure 79. The vertical axis represents the overload ratio, R, and the horizontal axis represents the corresponding allowable load, P_o, on the test area in pounds per square foot. The critical loads for the various overload ratios are selected and they are as follows:

For R = 1.00, P_o = 1701 lb./sq.ft.

For R = 1.50, P_o = 3371 lb./sq.ft.

For R = 2.00, P_o = 4411 lb./sq.ft.

For R = 2.50, P_o = 4844 lb./sq.ft.

For R = 3.00, P_o = 5278 lb./sq.ft.

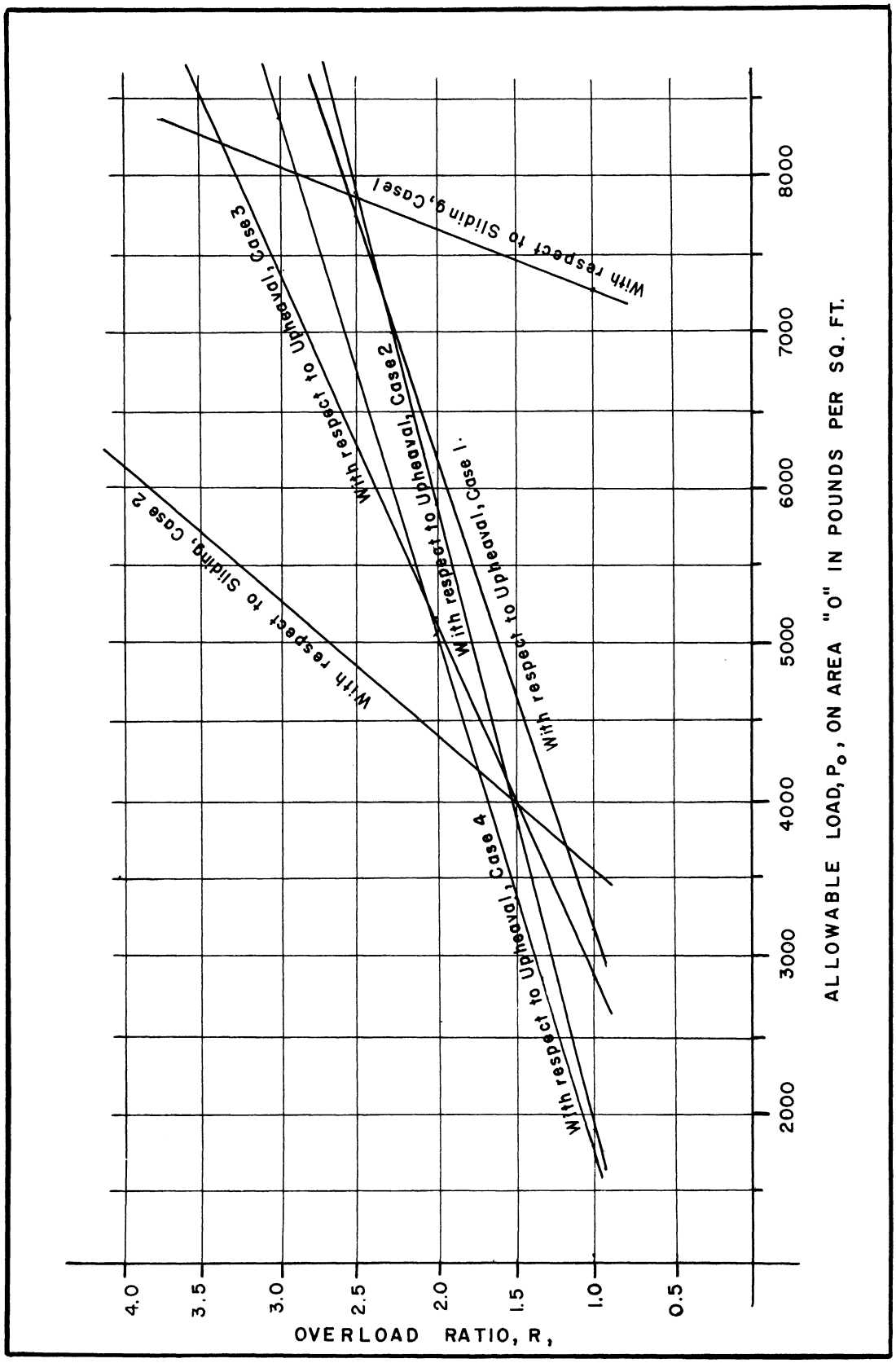

FIGURE 79. ALLOWABLE LOADS FOR VARIOUS OVERLOAD RATIOS WITH RESPECT TO MASS MOVEMENT (UPHEAVAL) AND SLIDING

CHAPTER VII

EVALUATING OF TEST AND CORRELATION OF RESULTS

The theoretical analysis discussed in Chapter IV shows that when this particular cofferdam will be subjected to the proposed loading, the mass stability of the cofferdam will be the critical cause of failure and will be controlling. Therefore, it was anticipated that the cofferdam will not collapse entirely but a mass movement of the soil mass supporting and surrounding the cofferdam will take place. When the test was run this was verified. The cofferdam did not collapse entirely but a mass movement took place in which there was a settlement depending upon the loading condition. This settlement has been evaluated in this chapter. The test has served basically to demonstrate the stability of the cofferdam with respect to mass movement. It also indicated, however, that the other causes of failure were not controlling.

The test results which were presented in Chapter V as settlements against time, as well as the general observations made during the test period, are used for this evaluation. The evaluation is made by means of two approaches. The first approach is made by translating the settlements into the rates of settlement taking place around the test load area for the various stages of loading, in order to study the mass movement taking place. The second approach is a mathematical evaluation of the rates of settlements with relation to the applied loads, from which the magnitude of an applied load that causes an overload ratio of one is determined.

The settlement charts were divided into two groups. The first group are for the outer points, those on rows P, J, 6, and 1, which are far from the boundary of the test load area. These points are supposed to have zero displacement. The values of the settlement ordinates, as indicated in the settlement charts, fell within the range of error. The range of error, in this case, is taken as $\pm$.005. Thus they are ignored when the rates of settlement are calculated. Those settlement charts are shown in Appendix C.

The second group of settlement charts are for those points on or within 48.5 feet of the boundary of the test load area, which had settlement ordinates greater than the range of error as indicated in the settlement charts. They are shown in Figures 56 to 71. The magnitude of the settlements of the points in this group are depended upon in determining the rates of settlements for the mass of soil surrounding the test load area.

The rates of settlements are determined by drawing a straight line through the settlements during the period when a certain load is placed on the test area, then calculating the slopes of these straight lines (see Figure 80). That is done by taking the vertical ordinate of each of these slopes, which is designated as Δ, dividing it by the duration of time in which these readings were taken, then converting it into inches per year. As an example of this, taking point M-4, the slope of the settlements is drawn graphically for the time when the load of 4500 tons was placed on the test load area and is found to be equal to .043 foot. This Δ is multiplied by the conversion factor for the period from September 22, 1956, to January 24, 1957, which is equal to $\frac{365}{124} \times 12 = 35.3$.

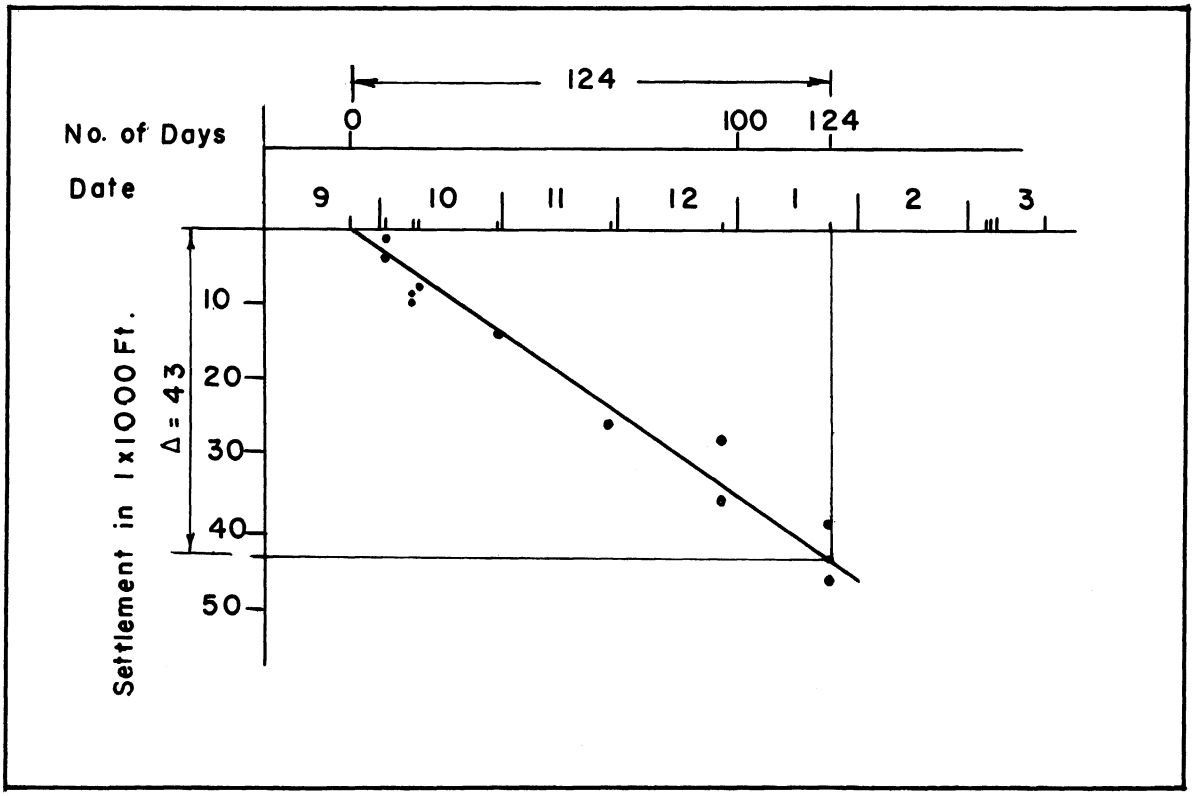

FIGURE 80. GRAPHICAL METHOD OF DETERMINING THE RATE OF SETTLEMENT

The rates of settlement are calculated in inches per year. Figure 80 illustrates this.

Based on this method the rates of settlement are calculated for the points on or within 48.5 feet of the boundary of the test load area, for the three stages of loading. Table II shows the tabulation of the values of Δ as determined from the settlement charts, as well as the rates of settlement. The rates of settlements are the product of the ordinate, Δ, times the corresponding conversion factor for each stage of loading. The conversion factors are calculated at the bottom of Table II.

To get a clearer picture of the rates of settlement taking place around the test load area, contours are drawn from the rates of settlement calculated in Table II. Figures 81 to 83 show the contours of the rates of settlement for the three stages of loading.

Figure 81 shows the contours for the rates of settlement when a load of 4500 tons was placed on the loading area. This figure shows clearly that there is greater yielding in the soil on the side which is away from the cofferdam, and it is centered around points L-3, L-4, M-4, and the center of the loading area. The reason for this is that the continuity effect of the cofferdam structure gives greater stability to the mass of soil adjacent to it when the shearing resistance between the cofferdam structure and the mass of soil adjacent to it is developed; thus the clay stratum at this side was not stressed to the extent of that on the opposite side which showed greater yielding.

TABLE II

VALUES OF Δ AND THE RATES OF SETTLEMENT

POINT	From 9-22-1956 To 4-1 -1957		From 3-24-1957 To 5-24-1957		From 8-3-1957 To 8-30-1957	
	Δ	Rate of Settl.	Δ	Rate of Settl.	Δ	Rate of Settl.
E-2	-.0115	-0.406	-.009	-1.011*	-.0045	-0.730
F-2	-.006	-0.212	-.012	-1.404*	-.0025	0.406
K-3	.000	0.000	.000	0.000**	-.0025	0.406
K-4	+.013	+0.459	.000	0.000**	-.003	-0.487
K-5	+.004	+0.141	+.008	+0.548**	-.000	-0.000
L-3	-.043	-1.518	-.027	-1.848**	-.007	-1.136
L-4	-.021	-0.741	-.024	-1.643**	-.007	-1.136
L-5	+.006	+0.212	+.011	+1.235*	-.004	-0.649
M-4	-.043	-1.518	-.034	-2.327**	-.0035	-.568
M-5	.000	0.000	.000	0.000**	lost	Lost
N-3	-.022	-0.777	-.020	-1.369**	.000	0.000
N-4	-.015	-0.530	-.022	-1.506**	.000	0.000
N-5	.000	0.000	-.003	-0.337*	Lost	Lost
O-3	+.010	+0.353	-.004	-0.450*	.000	0.000
O-4	.000	0.000	-.006	-0.674*	.000	0.000
O-5	.000	0.000	-.007	-0.786*	-.002	-.324

Conversion Factor $c_1 = 365 \times 12/124 = 35.3$

$c_2 = 365 \times 12/64 = 68.4$**

$c_2' = 365 \times 12/39 = 112.3$*

$c_3 = 365 \times 12/27 = 162.2$

Figure 82 shows the contours of the rates of settlement when a load of 5500 tons was placed on the loading area. The yielding of the soil started taking a more uniform shape and began to center around the points L-3, L-4, M-4, M-5, N-3, and the center of the test load area. However there is still greater yield on the side which is away from the cofferdam indicating the contributory strength due to the continuity of the cofferdam. Also another phenomenon of great importance is an upheaval movement of the soil which was centered between K-5, M-5, K-6, and M-6. This movement is an indication that the settlement which has taken place has caused all the resisting factors on the back side to be mobilized. This upheaval provided verification for the fact that all the soil resistance is fully mobilized when the load on the test area reaches 5500 tons.

Figure 83 shows the contours for the rates of settlement after unloading the test load area to 3199 tons. The rate of settlement decreased to 1.2 inches per year which is lower than the rate of settlement of 1.52 inches per year which was developed when the load of 4500 tons was placed on the test area. This value of 1.2 inches per year shows a proportionality when compared to that of the rates of settlements in stage one.

The rates of settlement on the side of row L appear to be greater than the rates of settlement on the side of row N (see Figure 81). This is explained by the fact that the ground at the dredged side of the cofferdam on the side of row L is lower than the ground at the dredged side of the cofferdam on the side of row N. These data were obtained from the soundings taken at the start of the test. Due to the difference

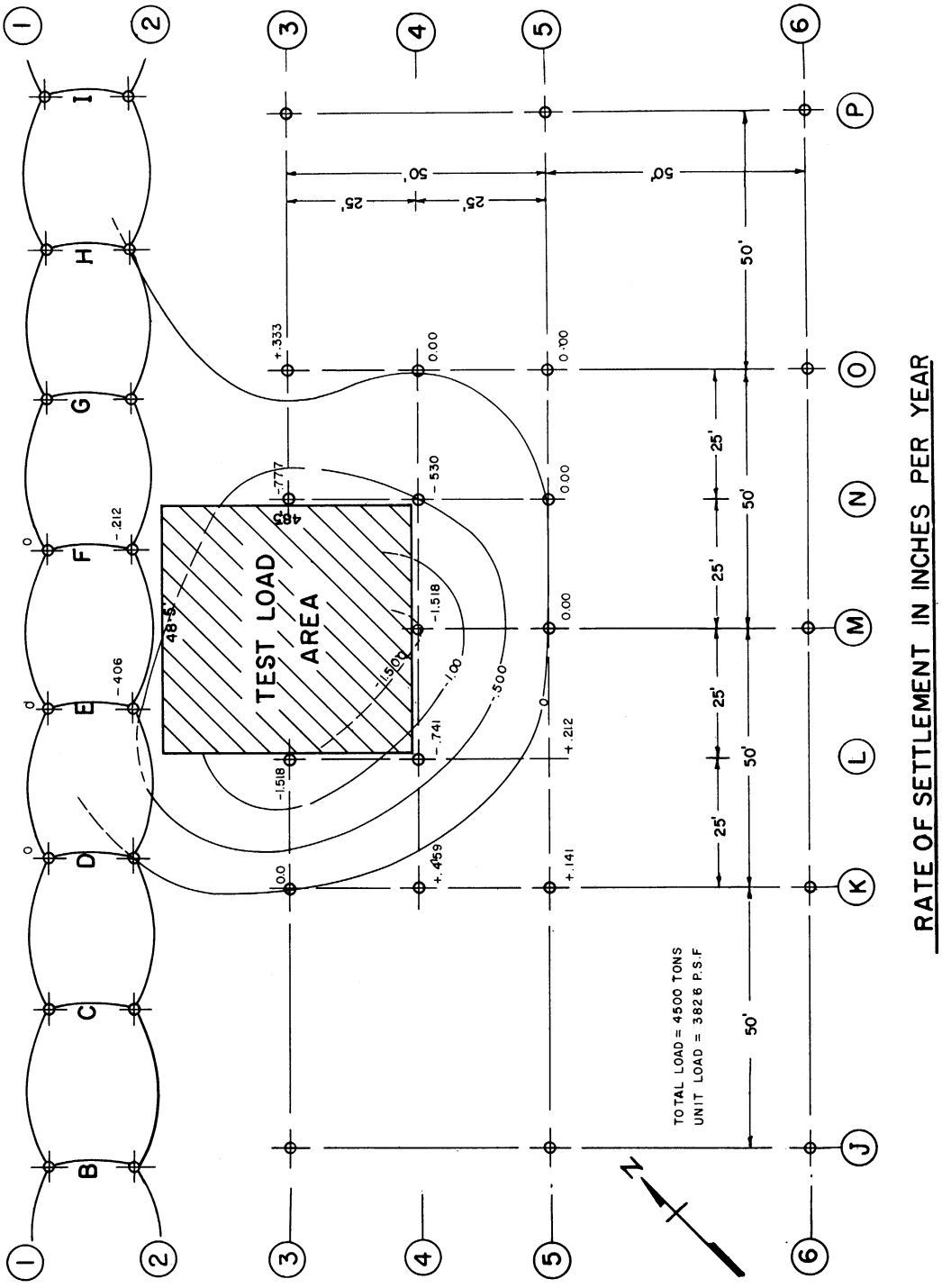

FIGURE 81. RATES OF SETTLEMENTS CONTOURS
FOR THE PERIOD 9-22-1956 TO 1-24-1957

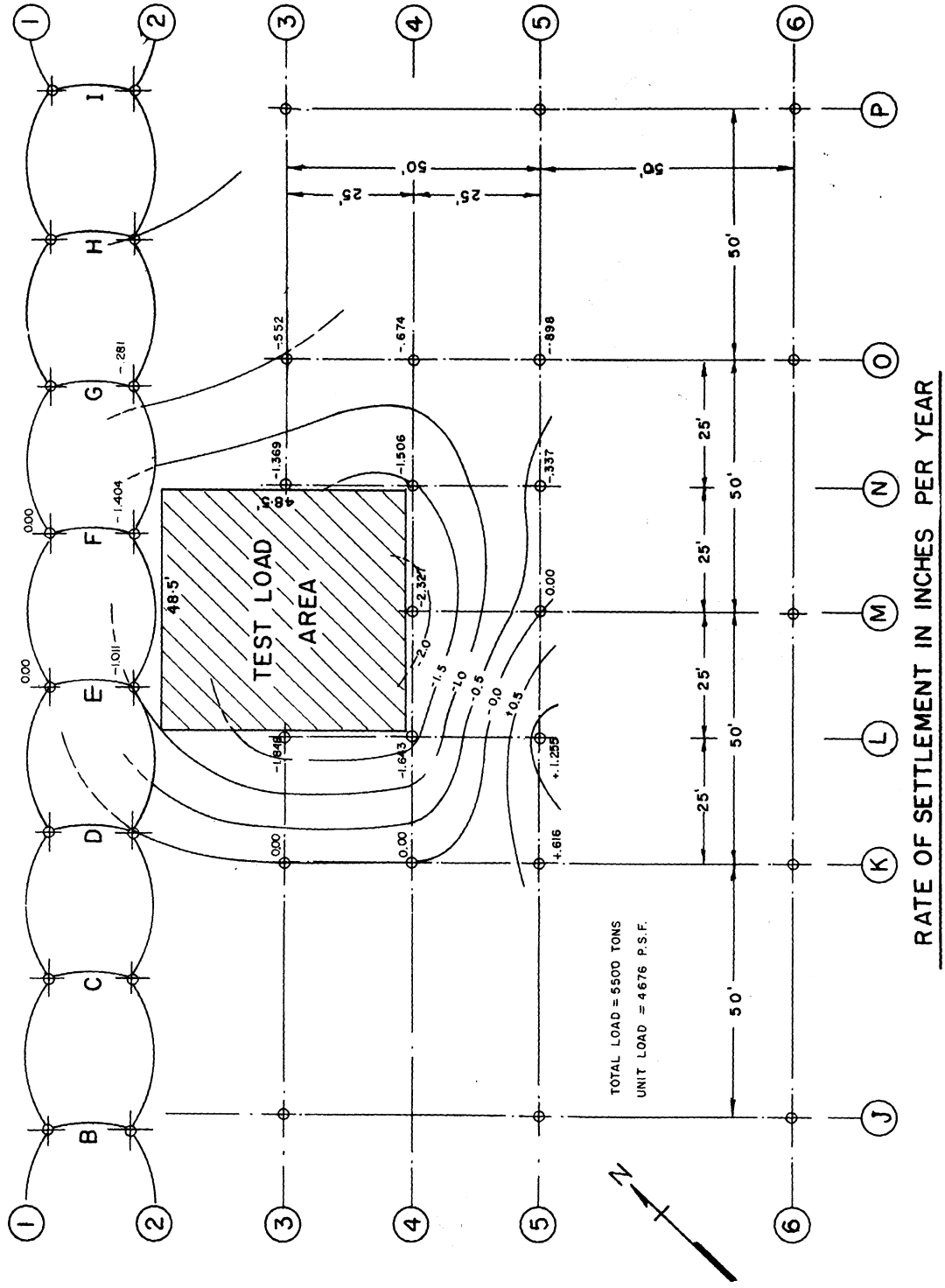

FIGURE 82. RATES OF SETTLEMENTS CONTOURS
FOR THE PERIODS 3-21-1957 TO 5-24-1957
AND 4-15-1957 TO 5-24-1957

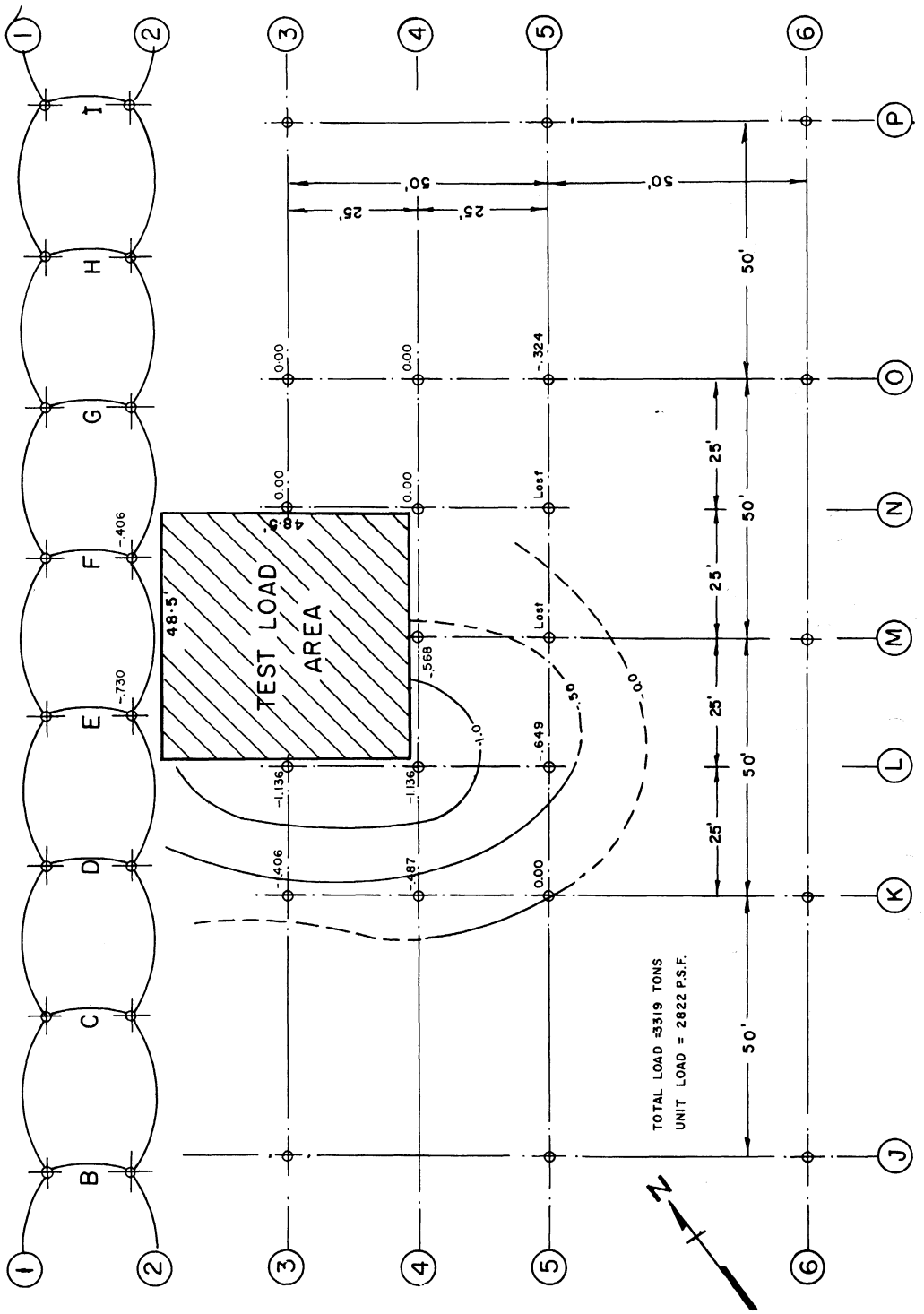

FIGURE 83. RATES OF SETTLEMENTS CONTOURS FOR THE PERIODS 3-21-1957 TO 5-24-1957 AND 4-15-1957 TO 5-24-1957

in the static heads, the resistance factors on the side of row N are higher than the resistance factors on the side of row L. Therefore, under the same loading condition, the shearing resistance in the clay strata on the side of row L will be mobilized to a greater extent than the shearing resistance in the clay strata on the side of row N. Therefore the side of row L was overstressed more than the side of row N. When the load was increased to 5500 tons on the test area the portion of the element on the side of row L yielded while the portion of the element on the side of row N became increasingly overstressed, bringing the rates of settlement into rates closer to the rates of settlement on the other side, as shown in Figure 82.

When the load of 5500 tons was placed on the test load area the corresponding rate of settlement reached a measurable value of 2.4 inches per year at some points. A rate of settlement of this magnitude is critical. This is a condition encountered frequently in plastic clay subjected to loading. It is a condition short of an actual failure of the soil but it will cause considerable trouble. However, when a rapid progressive settlement takes place it may result in the loss of some resistance factors which will lead to complete failure. Thus the load of 5500 tons represents the limit load to be placed on the test load area.

In the process of testing there was no indication of complete failure which could be represented by a collapse. Thus the cofferdam structure did not fail due to the applied loads, however the mass of soil deformed, allowing settlements to take place. These settlements indicated the overstressing of the underlying soft clay strata underneath

the cofferdam. Thus for this particular cofferdam the weakness lies in the ability of the underlying clay stratum to carry the applied loads. Therefore the mass stability of the soil mass supporting and surrounding the cofferdam is a major factor in determining the strength and stability of the cofferdam.

The mathematical evaluation of the rates of settlement is approached by drawing the yield value diagrams for the various rates of settlement against the corresponding load intensities. The points on the boundary of the test load area are depended upon in establishing the yield value diagram because these points are directly affected by the loading and they are within that mass of soil which will have to mobilize its resistances first.

The rates of settlement of the points are plotted against the load intensity. The horizontal ordinate represents the rate of settlement while the vertical ordinate represents the load intensity. The most fitted straight line which will represent these plotted points is determined by the method of least square. This method is discussed in Appendix E[27]. This straight line represents the yield value straight line.

The yield value straight line is obtained by taking into consideration the rates of settlement of the first stage of the test when the load was 4500 tons, where seven readings were taken, and the second stage of the test, when the load was 5500 tons, where five readings were taken. The straight line equation is found to be:

$$Y = .0008492\ X - 2.2321., \quad \ldots\ldots\ldots\ldots\ldots\ldots (1)$$

TABLE III

VALUES OF X, X^2, Y, AND XY USED IN DETERMINING THE YIELD VALUE STRAIGHT LINE USING 10 POINTS FOR THE FIRST AND SECOND STAGES OF LOADING

	X	X^2	Y	XY
1	3,826	14,638,276	1.518	5,807.868
2	3,826	14,638,276	0.741	2,835.066
3	3,826	14,638,276	1.518	5,807.868
4	3,826	14,638,276	0.777	2,972.802
5	3,826	14,638,276	0.530	2,027.780
6	4,676	21,864,976	1.848	8,641.248
7	4,676	21,864,976	1.643	7,682.668
8	4,676	21,864,976	2.327	10,881.052
9	4,676	21,864,976	1.369	6,401.444
10	4,676	21,864,976	1.506	7,042.056
Σ	42,510	182,516,260	13.777	60,099.852

$$b = \frac{n \Sigma XY - \Sigma X \Sigma Y}{n \Sigma X^2 - (\Sigma X)^2} = .0008492$$

$$a = \frac{\Sigma X^2 \Sigma Y - \Sigma X \Sigma XY}{n \Sigma X^2 - (\Sigma X)^2} = 2.2321$$

$$Y = .0008492\ X - 2.2321 \quad \ldots\ldots\ldots\ldots\ (1)$$

When Y equal to zero, X is equal to 2734 Pounds per square foot.

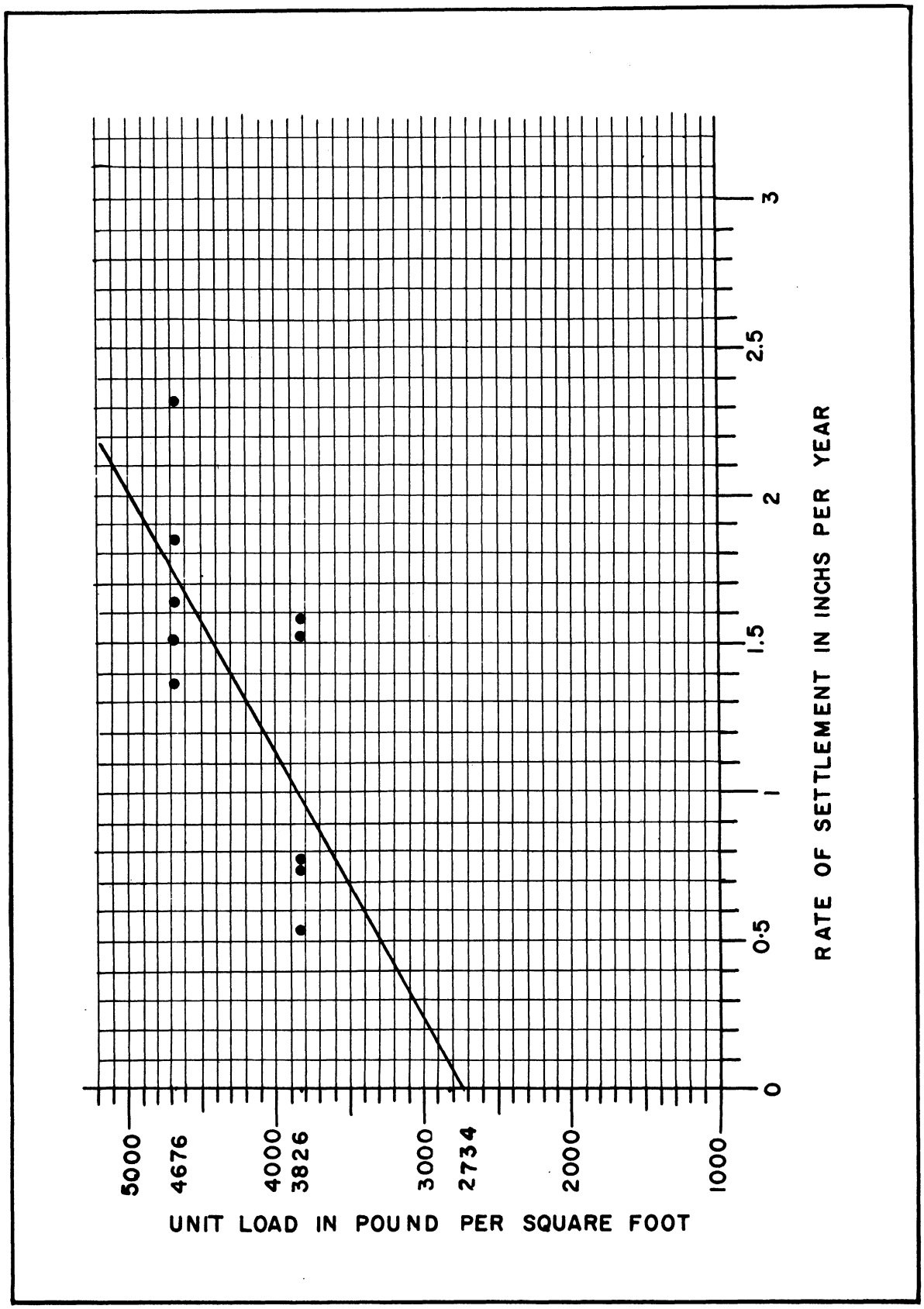

FIGURE 84. YIELD VALUE CURVE

This equation is illustrated in Figure 84. In Table III is shown the tabulation from which the yield value straight line equation is obtained, when ten plotted points of the first and the second stage of the test are considered.

Also the yield value straight line is obtained by taking into consideration the first stage, the second stage, and the third stage of the test when the load was 3199 tons, where three readings were taken. The straight line equation is found to be:

$$Y = .0006259\ X - 1.255 \quad \ldots\ldots\ldots\ldots\ldots\ldots (2)$$

This equation is illustrated in Figure 85. In Table IV is shown the tabulation from which the yield value straight line equation is obtained, when fifteen plotted points of the first, second, and third stages of the test are considered.

In order to determine the load capacity of the test load area for an overload ratio of one, the second yield value straight line equation is considered. This equation gives the relationship between the applied loads on the test load area and the corresponding rates of settlements. The rate of settlement is equal to zero for an overload ratio of one because the shearing stress is equal to or less than the yield value shearing resistance of the clay. Therefore, by substituting a zero rate of settlement in the second equation, the load which causes an overload ratio of one will be:

$$\frac{1.255}{.0006259} = 2040 \text{ lb./sq.ft.}$$

The allowable load on the test load area, as calculated in Chapter VI for an overload ratio of one, is 1701 pounds per square foot as shown on Page 182. The difference between the allowable load to be

TABLE IV

VALUES OF X, X^2, Y, AND XY USED IN DETERMINING THE YIELD VALUE STRAIGHT LINE USING 15 POINTS FOR THE FIRST, SECOND, AND THIRD STAGES OF LOADING

	X	X^2	Y	XY
1	3,826	14,638,276	1.518	5,807.868
2	3,826	14,638,276	0.741	2,835.066
3	3,826	14,638,276	1.518	5,807.868
4	3,826	14,638,276	0.777	2,972.802
5	3,826	14,638,276	0.530	2,027.780
6	4,676	21,864,976	1.848	8,641.248
7	4,676	21,864,976	1.643	7,682.668
8	4,676	21,864,976	2.327	10,881.052
9	4,676	21,864,976	1.369	6,401.444
10	4,676	21,864,976	1.506	7,042.056
11	2,822	7,963,684	1.136	3,205.792
12	2,822	7,963,684	1.136	3,205.792
13	2,822	7,963,684	0.568	1,602.896
14	2,822	7,963,684	0.000	0.000
15	2,822	7,963,684	0.000	0.000
Σ	56,620	222,334,680	16.617	68,114,332

$$b = \frac{n\Sigma XY - \Sigma X \Sigma Y}{n\Sigma X^2 - (\Sigma X)^2} = .0006259$$

$$a = \frac{\Sigma X^2 \Sigma Y - \Sigma X \Sigma XY}{n\Sigma X^2 \quad (\Sigma X)^2} = 1.255$$

$$Y = .0006259\ X - 1.255 \quad \text{.....(2)}$$

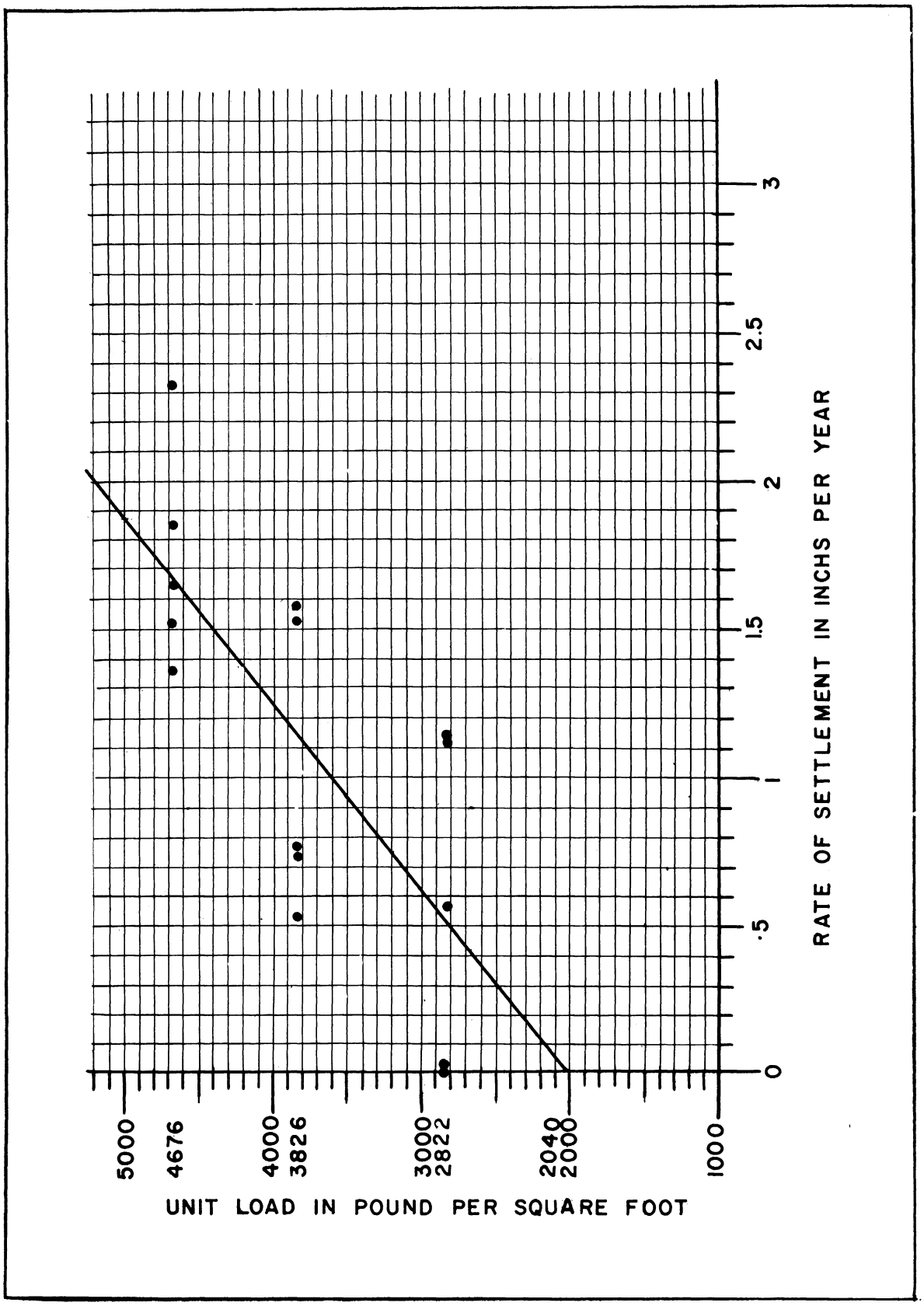

FIGURE 85. YIELD VALUE CURVE

placed on the test load area as determined theoretically and that as determined from the test results is 20 per cent. For a zero rate of settlement the allowable load as evaluated from the test results is greater than the allowable load calculated theoretically. This could be accounted for in the assumed design values. An example of that is the assumed angle of pressure transmission, θ, of the slag material. The angle of pressure transmission, could have been assumed steeper (smaller) because the slag material has developed an extra mechanical stability. This is due to the fact that there was a sufficiently long period for the slag fill to consolidate.

In order to determine the rate of settlement corresponding to each overload ratio the allowable load calculated theoretically is substituted in the straight line equation derived from the test results, obtaining the corresponding rate of settlement. Thus, for an overload ratio of 1.5, the allowable load calculated theoretically is 3371 pounds per square foot. By substituting this allowable load in the straight line equation derived from the best results, the rate of settlement is .77 inches per year. Accordingly, for an overload ratio of 2.0, the allowable load calculated theoretically is 4411 pounds per square foot and therefore the rate of settlement is 1.47 inches per year. For an overload ratio of 2.5, the allowable load calculated theoretically is 4844 pounds per square foot and therefore the rate of settlement is 1.85 inches per year. For an overload ratio of 3.0, the allowable load calculated theoretically is 5278 pounds per square foot and the rate of settlement is 2.09 inches per year.

From the above data, the overload ratios correspond to the rates of settlements as shown in Table V.

TABLE V

OVERLOAD RATIOS AND CORRESPONDING RATES OF SETTLEMENTS

Overload ratio R	Rate of settlement Inches per year	
	Calculated	Corrected by 120%
1.00	0.00	0.00
1.50	0.77	0.92
2.00	1.47	1.76
2.50	1.85	2.22
3.00	2.09	2.50

CHAPTER VIII

CONCLUSIONS AND RECOMMENDATIONS

The stability analysis of the cellular cofferdam as presented in this investigation has been conducted by both theoretical and experimental procedures. On the basis of this investigation the following conclusions can be drawn:

1. The allowable load on the test area, for an overload ratio of one, as determined from the revised theoretical analysis, is 1701 pounds per square foot. The allowable load on the test area, for an overload ratio of one (zero rate of settlement), as determined from the test, is 2040 pounds per square foot. Therefore there is a satisfactory correlation between the result of the theoretical analysis and that of the test. The values determined by the theoretical analysis are calculated on the basis of formulas for determining the active and passive lateral pressure given in Chapter II. Thus the determination of the active and passive lateral pressures, as calculated by the formulas given previously, gives a reliable method of determining these pressures, with definite consideration to the properties of the soil, as to whether it is purely granular, purely cohesive, or a mixed soil.
2. The test showed a maximum settlement of 2.32 inches per year at reference point M-4 on the boundary of the test area when the load of 4676 pounds per square foot was placed on the test area. Also there was no indication of structural failure of the cofferdam structure. The revised theoretical analysis in Chapter VI revealed that the cofferdam is critical with respect to mass stability, and the soft clay stratum of 38.5 feet thickness will control. Therefore, beside the general stability of the cofferdam structure, the

mass stability of the cofferdam is an important factor in designing and analyzing the cofferdam.

3. The lateral thrust applied on the cofferdam was delivered to the soft clay stratum to which the cell was driven. In order to achieve mass stability the cofferdam must reach the stiff clay stratum which would have sufficient strength to carry this lateral thrust. Therefore the depth and the stratum to which the sheet piles are driven have a great influence in determining the stability of the cofferdam.

4. It is established from the tested cofferdam that an overload ratio of 1 to 1.5 is recommended for a permanent cofferdam where the rate of settlement will not exceed 1/2 inch per year; while an overload ratio of 2 to 2.5 is recommended for a temporary cofferdam where the rate of settlement will be about 2 inches per year. This could be generalized whenever a sufficient confirmation is available. By choosing a suitable overload ratio (R) it is possible to design the cofferdam according to various rates of settlements.

5. The settlement contours show greater rates of settlements on row L than on row N. This is partially accounted for by the variation of static head on the dredged side where the depth of dredging is more at row L than at row N. Thus, due to this difference in surcharge, the element on row L was overstressed to a greater extent than that on side N. Therefore to increase the strength and stability of the cellular cofferdam a berm could be provided which would increase the strength of the cofferdam.

APPENDIX A

FULL MATHEMATICAL CALCULATIONS

FOR THE STABILITY ANALYSIS GIVEN IN CHAPTER IV

Soil Properties:
(Data are taken from Page 107)

Slag: Submerged weight, w_{s1} = 58.8 lb./cu.ft.

Wet weight, w_{t1} = 100.0 lb./cu.ft.

Angle of pressure transmission, θ = 27.5 degrees.

Angle of internal friction, ϕ = 45 degrees.

Sand: Submerged weight, w_{s2} = 68.2 lb./cu.ft.

Wet weight, w_{t2} = 115.0 lb./cu.ft.

Angle of pressure transmission, θ = 27.5 degrees.

Angle of internal friction, ϕ = 45 degrees.

Soft Clay:

Weight of clay, w_c = 130 lb./cu.ft.

Shearing resistance, S_{c_1} = 125 lb./sq.ft.

Between El.546.5 & 535.0 S_{uc_1} = 150 lb./sq.ft.

Between El.535.0 & 525.0 S_{uc_2} = 175 lb./sq.ft.

Between El.525.0 & 505.0 S_{uc_3} = 200 lb./sq.ft.

The average shearing resistance between

El.546.5 & El.505.0, S_{uc_4} = 180 lb./sq.ft.

Medium Clay:

Weight of clay, w_c = 130 lb./cu.ft.

Shearing resistance, S_{c_2} = 200 lb./sq.ft.

Shearing resistance, S_{uc_5} = 300 lb./sq.ft.

Note:

The weight of water, w_w = 62.4 lb./cu.ft.

$\tan \phi = \tan 45 = 1.0$

$\tan \theta = \tan 27.5 = 0.521$

$\tan^2\theta = \tan^2 27.5 = .271$, $\cot^2\theta = 3.69$.

Static Heads

	DREDGED SIDE		BACK SIDE	
	Increment lb./sq.ft.	Total lb./sq.ft.	Increment lb./sq.ft.	Total lb./sq.ft.
To El. 583.5	-----	-----	P_o	P_o
To El. 578.5	-----	-----	500	$P_o + 500$
To El. 556.0	1404*	1404*	1323 1404*	$P_o + 1823$ $P_o + 3227$
To El. 546.5	648 593*	648 2645	648 593*	$P_o + 2471$ $P_o + 4468$
To El. 543.5	390	3035	390	$P_o + 4858$

Numbers marked with (*) above are the static heads due to water only.

Active Lateral Pressures
(see Figure 86)

The active lateral pressures are determined as follows:

In the wet granular soil, $P_h = w_t\ h_t \text{Tan}^2\ \theta$.

In the submerged granular soil, $P_h = w_w\ h_w + w_s\ h_s\ \text{Tan}^2\ \theta$.

In the clay soil, P_h = Total static head - $2\ S_{uc} R$.

Dredged Side:

P_{h1} (at El. 556.0) = 1404 lb./sq.ft.

P_{h2} (at El. 546.5+) = .271 x 648 + 1997 = 2173 lb./sq.ft.

P_{h3} (at El. 546.5-) = 2645 - 300 R lb./sq.ft.

P_{h4} (at El. 543.5) = 3035 - 300 R lb./sq.ft.

Back Side:

P_{h5} (at El. 583.5) = $P_o \text{Tan}^2\theta$ = 0.271 P_o lb./sq.ft.

P_{h6} (at El. 578.5) = 0.271 P_o + .271x500 = .271 P_o+136 lb./sq.ft.

P_{h7} (at El. 556.0) = 0.271 P_o + 1898 lb./sq.ft.

P_{h8} (at El. 546.5+) = 0.271 P_o + 2667 lb./sq.ft.

P_{h9} (at El. 546.5-) = P_o + 4468 - 2 S_{uc_1}

= P_o + 4468 - 300 R lb./sq.ft.

P_{h10}(at El. 543.5) = P_o + 4858 - 300 R lb./sq.ft.

Passive Lateral Pressures

The passive lateral pressures are determined as follows:

In the wet granular soil, $P_h = w_t\ h_t\ Cot^2\theta$

In the submerged granular soil, $P_h = w_w\ h_w + w_s\ h_s\ Cot^2\theta$

In the clay soil, P_h = Total static head + 2 $S_{uc}R$

Dredged Side:

P'_{h1}(at El. 556.0) = 1404 lb./sq.ft.

P'_{h2}(at El. 546.5+) = 648 x $Cot^2\theta$ + $w_w\ h_w$

= 648 x 3.69 + 1997

= 2391 + 1997 = 4388 lb./sq.ft.

P'_{h3}(at El. 546.5-) = 2645 + 2 $S_{uc_1}R$

= 2645 + 300 R lb./sq.ft.

P'_{h4}(at El. 543.5) = 3035 + 300 R lb./sq.ft.

Active Lateral Forces

The lateral force is calculated as the area of the lateral pressure diagram. The active lateral forces are calculated as follows:

Dredged Side:

F_{h1} = $\frac{1}{2}$ (1404 x 22.5) = 15800 lb./ft. run

F_{h2} = $\frac{1}{2}$ (1404 + 2173) x 9.5 = 17000 lb./ft. run

F_{h3} = $\frac{1}{2}$ (2645-300R+3035-300R)x3 = 8520 + 900 R lb./ft. run

Total Active Lateral Force on the Dredged Side, F_{hd}, is equal to:

$$F_{hd} = F_{h1} + F_{h2} + F_{h3}$$
$$= 41320 - 900\ R \text{ lb./ft. run.}$$

Back Side:

$F_{h4} = \frac{1}{2}(.271P_o + .271P_o + 136)x5 = 1.35P_o + 340$ lb./ft. run.

$F_{h5} = \frac{1}{2}(.271P_o+136+.271P_o+1898)x22.5 = 6.10P_o+22900$ lb./ft. run.

$F_{h6} = \frac{1}{2}(.271P_o+1898+.271P_o+2667)x9.5 = 2.58P_o+21700$ lb./ft. run.

$F_{h7} = \frac{1}{2}(P_o+4468-300R+P_o+4858-300R)x3 = 3P_o+14000-900R$ lb./ft. run.

Total Active Lateral Force on the Back Side, F_{hb}, is equal to:

$$F_{hb} = F_{h4} + F_{h5} + F_{h6} + F_{h7}$$
$$= 13.03\ P_o + 58940 - 900\ R \text{ lb./ft. run.}$$

Passive Lateral Forces

Dredged Side:

$F'_{h1} = \frac{1}{2}(0 + 1404) \times 22.5 = 15800$ lb./ft. run.

$F'_{h2} = \frac{1}{2}(1404 + 4388) \times 9.5 = 27560$ lb./ft. run.

$F'_{h3} = \frac{1}{2}(2645+300R+3035+300R)x3 = 8520 + 900R$ lb./ft. run.

Total Passive Lateral Force on the Dredged Side, F'_{hd}, is equal to:

$$F'_{hd} = F'_{h1} + F'_{h2} + F'_{h3}$$
$$F'_{hd} = 51880 + 900\ R \text{ lb./ft. run.}$$

Vertical Shearing Resistance on the Dredged Side

Total Shearing Resistance $= 125R \times 3 + \frac{1}{2} \times 176 \times 9.5$

$$S_{hd} = 836 + 375\ R \text{ lb./ft.}$$

Average Shearing Resistance at the Dredged Side, S_{ad}, is:

$$S_{ad} = S_{hd}/h_1 = (836 + 375R)/12.5 = 30R + 66.88 \text{ lb./sq.ft.}$$

Vertical Shearing Resistance at the Back Side

$\frac{1}{2}$ (.271P_o + .271P_o + 136) x Tan ϕ x 5 = 1.35P_o+340 lb./ft.

$\frac{1}{2}$ (.271P_o+136+.271P_o+494) x Tan ϕ x 22.5 = 6.10P_o+7090 lb./ft.

$\frac{1}{2}$ (.271P_o+494+.271P_o+670) x Tan ϕ x 9.5 = 2.58P_o+5530 lb./ft.

3 S_{c_1} R = 3 x 125 x R = 375 R lb./ft.

Total Shearing Resistance at the Back Side, S_{hb}, is:

S_{hb} = 10.03 P_o + 12960 + 375 R lb./ft.

Average Shearing Resistance at the Back Side, S_{ab}, is:

$S_{ab} = S_{hb}/h = (10.03P_o+12960+375R)/40 = .251P_o+324+9.4R$ lb./sq.ft.

Average Shearing Resistance in the Clay Strata Below the Loading Plane (between El. 543.5 and El. 495.0)

$S_{c(Ave.)}$ = (125x38.5 + 200x10)/48.5 = 140 lb./sq.ft.

$S_{uc(Ave.)}$ = (180x38.5 + 300x10)/48.5 = 205 lb./sq.ft.

The Active Lateral Pressures and Force of the Fill of the Cell

P_{hf1} = .271 x 115 x 6 = 187 lb./sq.ft.

P_{hf2} = 187 + 35 (.271 x 68.2 + 62.4) = 3021 lb./sq.ft.

F_{hf} = (187 x 6)/2 + (187 + 3021) x 35/2

= 561 + 56140 = 56700 lb./ft. run of the cell.

The Passive Lateral Pressures and Force of the Fill of the Cell

P'_{hf1} = 3.69 x 115 x 6 = 2546 lb./sq.ft.

P'_{hf2} = 2546 + (68.2 x 3.69 + 62.4) x 35 = 13538 lb./sq.ft.

F'_{hf} = (2546 x 6)/2 + (2546 + 13538) x 35/2

= 7638 + 281470 = 289108 lb./ft. run.

$F''_{hf} = F'_{hf}$ - lateral force of water = 289108 - 62.4 x 35/2 = 250888

Stability Analysis with Respect to Mass Movement of the Soil Mass (Upheaval)

a) When all the area behind the cofferdam is loaded and the depth of the failing element is 48.5 feet:

This case is illustrated in Figure 86. The applied forces and the resisting forces are as follows:

The static head on the back side, wh_b, is equal to:

$$wh_b = P_o + 4858 \text{ lb./sq.ft.} \quad \text{(see Page 206)}$$

The active lateral force on the back side, F_{hb}, is equal to:

$$F_{hb} = 13.03\ P_o + 58940 - 900\ R \text{ lb./ft. run.} \quad \text{(see Page 208)}$$

The static head of the dredged side, wh_d, is equal to:

$$wh_d = 3035 \text{ lb./sq.ft.} \quad \text{(see Page 206)}$$

The active lateral force on the dredged side, F_{hd}, is equal to:

$$F_{hd} = 41320 - 900\ R \text{ lb./ft. run.} \quad \text{(see Page 208)}$$

The shearing resistance at El. 495.0, S_{t_2}, is equal to:

$$S_{t_2} = S_{a_2} = 200 \text{ lb./sq.ft.} \quad \text{(see Page 205)}$$

The average shearing resistance in the clay strata which are below the loading plane and above El. 495.0 is equal to:

$$S_{d(Ave.)} = 140 \text{ lb./sq.ft.} \quad \text{(see Page 209)}$$

$$S_{uc(Ave.)} = 205 \text{ lb./sq.ft.} \quad \text{(see Page 209)}$$

The average shearing resistance at the back side above the loading plane, S_{ab}, is equal to:

$$S_{ab} = (.251\ P_o + 324 + 9.4\ R) \quad \text{(see Page 209)}.$$

The average shearing resistance at the dredged side above the loading plane, S_{ad}, is equal to:

$$S_{ad} = (30\ R + 66.88) \quad \text{(see Page 208)}.$$

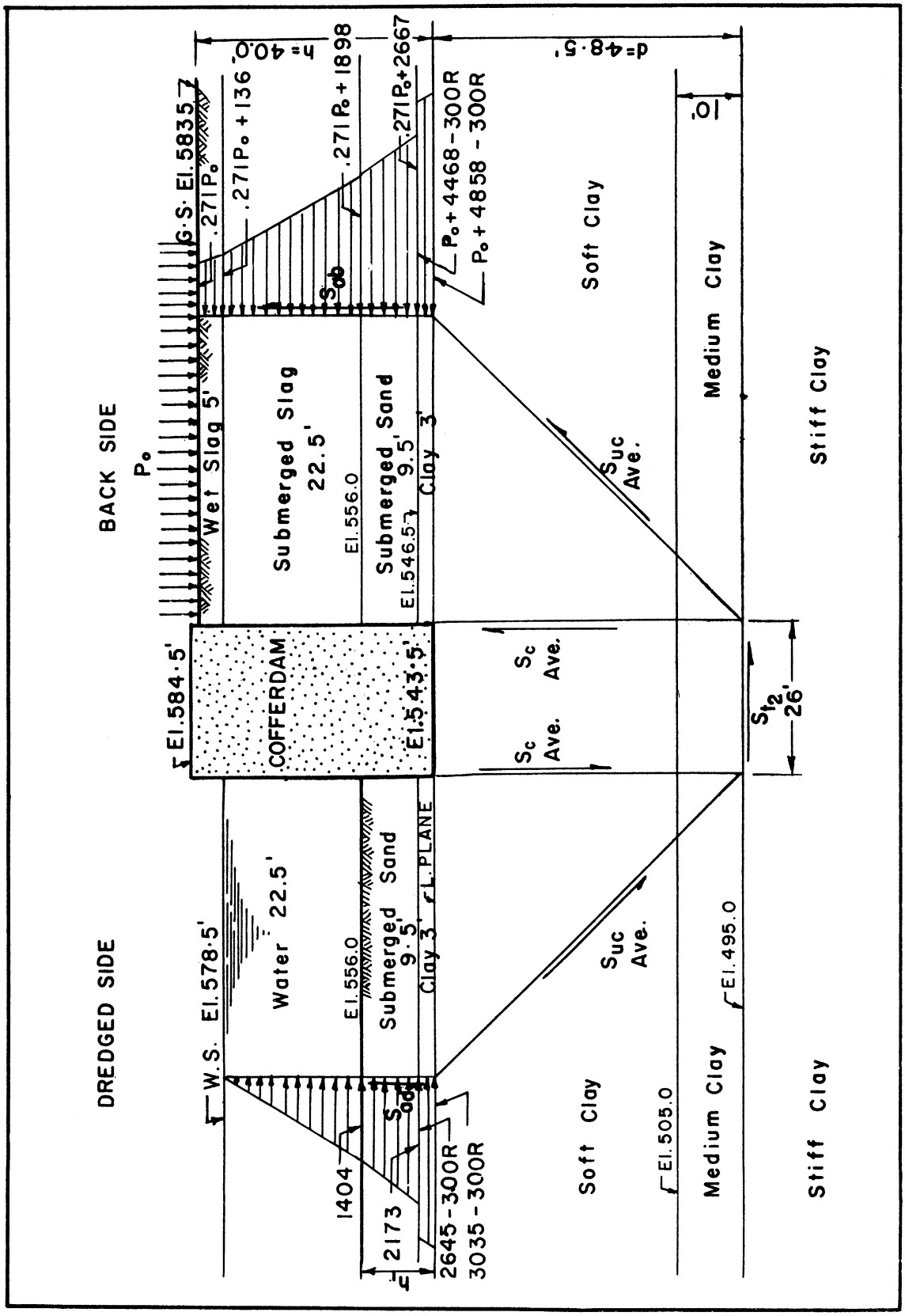

FIGURE 86. APPLIED AND RESISTING FORCES ACTING ON TEST COFFERDAM, FAILING ELEMENT DEPTH 48.5 FEET.

The weight transfer above the loading plane at the dredged side is determined as follows:

$$h_1 = 12.5 \text{ feet}, \quad d = 48.5 \text{ feet}, \quad h_1 < d$$

$$S_e = S_{t_2} R \frac{d}{h} = 200 R \frac{48.5}{12.5} = 776 R \leq S_{ad} = (30 R + 66.88)$$

$$S_e = (30 R + 66.88).$$

(776 R) is greater than (30R + 66.88) for values of R under consideration. Therefore the value of $S_{ad} \frac{h}{d}$, which is equal to S_{hd}/d, will be used for weight transfer at the dredged side.

The weight transfer above the loading plane at the back side is determined as follows:

$$h = 40', \quad d = 48.5', \quad h < d, \quad h/d = .825$$

$$S_e = S_{t_2} \frac{d}{h} \leq S_{ab}; \; S_e = 243R \leq (.251 P_o + 324 + 9.4 R).$$

When $S_e < S_{ab}$, the weight transfer at the back side is $S_{t_2}R=200R$.

When $S_e = S_{ab}$, the weight transfer at the back side is $S_{ab} \frac{h}{d}$

$$S_{ab} \frac{h}{d} = (.207 P_o + 267 + 7.75).$$

200 R can be more or less than $0.207 P_o + 267 + 7.75 R$ depending upon the values of P_o and the value of R. Therefore, the weight transfer at the back side will be either $S_{ab} \frac{h}{d}$ or $S_{t_2}R$ depending upon which one will control.

Therefore, the stability equation, using $S_{ab} \frac{h}{d}$ for weight transfer at the back side, is:

$$wh_b + F_{hb}/d - wh_d - F_{hd}/d - S_{hd}/d - 4 S_{uc(Ave.)}R$$

$$- 2 S_{c(Ave.)}R - S_{t_2} R \, b/d - S_{hb}/d = 0 .$$

$(P_o+4858)+(13.03P_o+58940-900R)/48.5-(3035)-(41320-900R)/48.5$

$-(836+375R)/48.5-(4x205R)-(2x140R)-(26x200R)/48.5$

$-(10.03P_o+12960+375R)/48.5 = 0$

$1.062\ P_o + 1902 - 1223\ R = 0$

For $P_o = 0$, $R = 1.55$, and $(h/d)S_{ab} = 279 < 200R$

For $R = 2.0$, $P_o = 510$, and $(h/d)S_{ab} = 388 < 200R$

For $R = 2.5$, $P_o = 1090$, and $(h/d)S_{ab} = 512 > 200R$*

For $R = 3.0$, $P_o = 1665$, and $(h/d)S_{ab} = 635 > 200R$*

For $R = 3.5$, $P_o = 2240$, and $(h/d)S_{ab} = 758 > 200R$*

$h/d = 40/48.5 = .825$, and $S_{ab} = 0.251\ P_o + 324 + 9.4R$.

When $(h/d)S_{ab}$ is greater than 200 R (where marked with * above) the stability equation using $S_{hb}\ \frac{h}{d}$ is not valid because the weight transfer is limited by $S_{t_2}R$. Therefore, the stability equation using S_{t_2} as the weight transfer will control.

The stability equation, with weight transfer using S_{t_2}, is:

$$wh_b + F_{hb}/d - wh_d - F_{hd}/d - S_{hd}/d - 4S_{uc(Ave.)}R - 2S_{c(Ave.)}R$$

$$- S_{t_2}R\ b/d - S_{t_2}R = 0$$

$(P_o+4858)+(13.03P_o+58940-900R)/48.5-(3035)-(41320-900R)/48.5$

$-(836+375R)/48.5-(4x205R)-(2x140R)-(26x200R)/48.5-200R = 0$

$1.269\ P_o + 2169 - 1415\ R = 0$

For $P_o = 0$, $R = 1.53$ and $(h/d)S_{ab} = 279 < 200R$*

For $R = 2.0$, $P_o = 520$ and $(h/d)S_{ab} = 390 < 200R$*

For $R = 2.5$, $P_o = 1080$ and $(h/d)S_{ab} = 509 > 200R$

For $R = 3.0$, $P_o = 1635$ and $(h/d)S_{ab} = 628 > 200R$

For $R = 3.5$, $P_o = 2190$ and $(h/d)S_{ab} = 747 > 200R$

When $(h/d)S_{ab}$ is smaller than 200 R in the above cases (where marked with * above) the shearing resistance S_{ab} controls and the stability equation using S_{t2} is not valid.

Summary of the results when all the area behind the cofferdam is loaded:

For R = 1.55, P_o = 0

For R = 2.00, P_o = 510 lb./sq.ft.

For R = 2.50, P_o = 1080 lb./sq.ft.

For R = 3.00, P_o = 1635 lb./sq.ft.

For R = 3.50, P_o = 2190 lb./sq.ft.

b) When area "0" of 48.5 feet times 48.5 feet is loaded and the depth of the failing element is 48.5 feet:

The allowable loads for various overload ratios, to be placed behind the cofferdam when all the area is loaded, were calculated previously, in which the problem was considered two dimensional.

To find the allowable loads on area "0" (see Figure 43), the problem will become three dimensional. The approach in this case is based on the assumption that the load capacity of areas 0, 1, 2, 3, 4, and 5 could be concentrated on area "0", providing there is sufficient shear in the vertical planes A-B, B-C, and C-D, in excess of what has already been mobilized for weight transfer, to distribute the concentration back to the five adjacent elements at the loading plane. This assumption has been abandoned as shown in Chapter VI.

The average shearing resistance on planes A-B, B-C, and C-D due to active lateral pressure is:

$$S_{ab} = 0.251\ P_o + 324 + 9.4\ R$$ (see Page 209) .

The shearing resistance mobilized for weight transfer along plane B-C when S_{t_2} controls is:

$$S_{t_2} \frac{d}{h} R = 200 R (48.5/40) = 243 R$$

Using the symbol P_o for the allowable load when all the area is loaded and the symbol P'_o for the allowable load when area "0", of 48.5 feet by 48.5 feet is loaded only, then the load P'_o will be as follows; $P'_o = 6 P_o$ or, as controlled by vertical shear,

$$P'_o = P_o + (3 S_{ab} - S_{ab}) \frac{hd}{d^2}$$

$$= P_o + 2 S_{ab} \frac{h}{d} \text{ when } S_{ab} \text{ controls.}$$

$$P'_o = P_o + (3 S_{ab} - S_{t_2} R \frac{d}{h}) \frac{hd}{d^2}$$

$$= P_o + (3 S_{ab} \frac{h}{d} - S_{t_2} R) \text{ when } S_{t_2} \text{ controls.}$$

By introducing the values of R and the corresponding values of P_o, the values of S_{ab}, S_{t_2}, h and d, the allowable loads for various overload ratios are calculated as follows:

For R = 2.0

P_o = 510 lb./sq.ft. (see Page 214)

P'_o = 510 x 6 = 3060 lb./sq.ft. or as controlled by vertical shear.

As controlled by vertical shear:

$$P'_o = P_o + 2 S_{ab} \frac{h}{d}$$

$$= 510 + 2(.251 P'_o + 324 + 18.1)40/48.5$$

$$0.586 P'_o = 1076$$

$$P'_o = 1830 \text{ lb./sq.ft.}$$

For R = 2.5

P_o = 1080 lb./sq.ft. (see Page 214)

P'_o = 6 x 1080 = 6480 lb./sq.ft. or as controlled by vertical shear.

As controlled by vertical shear:

$$P'_o = P_o + (3\, S_{ab} \frac{h}{d} - S_{t_2} R)$$

$$= 1080 + 3(.251\, P'_o + 324 + 23.5)40/48.5 - 200 \times 2.5$$

$$0.379\, P'_o = 1427$$

$$P'_o = 3760 \text{ lb./sq.ft.}$$

For R = 3.0

P_o = 1635 lb./sq.ft. (see Page 214)

P'_o = 6 x 1635 = 9810 lb./sq.ft. or as controlled by vertical shear.

As controlled by vertical shear:

$$P'_o = P_o + (3\, S_{ab} \frac{h}{d} - S_{t_2} R)$$

$$P'_o = 1635 + 3(.251\, P_o + 324 + 28.2)40/48.5 - 200 \times 3$$

$$0.379\, P'_o = 1905, \quad P'_o = 5040 \text{ lb./sq.ft.}$$

For R = 3.5

P_o = 2190 lb./sq.ft. (see Page 214)

P'_o = 6 x 2190 = 13140 lb./sq.ft. or as controlled by vertical shear.

As controlled by vertical shear:

$$P'_o = P_o + 3\, S_{ab} \frac{h}{d} - S_{t_2} R$$

$$P'_o = 2190 + 3(.251\, P'_o + 324 + 32.9)40/48.5 - 200 \times 3.5$$

$$0.379\, P'_o = 2370, \quad P'_o = 6250 \text{ lb./sq.ft.}$$

Summary of the results when area "O" is loaded:

For R = 2.00, P'_o = 1830 lb./sq.ft.

For R = 2.50, P'_o = 3760 lb./sq.ft.

For R = 3.00, P'_o = 5040 lb./sq.ft.

For R = 3.50, P'_o = 6250 lb./sq.ft.

c) When all the area behind the cofferdam is loaded and the depth of the failing element is 38.5 feet:

This case is illustrated in Figure 87. The applied forces and the resisting forces are as follows:

The static head on the back side, wh_b, is equal to:

$$wh_b = P_o + 4858 \text{ lb./sq.ft.} \quad \text{(see Page 206)}$$

The active lateral force on the back side, F_{hb}, is equal to:

$$F_{hb} = 13.03\ P_o + 58940 - 900\ R \text{ lb./ft. run.} \quad \text{(see Page 208)}$$

The static head on the dredged side, wh_d, is equal to:

$$wh_d = 3035 \text{ lb./sq.ft.} \quad \text{(see Page 206)}$$

The active lateral force on the dredged side, F_{hd}, is equal to:

$$F_{hd} = 41320 - 900\ R \text{ lb./ft. run.} \quad \text{(see Page 208)}$$

The shearing resistance at El. 505.0, S_{t_1}, is equal to:

$$S_{t_1} = S_{c_1} = 125 \text{ lb./sq.ft.} \quad \text{(see Page 205)}$$

The average shearing resistance in the clay stratum which is below the loading plane and above El. 505.0 is equal to:

$$S_{c_1} = 125 \text{ lb./sq.ft.} \quad \text{(see Page 205)}$$

$$S_{uc_4} = 180 \text{ lb./sq.ft.} \quad \text{(see Page 205)}$$

The average shearing resistance at the back side above the loading plane, S_{ab}, is equal to:

$$S_{ab} = (.251\ P_o + 324 + 9.4\ R) \quad \text{(see Page 209)}.$$

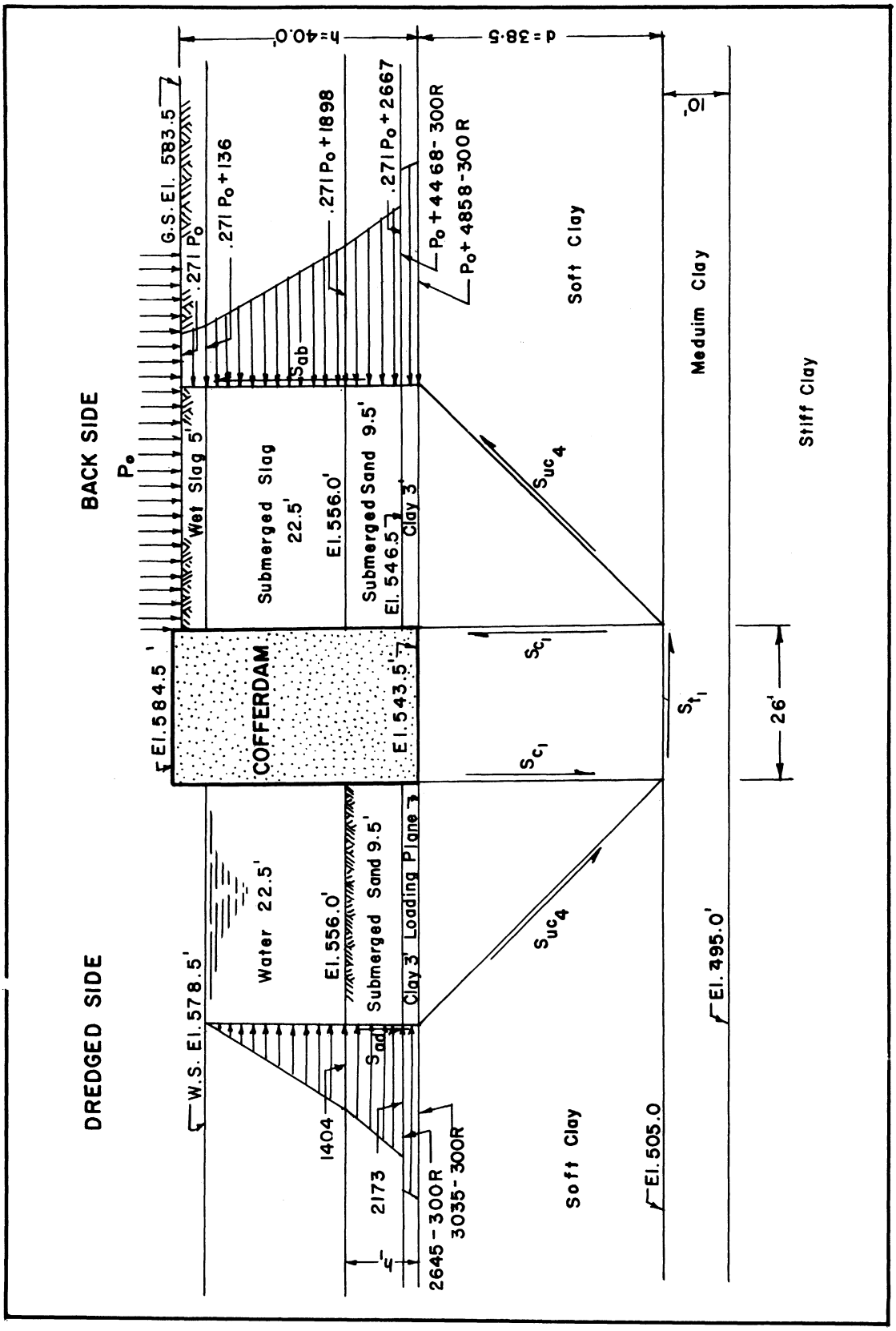

FIGURE 87. APPLIED AND RESISTING FORCES ACTING ON TEST COFFERDAM, FAILING ELEMENT DEPTH 38.5 FEET.

The average shearing resistance at the dredged side above the loading plane, S_{ad} = (30 + 66.88) (see Page 208) .

The weight transfer above the loading plane at the dredged side is determined as follows:

$$h_1 = 12.5 \text{ feet}, \quad d = 38.5 \text{ feet}, \quad h_1 < d$$

$$S_e = S_{t_1} R \frac{d}{h_1} \leq S_{ad}, \text{ therefore}$$

$$S_e = 125 \times \frac{38.5}{12.5} R = 385 R \leq (30 R + 66.88)$$

$$S_e = (30 R + 66.88) .$$

Therefore, when S_e is equal to or greater than S_{ad}, the reduction in the static head will be $S_{ad} \frac{h_1}{d}$, which is equal to S_{hd}/d.

The weight transfer above the loading plane at the back side is determined as follows:

$$h = 40', \quad d = 38.5', \quad h > d$$

$$S_e = S_{t_1} R \leq S_{ab}, \text{ therefore, } S_e = 125 R \leq (.251 P_o + 324 + 9.4 R)$$

When $S_e < S_{ab}$, the weight transfer at the back side is $S_{t_1} R = 125R$.

When $S_e > S_{ab}$, the weight transfer at the back side is S_{ab} .

125 R can be more or less than .251 P_o + 324 + 9.4 R depending upon the values of P_o and the value of R. Therefore the weight transfer at the back side will be either S_{ab} or S_{t_1} R, depending upon which one will control.

The stability equation will be set with the assumption that $S_{t_1} R$ will control. This will be verified later. Therefore the stability

equation will be:

$$wh_b + F_{hb}/d - wh_d - F_{hd}/d - S_{hd}/d - 4\,S_{uc4}R - 2\,S_{c_1}R - S_{t_1}R\,b/d - S_{t_1}R = 0$$

$$(P_o+4858)+(13.03P_o+58940-900R)/38.5-(3035)-(41320-900R)/38.5 -(836+375R)/38.5-(4x180R)-(2x125R)-(26x125R)/38.5- 125R = 0$$

$$1.338\,P_o + 2258 - 1189\,R = 0$$

For $P_o = 0$, $R = 1.9$ and $S_{ab} = 342 > 125R$

For $R = 2.0$, $P_o = 90$ and $S_{ab} = 365 > 125R$

For $R = 2.5$, $P_o = 535$ and $S_{ab} = 482 > 125R$

For $R = 3.0$, $P_o = 980$ and $S_{ab} = 598 > 125R$

For $R = 3.5$, $P_o = 1420$ and $S_{ab} = 712 > 125R$

The values of S_{ab} as shown above, for the various overload ratios, R, and the corresponding P_o, are always greater than 125 R. Thus the assumption that S_{t_1} will control is valid and therefore the weight transfer at the back side is controlled by $S_{t_1}R$.

d) When Area "0" of 38.5 feet times 38.5 feet is loaded and the depth of the failing element is 38.5 feet:

The allowable loads for various overload ratios, to be placed behind the cofferdam when all the area is loaded, were calculated previously, in which the problem was considered two dimensional.

To find the allowable loads on area "0" (see Figure 45), the problem will become three dimensional. The approach in this case is based on the assumption that the load capacity of areas 0, 1, 2, 3, 4, and 5 could be concentrated on area "0", providing there is sufficient shear in the vertical planes A-B, B-C, and C-D, in excess of what has

already been mobilized for weight transfer, to distribute the concentration back to the five adjacent elements at the loading plane. This assumption has been abandoned as shown in Chapter VI.

For R = 2.0

P_o = 90 lb./sq.ft. (see Page 220)

P'_o = 90 x 6 = 540 or as controlled by vertical shear.

As controlled by vertical shear:

$$P'_o = P_o + (3S_{ab} - S_{t_1}) \frac{h \times d}{d \times d} = P_o + 3S_{ab} \frac{h}{d} - S_{t_1} R \frac{h}{d}$$

$$= 90 + 3(.251\ P'_o + 324 + 18.8)40/38.5 - 125 \times 2.0 \times 40/38.5$$

P'_o = 4130 lb./sq.ft.

Therefore for R = 2.0, P'_o = 540 lb./sq.ft.

For R = 2.5

P_o = 535 lb./sq.ft. (see Page 220)

P'_o = 6 x 535 = 3210 lb./sq.ft. or as controlled by vertical shear.

As controlled by vertical shear:

$$P'_o = P_o + (3S_{ab} \frac{h}{d} - S_{t_1} R \frac{h}{d})$$

$$= 535 + 3(.251\ P'_o + 324 + 23.5)40/38.5 - 125 \times 2.5 \times 40/38.5$$

$$= 5940 \text{ lb./sq.ft.}$$

Therefore for R = 2.5, P'_o = 3210 lb./sq.ft.

For R = 3.0

P_o = 980 lb./sq.ft. (see Page 220)

P'_o = 6 x 980 = 5880 lb./sq.ft. or as controlled by vertical shear.

As controlled by vertical shear:

$$P'_o = P_o + (3S_{ab}\frac{h}{d} - S_{t_1}R\frac{h}{d})$$

$$P'_o = 980 + 3(.251\ P_o + 324 + 28.2)40/38.5 - 125 \times 3x40/38.5$$

$$= 7740 \text{ lb./sq.ft.}$$

Therefore for R = 3.0, P'_o = 5880 lb./sq.ft.

For R = 3.5

P_o = 1420 lb./sq.ft. (see Page 220)

P'_o = 6 x 1420 = 8520 lb./sq.ft. or as controlled by vertical shear.

As controlled by vertical shear:

$$P'_o = P_o + 3\ S_{ab}\frac{h}{d} - S_{t_1}\ R\frac{h}{d}$$

$$P'_o = 1420 + 3(.251\ P'_o + 324 + 32.9)40/38.5-125x3.5x40/38.5$$

$$= 9530 \text{ lb./sq.ft.}$$

Therefore for R = 3.5, P'_o = 8520 lb./sq.ft.

Summary of the results when area "0" of 38.5 feet by 38.5 feet is loaded: (d = 38.5')

For R = 2.00, P'_o = 540 lb./sq.ft.

For R = 2.50, P'_o = 3210 lb./sq.ft.

For R = 3.00, P'_o = 5880 lb./sq.ft.

For R = 3.50, P'_o = 8520 lb./sq.ft.

e) When the area "0" of 48.5 feet times 48.5 feet is loaded and the depth of the failing element is 38.5 feet:

The allowable loads for various overload ratios, to be placed behind the cofferdam when all the area is loaded, are calculated on Page

To find the allowable loads on area "0" (see Figure 46), the approach in this case is based on the assumption that the load capacity of areas 0, 1, 2, 3, 4, and 5 could be concentrated on Area "0", providing there is sufficient shear in the vertical planes A-B, B-C, and C-D, in excess of what has already been mobilized for weight transfer, to distribute the concentration back to the five adjacent elements at the loading plane. This assumption has been abandoned as shown in Chapter VI.

The average shearing resistance on planes A-B, B-C, and C-D due to the active lateral pressure is:

$$S_{ab} = 0.251\ P_o + 324 + 9.4\ R \quad \text{(see Page 209)}$$

The shearing resistance mobilized for weight transfer along plane B-C is S_{t_1} and is equal to 125 R.

Using the symbol P_o for the allowable load when all the area is loaded and the symbol P_o' for the allowable load when area "0" of 48.5 by 48.5 feet is loaded only, then the load P_o' will be determined as follows:

$$P_o' = P_o \times 6 \times (38.5 \times 38.5)/(48.5 \times 48.5)$$

$$P_o' = 3.78\ P_o \text{ or, as controlled by vertical shear,}$$

$$P_o' = P_o + (3\ S_{ab} - S_{t_1}R)\ \frac{hxd}{dxd}$$

$$P_o' = P_o + (3\ S_{ab} - S_{t_1}R)\ 40x48.5/48.5x48.5$$

$$P_o' = P_o + .825(3\ S_{ab} - S_{t_1}R)$$

By introducing the values of R and the corresponding values of P_o, the values of S_{ab}, and the value of S_{t_1}, the allowable loads for various overload ratios are calculated as follows:

For R = 2.0, P_o = 90 lb./sq.ft. (see Page 220)

$P'_o = 3.78\ P_o = 3.78 \times 90 = 340$ lb./sq.ft. or as controlled by vertical shear.

As controlled by vertical shear:

$$P'_o = P_o + .825(3\ S_{ab} - S_{t_1} R)$$

$$P'_o = 90 + .825 \times 3(.251\ P_o + 324 + 9.4\ R) - .825 \times 125 \times 2.0$$

P'_o = 1932 lb./sq.ft. which is greater than 340 lb./sq.ft.

Therefore; For R = 2.0, P'_o = 340 lb./sq.ft.

For R = 2.50, P_o = 535 lb./sq.ft. (see Page 220)

$P'_o = 3.78\ P_o = 3.78 \times 535 = 2022$ lb./sq.ft. or as controlled by vertical shear.

As controlled by vertical shear:

$$P'_o = P_o + .825\ (3\ S_{ab} - S_{t_1} R)$$

$$P'_o = 535 + .825 \times 3\ (.251\ P_o + 324 + 23.5) - .825 \times 125 \times 2.5$$

P'_o = 2998 lb./sq.ft. which is greater than 2022 lb./sq.ft.

Therefore for R = 2.50, P'_o = 2022 lb./sq.ft.

For R = 3.0, P_o = 980 lb./sq.ft. (see Page 220)

$P'_o = 3.78\ P_o = 3.78 \times 980 = 3702$ lb./sq.ft. or as controlled by vertical shear.

As controlled by vertical shear:

$$P'_o = P_o + .825\ (3\ S_{ab} - S_{t_1} R)$$

$$P'_o = 980 + .825 \times 3(.251\ P_o + 324 + 28.2) - .825 \times 125 \times 3.0$$

P'_o = 4078 lb./sq.ft. which is greater than 3702 lb./sq.ft.

Therefore for R = 3.0, $P_o' = 3702$ lb./sq.ft.

For R = 3.50, $P_o = 1420$ lb./sq.ft. (see Page 220)

$P_o' = 3.78\ P_o = 3.78 \times 1420 = 5368$ lb./sq.ft. or as controlled by vertical shear.

As controlled by vertical shear:

$$P_o' = P_o + .825\ (3\ S_{ab} - S_{t_1} R)$$

$$P_o' = 1420 + .825x3(.251\ P_o + 324 + 32.9) - .825x125x3.5$$

$P_o' = 5125$ lb./sq.ft. which is less than 5368 lb./sq.ft.

Therefore for R = 3.5, $P_o' = 5125$ lb./sq.ft.

Summary of the results when area "0" of 48.5 feet by 48.5 feet is loaded and the failing element depth is 38.5 feet:

For R = 2.0, $P_o' = 340$ lb./sq.ft.

For R = 2.5, $P_o' = 2022$ lb./sq.ft.

For R = 3.0, $P_o' = 3702$ lb./sq.ft.

For R = 3.5, $P_o' = 5125$ lb./sq.ft.

Stability Analysis with Respect to Sliding

Two cases are considered; the first is when all the area behind the cofferdam is loaded and the second case is when the square area of 48.5 feet by 48.5 feet is loaded only.

When all the area is loaded

The active lateral pressure on the back side will be resisted by the passive lateral pressure on the dredged side and the shearing resistance at the base of the cofferdam. (See Figure 88). Therefore the

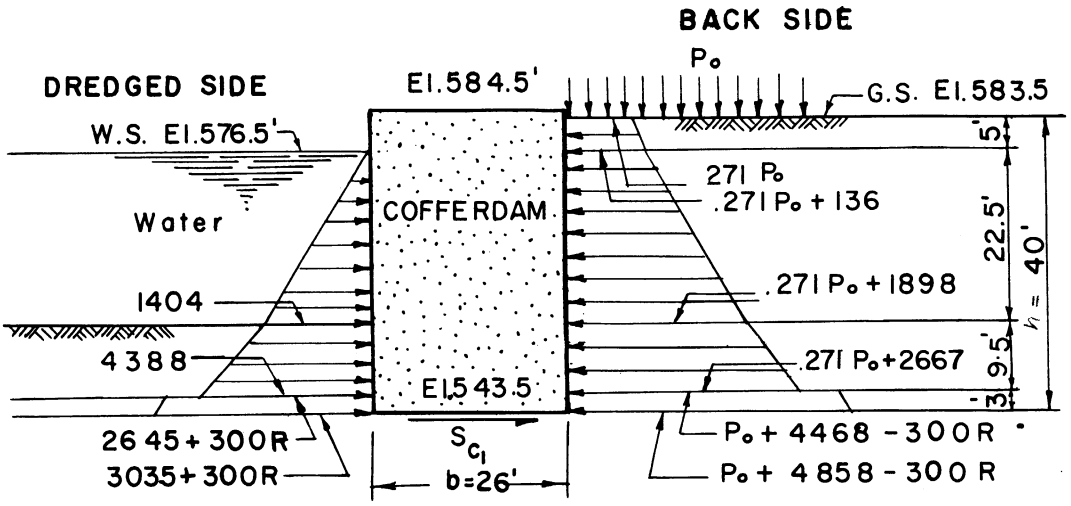

FIGURE 88. FORCES ACTING ON TEST COFFERDAM WITH RESPECT TO SLIDING

stability equation will be:

$$F_{hb}(\text{active}) - F'_{hd}(\text{passive}) - S_{c_1} R\, b = 0$$

$$(13.03P_o + 58940 - 900R) - (51880 + 900\,R) - (26 \times 125R) = 0$$

$$P_o = 388\,R - 538$$

For $P_o = 0$ $\qquad R = 1.38$

For $R = 2.00$ $\qquad P_o = 232$ lb./sq.ft.

For $R = 2.50$ $\qquad P_o = 430$ lb./sq.ft.

For $R = 3.00$ $\qquad P_o = 624$ lb./sq.ft.

For $R = 3.50$ $\qquad P_o = 818$ lb./sq.ft.

When Area "O" is loaded only

The stability equation is set taking into consideration the continuity effect of the cofferdam's structure.

The applied force on the cofferdam is the active lateral force on the back side, F_{hb}, and is equal to:

$(13.03\,P_o + 58940 - 900\,R)$ lb./ft. (see Page 208)

The resisting forces are the passive lateral pressure on the dredged side, the resistance to sliding at the base of the cofferdam and the resistance due to the continuity effect of the unloaded portion of the cofferdam. The passive lateral force on the dredged side is equal to:

$F'_{hd} = (51880 + 900\,R)$ lb./ft. (see Page 208)

The resistance to sliding at the base of the cofferdam is equal to:

$$S_{c_1} R\, b = 125 \times 26\,R = 3250\,R \text{ lb./ft.}$$

The resistance due to the effect of the continuity will be the total resistance of the unloaded portion of the cofferdam in excess of what has been mobilized for the stability of the unloaded portion of the cofferdam.

The resistance of the unloaded portion of the cofferdam against sliding which is in excess of what has been mobilized for the stability of the unloaded portion of the cofferdam is calculated on the following basis. For any value of R greater than 1.38, which is the overload ratio for P_o equal to zero, the increase in the value of R will affect the clay strata. This increase in the resistance will be equal to:

$(2 \times 900 + 125 \times 26)\ (R - 1.38)$ lb./ft. run of the cofferdam. The total resistance over the length of the unloaded portion of the cofferdam is:

$397^*(2 \times 900 + 125 \times 26)\ (R - 1.38)$ lb.

The resistance per foot run of the unloaded portion of the cofferdam is equal to:

$$397^*(2 \times 900 + 125 \times 26)\ (R - 1.38)/48.5$$
$$= 397 \times 5050(R - 1.38)/48.5$$
$$= 41337\ (R - 1.38) \text{lb./ft.}$$

Therefore the stability equation with respect to sliding will be set as follows:

$$F_{hb} - F'_{hd} - S_{c_1} R\ b - 41337\ (R - 1.38) = 0$$
$$(13.03\ P_o + 58940 - 900\ R) - (51880 + 900\ R) - (3250\ R)$$
$$- (41337\ R - 57045) = 0$$
$$13.03\ P_o + 58940 - 900\ R - 51880 - 900\ R - 3250\ R$$
$$- 41337\ R + 57045 = 0$$

Therefore $13.03\ P_o + 64105 - 46387\ R = 0$

*The length of the unloaded portion of the cofferdam is 397 feet.

$P_o = 3560\ R - 4915$

For R = 2.00, P_o = 2205 lb./sq.ft.

For R = 2.50, P_o = 3985 lb./sq.ft.

For R = 3.00, P_o = 5765 lb./sq.ft.

For R = 3.50, P_o = 7545 lb./sq.ft.

Tension in the interlock:

The active lateral pressure acting on the back wall of the cofferdam will be transmitted to the front wall provided that there is sufficient passive lateral pressure in the fill of the cell. This pressure will be resisted by the passive lateral pressure on the dredged side. The resultant pressure will be transmitted to the back wall through the diaphragm causing a tension in the interlock. (see Figure 48).

The active lateral pressures on the back side are calculated on page 208 and the total active force is F_{hb}.

$F_{hb} = 13.03P_o + 58940 - 900R$ lb./ft. run of the cofferdam.

The passive lateral pressure on the dredged side is calculated on page 208 and the total passive force on the dredged side is F'_{hd}.

$F'_{hd} = 51880 + 900\ R$ lb./ft. run of the cofferdam.

The net pressure on the front wall is:

$$F_{hb} - F'_{hd} = (13.03\ P_o + 58940 - 900\ R) - (51880 + 900\ R)$$

$$= 13.03\ P_o + 7060 - 1800\ R$$

This net pressure will be carried to the back wall by the diaphragm causing the tension in the interlock. The tension in the interlock is:

$$T = \frac{(F_{hb} - F'_{hd}) \times 3L}{4\ b\ \text{Tan}\ \theta \times 12} = \frac{(13.03P_o + 7060 - 1800R) \times 30 \times 3}{4 \times 26 \times \text{Tan}\ 27.5 \times 12}$$

where 30 is the length of the three cells of the cofferdam in front of the test area, 4 is the number of diaphragms by which the tension is carried, and b Tan θ is the length of the interlock which is effective in carrying the tension.

$$T = (13.03\ P_o + 7060 - 1800R)/10.4 \times .521 \times 1.33$$

$$= (13.03\ P_o + 7060 - 1800R)/7.225$$

If the allowable tension in the interlock is 10000 pounds per inch of the interlock, then the allowable loads to be placed behind the cofferdam without exceeding the allowable tension in the interlock are:

$$10000 = (13.03\ P_o + 7060 - 1800R)/7.225$$

$$65025 = 13.03\ P_o - 1800R$$

$$P_o = 138\ R + 4990$$

Therefore for various assumed overload ratios, P_o is:

When R = 2.00, P_o = 5262 lb./sq.ft.

When R = 2.50, P_o = 5331 lb./sq.ft.

When R = 3.00, P_o = 5400 lb./sq.ft.

When R = 3.50, P_o = 5469 lb./sq.ft.

The above equation for the tension in the interlock is based on the assumption that the total active force on the back side will be transmitted to the front wall. The maximum force that could be transmitted through the fill is limited by the passive lateral pressure of the fill in the cell.

When the load P_o is equal to 5469 pounds per square foot the lateral pressure, F_{hb}, is:

$$F_{hb} = 5469 \times 13.03 + 58940 - 900 \times 3.5$$

$$= 71261 + 58940 - 3150$$

$$= 127051 \text{ lb./ft. run.}$$

The passive lateral pressure of the fill in the cell is calculated on page 209 and is equal to 289108 which is greater than 127051 pounds per foot. Therefore there is sufficient passive lateral pressure in the cell to transfer the applied lateral pressure, F_{hb}, from the back wall to the front wall of the cofferdam.

Allowable load, P_o, with respect to overturning when all area is loaded:

The applied moment due to the active lateral pressure on the back side: (see Figure 89)

Between El. 583.5 and El. 578.5

$$M_{a1} = 5 \times .271\ P_o \times 37.5 + \tfrac{1}{2} \times 136 \times 36.67 \times 5$$

$$= 51.5\ P_o + 12470 \text{ lb.ft./ft. run.}$$

Between El. 578.5 and El. 556.0

$$M_{a2} = (.271\ P_o + 136) \times 22.5 \times 23.75 + 1762 \times 22.5 \times \tfrac{1}{2} \times 20$$

$$= 145\ P_o + 469700 \text{ lb.ft./ft. run of cofferdam.}$$

Between El. 556.0 and El. 546.5

$$M_{a3} = (.271\ P_o + 1898) \times 9.5 \times 7.75 + \tfrac{1}{2} \times 769 \times 9.5 \times 6.167$$

$$= 19.9\ P_o + 36540 \text{ lb.ft./ft. run of cofferdam.}$$

Between El. 546.5 and El. 543.5

$$M_{a4} = (P_o + 4468 - 300\ R) \times 3 \times 1.5 + 390 \times 1 \times 3 \times \tfrac{1}{2}$$

$$= 4.5\ P_o + 20690 - 1350\ R \text{ lb.ft./ft. run of cofferdam.}$$

The total applied moment due to the active lateral pressure on the back side is M_a and is equal to:

$$M_a = 220.3\ P_o + 539400 - 1350\ R \text{ lb.ft./ft. run of cofferdam.}$$

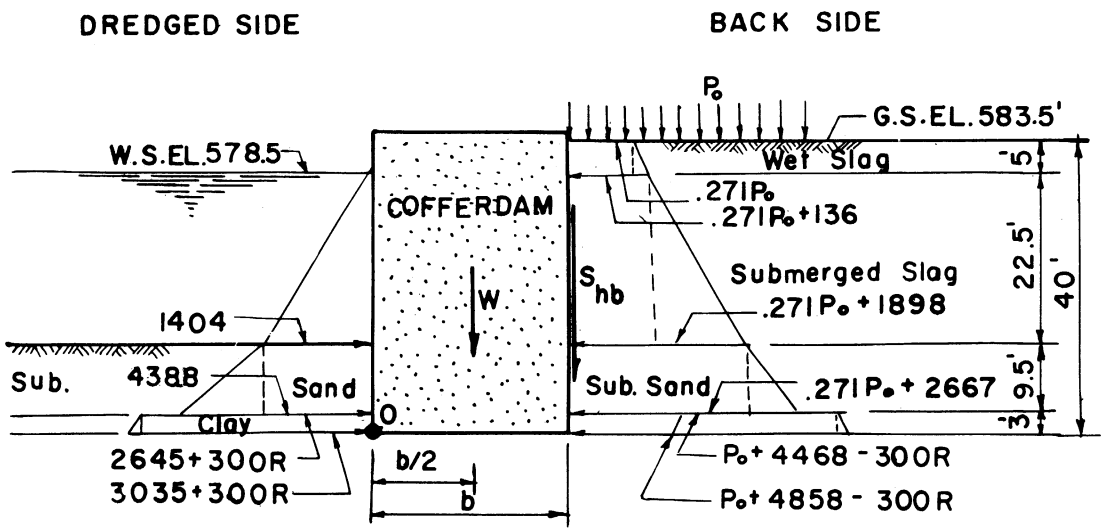

FIGURE 89. FORCES ACTING ON TEST COFFERDAM WITH RESPECT TO OVERTURNING

The resisting moment due to the passive lateral pressure on the dredged side:

Between El. 578.5 and El. 556.0

$$M'_{r1} = (\tfrac{1}{2} \times 1404 \times 22.5)(12.5 + 22.5/3)$$

$$= 316000 \text{ lb.ft./ft. run of cofferdam.}$$

Between El. 556.0 and El. 546.5

$$M'_{r2} = \tfrac{1}{2}(1404 + 4388) \times 9.5 \times (3 + 3.94)$$

$$= 191000 \text{ lb.ft./ft. run of cofferdam.}$$

Between El. 546.5 and El. 543.5

$$M'_{r3} = \tfrac{1}{2}(2645 + 300\ R) \times 3 \times 3 + (\tfrac{1}{2} \times 390 \times 3) \times 1$$

$$= 12500 + 1350\ R \text{ lb.ft./ft. run of cofferdam.}$$

The total moment due to the passive lateral pressure on the dredged side is M'_{rd} and is equal to $(M'_{r1} + M'_{r2} + M'_{r3})$.

$$M'_{rd} = 519500 + 1350\ R \text{ lb.ft./ft. run of cofferdam.}$$

The resisting moment due to the weight of the cofferdam about the toe (Point 0, see Figure 89).

$$W = (6 \times 115 + 35 \times 68.2)\ 26$$

$$= 3077 \times 26 = 80000 \text{ lb./ft. of cofferdam.}$$

The resisting moment due to the weight is M_{rw} and is equal to:

$$M_{rw} = 80000 \times 26/2 = 80000 \times 13 = 1040000 \text{ lb.ft./ft.}$$

The resisting moment due to the shearing force at the outer face of the back wall:

The shearing resistance of the soil mass at the back side is calculated on page 209 and is equal to:

$$S_{hb} = 10.03\ P_o + 12960 + 375\ R\ .$$

Assuming the coefficient of friction between the soil mass and the steel sheet-pile is 0.3, therefore, the shearing resistance at the outer face of the cofferdam at the back side is equal to:

$$.3\ S_{hb} = .3(10.03\ P_o + 12960 + 375\ R).$$

The moment of this force about the toe is:

$$M_{rs} = .3 \times S_{hb} \times b = 7.8(10.03\ P_o + 12960 + 375\ R)$$

$$M_{rs} = 78.234\ P_o + 101088 + 2925\ R.$$

The total resisting moment is designated as M_r and is equal to $M'_{rd} + M_{rw} + M_{rs}$ which are calculated above.

$$M_r = (519500 + 1350\ R) + (1040000) + (78.234\ P_o + 101088 + 2925\ R)$$

$$M_r = 78.234\ P_o + 1660588 + 4275\ R.$$

Equating the applied moment, M_a, to the resisting moment, M_r, the stability equation with respect to overturning will be:

$$(220.3\ P_o + 539400 - 1350\ R) - (78.234\ P_o + 1660588 + 4275\ R) = 0$$

$$142.066\ P_o - 1121188 - 5625\ R = 0$$

$$P_o - 7895 - 40.0\ R = 0$$

$$P_o = 7895 + 40\ R.$$

For R = 1.00, P_o = 7935

For R = 1.50, P_o = 7955

For R = 2.00, P_o = 7975

For R = 2.50, P_o = 7995

For R = 3.00, P_o = 8015

For R = 3.50, P_o = 8035

In the stability equation above the mobilized shearing resistance at the outer face of the back wall must not exceed the passive shearing resistance in the fill of the cell, S'_{hf}. The shearing resistance, S_{hb}, will be equal to S'_{hf} when the load, P_o, placed behind the cofferdam reaches the value 23346 which is calculated as follows:

$S_{hb} = 10.03\ P_o + 12960 + 375\ R$ lb./ft. (see Page 209)

$S'_{hf} = F''_{hf} \times \text{Tan}\ \phi = 250888 \times 1$ lb./ft. (see Page 209)

$10.03\ P_o + 12960 + 375\ R = 250888$

$10.03\ P_o = 250888 - 12960 - 375\ R$

$P_o = 23720 - 374\ R$ (taking R equal to one)

$P_o = 23346$ lb./sq.ft.

The value of P_o is very high. Therefore the shearing resistance on the outer face of the back wall, S_{hb}, will control.

The previous solution is made on the assumption that all the area behind the cofferdam is loaded. Therefore, if an area "O" is loaded, the cofferdam will maintain its stability as if all the area is loaded and then a portion of the area is unloaded. This makes it unnecessary to investigate the case when area "O" is loaded.

Allowable Load, P_o, With Respect to Vertical Shear When All Area is Loaded

The total applied moment due to the active lateral pressure acting against the cofferdam on the back side equals: (see Page 231)

$M_a = 220.3\ P_o + 539400 - 1350\ R$ lb.ft./ft. run of cofferdam.

The total resisting moment due to the passive lateral pressure acting against the cofferdam on the dredged side equals:

$$M'_{rd} = 519500 + 1350\ R \text{ lb.ft./ft. run of cofferdam.}$$

(see Page 233)

The resisting moment due to the shearing resistance on the outer faces of the cofferdam wall, M_{rsd}, is calculated as follows:

$$S_{hb} = 10.03\ P_o + 12960 + 375\ R \quad \text{(see Page 209)}$$

$$S'_{hd} = (3.69 \times 648) + (3 \times 125\ R) = 2391 + 375\ R$$

$S'_{hd} \leq S_{hb}$ and therefore S'_{hd} controls.

$$M_{rsd} = 0.3\ S'_{hd}\ b = 26(2391 + 375\ R) \times 0.3$$

The net moment causing the vertical shear in the cofferdam is M_{rv} and is equal to:

$$M_{rv} = M_a - M'_{rd} - 0.3\ S'_{hd}\ b \text{ (moments are about center line of cofferdam)}$$

$$M_{rv} = (220.3\ P_o + 539400 - 1350\ R) - (519500 + 1350\ R) - 26(2391 + 375\ R) \times 0.3$$

$$M_{rv} = 220.3\ P_o + 1250 - 5625\ R$$

This resultant moment will cause the vertical shear in the cell which is symbolized by Q and is equal to:

$$220.3\ P_o + 1250 - 5625\ R = \frac{5}{8} \times 26 \times Q$$

The shearing resistance in the fill of the cell is equal to the lateral pressure in the fill times Tan ϕ. The lateral pressure in the fill is greater than the active lateral pressure of the fill of the cell due to the applied lateral pressure on the back side. However, the lateral pressure in the fill must not exceed the passive lateral

pressure in the fill. The shearing resistance of the fill in the cell, S_v, is calculated as follows:

$F_{hf} = 56700 - \frac{1}{2} \times 62.4 \times 35 \times 35 = 18480$ lb./ft. (see Page 209)

$F'_{hb} = 13.03\ P_o + 58940 - 900\ R$ lb./ft. (see Page 208)

$F''_{hf} = 250888$ lb./ft. (see Page

$F_{hf} < F'_{hb} < F''_{hf}$

$S_v = F_{hb} \times \text{Tan}\ \phi = (13.03\ P_o + 58940 - 900\ R) \times 1$

$S_v = 13.03\ P_o + 58940 - 900\ R$

The stability criterion with respect to vertical shear is that the shearing stress, Q, must not exceed the shearing resistance, S_v. Thus substituting S_v in the equation for Q on Page 236, the stability equation with respect to vertical shear in the cell is:

$220.3\ P_o + 1250 - 5625\ R = \frac{5}{8} \times 26\ (13.03\ P_o + 58940 - 900\ R)$

$220.3\ P_o + 1250 - 5625\ R = 211.7\ P_o + 957775 - 14625\ R$

$8.6\ P_o = 956525 - 9000\ R$ (taking R = 1.0)

$P_o = 111223 - 1047 = 110176$ lb./sq.ft. which is very high value. Thus the vertical shear in the cell is not a critical factor in the stability of this cofferdam.

APPENDIX B

FULL MATHEMATICAL CALCULATIONS FOR THE REVISED STABILITY ANALYSIS GIVEN IN CHAPTER VI

Static Heads

Back Side:

wh_b = P_o + 4858 lb./sq.ft. when all area is loaded (see Page 206)

wh_{bo} = .2068 P_o + 4858 lb./sq.ft. when area "0" is loaded only.

The coefficient .2068 is calculated as follows: When area "0" is loaded only, the load placed behind the cofferdam, P_o, will be distributed within the limit of load distribution of 1:1. Thus the static head on the loading plane due to the effect of the surcharge load, P_o, will be in the ratio of the area loaded, A, to the area which is within the load distribution at the loading plane, A'.

$$c = \frac{A}{A'} = \frac{48.5 \times 48.5}{88.5 \times 128.5} = \frac{2352.25}{11372.25} = .2068 .$$

Dredged Side:

The static head at the dredged side, assuming the ground surface is at El. 556.0, is calculated on Page 206 and is:

wh_d = 3035 lb./sq.ft.

The static head on the dredged side based on the actual ground surface is calculated as follows:

The static head above the loading plane, assuming the failing element has a depth, d, equal to 48.5 feet and failure is occurring next to the cofferdam directly, is wh_{dl} and is equal to:

wh_{dl} = wh_d + average weight of submerged berm above El. 556.0 within 48.5 feet of the front wall of the cofferdam.

$wh_{dl} = wh_d + w_{s2} \frac{A_1}{d}$ where A_1 is the sectional area of the berm above 556.0 within 48.5 feet of the front wall. A_1 = 689.8 sq.ft.

wh_{dl} = 3035 + 68.2 x 689.8/48.5

= 3035 + 969 = 4004 lb./sq.ft.

The static head above the loading plane, assuming the failing element has a depth, d, equal to 38.5 feet and failure is occurring next to the cofferdam directly, is wh_{d2} and is equal to:

wh_{d2} = wh_d + average weight of submerged berm above El. 556.0 within 38.5 feet of the cofferdam.

$wh_{d2} = wh_d + w_{s2} \frac{A_2}{d}$ where A_2 is the sectional area of the berm above El. 556.0 within 38.5 feet of the cofferdam.

A_2 = 616 sq.ft.

wh_{d2} = 3035 + 68.2 x 616/38.5 = 3035 + 1093 = 4128 lb./sq.ft.

The static head above the loading plane, assuming the failure is occurring beyond the toe of the berm, is wh_{d3} and is equal to:

$wh_{d3} = wh_{d1} + w_{s2}\, h_s = 3035 + 68.2 \times 6.5 = 3035 + 443$

= 3478 lb./sq.ft.

Lateral Pressures and Lateral Forces

Active lateral pressures and forces on the back side:

The active lateral force on the back side is calculated on Page 208 and is equal to:

$F_{hb} = 13.03\, P_o + 58940 - 900\, R$ lb./ft. run.

Active lateral pressures and forces on the dredged side:

The active lateral pressures on the dredged side at Section X-X (see Figure 90) is calculated as follows:

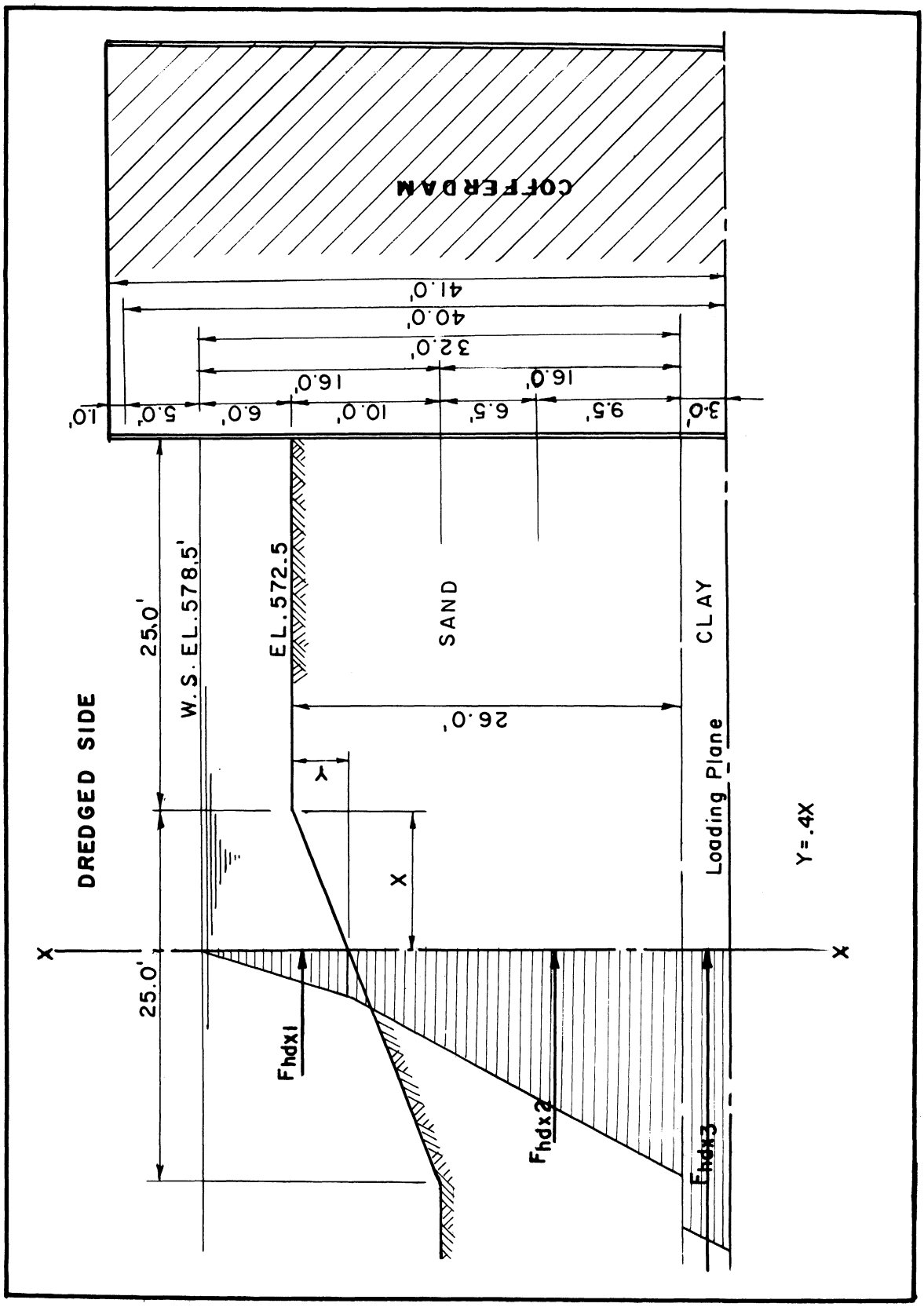

FIGURE 90. LATERAL PRESSURES ON THE DREDGED SIDE

$$P_{hx1} = 62.4\ (6 + .4\ X) = 374.4 + 24.96\ X\ .$$

$$P_{hx2} = 62.4 \times 32 + 68.2 \times .271\ (26 - .4\ X)$$

$$= 1997 + 18.4822\ (26 - .4\ X)$$

$$= 1997 + 480.5 - 7.393\ X$$

$$= 2477.5 - 7.393\ X\ .$$

$$P_{hx3} = 62.4 \times 32 + 68.2\ (26 - X) - 2 \times 150\ R$$

$$= 1997 + 1773.2 - 27.28\ X - 300\ R$$

$$= 3770 - 27.28\ X - 300\ R\ .$$

$$P_{hx4} = 62.4 \times 32 + 68.2\ (26 - X) + 3 \times 130 - 2 \times 150\ R$$

$$= 4160 - 27.28\ X - 300\ R\ .$$

In the above calculation $w_w = 62.4$ the weight of the water in pounds per cubic foot, $w_s = 68.2$ the weight of the submerged sand in pounds per cubic foot, $Tan^2\theta = .271$, and $S_{uc_1} = 150$ pounds per square foot.

The lateral force is calculated as follows:

$$F_{hdx1} = \tfrac{1}{2}\ (374.4 + 24.96\ X)(6 + .4\ X)$$

$$= 1123.2 + 4.992\ X^2 + 149.76\ X\ .$$

$$F_{hdx2} = \tfrac{1}{2}\ (374.4 + 24.96\ X + 2477.5 - 7.393\ X)(26 - .4\ X)$$

$$= (1426 + 8.78\ X)(26 - .4\ X)$$

$$= 37076 - 342.1\ X - 3.512\ X^2\ .$$

$$F_{hdx3} = \tfrac{1}{2}\ (3770 - 27.28\ X - 300\ R + 4160 - 27.28\ X - 300\ R) \times 3$$

$$= 11895 - 81.84\ X - 900\ R\ .$$

The total active lateral force equals:

$$F_{hdx} = F_{hdx1} + F_{hdx2} + F_{hdx3}$$

$$= 50094 + 1.48\ X^2 - 274.18\ X - 900\ R\ \text{lb./ft. run.}$$

Passive lateral pressure and forces on the dredged side:

The passive lateral pressures on the dredged side at a section X-X as shown in Figure 90 is calculated as follows:

$\text{Cot}^2\theta = \text{Cot}^2 27.5 = 3.69.$

$P'_{hx1} = 62.4\ (6 + .4\ X) = 374.4 + 24.96\ X\ .$

$P'_{hx2} = 62.4 \times 32 + 68.2 \times 3.69(26 - .4\ X)$

$= 1997 + 251.658(26 - .4\ X)$

$= 1997 + 6543 - 100.66\ X = 8540 - 100.66\ X\ .$

$P'_{hx3} = 3770 - 27.28\ X + 300\ R\ .$

$P'_{hx4} = 4160 - 27.28\ X + 300\ R\ .$

The passive lateral force is calculated as follows:

$F'_{hdx1} = \frac{1}{2}(374.4 + 24.96\ X)(6 + .4\ X)$

$= 1123.2 + 4.992\ X^2 + 149.76\ X.$

$F'_{hdx2} = \frac{1}{2}(374.4 + 24.96\ X + 8540 - 100.66\ X)(26 - .4\ X)$

$= \frac{1}{2}(8914.4 - 75.70\ X)(26 - .4\ X)$

$= 115887 - 2766.98\ X + 15.140\ X^2.$

$F'_{hdx3} = 11895 - 81.84\ X + 900\ R\ .$

The total passive force equals:

$F'_{hdx} = F'_{hdx1} + F'_{hdx2} + F'_{hdx3}$

$= 128905 + 20.132\ X^2 - 2699.06\ X + 900\ R$ lb./ft. run.

Shearing Resistances at the Dredged Side

Active shearing resistance at the dredged side at section X-X:

The active shearing resistance at the dredged side at section X-X is calculated as follows:

$S_{hdx} = \frac{1}{2}[0 + 68.2 \times .271(26 - .4\ X)][26 - .4\ X]\ \text{Tan}\ \phi + 3 \times 125\ R\ .$

$\text{Tan}\ \phi = \text{Tan}\ 45^\circ = 1\ .$

$S_{hdx} = 9.2411(26 - .4\ X)^2 + 375\ R$

$= 9.2411(676 - 20.8\ X + .16\ X^2) + 375\ R\ .$

$S_{hdx} = 6247 - 192.2\ X + 1.479\ X^2 + 375\ R$ lb./ft. run.

Passive shearing resistance at the dredged side at section X-X:

The passive shearing resistance at the dredged side at section X-X is calculated as follows:

$$S'_{hdx} = \tfrac{1}{2} [0 + 68.2 \times 3.69 (26 - .4 X)][26 - .4 X] \operatorname{Tan} \phi + 375 R$$

$$= \tfrac{1}{2} \times 251.658 (26 - .4 X)^2 + 375 R$$

$$= 125.829 (676 - 20.8 X + .16 X^2) + 375 R \cdot$$

$$S'_{hdx} = 85058 - 2617.24 X + 20.133 X^2 + 375 R \text{ lb./ft. run.}$$

Stability Analysis With Respect to the Mass Movement of the Soil Mass (Upheaval)

a) When the depth of the failing element, d, equals 48.5 feet and the failing element is at the dredged side next to the cofferdam:

This case is illustrated in Figure 76. The applied forces and the resisting forces are as follows:

The static head on the back side, wh_{bo}, is equal to:

$wh_{bo} = .2068 P_o + 4858$ lb./sq.ft. (see Page 239).

The active lateral force on the back side, F_{hb}, is equal to:

$F_{hb} = 13.03 P_o + 58940 - 900 R$ lb./ft. run (see Page 208).

The static head on the dredged side, wh_{dl}, is equal to:

$wh_{dl} = 4004$ lb./sq.ft. (see Page 239).

The active lateral force on the dredged side, F_{hdl}, is equal to:

$F_{hdl} = 44468 - 900 R$ lb./sq.ft. (see Page 171).

The average shearing resistance at the back side, S_{ab}, is equal to:

$S_{ab} = .251 P_o + 324 + 9.4 R$ lb./sq.ft. (see Page 209).

The average shearing resistance at the dredged side, S_{adl}, is equal to:

$S_{adl} = (2447 + 375 R)/19.6$ (see Page 172).

The average shearing resistance in the clay strata which are above El. 495.0 and below the loading plane is equal to: (see Page 209) .

$S_{c(Ave.)}$ = 140 lb./sq.ft. and $S_{uc(Ave.)}$ = 205 lb./sq.ft.

The shearing resistance at El. 495.0, S_{t_2}, is equal to:

$S_{t_2} = S_{c_2}$ = 200 lb./sq.ft. (see Page 205).

The weight transfer above the loading plane at the dredged side is calculated as follows:

h_3 = 19 + .4(50 - 48.5) = 19.6 feet. $h_3 = 19.6$, $d = 48.5$, $h_3 < d$, therefore,

$S_{e1} = S_{t_2} d/h_3 \leq S_{adl}$, $S_{e1} = 200\ R \times 48.5/19.5 = 495\ R > (125+19.1\ R)$

$\therefore S_{e1} = (125 + 19.1\ R)$.

The reduction in the static head is equal to $(125 + 19.1\ R)\ 19.6/48.5$

$= (2447 + 375\ R)/48.5$ lb./sq.ft.

The weight transfer above the loading plane at the back side is calculated as follows:

$h = 40$, $d = 48.5$, $h < d$,

therefore,

$S_{e2} = S_{t_2} d/h \leq S_{ab}$, $S_{e2} = 200\ R \times 48.5/40 = 253R \leq (.251P_o + 324 + 9.4R)$

$\therefore S_{e2} = 253\ R$.

The reduction in the static head is equal to S_{t_2} = 200 R lb./sq.ft.

The stability equation will be:

$$wh_{bo} + F_{hb}/d - wh_{dl} - F_{hdl}/d - 4S_{uc(Ave.)}\ R - 2S_{c(Ave.)}\ R - S_{t_2} Rb/d - S_{hdl}/d - S_{t_2} R = 0.$$

$$(.2068\ P_o + 4858) + (13.03P_o + 58940 - 900\ R)/48.5 - (4004)$$

$$- (44468 - 900\ R)/48.5 - (4 \times 205\ R) - (2 \times 140\ R) - (26 \times 200\ R)/48.5$$

$$- (2447 + 375\ R)/48.5 - 200\ R = 0$$

$$.4755\ P_o + 1102 - 1415\ R = 0.$$

For P_o equal to zero the overload ratio will be equal to:

$R = 1102/1415 = 0.78.$

When the load, P_o, will be increased the overload ratio will exceed one, thus the passive lateral pressure on the dredged side will be developed. Therefore the stability equation, using the passive lateral pressure for the dredged side, will be:

$(.2068\ P_o + 4858) + (13.03\ P_o + 58940 - 900\ R)/48.5 - (4004)$

$- (76595 + 900\ R)/48.5 - (4x205\ R) - (2x140\ R) - (26x200\ R)/48.5$

$- (2447 + 375R)/48.5 - (200\ R) = 0$

$.4755\ P_o - 56 - 1453\ R = 0.$ Therefore, $P_o = 3056\ R + 118$

For R = 1.00, $P_o = 3174$ lb./sq.ft.

For R = 1.50, $P_o = 4702$ lb./sq.ft.

For R = 2.00, $P_o = 6230$ lb./sq.ft.

For R = 2.50, $P_o = 7758$ lb./sq.ft.

For R = 3.00, $P_o = 9286$ lb./sq.ft.

For R = 3.50, $P_o = 10814$ lb./sq.ft.

b) When the depth of the element, d, equals 48.5 and the failing element is at the dredged side at the toe of the berm:

This case is illustrated in Figure 77. The applied forces and the resisting forces are as follows:

The static head on the back side, wh_{bo}, is equal to:

$wh_{bo} = .2068\ P_o + 4858$ lb./sq.ft. (see Page 239).

The active lateral force on the back side, F_{hb}, is equal to:

$F_{hb} = 13.03\ P_o + 58940 - 900\ R$ lb./ft. run. (see Page 208).

The static head on the dredged side, wh_{d3}, is equal to:

$wh_{d3} = 3478$ lb./sq.ft. (see Page 240).

The active lateral force on the dredged side, F_{hd3}, is equal to:

F_{hd3} = 44164 - 900 R lb./ft. run. (see Page 171).

The passive lateral force on the dredged side, F'_{hd3}, is equal to:

F'_{hd3} = 74011 + 900 R lb./ft. run. (see Page 171).

The average shearing resistance at the back side, S_{ab}, is equal to:

S_{ab} = .251 P_o + 324 + 9.4 R lb./sq.ft. (see Page 209).

The average shearing resistance at the dredged side, S_{ad3}, is equal to:

S_{ad3} = (2366 + 375 R)/19.0 lb./sq.ft. (see Page 172).

The average shearing resistance in the clay strata which are below the loading plane and above El. 495.0 is equal to:

$S_{c(Ave.)}$ = 140 lb./sq.ft. (see Page 209).

$S_{uc(Ave.)}$ = 205 lb./sq.ft. (see Page 209).

The shearing resistance at El. 495.0, S_{t_2}, is equal to:

S_{t_2} = 200 lb./sq.ft. (see Page 205).

The weight transfer above the loading plane at the dredged side due to the shearing resistance at the left side is calculated as follows:

h_2 = 19.0, d = 48.5, $h_2 < d$, therefore,

$S_{e3} = S_{t_2} h_2/d \leq S_{ad3}$, S_{e3} = 200 R x 48.5/19.0 = 511 R > 124 + 19.7 R

$\therefore S_{e3}$ = 124 + 19.7.

The reduction in the static head at the dredged side due to the shearing resistance at the left side is equal to:

(124 + 19.7 R) x 19.0/48.5 = (2366 + 375 R)/48.5 lb./sq.ft.

The weight transfer above the loading plane at the dredged side, due to the shearing resistance at the right side, is calculated as follows. The shearing resistance above the loading plane at the right side of the failing element at the dredged side could be mobilized to a certain extent in which

the weight transfer to the adjacent element at the right plus the loss of shearing resistance at the failure plane, $S_{t_2}d/d$, is less than the extra static head on the adjacent element at the right due to the submerged weight of the berm in order that the adjacent element on the right will not become critical. The static head due to the weight of the submerged berm on the adjacent element at the right is:

$$68.2(10 \times 25 \times 1/2 + 23.5 \times 10)/48.5 = 506 \text{ lb./sq.ft.}$$

The weight transfer plus the loss of shearing resistance at the failure plane is:

$$(2366 + 375\ R)/48.5 + 200\ R \text{ lb./sq.ft.}$$

These two factors will be equal when the value of R is 2.2, which is calculated as follows:

$$506 = 49 + 208\ R \quad , \quad \text{then} \quad R = 457/208 = 2.2 \quad .$$

Therefore for any value of R less than 2.2 the weight transfer will be equal to $(2366 + 375\ R)/48.5$ and for any value of R greater than 2.2 the weight transfer will be equal to:

$$(2366 + 375 \times 2.2)/48.5 = 49 + 18 = 57 \text{ lb./sq.ft.}$$

The weight transfer above the loading plane at the back side due to the shearing resistance at the right side is calculated on Page 245 and is equal to 200 R pounds per square foot.

The weight transfer above the loading plane at the back side due to the shearing resistance at the left side is calculated as follows. The coefficient of frictional resistance between the soil mass and the steel sheet-pile is assumed to be equal to 0.3. The shearing resistance at the back side of the cofferdam at the soil mass is S_{hb} and is equal to:

$$S_{hb} = 10.03\ P_o + 12960 + 375\ R \quad \text{(see Page 209).}$$

$.3\ S_{hb}/d = .062\ P_o + 80 + 2.3\ R$. The value of S_{hb} depend upon the value of P_o and R. In order to set up the stability equation it is assumed now that this value of shearing resistance will control and the weight transfer, due to it, to the adjacent element will not make the next element critical. This will be verified later.

The stability equation using the active lateral pressure on the dredged side will be:

$$wh_{bo} + F_{hb}/d - wh_{d3} - F_{hd3}/d - 4\ S_{uc(Ave.)}R - 2\ S_{c(Ave.)}R - S_{t_2}R\ (50+b)/d$$
$$- 2\ S_{hd3}/d - S_{t_2}R - .3\ S_{hb}/d = 0.$$
$$(.2068\ P_o + 4858) + (13.03\ P_o + 58940 - 900\ R)/48.5 - (3478)$$
$$- (44164 - 900\ R)/48.5 - (4 \times 205\ R) - (2 \times 140\ R)$$
$$- (76 \times 200\ R)/48.5 - 2\ (2366 + 375\ R)/48.5 - (200\ R)$$
$$- (.062\ P_o + 80 + 2.3\ R) = 0.$$
$$.2068\ P_o + 4858 + .2687\ P_o + 1215 - 18.6R - 3478 - 911 + 18.6R$$
$$- 820\ R - 280R - 313.4R - 98 - 15.5R - 200R - .062\ P_o - 80 - 2.3R = 0$$
$$.4135\ P_o + 1506 - 1631.2\ R = 0.$$

For P_o equal to zero the overload ratio is:

$$R = 1506/1631.2 = .924.$$

When the load, P_o, increases, the passive lateral pressure on the dredged side will be developed. Thus the stability equation, using the passive lateral pressure on the dredged side, for values of R less than 2.2, will be:

$$wh_{bo} + F_{hb}/d - wh_{d3} - F'_{hd3}/d - 4S_{uc(Ave.)} - 2S_{c(Ave.)}\ R$$
$$- S_{t_2}R(50 + b)/d - 2S_{hd3}/d - S_{t_2}R - .3\ S_{hb}/d = 0.$$
$$(.2068\ P_o + 4858) + (13.03\ P_o + 58940 - 900\ R)/48.5 - (3478)$$
$$- 2(2366 + 375R)/48.5 - (200R) - (.062\ P_o + 80 + 2.3R) = 0$$

$.4135\ P_o + 892 - 1668\ R = 0.$

$P_o = 4034\ R - 2157$. (for values of R less than 2.2)

For values of R greater than 2.2 the stability equation will be:

$(.4135\ P_o + 892 - 1668\ R) + (2366 + 375\ R)/48.5 - 57 = 0$

$.4135\ P_o + 884 - 1660\ R = 0.$

$P_o = 4014\ R - 2137$ (for values of R greater than 2.2)

Therefore,

For R = 1.00, P_o = 1877 lb./sq.ft.

For R = 1.50, P_o = 3894 lb./sq.ft.

For R = 2.00, P_o = 5911 lb./sq.ft.

For R = 2.50, P_o = 7884 lb./sq.ft.

For R = 3.00, P_o = 9891 lb./sq.ft.

For R = 3.50, P_o = 11898 lb./sq.ft.

The shearing resistance at the left side, at the back side, will transfer the weight to the adjacent element and the static head will increase by the value $.3\ S_{hb}/d = (.062\ P_o + 80 + 2.3\ R)$. For the overload ratio of 3.5 and the corresponding value of P_o of 11898 pounds per square foot, the weight transfer is:

$(.062 \times 11898 + 80 + 2.3\ R) = 826$ lb./sq.ft.

The static head due to the surcharge and the loss of horizontal shearing resistance at the failure plane of the main element are:

$.2068\ P_o - 200\ R = 1760$ lb./sq.ft. (Taking R equal to 3.5 and P_o equal to 11898.)

The static head due to the surcharge and the loss of the horizontal shearing resistance on the main element is less than the weight transferred to the adjacent element. Thus the adjacent element is not critical.

c) When the depth of the element, d, equals 38.5 feet and the failing element is at the dredged side next to the cofferdam:

This case is illustrated in Figure 77. The applied forces and the resisting forces are as follows:

The static head on the back side, wh_{bo}, is equal to:

$wh_{bo} = .2068\ P_o + 4858$ lb./sq.ft. (see Page 239).

The active lateral force on the back side, F_{hb}, is equal to:

$F_{hb} = 13.03\ P_o + 58940 - 900$ lb./sq.ft. (see Page 208).

The static head on the dredged side, wh_{d2}, is equal to:

$wh_{d2} = 4128$ lb./sq.ft. (see Page 240).

The active lateral force on the dredged side, F_{hd2}, is equal to:

$F_{hd2} = 46663 - 900\ R$ (see Page 171).

The passive lateral force on the dredged side, F'_{hd2}, is equal to:

$F'_{hd2} = 96137 + 900\ R$ (see Page 171).

The average shearing resistance at the back side, S_{ab}, is equal to:

$S_{ab} = .251\ P_o + 324 + 9.4\ R$ lb./sq.ft. (see Page 209).

The average shearing resistance at the dredged side, S_{ad2}, is equal to:

$S_{ad2} = S_{hd2}/h_4 = (3922 + 375\ R)/24.4$ (see Page 172).

The shearing resistances in the soft clay stratum below the loading plane, S_{c_1}, and S_{uc_4}, are equal to:

$S_{c_1} = 125$ lb./sq.ft. and $S_{uc_4} = 180$ lb./sq.ft. (see Page 205).

The shearing resistance at El. 505.0, S_{t_1}, is equal to:

$S_{t_1} = S_{c_1} = 125$ lb./sq.ft. (see Page 205).

The weight transfer above the loading plane at the back side is calculated as follows:

$h = 40$ feet, $d = 38.5$ feet. $h > d$

$S_{e_4} = S_{t1}\, Rd/d \leq S_{ab}$, $S_{e_4} = 125\ R < (.251\ P_o + 324 + 9.4\ R)$

$S_{e_4} = 125\ R$.

Therefore the reduction in the static head is equal to: 125 R.

The weight transfer above the loading plane at the dredged side is calculated as follows:

$h_4 = 24.4$ feet, $d = 38.5$ $h_4 < d$ therefore,

$S_{e_5} = S_{t_1} d/h_4 \leq S_{ab}$,

$S_{e_5} = 125R \times 38.5/24.4 = 197\ R > (3922 + 375\ R)/24.4 = 161 + 15.4\ R$

$S_{e_5} = 161 + 15.4\ R.$

The reduction in the static head is equal to $(161 + 15.4) \times 24.4/38.5$

$= (3922 + 375\ R)/38.5$ lb./sq.ft.

The stability equation using the active lateral pressure on the dredged side will be:

$$wh_{bo} + F_{hb}/d - wh_{d2} - F_{hd2}/d - 4S_{uc_4}\ R - 2S_{c_1}R - S_{t_1}R\ b/d$$

$$- S_{hd2}/d - S_{t_1}R = 0.$$

$$(.2068\ P_o + 4858) + (13.03\ P_o + 58940 - 900\ R)/38.5 - (4128)$$

$$- (46663 - 900\ R)/38.5 - (4x180\ R) - (2x125\ R) - (125x26\ R)/38.5$$

$$- (3922 + 375\ R)/38.5 - 125\ R = 0$$

$$.2068\ P_o + 4858 + .3382\ P_o + 1531 - 23.4\ R - 4128 - 1215$$

$$+ 23.4\ R - 720\ R - 250\ R - 84.4\ R - 102 - 9.8\ R - 125\ R = 0$$

$$.5450\ P_o + 944 - 1189.2\ R = 0.$$

For P_o equal to zero the overload ratio is:

$R = 944/1189.2 = 0.79.$

When the load P_o will be placed behind the cofferdam the passive lateral pressure on the dredged side will be developed. Therefore, the stability equation, using the passive lateral pressure on the dredged side, will be:

$$wh_{bo} + F_{hb}/d - wh_{d2} - F'_{hd2}/d - 4S_{uc_4} R - 2S_{c_1} R - S_{t_1} R\, b/d$$
$$- S_{hd2}/d - S_{t_1} R = 0.$$
$$(.2068\ P_o + 4858) + (13.03\ P_o + 58940 - 900\ R)/38.5 - (4128)$$
$$- (96137 + 900\ R)/38.5 - (4x180\ R) - (2x125\ R) - (125x26\ R)/38.5$$
$$- (3922 + 375\ R)/38.5 - (125\ R) = 0$$
$$.2068\ P_o + 4858 + .3382\ P_o + 1531 - 23.4\ R - 4128 - 2500$$
$$- 23.4\ R - 720\ R - 250\ R - 84.4\ R - 102 - 9.8\ R - 125\ R = 0$$
$$.5450\ P_o - 341 - 1236.0\ R = 0.$$
$$P_o = 2268\ R + 626.$$

For R = 1.00, P_o = 2894 lb./sq.ft.

For R = 1.50, P_o = 4028 lb./sq.ft.

For R = 2.00, P_o = 5162 lb./sq.ft.

For R = 2.50, P_o = 6296 lb./sq.ft.

For R = 3.00, P_o = 7430 lb./sq.ft.

For R = 3.50, P_o = 8564 lb./sq.ft.

d) When the depth of the element, d, equals 38.5 feet and the failing element is at the dredged side at the toe of the berm:

This case is illustrated in Figure 77d. The applied forces and the resisting forces are as follows:

The staic head on the back side, wh_{bo}, is equal to:

wh_{bo} = .2068 P_o + 4858 lb./sq.ft. (see Page 239).

The active lateral force on the back side, F_{hb}, is equal to:

F_{hb} = 13.03 P_o + 58940 - 900 R lb./sq.ft. (see Page 208).

The static head on the dredged side, wh_{d3}, is equal to:

wh_{d3} = 3478 lb./sq.ft. (see Page 240).

The active lateral force on the dredged side, F_{hd3}, is equal to:

F_{hd3} = 44164 - 900 R lb./sq.ft. (see Page 171).

The passive lateral force on the dredged side, F'_{hd3}, is equal to:

F'_{hd3} = 74011 + 900 R lb./sq.ft. (see Page 171) .

The average shearing resistance at the dredged side, S_{ad3}, is equal to:

S_{ad3} = (2366 + 375 R)/19.0 lb./sq.ft. (see Page 172).

The average shearing resistance at the back side, S_{ab}, is equal to:

S_{ab} = .251 P_o + 324 + 9.4 R lb./sq.ft. (see Page 209).

The shearing resistance in the clay statum below the loading plane is equal to:

S_{c_1} = 125 lb./sq.ft. (see Page 205) .

S_{uc_4} = 180 lb./sq.ft. (see Page 205) .

The shearing resistance at El. 505.0, S_{t_1}, is equal to:

S_{c_1} = 125 lb./sq.ft. (see Page 205) .

The weight transfer above the loading plane at the dredged side due to the shearing resistance at the left side is calculated as follows:

h_2 = 19.0 feet, d = 38.5 feet, $h_2 < d$, therefore,

$S_{e6} = S_{t_1} h_2/d \leq S_{ad3}$, S_{e6} = 125 R x 38.5/19.0 = 253 R > 124+19.7R

S_{e6} = 124 + 19.7 R .

The reduction in the static head at the dredged side due to the shearing resistance at the left side is equal to:

(124 + 19.7 R) x 19.0/38.5 = (2366 + 375 R)/38.5 lb./sq.ft.

The weight transfer above the loading plane at the dredged side due to the shearing resistance at the right side, is calculated as follows. The shearing resistance above the loading plane at the right side of the failing element at the dredged side could be mobilized to a certain extent in which the weight transfer to the adjacent element at the right plus the loss of shearing resistance at the failure plane, S_{t_1} d/d, are less than the extra static head on the adjacent element at the right, due to the submerged weight of the berm in order that the adjacent element on the right will not become critical. The static head due to the weight of the submerged berm on the adjacent element at the right is:

$$68.2(10 \times 25 \times \tfrac{1}{2} + 23.5 \times 10)/38.5 = 637 \text{ lb./sq.ft.}$$

The weight transfer plus the loss of shearing resistance at the failure plane is:

$$(2366 + 375\ R)/38.5 + 125\ R = 62 + 135\ R \text{ lb./sq.ft.}$$

$$637 = 62 + 135\ R$$

$$R = 575/135 = 4.3$$

Therefore, for any value or R less than 4.3 the weight transfer will be equal to $(2366 + 375\ R)/38.5$.

The weight transfer above the loading plane at the back side due to the shearing resistance at the right side is calculated on Page 252 and is equal to 125 R pounds per square foot.

The weight transfer above the loading plane at the back side due to the shearing resistance at the left side is calculated as follows. The coefficient of frictional resistance between the soil mass and the steel sheet pile is assumed to be equal to 0.3. The shearing resistance at the back side

of the cofferdam at the soil mass is S_{hb} and is equal to:

$$S_{hb} = 10.03\ P_o + 12960 + 375\ R \quad \text{(see Page 209).}$$

$.3\ S_{hb}/d = .0781 + 101 + 2.9\ R$. The value of S_{hb} depend upon the value of P_o and R. In order to set up the stability equation it is assumed now that this value of shearing resistance will control and the weight transfer, due to it, to the adjacent element will not make the next element critical. This will be verified later.

The stability equation using the active lateral pressure on the dredged side will be:

$$wh_{bo} + F_{hb}/d - wd_{d3} - F_{hd3}/d - 4\ S_{uc_4}\ R - 2\ S_{c_1} R - S_{t_1} R(50 + b)/d$$
$$- 2\ S_{hd3}/d - S_{t_1}\ R - .3\ S_{hb}/d = 0 .$$
$$(.2068\ P_o + 4858) + (13.03\ P_o + 58940 - 900\ R)/38.5 - (3748)$$
$$- (44164 - 900\ R)/38.5 - (4 \times 180\ R) - (2 \times 125\ R)$$
$$- (76 \times 125\ R)/38.5 - 2(2366 + 375\ R)/38.5 - 125\ R$$
$$- (.0781\ P_o + 101 + 2.9\ R) = 0$$
$$.2068\ P_o + 4858 + .3382\ P_o + 1531 - 23.4\ R - 3478 - 1145 + 23.4\ R$$
$$- 720\ R - 250\ R - 394.8\ R - 123 - 19.5\ R - 125\ R - .0781\ P_o$$
$$- 101 - 2.9\ R = 0$$
$$.4669\ P_o + 1542 - 1512.2\ R = 0 .$$

For P_o equal to zero, the overload ratio is:

$$R = 1542/1512.2 = 1.02 .$$

When the load, P_o, is placed on the test area and the overload ratio increases, the passive lateral pressure on the dredged side will be developed. Thus the stability equation, using the passive lateral pressure on the dredged side, for values of R less than 4.3, will be:

$wh_{bo} + F_{hb}/d - wh_{d3} - F'_{hd3}/d - 4\ S_{uc_4}R - 2\ S_{c_1}R - S_{t_1}R\ (50 + b)/d$

$- 2\ S_{hd3}/d - S_{t_1}\ R - .3\ S_{hb}/d = 0.$

$(.2068\ P_o + 4858) + (13.03\ P_o + 58940 - 900\ R)/38.5 - (3478)$

$- (74011 + 900\ R)/38.5 - (4 \times 180\ R) - (2 \times 125\ R) - (76 \times 125R)/38.5$

$- 2(2366 + 375\ R)/38.5 - 125\ R - (.0781\ P_o + 101 + 2.9\ R) = 0$

$.2068\ P_o + 4858 + 3382\ P_o + 1531 - 23.4\ R - 3478 - 1922 - 23.4\ R$

$- 720\ R - 250\ R - 394.8\ R - 123 - 19.5\ R - 125\ R - .0781\ P_o - 101$

$- 2.9\ R = 0.$

$.4469\ P_o + 765 - 1559\ R = 0$

$P_o = 3339\ R - 1638$ (for values of R less than 4.3)

For R = 1.00, P_o = 1701 lb./sq.ft.

For R = 1.50, P_o = 3371 lb./sq.ft.

For R = 2.00, P_o = 5040 lb./sq.ft.

For R = 2.50, P_o = 6710 lb./sq.ft.

For R = 3.00, P_o = 8379 lb./sq.ft.

For R = 3.50, P_o = 10049 lb./sq.ft.

Stability Analysis With Respect to Sliding

Two cases are to be considered in determining the load capacity of the test load area and the stability of the cofferdam with respect to sliding. These two cases are illustrated in Figure 78. In the first case, the lateral pressures acting on the cofferdam directly are considered. In the second case, the lateral pressure on the back side directly and the lateral pressure on the dredged side at the toe of the berm, which is less than the lateral pressure on the cofferdam directly, are considered. Also

in both cases the active or the passive lateral pressures on the dredged side are used.

a) Case one, using the active lateral pressure on the dredged side:

The applied and the resisting forces are as follows:

The active lateral force on the back side, F_{hb}, is equal to:

$F_{hb} = 13.03\ P_o + 58940 - 900\ R$ lb./ft. run. (see Page 208).

The active lateral force on the dredged side directly, F_{hd4}, is equal to:

$F_{hd4} = 50094 - 900\ R$ lb./ft. run. (see Page 171).

The shearing resistance contributed from the cofferdam structure is:

$$(F_{hf} - 62.4 \times 35 \times 35/2) \tan \phi \times 2 \times b/48.5$$
$$= (56700 - 38220) \times 1 \times 2 \times 26/48.5$$
$$= 18480 \times 52/48.5 = 19810 \text{ lb./ft. run.}$$

The shearing resistance at the base of the cofferdam is:

$S_{c_1} \times b \times R = 125 \times 26\ R = 3250\ R$ lb./ft. run.

The stability equation with respect to sliding is:

$F_{hb} - F_{hd4} - 19810 - S_{c_1}\ b\ R = 0$.

$(13.03\ P_o + 58940 - 900\ R) - (50094 - 900\ R)$

$- 19810 - 3250\ R = 0$

$13.03\ P_o - 10964 - 3250\ R = 0$.

$P_o = 841 + 249\ R$ For $R = 1.0$, $P_o = 1090$ lb./sq.ft.

b) Case one, using the passive lateral pressure on the dredged side:

The applied and the resisting forces are as follows:

The active lateral force on the back side, F_{hb}, is equal to:

$F_{hb} = 13.03\ P_o + 58940 - 900\ R$ lb./ft.run. (see Page 208).

The passive lateral force on the dredged side directly, F'_{hd4}, is equal to:

F'_{hd4} = (128905 + 900 R) lb./ft. run. (see Page 171).

The shearing resistance contributed from the cofferdam's structure is:

19810 lb./ft. run. (see Page 258).

The shearing resistance at the base of the cofferdam is:

3250 lb./ft. run. (see Page 258).

The stability equation with respect to sliding is:

$F_{hb} - F'_{hd4} - 19810 - 3250\ R = 0.$

$(13.03\ P_o + 58940 - 900\ R) - (128905 + 900\ R)$

$- 19810 - 3250\ R = 0.$

$13.03\ P_o - 89775 - 5050\ R = 0.$

$P_o = 6889 + 387\ R$

For R = 1.00, P_o = 7276 lb./sq.ft.

For R = 1.50, P_o = 7469 lb./sq.ft.

For R = 2.00, P_o = 7662 lb./sq.ft.

For R = 2.50, P_o = 7855 lb./sq.ft.

For R = 3.00, P_o = 8049 lb./sq.ft.

For R = 3.50, P_o = 8232 lb./sq.ft.

c) Case two, using the active lateral pressure at the toe of the berm on the dredged side:

The applied and resisting forces are:

The active lateral force on the back side, F_{hb}, is equal to:

$F_{hb} = 13.03\ P_o + 58940 - 900\ R$ lb./ft. run. (see Page 208).

The active lateral force at the toe of the berm on the dredged side is equal to:

F_{hd3} = (44164 - 900 R) lb./ft. run. (see Page 171).

The shearing resistance contributed by the cofferdam's structure is equal to:

19810 lb./ft. run. (see Page 258).

The shearing resistance at the loading plane is:

S_{c_1} x (b + 50)R = 125 x 76 R = 9500 R.

The stability equation with respect to sliding is:

$F_{hb} - F_{hd3} - 19810 - 9500 R = 0$.

$(13.03 P_o + 58940 - 900 R) - (44164 - 900 R)$

$- 19810 - 9500 R = 0$

$13.03 P_o - 5034 - 9500 R = 0$

$P_o = 386 + 728 R.$

d) Case two, using the passive lateral pressure at the toe of the berm on the dredged side:

The applied and the resisting forces are:

The active lateral force on the back side, F_{hb}, is equal to:

$F_{hb} = 13.03 P_o + 58940 - 900 R$ lb./ft. run. (see Page 208).

The passive lateral force at the toe of the berm on the dredged side, F'_{hd3}, is equal to:

F'_{hd3} = (74011 + 900 R) lb./ft. run. (see Page 171).

The shearing resistance contribued by the cofferdam's structure is equal to:

19810 lb./ft. run. (see Page 258).

The shearing resistance at the loading plane is:

9500 R lb./ft. run. (see Page 258).

The stability equation with respect to sliding is:

$F_{hb} - F'_{hd3} - 19810 - 9500\ R = 0$

$(13.03\ P_o + 58940 - 900\ R) - (74011 + 900\ R)$

$- 19810 - 9500\ R = 0$

$13.03\ P_o + 58940 - 900\ R - 74011 - 900\ R - 19810 - 9500\ R = 0$

$13.03\ P_o - 34881 - 11300\ R = 0$

$P_o = 2677 + 867\ R.$

For R = 1.00, P_o = 3544 lb./sq.ft.

For R = 1.50, P_o = 3977 lb./sq.ft.

For R = 2.00, P_o = 4411 lb./sq.ft.

For R = 2.50, P_o = 4844 lb./sq.ft.

For R = 3.00, P_o = 5278 lb./sq.ft.

For R = 3.50, P_o = 5706 lb./sq.ft.

APPENDIX C

SETTLEMENT CHARTS FOR THE POINTS

A-1, A-2, B-1, B-2, C-1, C-2, D-1, D-2, E-1, F-1, G-1, G-2, H-1, H-2, I-1, I-2, J-3, J-5, J-6, K-6, M-6, O-6, P-3, P-5, and P-6

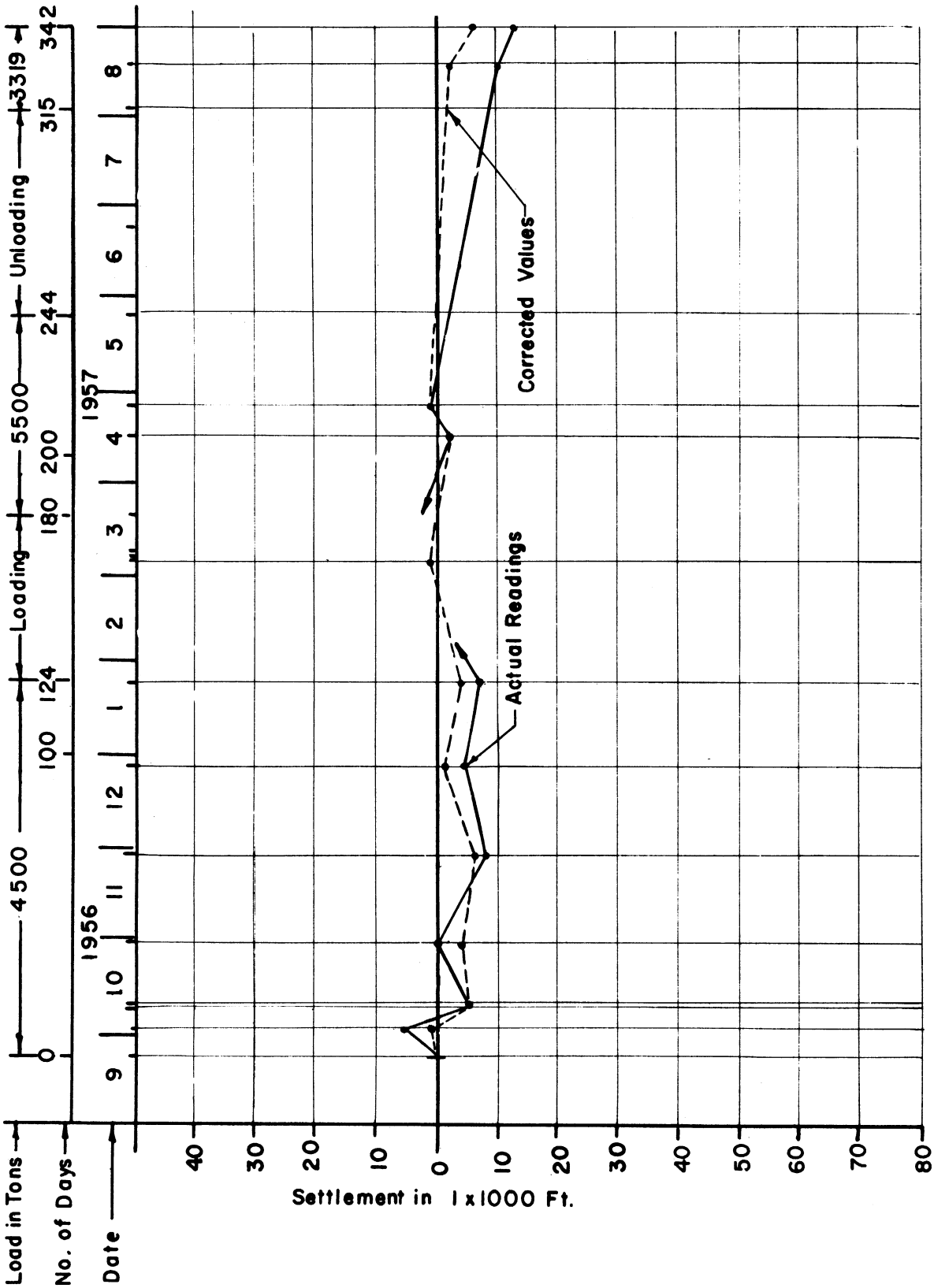

FIGURE 91. SETTLEMENT OF POINT A-1

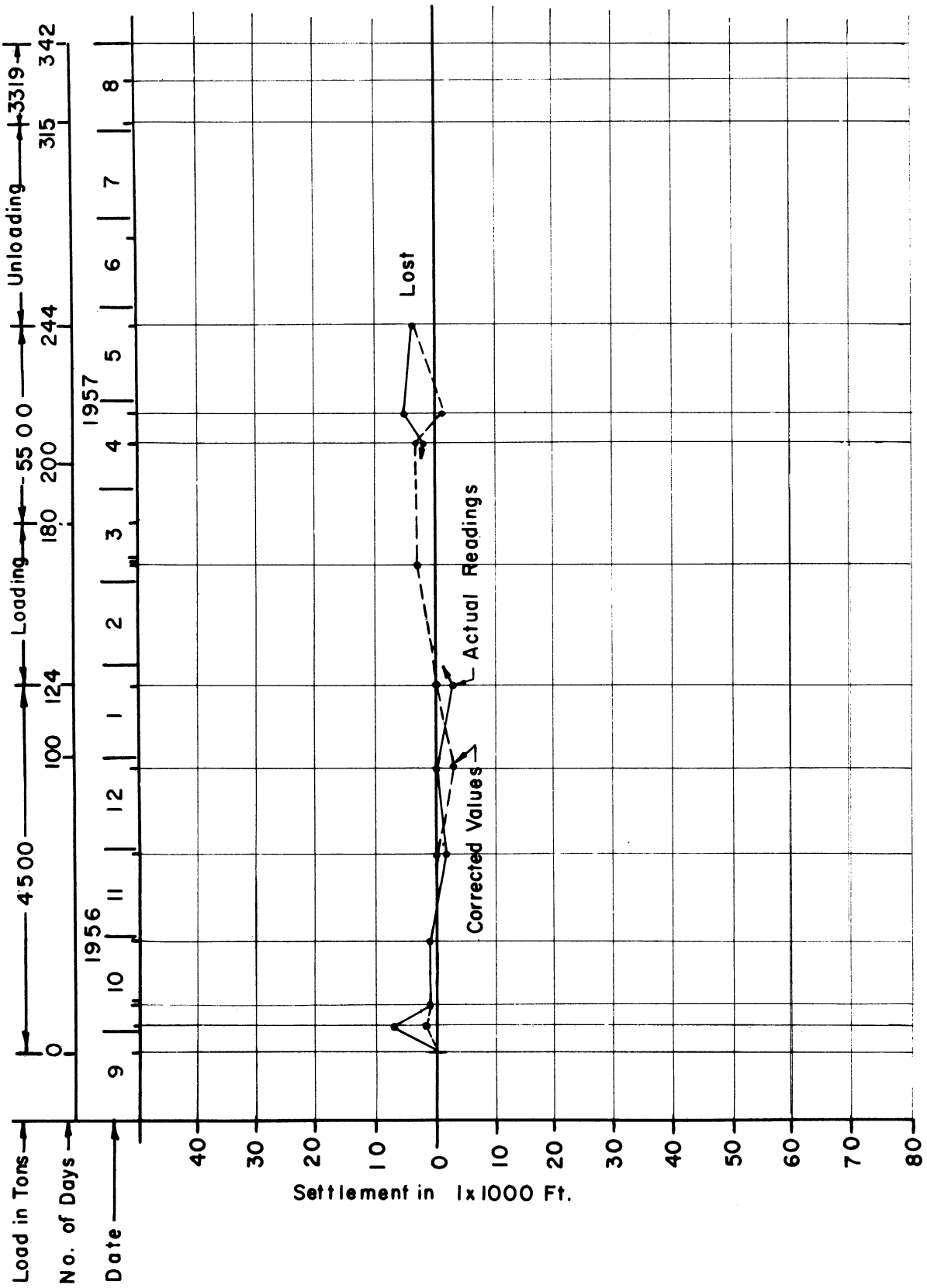

FIGURE 92. SETTLEMENT OF POINT A-2

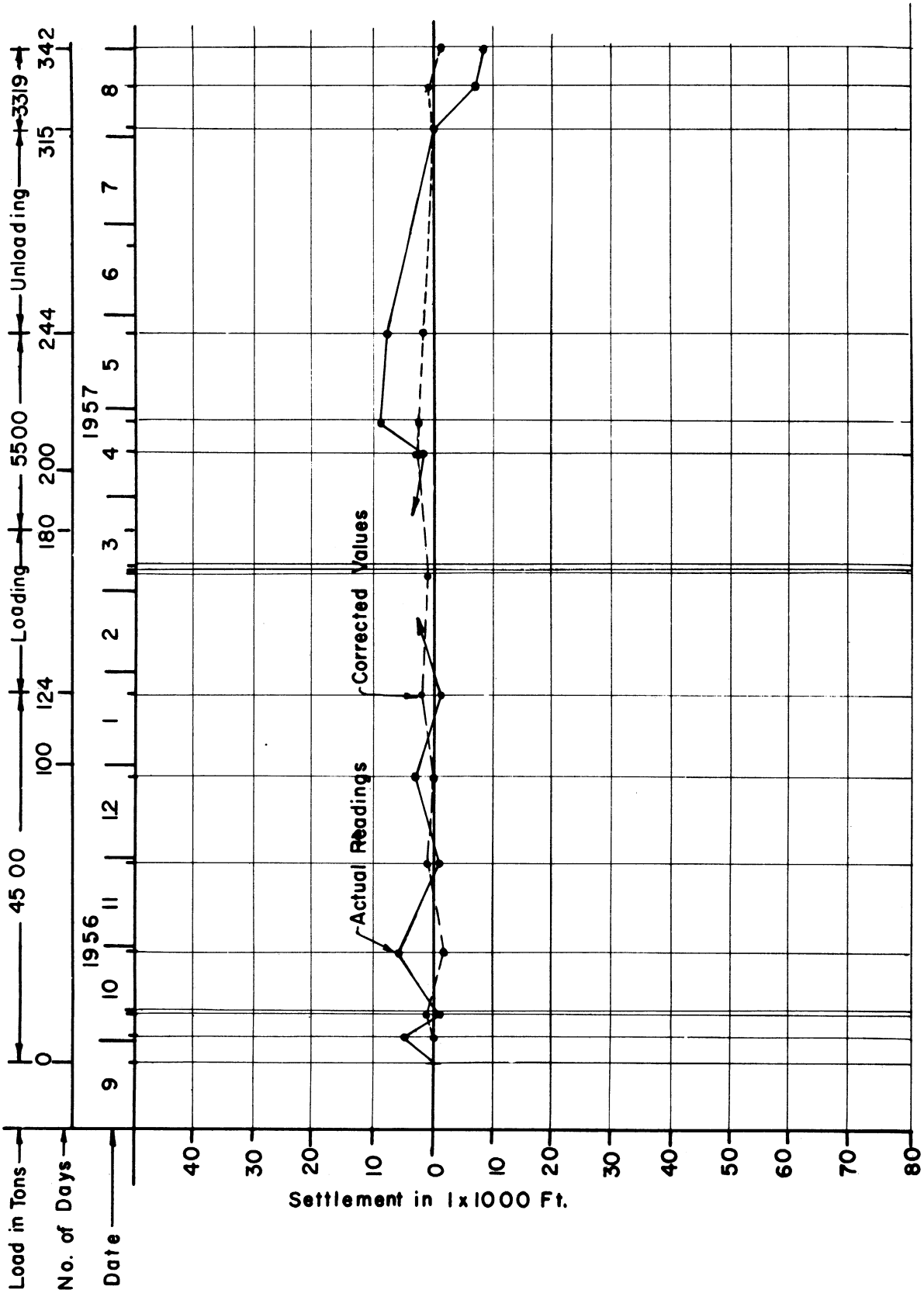

FIGURE 93. SETTLEMENT OF POINT B-1

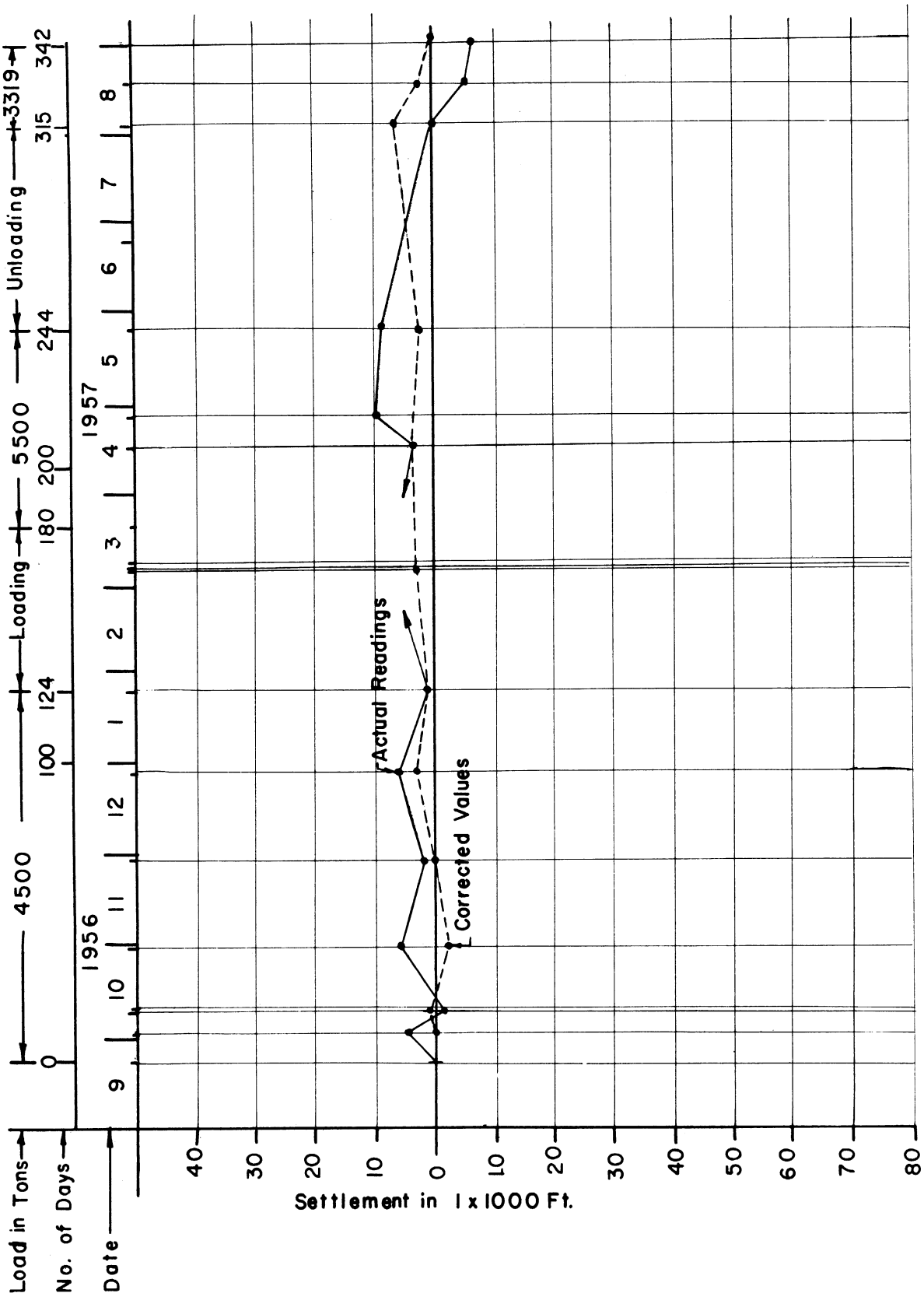

FIGURE 94. SETTLEMENT OF POINT B-2

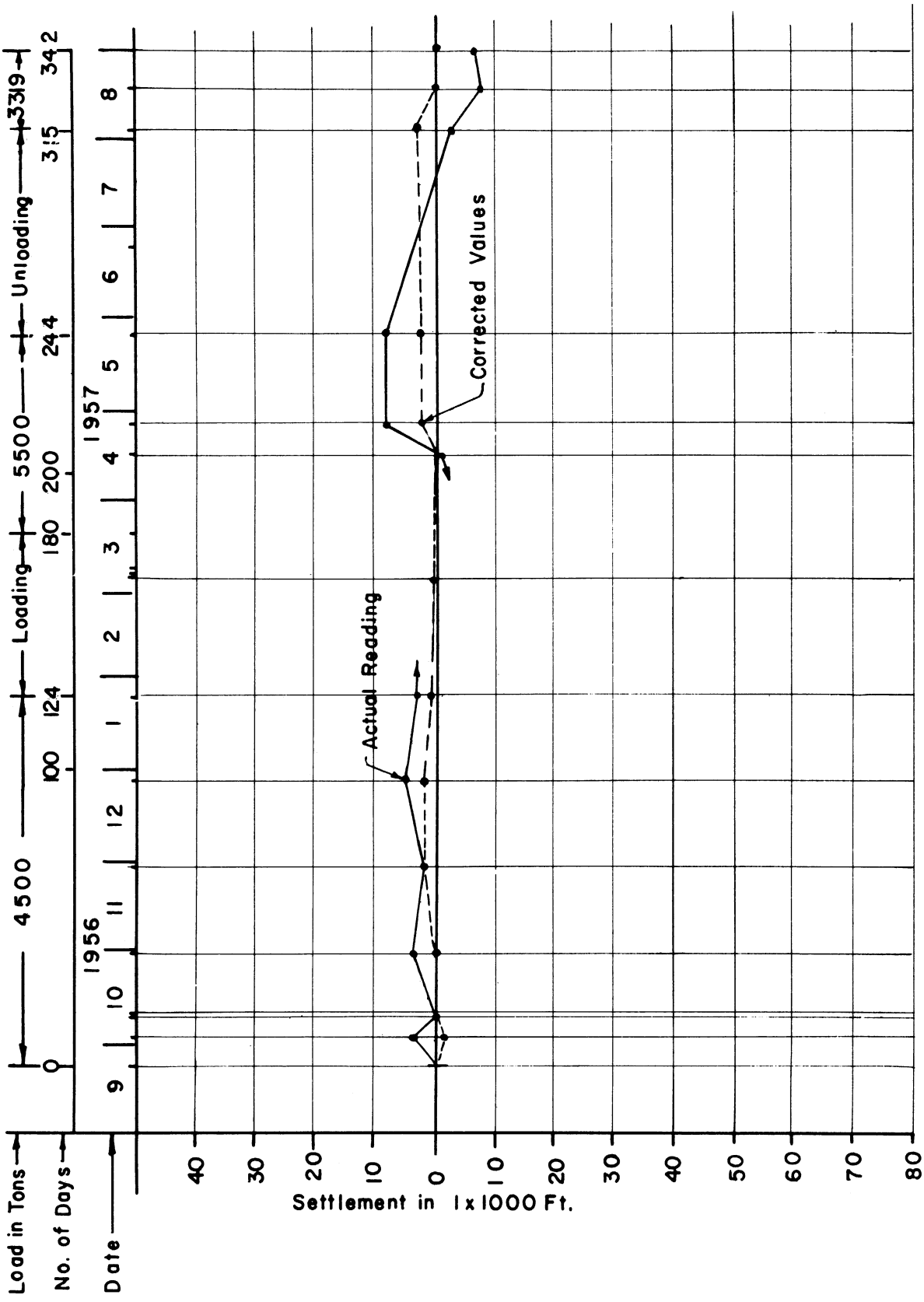

FIGURE 95. SETTLEMENT OF POINT C-1

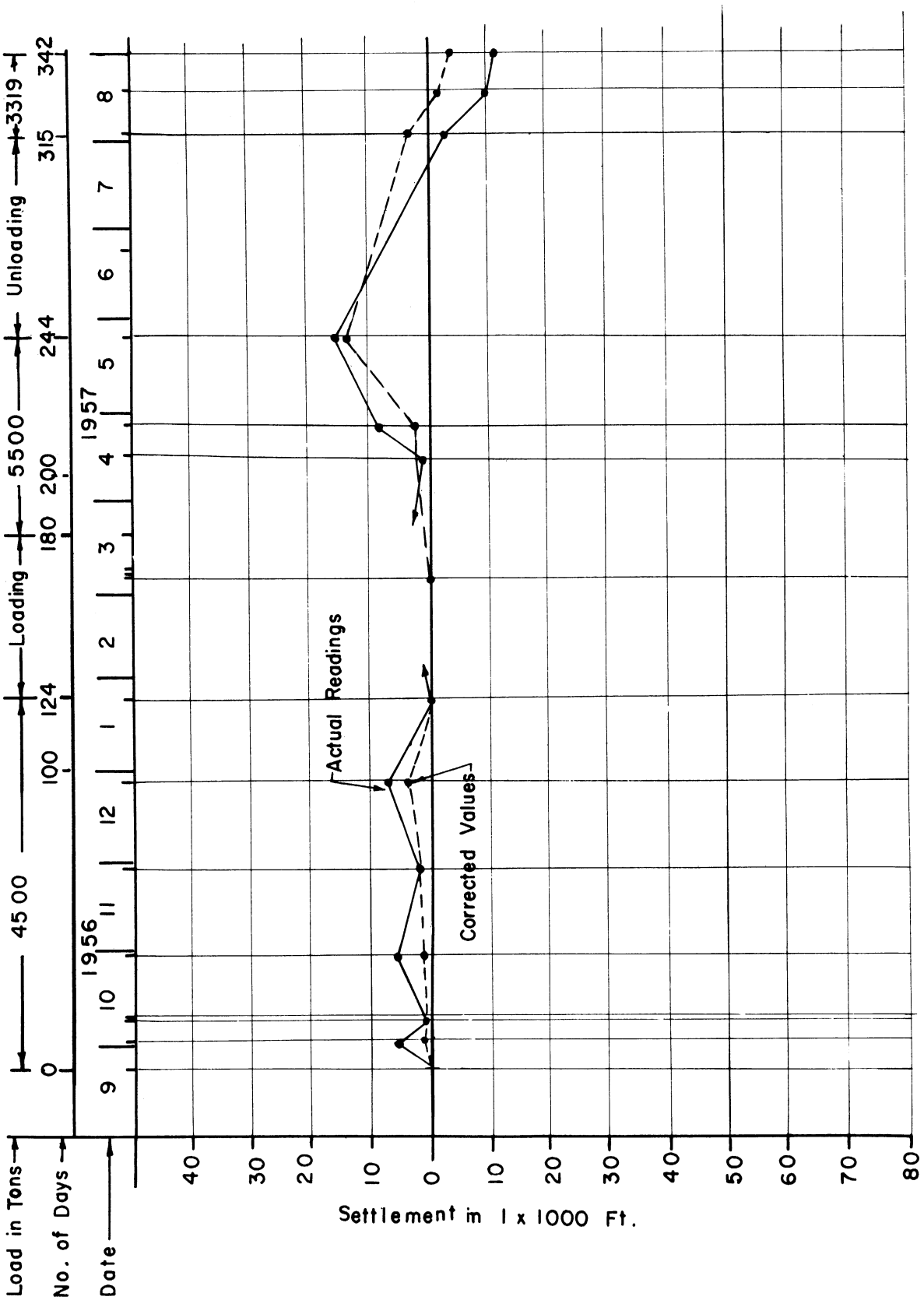

FIGURE 96. SETTLEMENT OF POINT C-2

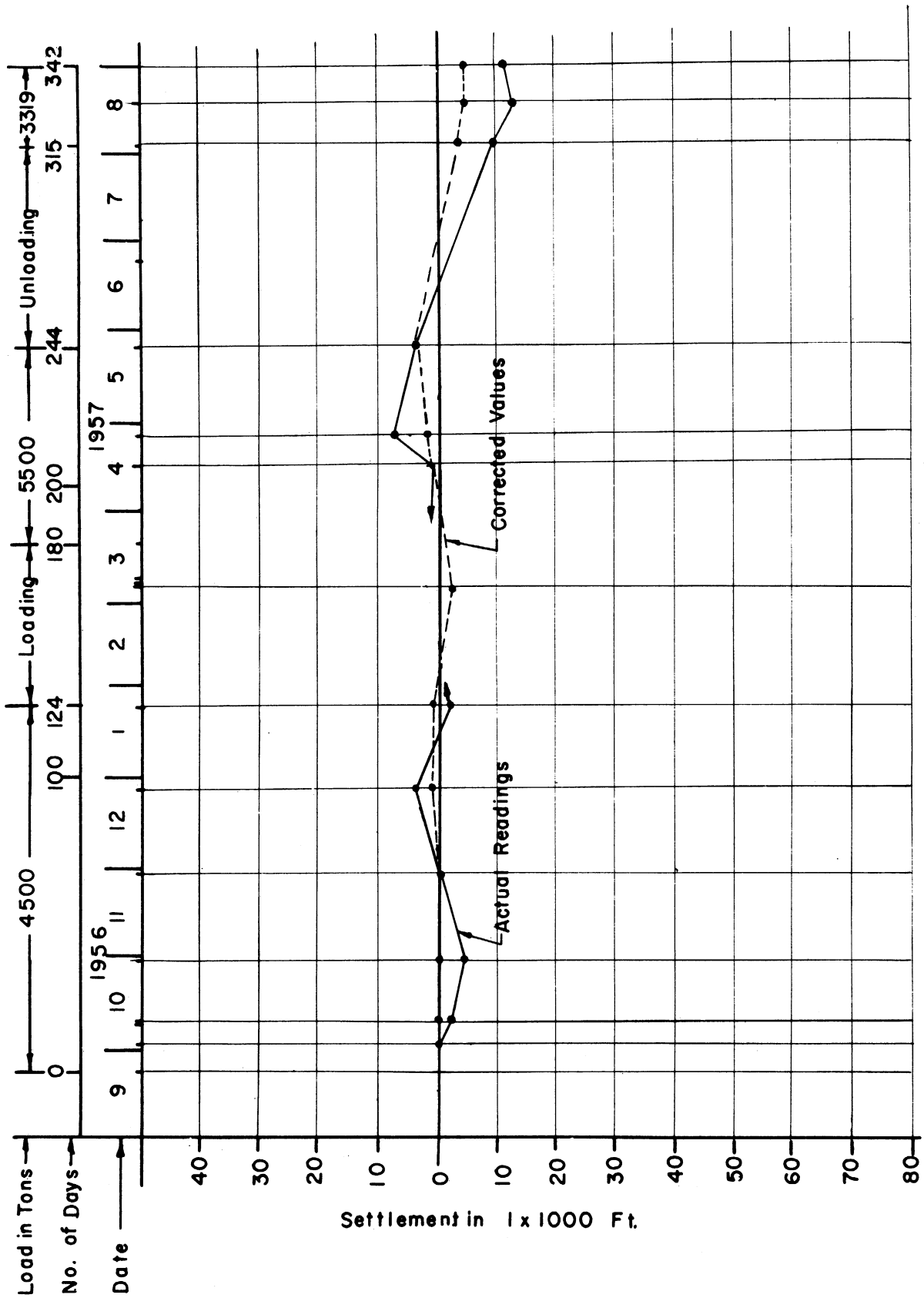

FIGURE 97. SETTLEMENT OF POINT D-1

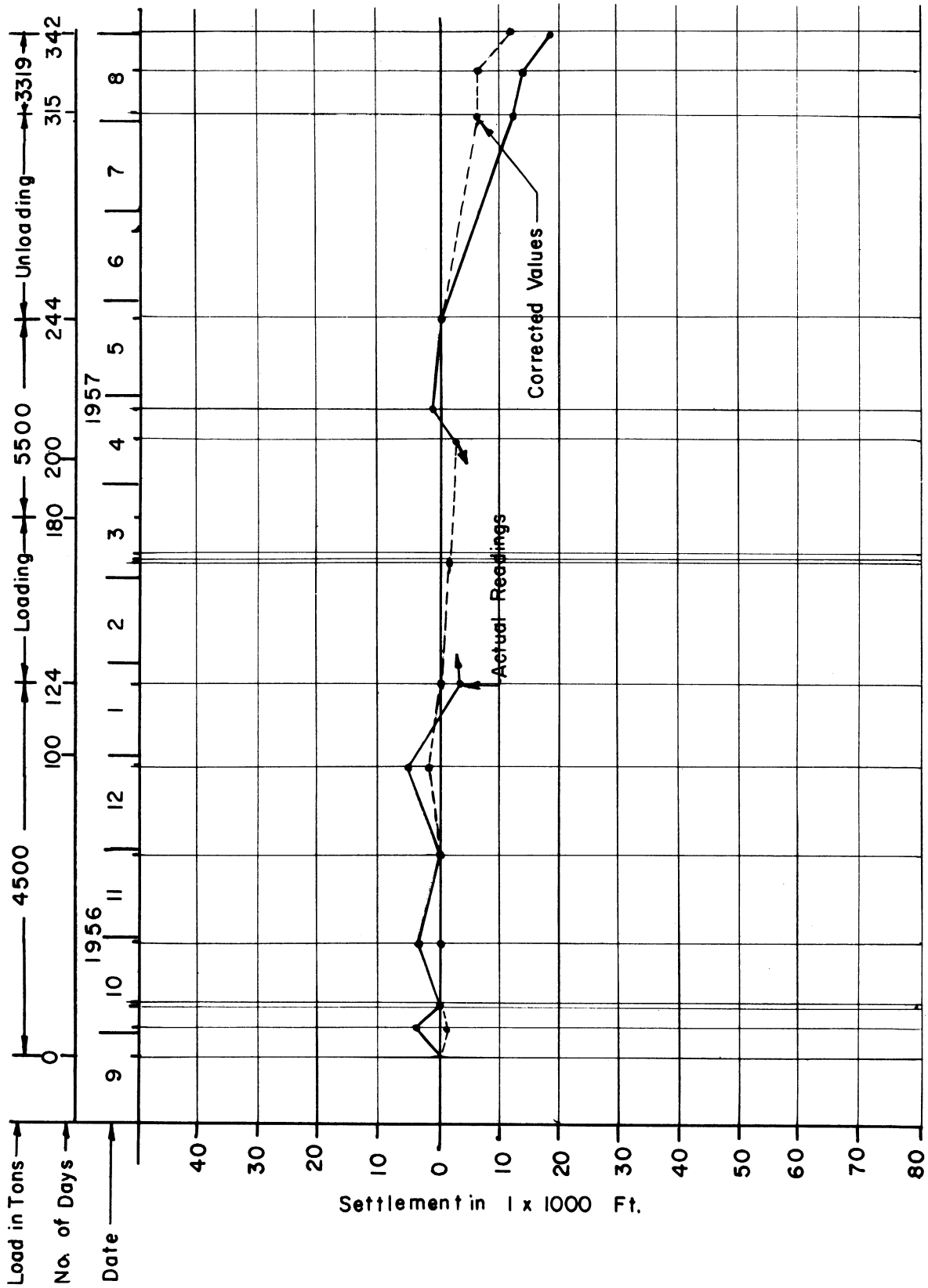

FIGURE 98. SETTLEMENT OF POINT D-2

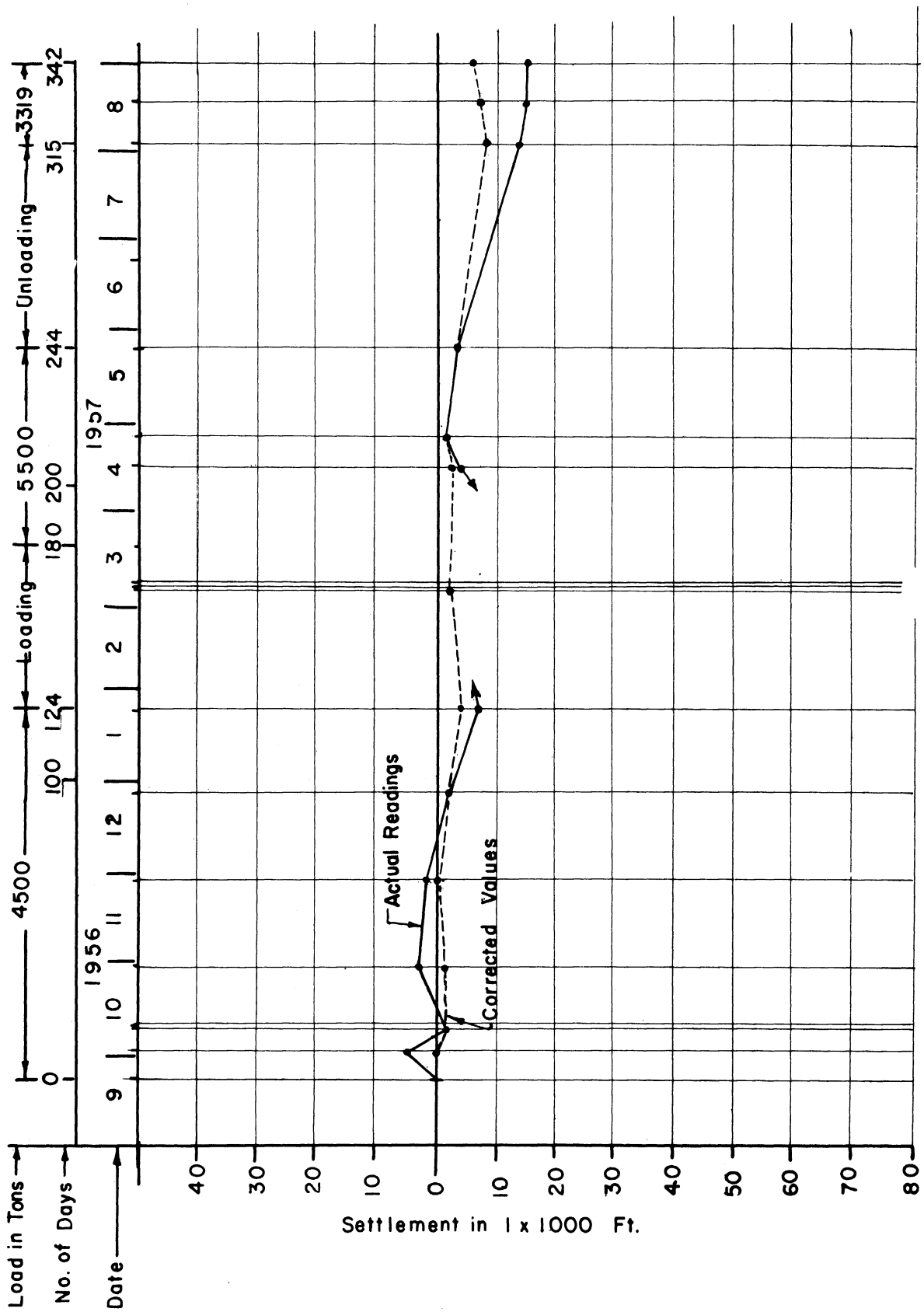

FIGURE 99. SETTLEMENT OF POINT E-1

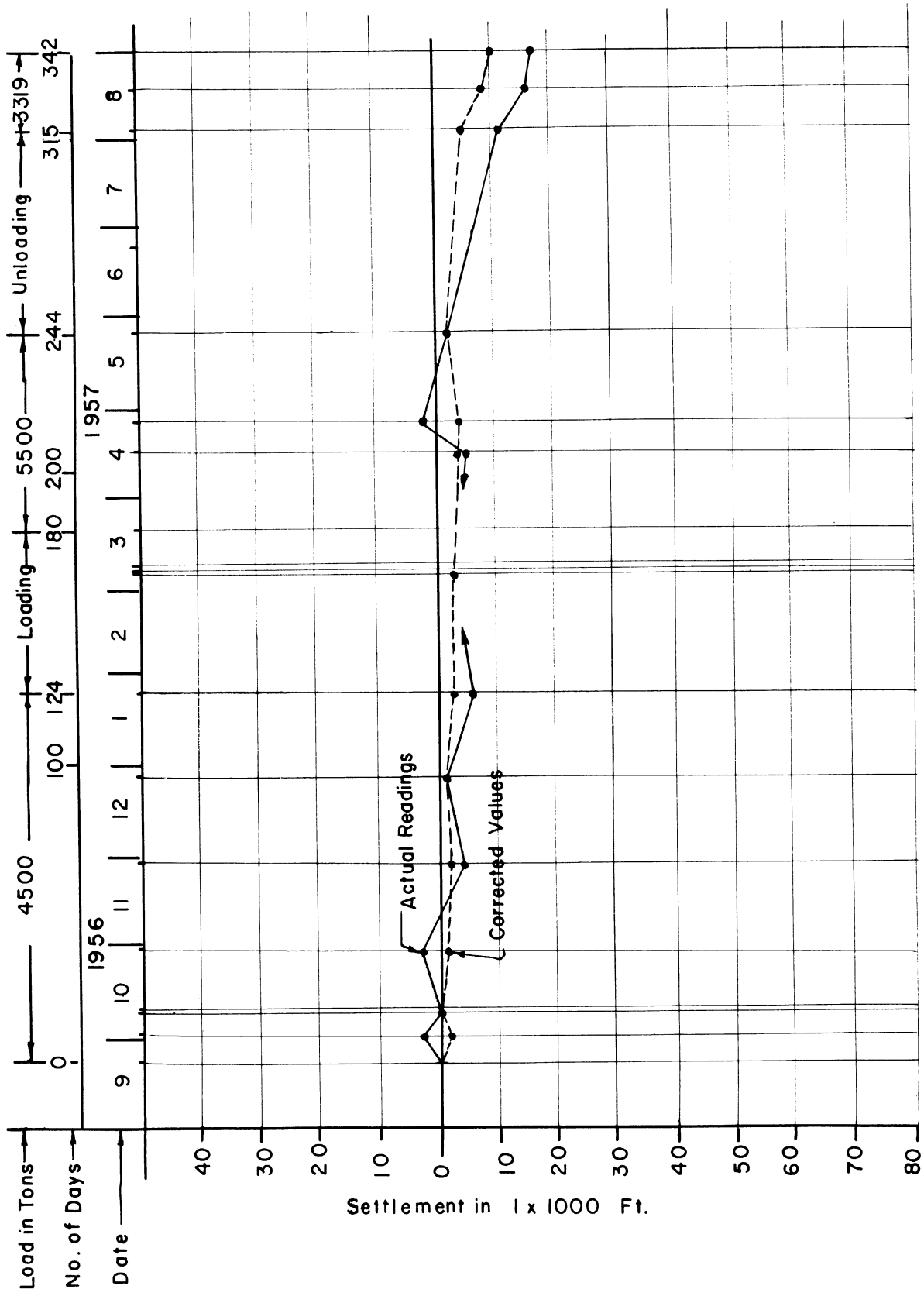

FIGURE 100. SETTLEMENT OF POINT F-1

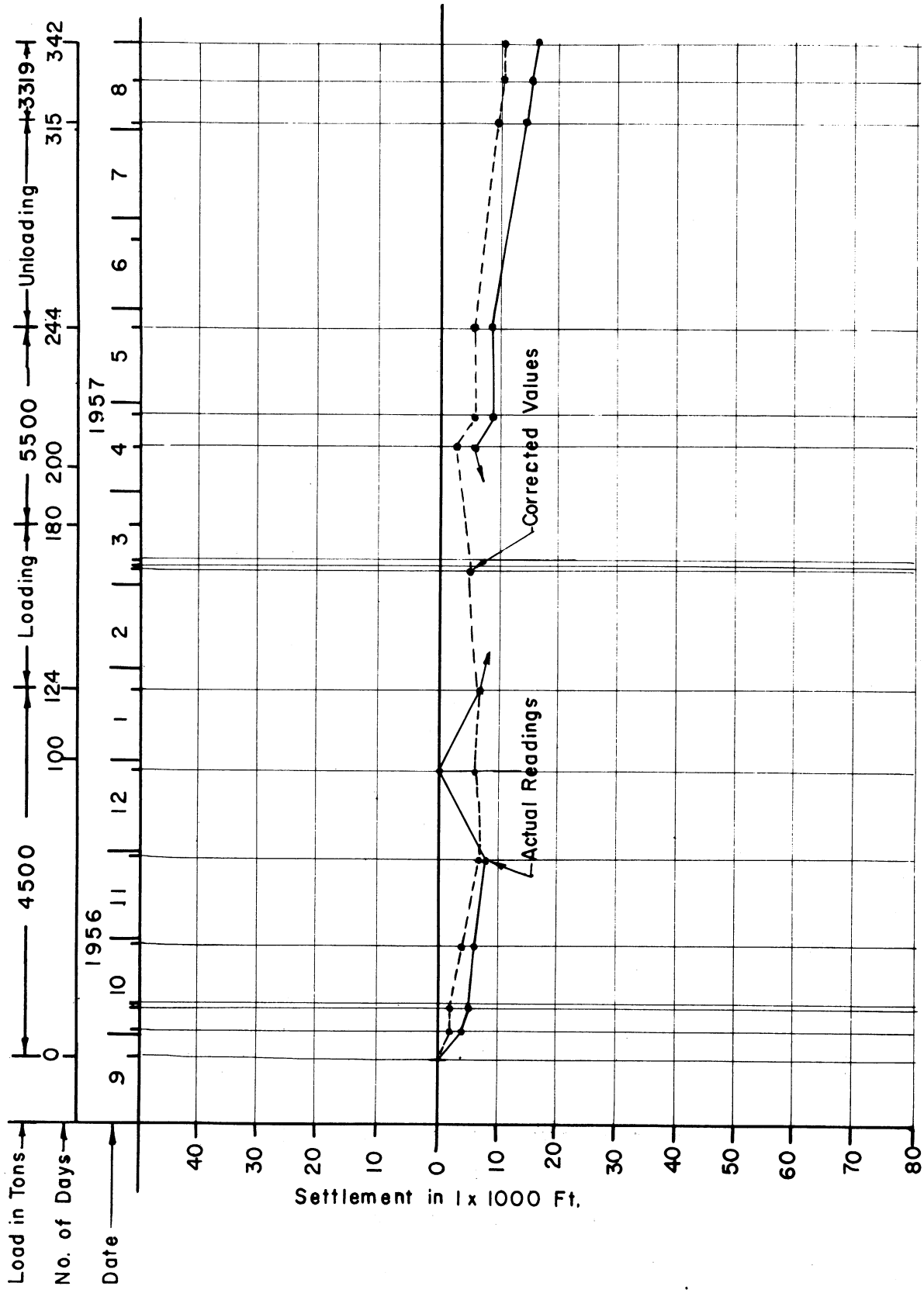

FIGURE 101. SETTLEMENT OF POINT G-1

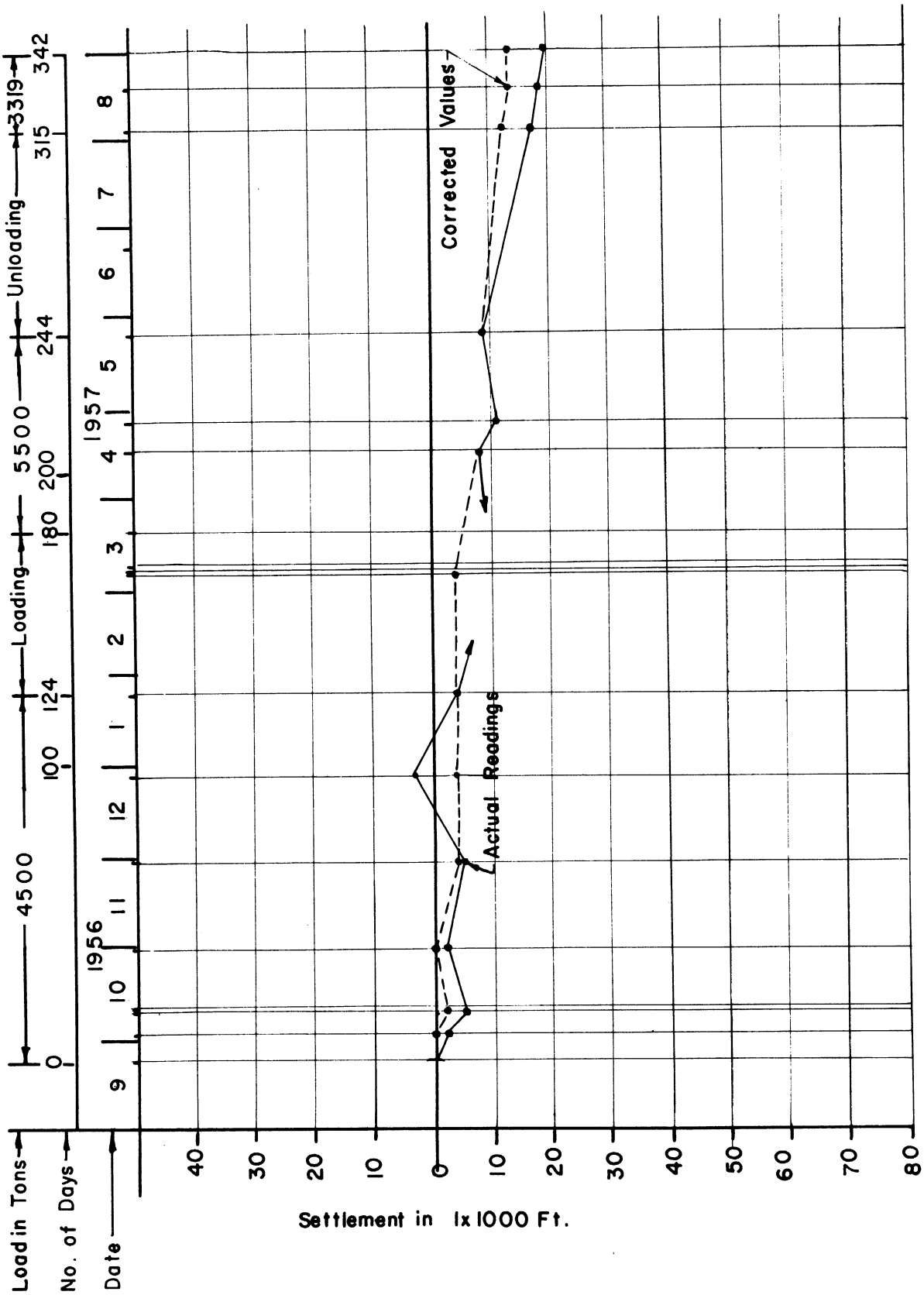

FIGURE 102. SETTLEMENT OF POINT G-2

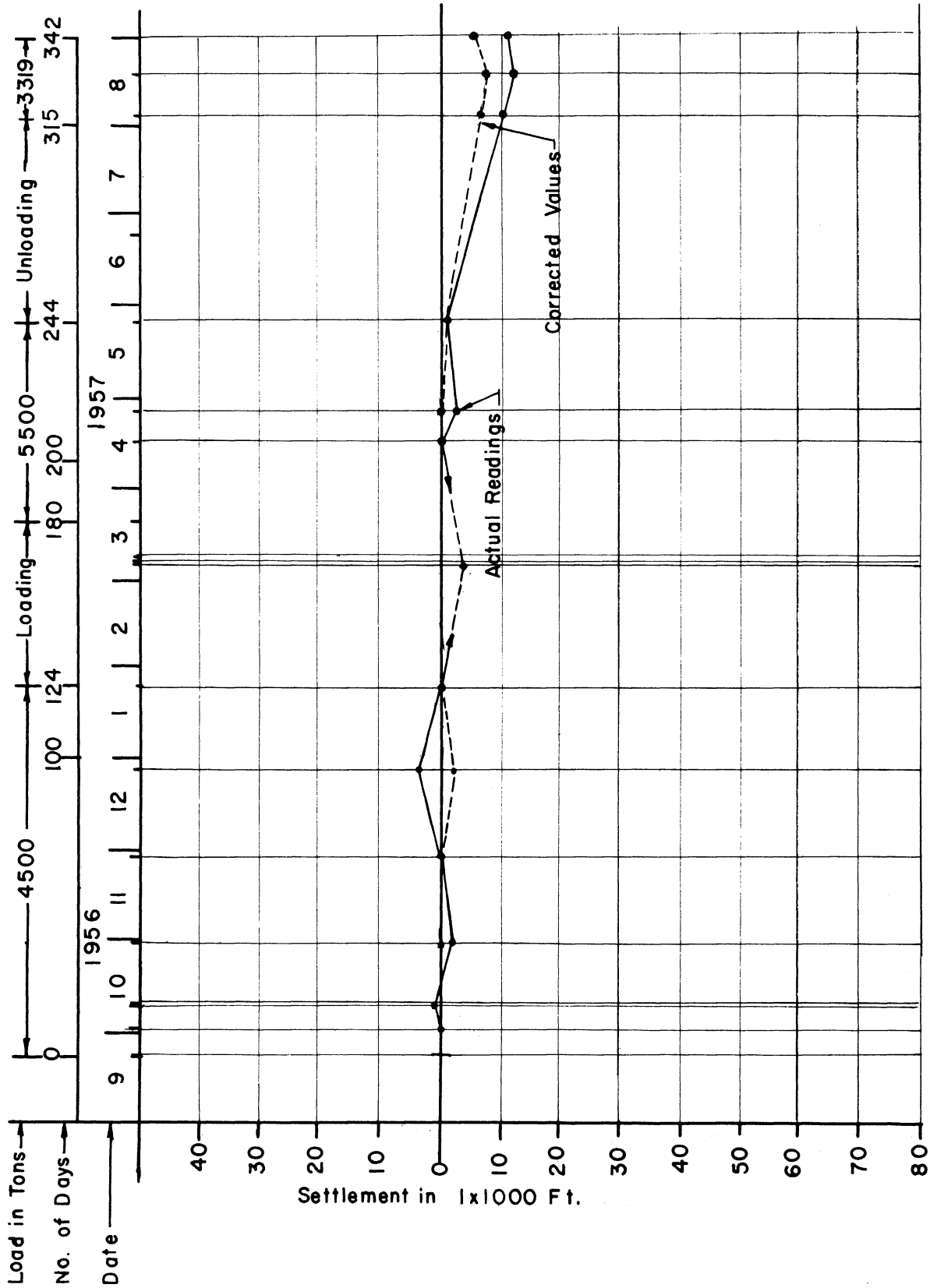

FIGURE 103. SETTLEMENT OF POINT H-1

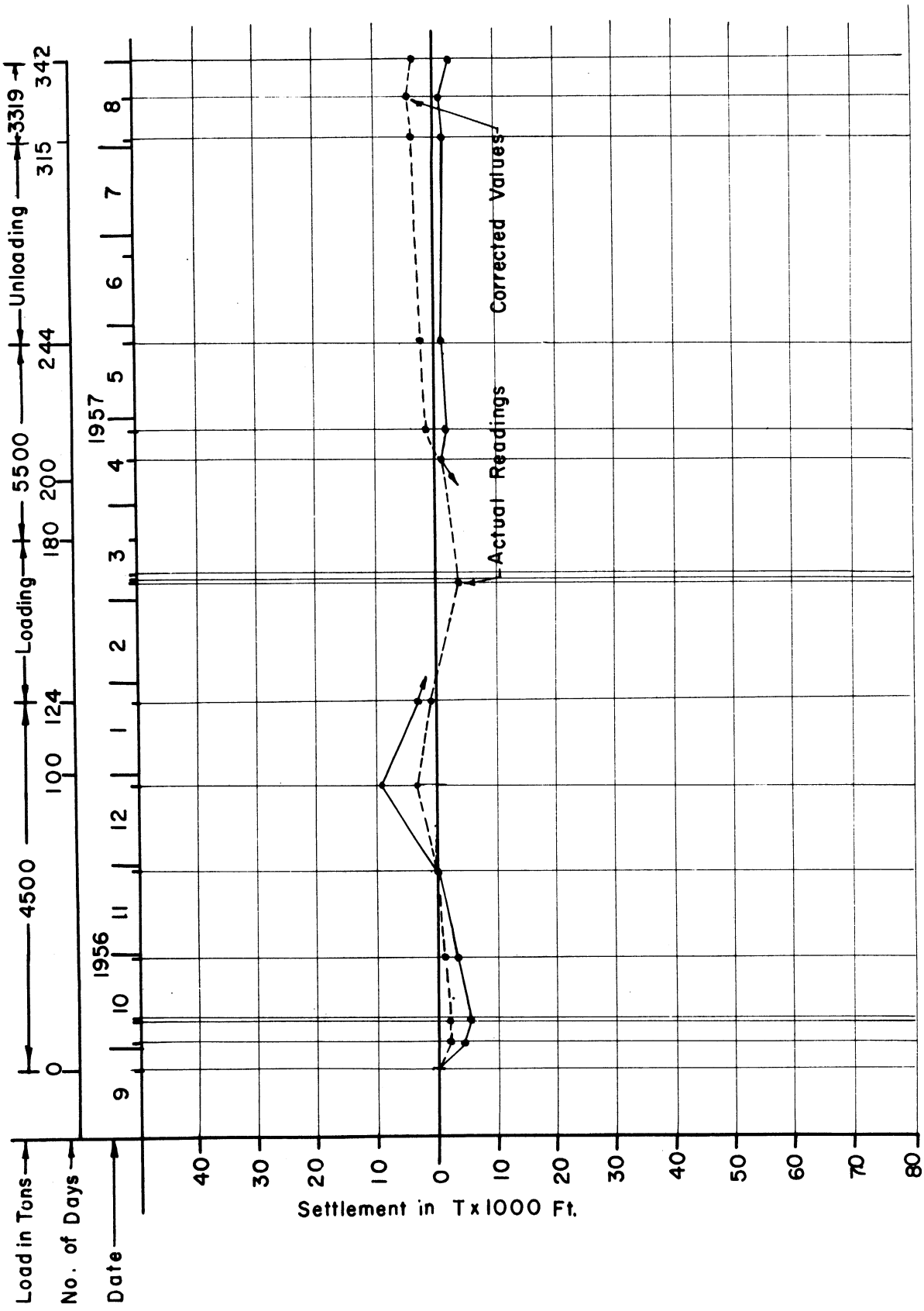

FIGURE 104. SETTLEMENT OF POINT H - 2

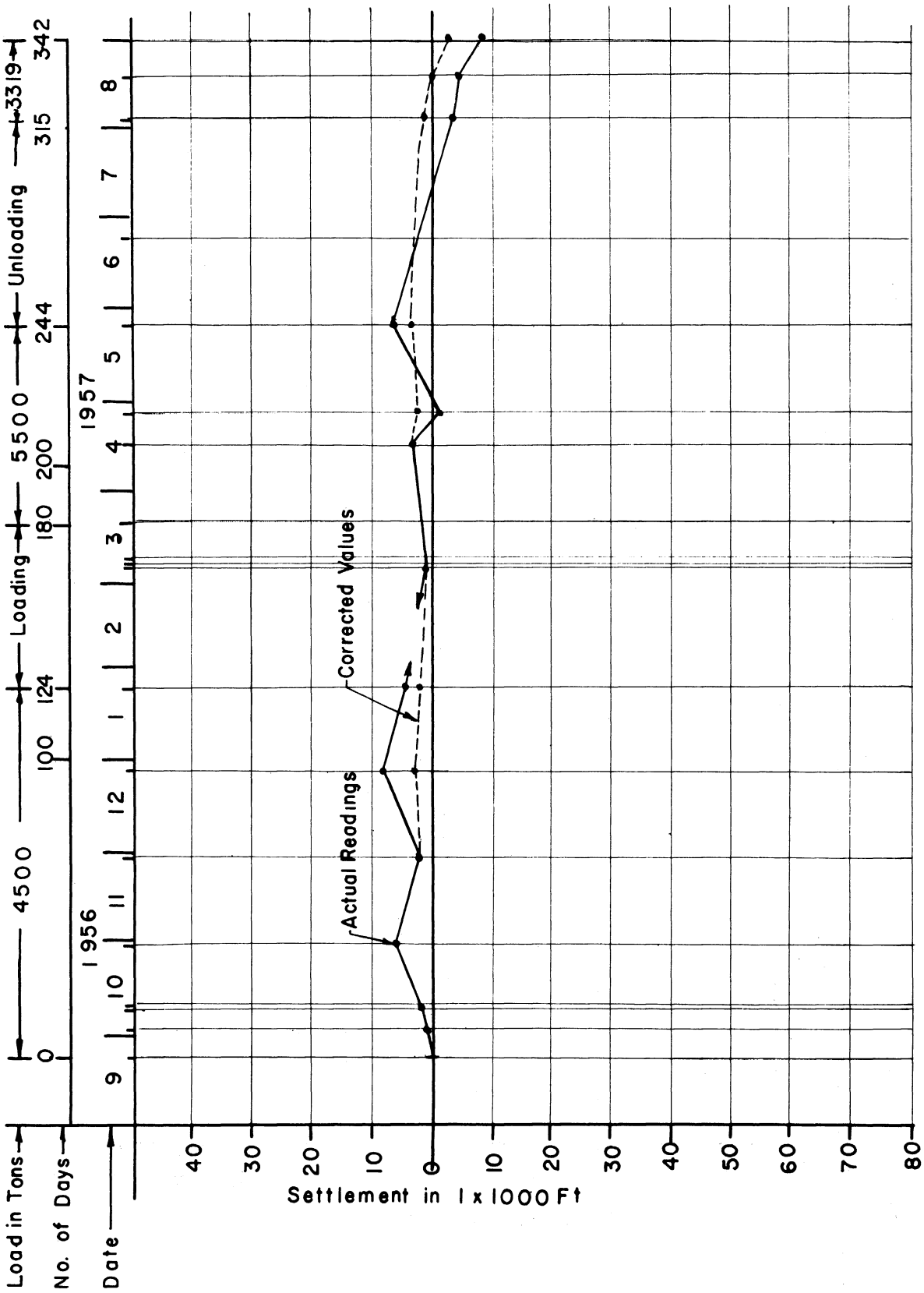

FIGURE 105. SETTLEMENT OF POINT I-1

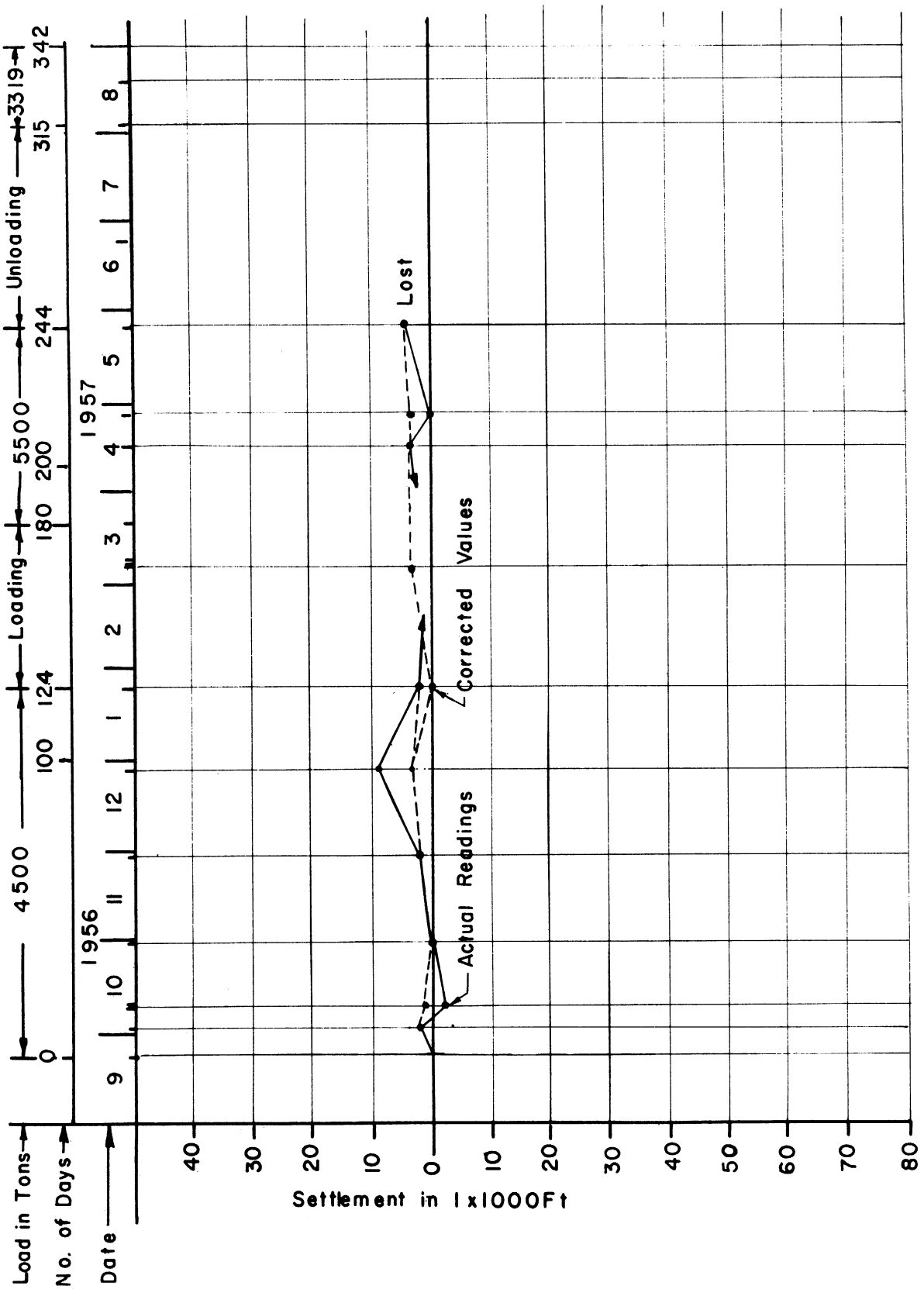

FIGURE 106 . SETTLEMENT OF POINT I-2

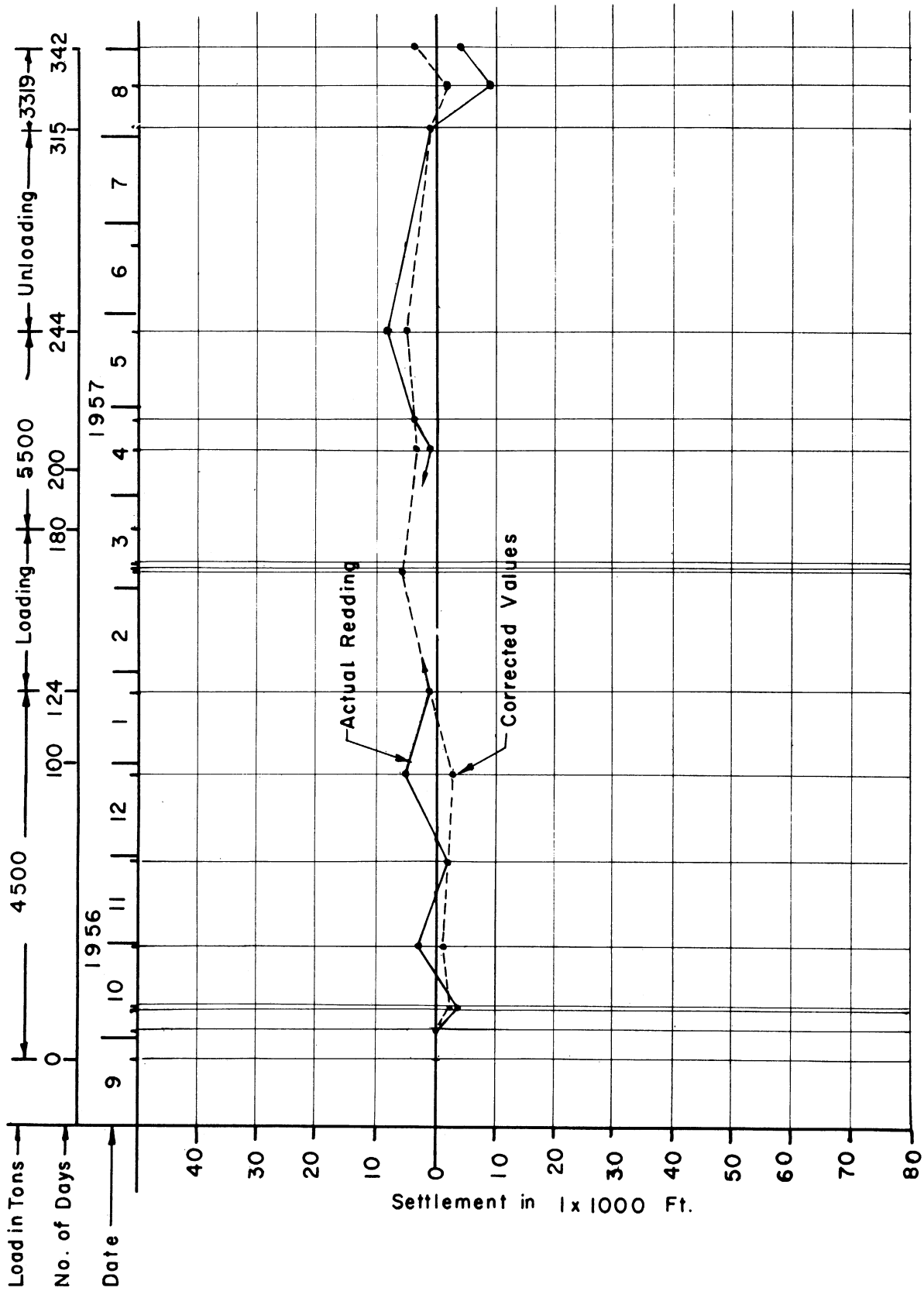

FIGURE 107 .SETTLEMENT OF POINT J-3

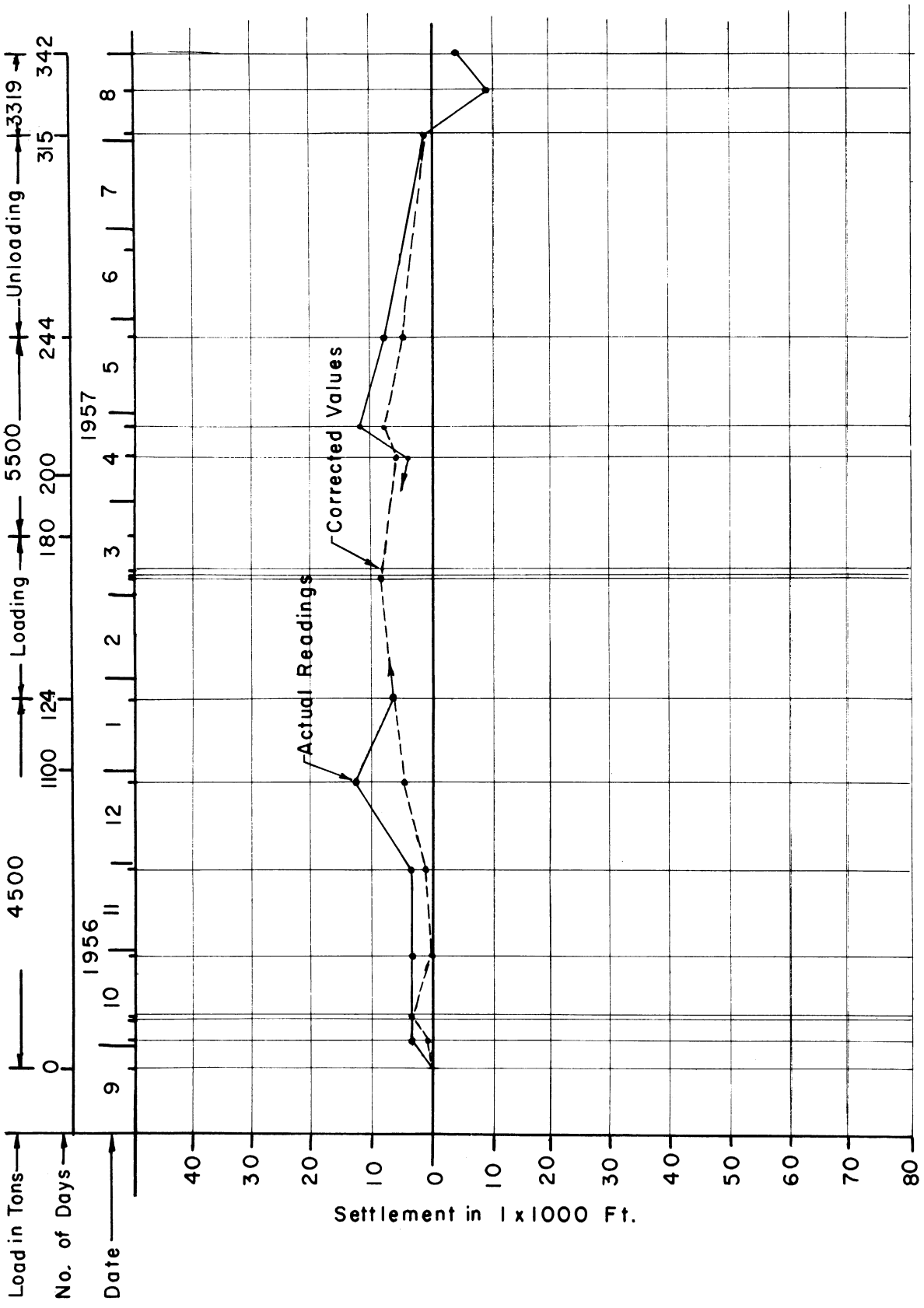

FIGURE 108. SETTLEMENT OF POINT J-5

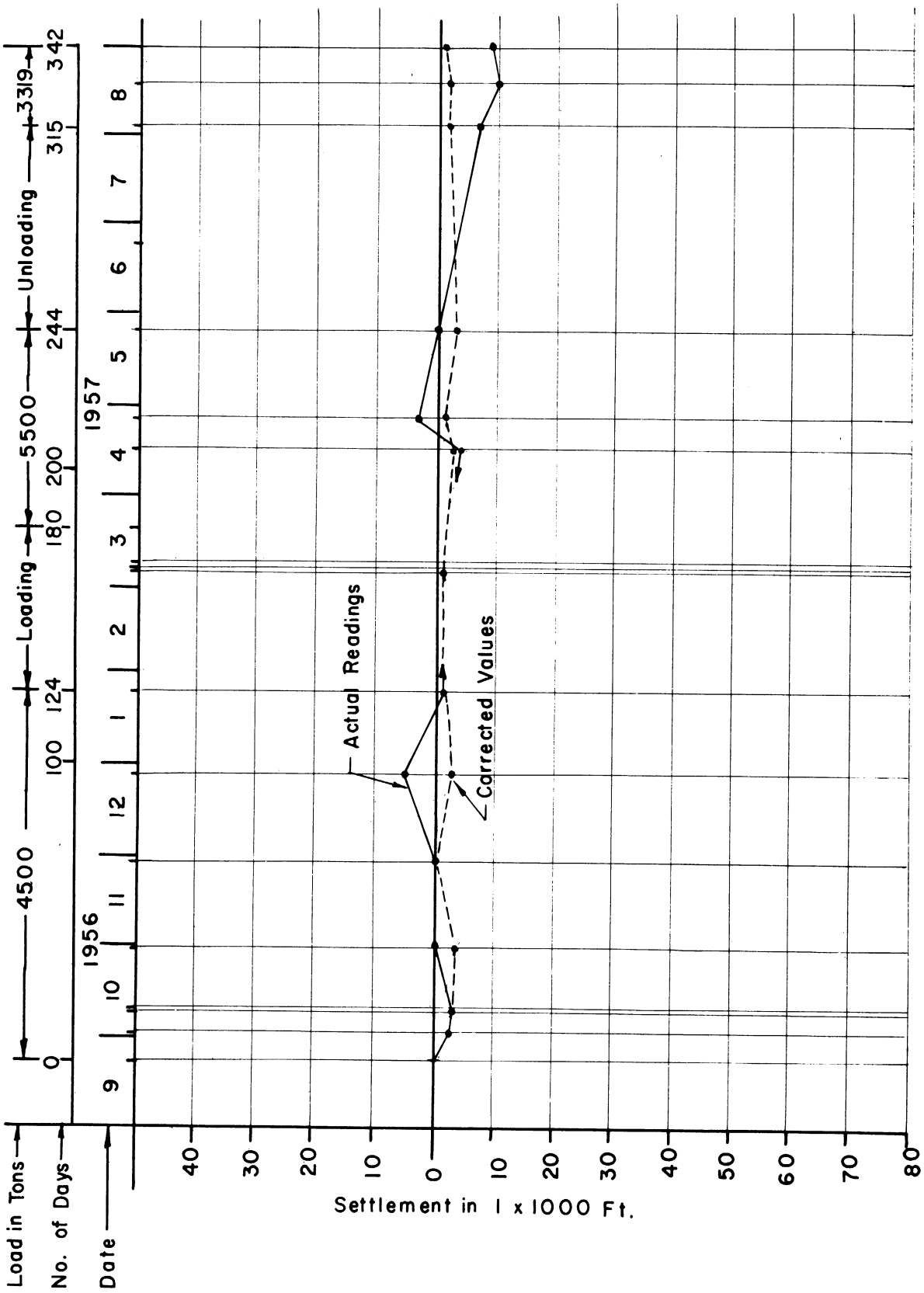

FIGURE 109 . SETTLEMENT OF POINT J-6

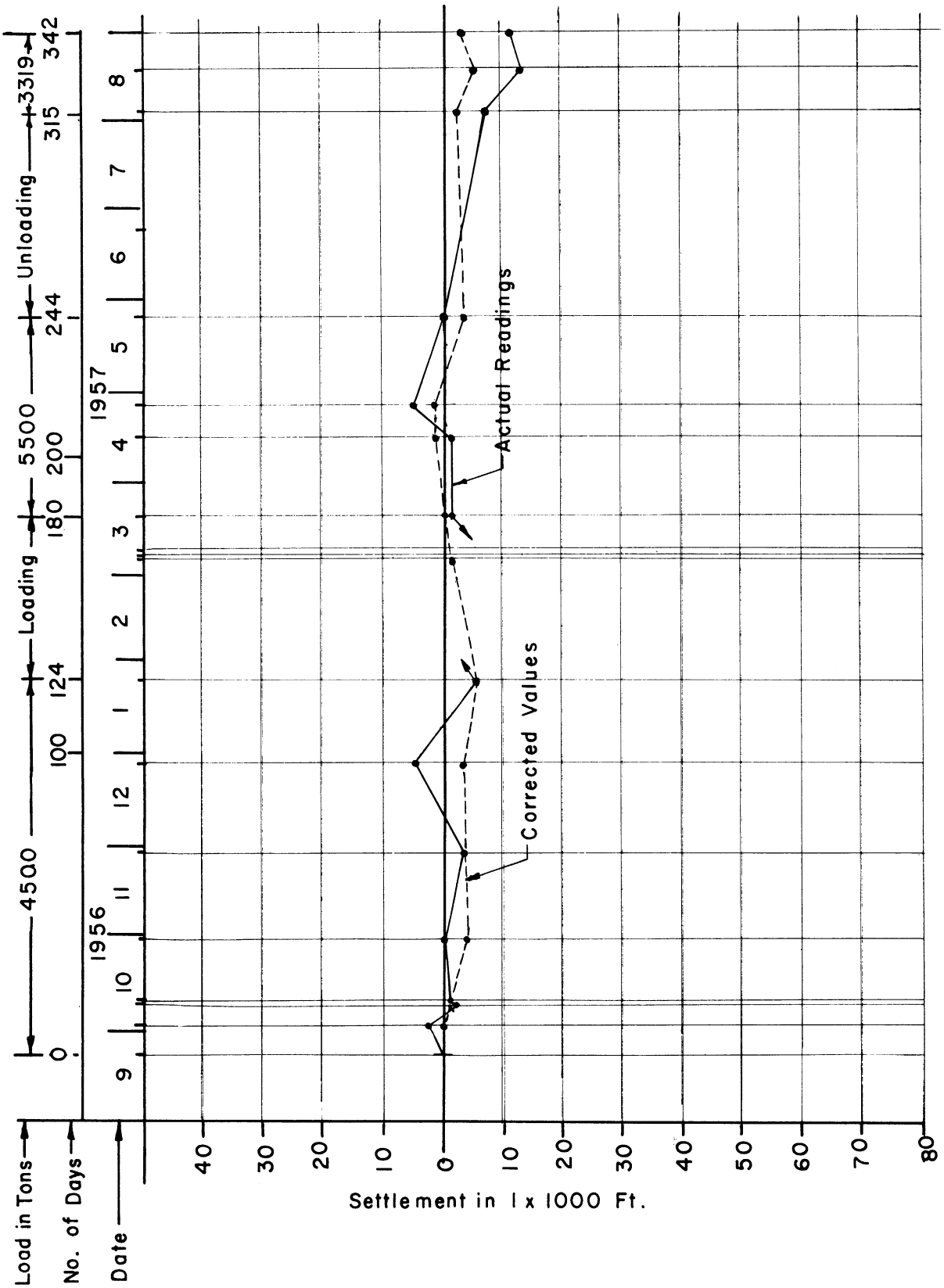

FIGURE 110. SETTLEMENT OF POINT K-6

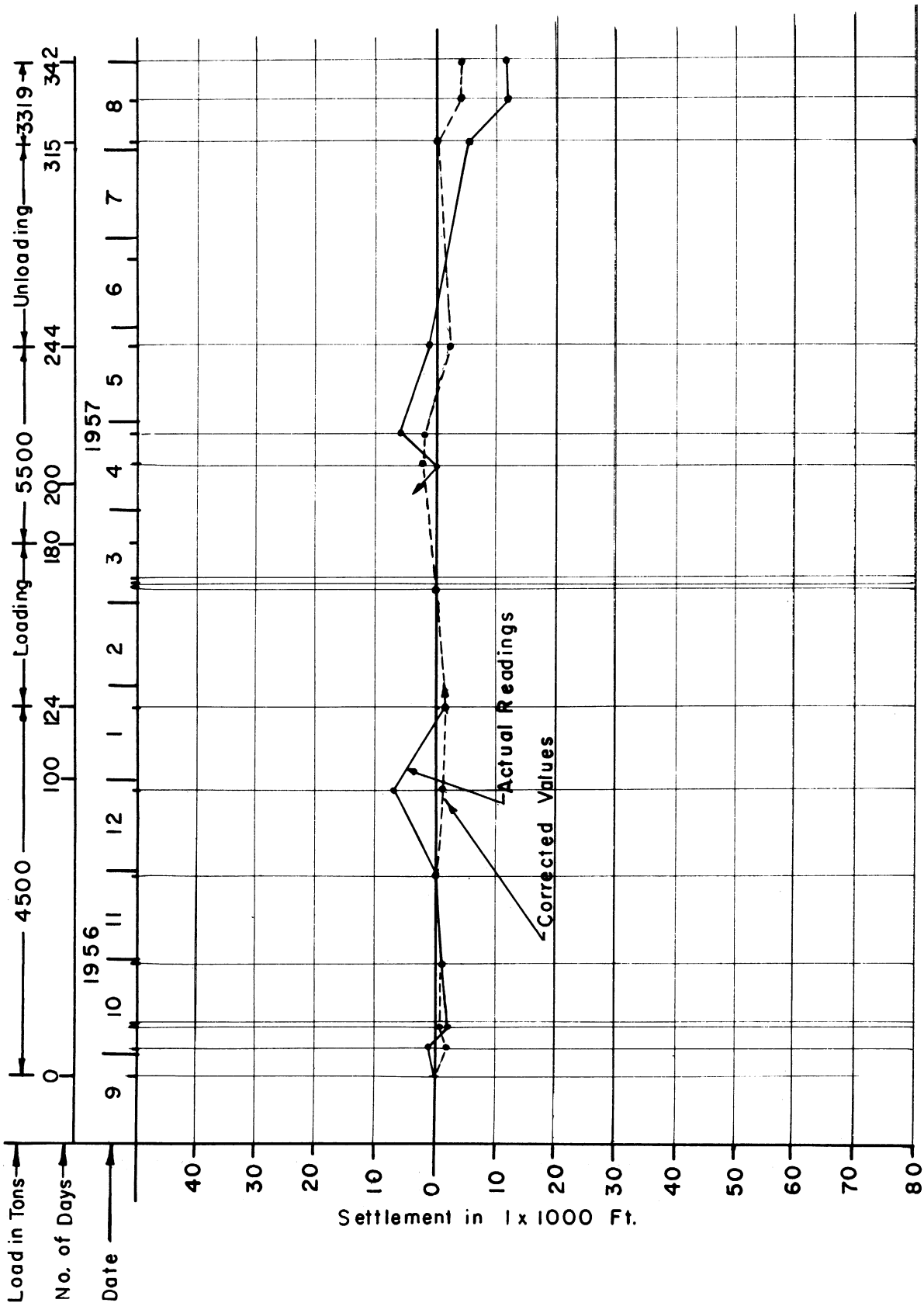

FIGURE III. SETTLEMENT OF POINT M-6

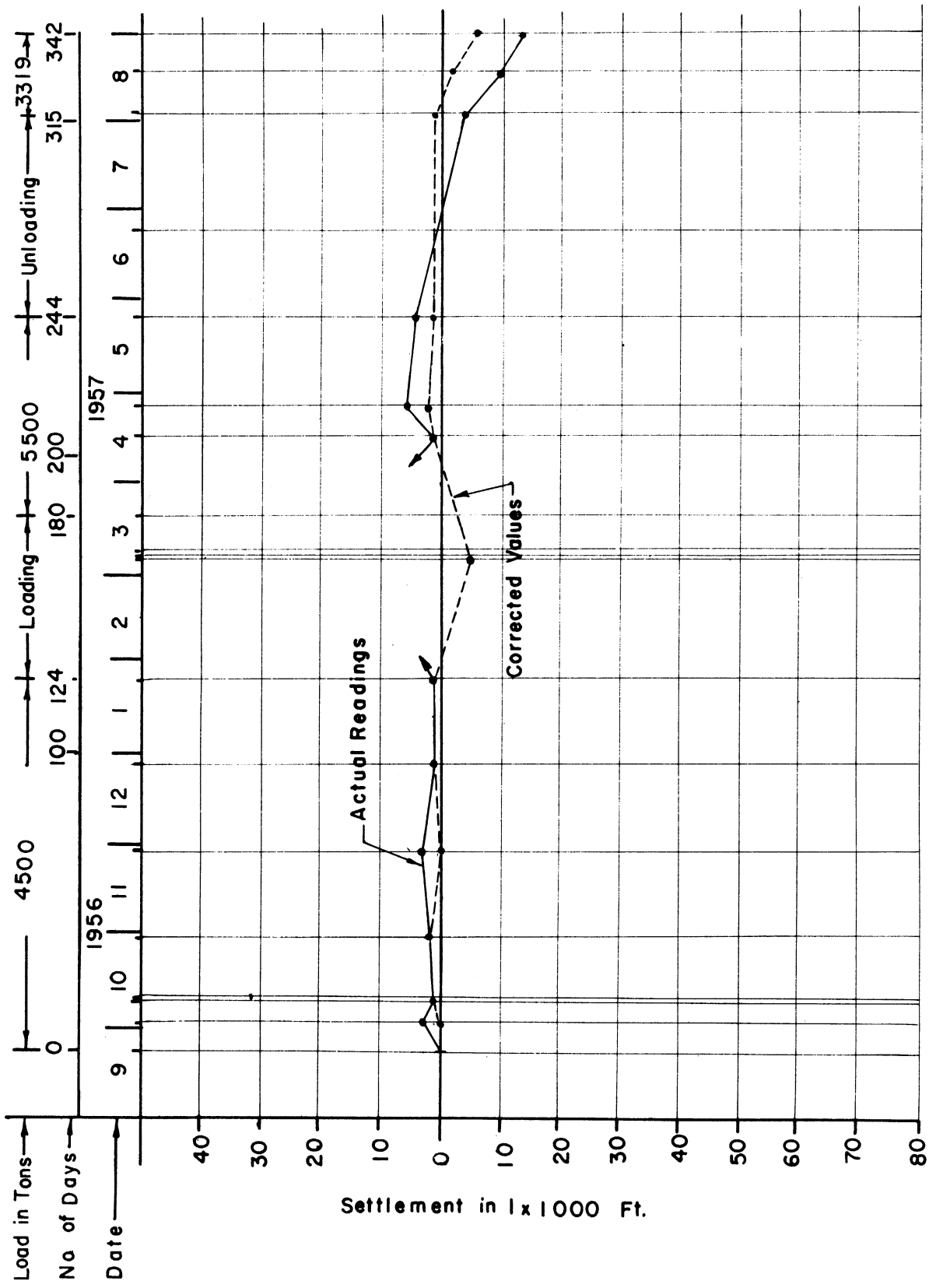

FIGURE 112. SETTLEMENT OF POINT O-6

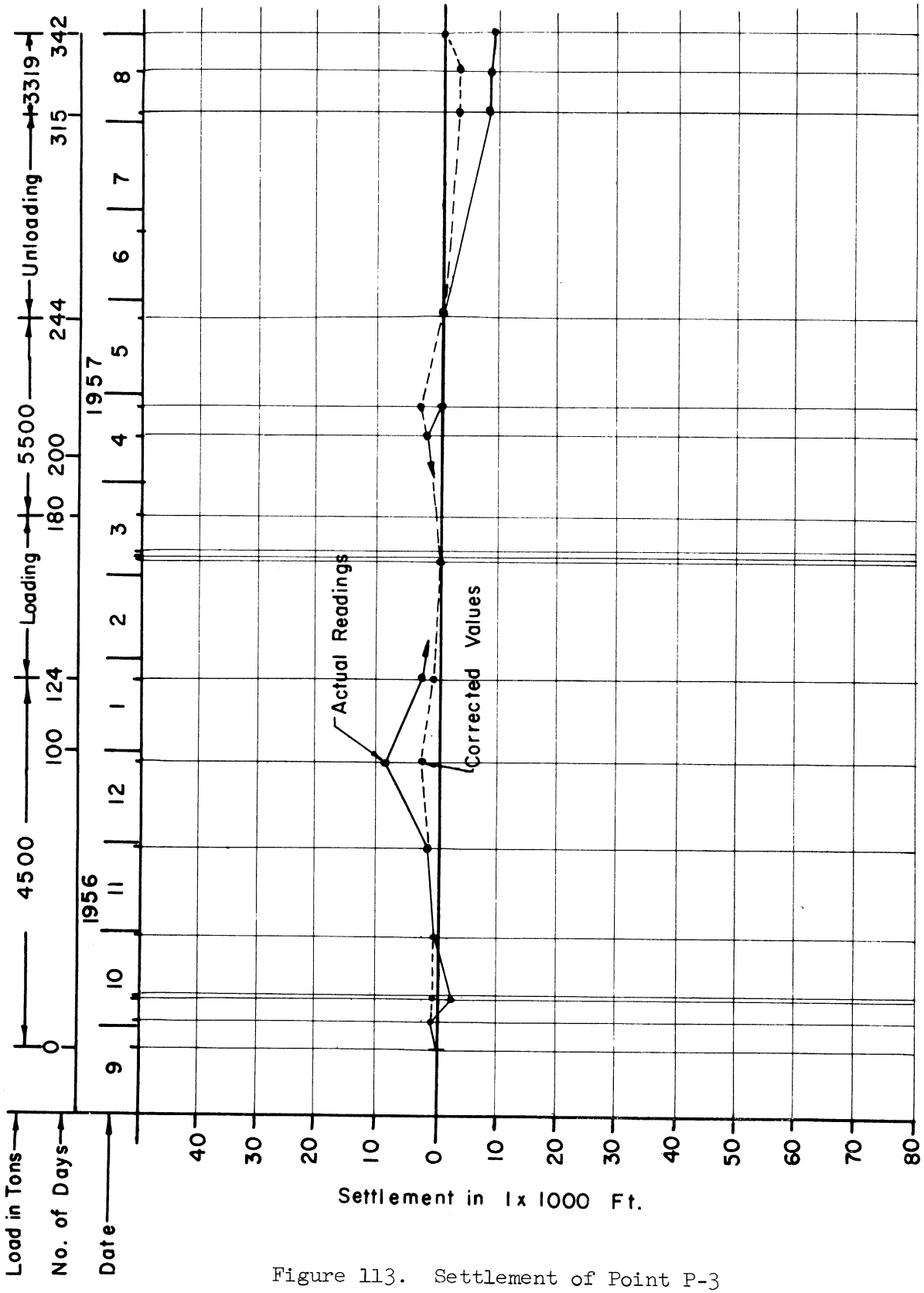

Figure 113. Settlement of Point P-3

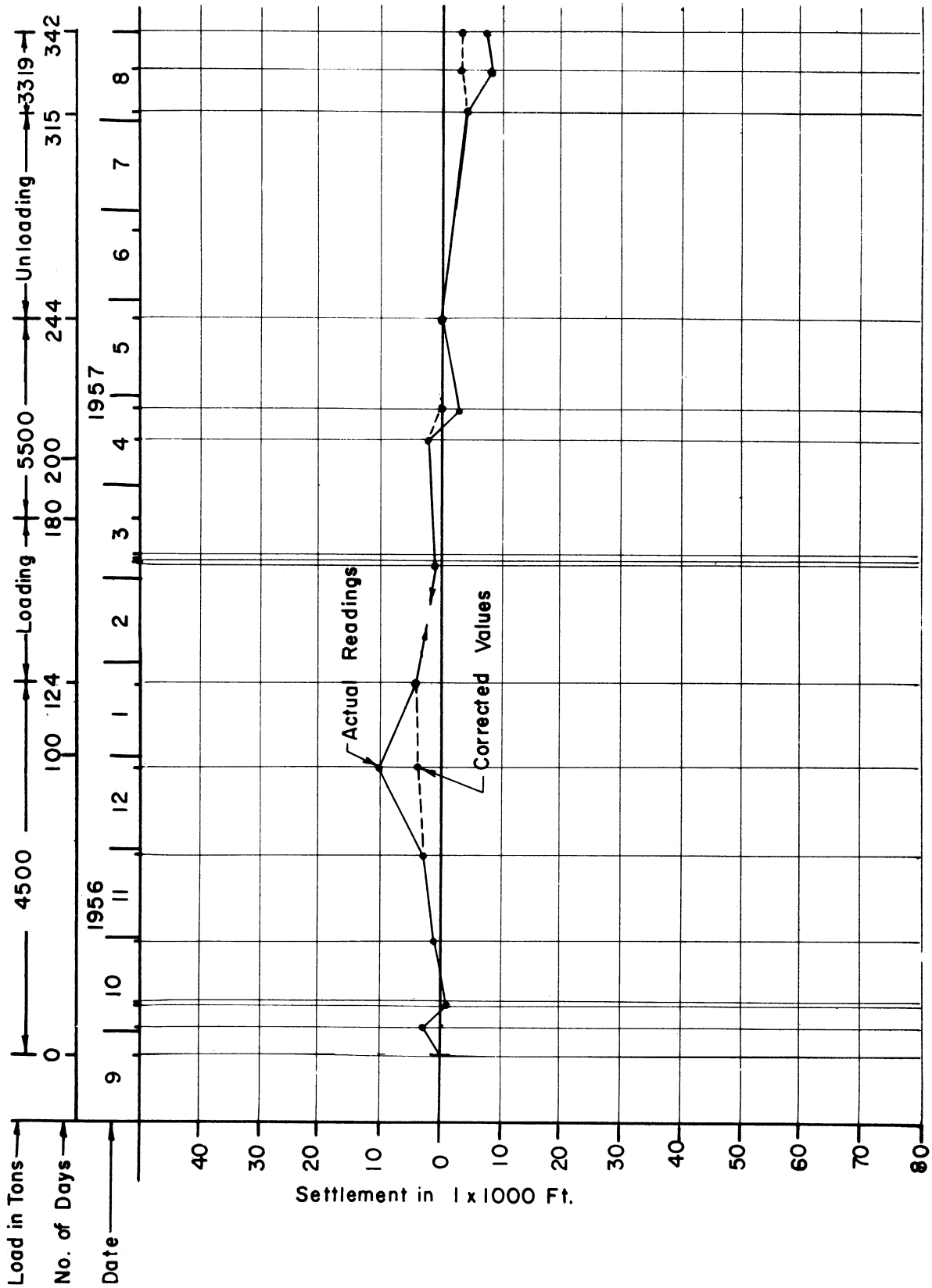

FIGURE 114. SETTLEMENT OF POINT P- 5

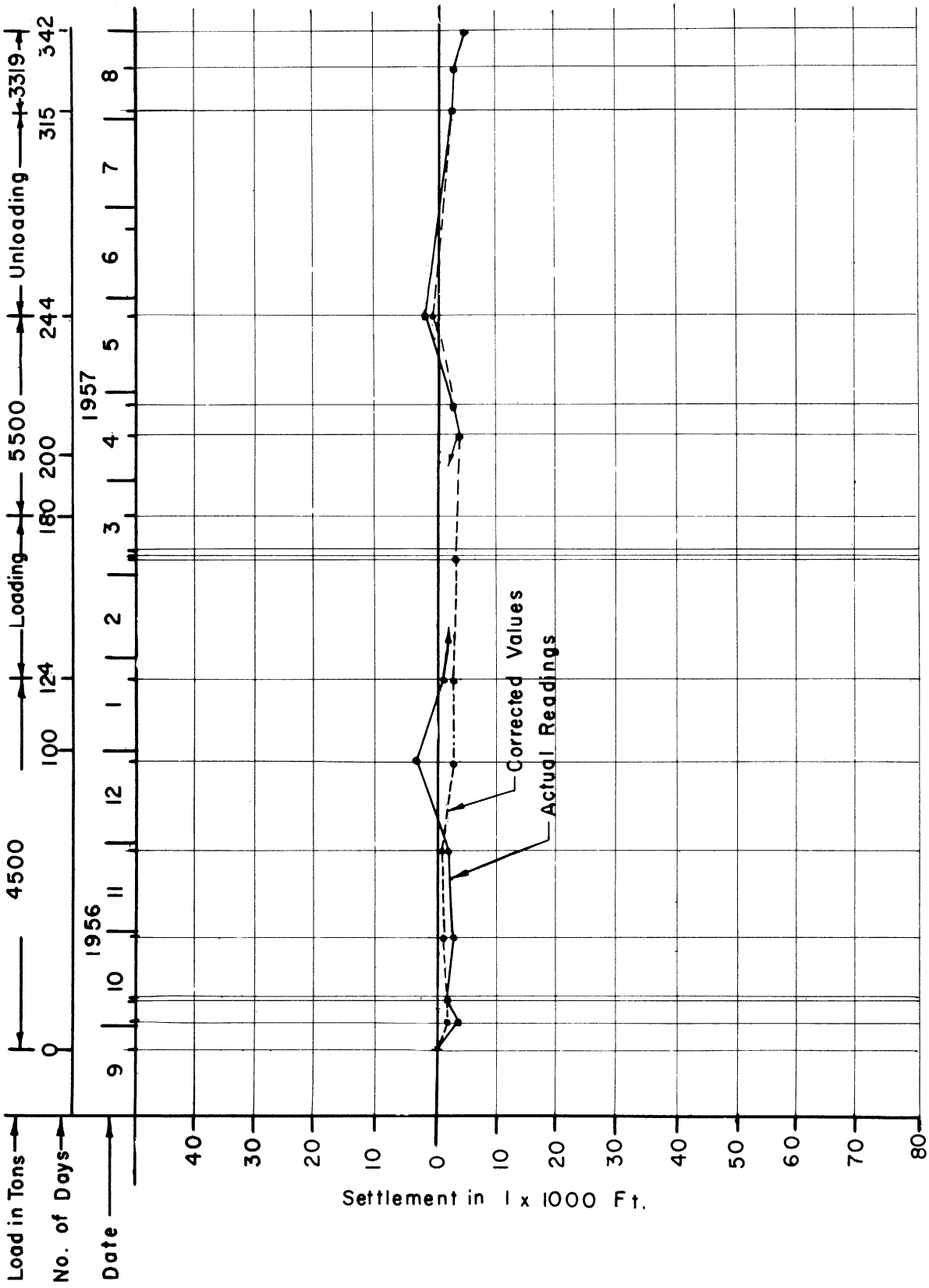

FIGURE 115. SETTLEMENT OF POINT P-6

APPENDIX D

TABLES SHOWING THE READINGS OF ELEVATIONS DURING THE TEST PERIOD, AS SUBMITTED BY INLAND STEEL COMPANY, INDIANA HARBOR, INDIANA

TABLE VI-a

READINGS OF ELEVATIONS OF MONUMENTS
DURING THE TEST

Date	9-22-56	10-2-56	10-9-56	10-10-56	10-30-56
Load	4500 T	4500 T	4500 T	4500 T	4500 T
BM1	6.951	6.951	6.951	6.951	6.951
BM2	5.756	5.756	5.756	5.756	5.756
J6	5.805	5.800	5.800	----	5.803
K6	5.451	5.454	5.449	5.450	5.448
M6	4.899	4.900	4.897	----	4.898
O6	6.917	6.920	6.919	----	6.919
P6	7.621	7.617	7.619	----	7.618
J5	5.019	5.023	5.025	----	5.023
K5	4.730	4.731	4.730	----	4.731
L5	4.790	4.794	4.789	----	4.795
M5	4.479	4.481	4.477	4.479	4.478
N5	4.332	4.331	4.332	----	4.332
O5	5.501	5.499	5.494	----	5.497
P5	6.642	6.645	6.641	----	6.643
K4	4.757	4.761	4.759	----	4.771*

Date	11-20-56	11-26-56	Correction	12-27-56	1-24-57
Load	4500 T	4500 T	Factor	4500 T	4500 T
BM1	6.951	6.951	----	6.925	6.951
BM2	5.756	5.756	----	----	----
J6	5.803	5.808	.005	5.813	5.807
K6	5.448	5.447	-.001	5.455	5.445
M6	4.889	4.892	.003	4.893	4.894
O6	6.920	6.929	.009	6.927	6.927
P6	7.619	7.634	.015	7.639	7.635
J5	5.023	5.027	.004	5.036	5.030
K5	4.731	4.736	.005	4.744	4.745
L5	4.794	4.797	.003	4.803	4.809
M5	4.474	4.485	.011	4.487	4.489
N5	4.331	4.343	.012	4.341	4.342
O5	5.501	5.512	.011	5.518	5.510
P5	6.645	6.654	.009	6.661	6.655
K4	4.767	4.768	.001	4.776	4.773

Date	3-3-57	3-6-57	3-8-57	3-21-57	4-15-57
Load	4550 T	4600 T	4856 T	5500 T	5500 T
BM1	6.951	----	----	----	6.951
BM2	----	----	----	----	----
J6	5.907	----	----	----	5.803
K6	5.549	----	----	----	5.449
M6	4.992	----	----	----	4.892
O6	7.021	----	----	----	6.927
P6	7.633	----	----	----	7.632
J5	5.132	----	----	----	5.027
K5	4.837	----	----	4.728	4.735
L5	4.845	----	----	----	4.747
M5	4.466	4.468	4.480	4.475	4.473
N5	4.337	----	----	----	4.337
O5	5.509	----	----	----	5.486
P5	6.652	----	----	----	6.653
K4	4.853	----	----	4.757	4.753

Date	4-26-57	5-24-57	8-3-57	8-17-57	8-30-57
Load	5500 T	5500 T	3319 T	3319 T	3319 T
BM1	6.951	6.951	6.951	6.951	6.951
BM2	----	----	----	----	----
J6	4.811	5.808	5.801	5.798	5.799
K6	4.455	5.450	5.443	5.437	5.439
M6	4.890	5.893	4.887	4.880	4.880
O6	6.932	6.930	6.922	6.916	6.912
P6	7.633	7.638	7.634	7.633	7.631
J5	5.035	5.030	5.025	5.020	5.022
K5	4.739	4.736	4.729	4.722	4.724
L5	4.761	4.753	4.707	4.700	5.703
M5	4.479	4.475	----	----	----
N5	4.334	4.336	4.323	----	----
O5	5.483	5.486	5.477	5.476	5.473
P5	6.648	6.651	6.647	6.643	6.644
K4	4.762	4.755	4.726	4.719	4.720

TABLE VI-b

READINGS OF ELEVATIONS OF MONUMENTS
DURING THE TEST

Date	9-22-56	10-2-56	10-9-56	10-10-56	10-30-56
Load	4500 T	4500 T	4500 T	4500 T	4500 T
L4	4.349	4.353	4.349	4.350	4.349
M4	4.097	4.096	4.097	4.099	4.093
N4	4.390	4.389	4.393	4.396	4.393
O4	5.230	5.226	5.227	-----	5.226
J3	5.513	5.513	5.509	----	5.516
K3	4.665	4.667	4.664	----	4.667
L3	4.266	4.266	4.262	4.266	4.258
N3	4.645	4.644	4.637	4.640	4.634
O3	5.193	5.194	5.190	----	5.196
P3	5.253	5.254	5.251	----	5.254
A2	5.093	5.100	5.094	----	5.094
B2	5.388	5.393	5.387	----	5.394
C2	5.432	5.438	5.433	----	5.430
D2	5.501	5.505	5.501	-----	5.505
E2	5.661	5.665	5.658	----	5.661

Date	11-28-56	11-28-56	Correction	12-27-56	1-24-57
Load	4500 T	4500 T	Factor	4500 T	4500 T
L4	4.342	4.354	.012	4.355	4.343
M4	4.071	4.075	.004	4.073	4.062
N4	4.383	4.393	.010	4.393	4.386
O4	5.230	5.244	.014	5.252	5.244
J3	5.514	5.517	.003	5.521	5.517
K3	4.663	4.665	.002	4.669	4.665
L3	4.248	4.255	.007	4.251	4.242
N3	4.630	4.635	.005	4.639	4.628
O3	5.199	5.202	.003	5.211	5.204
P3	5.255	5.265	.010	5.272	5.266
A2	5.091	5.094	.003	5.096	5.093
B2	5.390	5.394	.004	5.398	5.393
C2	5.434	5.432	-.002	5.437	5.430
D2	5.501	5.502	.001	4.507	5.499
E2	5.654	5.663	.009	5.662	5.657

Date	3-5-57	3-6-57	3-8-57	3-21-57	4-13-57
Load	4550 T	4600 T	4856 T	5500 T	5500 T
L4	4.415	4.334	4.334	4.322	4.311
M4	4.146	4.041	4.040	4.014	3.999
N4	4.378	4.368	4.372	4.368	4.363
O4	5.238	——	——	——	5.211
J3	5.622	——	——	——	5.517
K3	4.758	——	——	——	4.661
L3	4.334	4.230	4.239	4.216	4.205
N3	4.618	4.615	4.607	4.604	4.595
O3	5.197	——	——	——	5.198
P3	5.262	——	——	——	5.265
A2	5.203	——	——	——	5.098
B2	5.499	——	——	——	5.395
C2	5.534	——	——	——	5.431
D2	5.601	——	——	——	5.500
E2	5.759	——	——	——	5.654

Date	4-26-57	5-24-57	8-3-57	8-17-57	8-30-57
Load	5500 T	5500 T	3319 T	3319 T	3319 T
L4	4.307	4.301	4.312	4.307	4.294
M4	3.997	3.985	3.994	3.990	3.990
N4	4.343	4.355	4.353	4.357	4.351
O4	5.209	5.208	5.203	5.203	5.202
J3	5.520	5.524	5.517	5.507	5.512
K3	4.668	4.662	4.659	4.654	4.653
L3	4.198	4.193	4.198	4.192	4.191
N3	4.590	4.590	4.585	4.587	4.585
O3	5.194	5.196	5.188	5.189	5.189
P3	5.263	5.263	5.255	5.255	5.254
A2	5.101	5.100	----	----	----
B2	5.401	5.400	5.394	5.385	5.385
C2	5.438	5.455	5.427	5.420	5.419
D2	5.503	5.502	5.490	5.488	5.484
E2	5.657	5.654	5.643	5.642	5.640

TABLE VI-c

READINGS OF ELEVATIONS OF MONUMENTS
DURING THE TEST

Date	9-22-56	10-2-56	10-9-56	10-10-56	10-30-56
Load	4500 T	4500 T	4500 T	4500 T	4500 T
F2	5.479	5.482	5.477	5.483	5.478
G2	5.864	5.862	5.859	----	5.862
H2	5.903	5.899	5.898	----	5.900
I2	5.408	5.410	5.406	----	5.408
A1	5.295	5.301	5.290	----	5.295
B1	5.388	5.393	5.387	----	5.394
C1	5.154	5.158	5.154	----	5.158
D1	5.360	5.360	5.358	----	5.364
E1	5.925	5.930	5.924	----	5.928
F1	5.409	5.412	5.409	----	5.412
G1	6.603	6.299	6.298	----	6.297
H1	6.360	6.360	6.361	----	6.358
I1	6.236	6.237	6.239	----	6.242

Date	11-28-56	11-28-56	Correction	12-27-56	1-24-57
Load	4500 T	4500 T	Factor	4500 T	4500 T
F2	5.473	5.477	.004	5.484	5.477
G2	5.859	5.867	.008	5.875	5.868
H2	5.903	5.914	.011	5.923	5.917
I2	5.410	5.418	.008	5.925	5.418
A1	5.287	5.288	.001	5.286	5.289
B1	5.387	5.389	.002	5.393	5.389
C1	5.156	5.158	.002	5.161	5.155
D1	5.360	5.341	.019	5.345	5.339
E1	5.923	5.919	.004	5.919	5.914
F1	5.405	5.407	.002	5.410	5.405
G1	6.295	6.305	.010	6.313	6.306
H1	6.360	6.371	.011	6.375	6.371
I1	6.238	6.238	.000	6.244	6.240

Date	3-5-57	3-6-57	3-8-57	3-21-57	4-15-57
Load	4550 T	4600 T	4856 T	5500 T	5500 T
F2	5.471	——	——	——	5.473
G2	5.862	——	——	——	5.864
H2	5.900	——	——	——	5.913
I2	5.417	——	——	——	5.419
A1	5.399	——	——	——	5.294
B1	5.495	——	——	——	5.392
C1	5.259	——	——	——	5.155
D1	5.443	——	——	——	5.342
E1	6.019	——	——	——	5.917
F1	5.508	——	——	——	5.406
G1	6.302	——	——	——	6.307
H1	6.367	——	——	——	6.371
I1	6.237	——	——	——	6.239

Date	4-26-57	5-24-57	8-3-57	8-17-57	8-30-57
Load	5500 T	5500 T	3319 T	3319 T	3319 T
F2	5.467	5.463	5.463	5.455	5.461
G2	5.861	5.863	5.854	5.853	5.852
H2	5.912	5.913	5.902	5.903	5.901
I2	5.416	5.420	----	----	----
A1	5.297	-----	----	5.286	5.283
B1	5.399	5.398	5.390	5.384	5.382
C1	5.164	5.164	5.153	5.148	5.149
D1	5.349	5.345	5.333	5.329	5.330
E1	5.920	5.918	5.907	5.906	5.906
F1	5.413	5.409	5.400	5.395	5.394
G1	6.304	6.304	6.298	6.296	6.296
H1	6.368	6.373	6.360	6.358	6.359
I1	6.235	6.241	6.232	6.231	6.227

APPENDIX E

DETERMINATION OF EQUATION OF TWO VARIABLES BY METHOD OF LEAST SQUARES

APPENDIX E

When a set of points has a linear trend, the problem is to determine the best-fitting line. The general equation of a straight line is:

$$Y = b\,X + a$$

In this equation X is the independent variable and Y is the dependent variable. The best-fitting line for these points is the one that has the constants determined by minimizing the sum of the squares of the Y-residuals.

The Y-residual = $\Delta Y = Y_i - b\,X_i - a$.

The square of the Y-residual = $\Delta Y^2 = (Y_i - b\,X_i - a)^2$.

The sum of the square of the Y-residual is:

$$\Sigma\,\Delta Y^2 = \Sigma\,(Y_i - b\,X_i - a)^2$$

The conditions for the sum of the squares of the Y-residuals to be minimum are that the first partial derivatives $\Sigma\,\Delta\,Y^2$, with respect to "b" and "a", be equal to zero

$$\frac{d(\Sigma\,\Delta Y^2)}{d\,b} = 0$$

$$\frac{d(\Sigma\,\Delta Y^2)}{d\,a} = 0$$

resulting in the normal equations

$$\Sigma\,X_i\,Y_i - b\,\Sigma\,X_i^2 - a\,\Sigma\,X_i = 0$$

$$\Sigma\,Y_i - b\,\Sigma\,X_i - a\,n = 0$$

By solving the normal equations simultaneously

$$b = \frac{n\,\Sigma\,X\,Y - \Sigma\,X\,\Sigma\,Y}{n\,\Sigma\,X^2 - (\Sigma\,X)^2}$$

$$a = \frac{\Sigma X^2 \Sigma Y - \Sigma X \Sigma XY}{n \Sigma X^2 - (\Sigma X)^2}$$

The coefficient of correlation, or measure for goodness of fit, is expressed as:

$$r = \frac{n \Sigma XY - \Sigma X \Sigma Y}{\sqrt{n \Sigma X^2 - (\Sigma X)^2} \quad \sqrt{n \Sigma Y^2 - (\Sigma Y)^2}}$$

APPENDIX F

TRIAXIAL CHART FOR THE TEXTURAL CLASSIFICATION OF SOILS

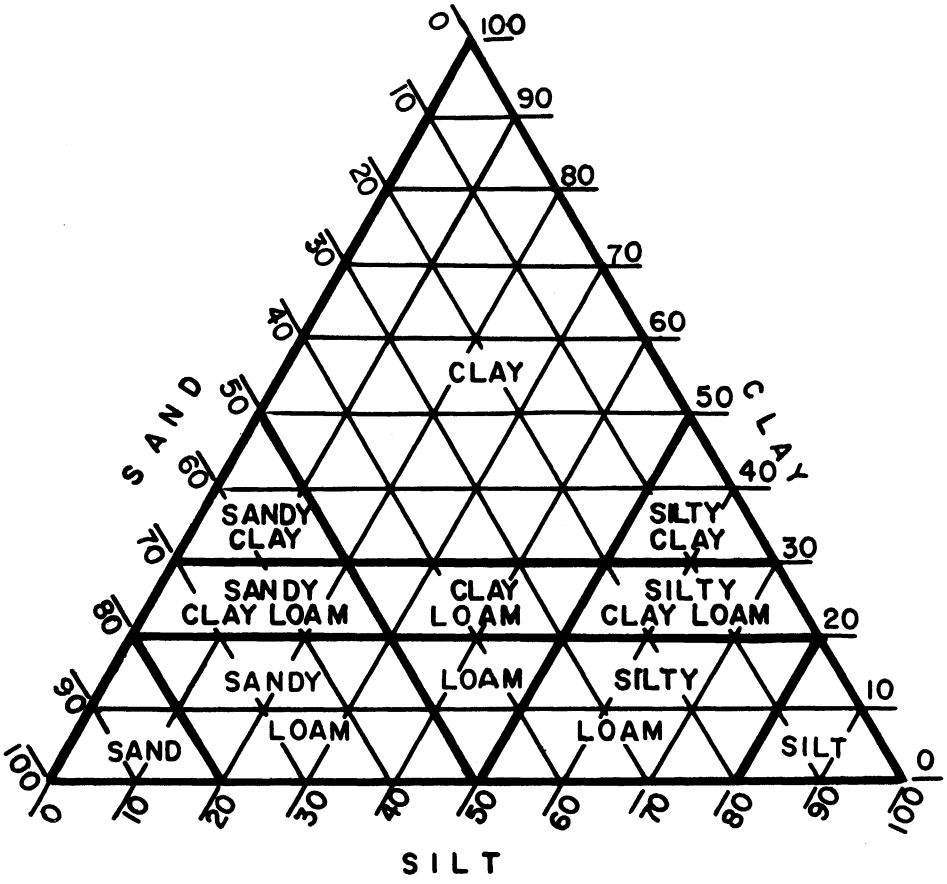

FIGURE. 116 . TRIAXIAL CHART FOR TEXTURAL CLASSIFICATION OF SOILS (17)

BIBLIOGRAPHY A

This bibliography lists the references used and referred to in this dissertation.

BIBLIOGRAPHY

1. Ackerman, A. J., "Discussion, Ackerman on Cellular Cofferdams," Transactions of the American Society of Civil Engineers, Vol. 110, 1945, pp. 1155-1161.

2. Carnegie Steel Sheet Piling, Carnegie Steel Company, Pittsburgh, Pa., First Edition, 1931, 92 pages.

3. Engineering News-Record, "Contractors Win River Battle," Engineering News-Record, Vol. 119, 1937, pp. 13-16.

4. Engineering News-Record, "New York Piers for 1000-Foot Ships," Engineering News-Record, August 3, 1933, pp. 123-126.

5. Greulich, G. G., "Discussion, Greulich on Cellular Cofferdams," Transactions of the American Society of Civil Engineers, Vol. 110, 1945, pp. 1120-1124.

6. Epstein, Harris, "Design of a Cellular Cofferdam," Proceedings, 17th Annual Meeting, Highway Research Board, National Research Council, Vol. 17, 1937, pp. 481-493.

7. Harroun, D. T., Stability of Cohesive Earth Masses in Embankments, Thesis, University of Michigan, Ann Arbor, Michigan, 1941.

8. Hedman, A. F., "Cofferdam Design for Kentucky Dam," Engineering News-Record, Vol. 128, (January 1, 1942) pp. 50-55.

9. Housel, W. S., "Experimental Soil-Cement Stabilization at Cheboygan, Michigan," Proceedings, 17th Annual Meeting, Highway Research Board, National Research Council, 1937.

10. Housel, W. S., "Internal Stability of Granular Materials," American Society Testing Materials, Vol. 36, Part II, (1936).

11. Housel, W. S., "Shearing Resistance of Soil, Its Measurement and Practical Significance," Proceedings, American Society for Testing Materials, Vol. 39, 1939.

12. Housel, W. S., Notes on Stability of Embankments, Soil Mechanics Research Laboratory, Michigan State Highway Department, January, 1947.

13. Housel, W. S., "Interpretation of Triaxial Compression Test on Granular Mixtures," Proceedings, Association of Asphalt Paving Technologist, Vol. 19, 1950.

14. Housel, W. S., "Misconceptions in the Use of Surface Tension in Capillarity," Proceedings, 30th Annual Meeting, Highway Research Board, December, 1950.

15. Housel, W. S., Design Memorandum on Embankment Stability, Lateral Distribution or Weight Transfer Above the Loading Plane, Soil Mechanics Laboratory, Department of Civil Engineering, University of Michigan, April, 1952.

16. Housel, W. S., Design Memorandum on Bearing Capacity of Spread Footings on Cohesive Soil, Soil Mechanics Laboratory, Department of Civil Engineering, University of Michigan, June, 1952.

17. Housel, W. S., Applied Soil Mechanics, Edwards Brothers, Inc., Ann Arbor, Michigan, 1955.

18. Housel, W. S., "Field and Laboratory Determinations of the Bearing Capacity of Hardpan for Design of Deep Foundations," American Society of Testing Materials, Vol. 56, 1956, pp. 1320-1350.

19. Housel, W. S., Applied Soil Mechanics, Laboratory Manual of Soil Testing Procedures, Edwards Brothers, Inc., Ann Arbor, Michigan, 1957.

20. Housel, W. S., "Embankment Stability as a Factor in Adequate Sheeting and Bracing," Journal of American Water Works Association, Vol. 50, No. 2, February, 1958.

21. Jacoby, J. S. and Davis, R. P., The Foundations of Bridges and Buildings, McGraw-Hill Book Company, Third Edition, 1941, pp. 238-274.

22. Miller, J. S., "Discussion, Miller on Cellular Cofferdams," Transactions of the American Society of Civil Engineers, Vol. 110, 1945, pp. 1171-1173.

23. Pennoyer, R. P., "Design of Steel Sheet-Piling Bulkheads," Civil Engineering, Vol. 3, 1933, pp. 615-619.

24. Pennoyer, R. P., "Gravity Bulkheads and Cellular Cofferdams," Civil Engineering, Vol. 4, 1934, pp. 301-305.

25. Pennoyer, R. P., "Discussion, Pennoyer on Cellular Cofferdams," Transactions of the American Society of Civil Engineers, Vol. 110, 1945, pp. 1124-1133.

26. Prentis, Edmund A., and White, Lazarus, Cofferdams, Columbia University Press, New York, N.Y., 1950.

27. Richardson, C. H., An Introduction to Statistical Analysis, Harcourt Brace and Co., New York, 1944, pp. 474.

28. Terzaghi, K. A., "Stability and Stiffness of Cellular Cofferdams," Proceedings of the American Society of Civil Engineers, Vol. 70, No. 7, September, 1944.

29. Terzaghi, K. A., "Shipway with Cellular Cofferdam on Marl Foundation," Transaction of the American Society of Civil Engineers, Vol. 71, No. 9, November 1945, pp. 1327-1353.

30. Trans. ASCE, Transactions of the American Society of Civil Engineers, Vol. LXXXI, (1917), pp. 544-545.

31. Trans. ASCE, Transactions of the American Society of Civil Engineers, Vol. LXXXI, (1917), pp. 553-569.

32. Watt, D. A., "Steel Sheetpile Cofferdam for Troy Lock and Dam," Engineering News, Vol. 76, 1916, pp. 533-540.

BIBLIOGRAPHY B

This bibliography is a general bibliography on cofferdams. It was used in the general study of the problem. There is no direct reference to it.

BIBLIOGRAPHY ON COFFERDAMS

Ackerman, A. J. "Planning and Plant for Heavy Construction," Construction Methods, Vol. 18, No. 6 (June, 1936), pp. 50-54.

Albertson, E. R. "Cofferdaming Difficulties in Narrow Tideway," Engineering News-Record, Vol. 118, No. 20 (May 20, 1937), pp. 729-732.

Bailey, S. C. "Construction of Cofferdams," Dock and Harbor Authority, Vol. 29, No. 337 (November, 1948), pp. 172-177.

Bengston, O. R. "Template Takes Trouble Out of Driving 70 Foot Cofferdam Cells," Engineering News-Record, Vol. 148, No. 3 (January 17, 1952), pp. 34-35.

Brink, L. L. "Unique Two-Barge Technique Expedites in Placing of Cofferdam," Civil Engineer, Vol. 19, No. 4 (April, 1949), pp. 32-33.

Caples, W. G. "Steel Breakwaters," Military Engineer, March-April, 1932, pp. 120-122.

Carnegie Steel Company Carnegie Steel Sheet Piling, Carnegie Steel Company, Pittsburgh, 1931, 92 pages.

Chamberlin, H. "Liquid Mud Lifts Ship," Engineering News-Record, August 5, 1937, p. 235.

Chambers, R. H. "Survey of Foundation Construction Method," Civil Engineer, Vol. 11, No. 1 (1941), pp. 31-34.

Chambers, R. H. "Intake Tunnel through New Orleans Levee in Sheet Pile Cofferdams," Engineering News-Record, April 3, 1924.

Chivers, N. M. "The Cofferdam at Lock #2, Cape Fear River, North Carolina," U.S. Corps of Engineers, Vol. 8, No. 19 (1916), pp. 608 ff.

Civil Engineering "Novel Construction Plan for Graving Dock Suggested by Soil Studies," August, 1944, pp. 323-328.

Clark, A. W. "Construction Features of Osage Hydro-electric Development," Engineering News-Record, March 26, 1931, pp. 523-528.

Colburn, R. T. "Sheet-pile Cofferdam and Test Cell for TVA Projects," Civil Engineering, Vol. 9, No. 9, (September, 1939), pp. 551-553.

Condron, T. L. "Cellular Steel Breakwater for Calumet Harbor," Engineering News-Record, Vol. 115 (1935), pp. 86-91.

Construction Methods "Building Cofferdams for Arlington Bridge Piers," Vol. 10, No. 4 (April, 1928), pp. 16-19.

"Cellular Cofferdam Encloses 18 Acre Area for Building Steamship Piers 1100 Feet Long," Vol. 16, No. 9 (September, 1934), pp. 32-37.

"Well Points, Pile Jets and Crib Cofferdams," Vol. 24, No. 5 (May, 1942), pp. 48, 92, 94, 100-101.

"Walls Keep Riverside Cofferdam Dry," Vol. 29, No. 4 (April, 1947) pp. 84 ff.

"Rock Fill Cofferdam in Soo Rapids," Vol. 30, No. 10, (October, 1948), pp. 36-41.

"Something New...Concrete Cofferdam at Bull Shoals," Vol. 30, No. 4 (April, 1948), pp. 86-90.

"Deep Cofferdam," Vol. 31, No. 8 (August, 1949), pp. 50 ff.

"Clay and Stone Placed to Make Good Dike," Vol. 37, No. 3 (March, 1953), pp. 74, 78, 82, 84.

"Guyed Shield Deflects Niagara for Daring Cofferdam Construct," Vol. 37, No. 5 (May, 1955), pp. 59-62.

Construction "Cofferdam Built on Shore," Vol. 12, No. 3 (March, 1930), pp. 61-63.

Contractors and Engineers Monthly

"Methods and Machines Used in Building Montgomery Locks on the Ohio River," Vol. 28, No. 3 (March, 1934), pp. 22-26.

Davies, H. A. "Stress Computation in Single Wall Cofferdam," Cornell Civil Engineering, Vol. 33, No. 2, (1924), pp. 31-35.

Donegian, M. N. "Canvas Lining for Cofferdam Controls Water in Previous Soil," Engineering News-Record, Vol. 131, No. 21, (November, 1943) pp. 756 ff.

Engineering "Sheet Pile Cofferdams for the Arlington Memorial Bridge," Vol. 126, No. 3272 (September 28, 1928), pp. 383-385.

Engineering Journal "Demolition of Cofferdams Below Great Falls Power Development on Umnipes River," Vol. 6, No. 11 (November 11, 1923), pp. 513-514.

Engineering News-Record "Cofferdam for the 39th Street Pumping Station at Chicago," December 17, 1903.

"Steel Piling Cofferdam for Bridge Piers," April 21, 1906.

"Heavy Bracing Gives Large Open Pockets in Deep Cofferdam," January 27, 1917.

"New-Type Thin Wall Cofferdam," Vol. 83, No. 18 (October, 1919), pp. 817-818

"West Palm Beach Water Co. Builds 20-M.G.D. Purification and Pumping Plant in Ten Months," June 30, 1927, pp. 1048-1052.

"Sheeting Interlocked on Barge for Cofferdam Wall," Vol. 110, No. 6, (February 9, 1933), p. 191.

"New York Piers for 1000 Foot Ships," Vol. 111, No. 5 (August 3, 1933), pp. 123-126.

Engineering News-Record (Continued)

"Roller-Gate Dam for Kanawha River," September 21, 1934, pp. 337-342.

"Pier Construction in 20 Foot Tide," Vol. 112, No. 7 (February 15, 1934), pp. 219-224.

"Sinking Open Cofferdams Through Glacial Drift," January 3, 1935, pp. 1-5.

"Progressive Cofferdaming for Long Low Dam," Vol. 114, No. 14, (April 4, 1935), pp. 473-477.

"Well Points Dry up Wet Excavation for N. Y. Incinerator Plant," April 11, 1935, pp. 515-516.

"Constructing the First Cofferdam at Grand Coulee," August 1, 1935, pp. 148-151.

"Cofferdam in Swift Water for Bonneville Dam," September 5, 1935, pp. 315-318.

"Construction Steps up at Pickwick, Third TVA Dam," April 16, 1936, pp. 549-552.

"Jetty Construction Methods Used to Repair Bonneville Cofferdam," October 1, 1936, pp. 461-463.

"Pile Pulling and Reuse Cuts Cofferdam Cost," Vol. 118, No. 16 (March 4, 1937), pp. 327-328.

"Serious Leak in Cofferdam at Grand Coulee," Vol. 118, No. 16 (April 22, 1937), pp. 595-597.

"Contractors Win River Battle," Vol. 119, No. 1 (July 1, 1937), pp. 13-16.

"Grand Coulee Cofferdam Removal," Vol. 119, No. 10, (September 2, 1937), p. 401.

"Deep Steel Sheet-Pile Cofferdams at Arlington Bridge," July 21, 1927, pp. 92-93.

"Open-Cut Subway, N. Y. City, Built under Unusual Conditions," August 18, 1927.

Engineering News-Record (Continued)

"Building Substructure of Arthur Kill Bridges," November 10, 1927, pp. 744-748.

"Foundation Problems in Enlarging Center Pier of Swing Bridge at Providence," December 8, 1927, pp. 927-929.

"Toe of Cofferdam at Hudson Bridge Falls; Three Drown," December 29, 1927, p. 1057.

"Old Cofferdam Removed by Power Scraper Bucket," Vol. 101, No. 11 (September 3, 1928), pp. 409-410.

"Deep Trench Emergency Intake for Pittsburgh Water Works," April 18, 1929, pp. 638-640.

"Building a Lock and Dam on the Illinois River," May 16, 1929, pp. 778-782.

"Deep Foundations for Lake Champlain Bridge Built with Open Cofferdam, November 21, 1929, pp. 796-800.

"N. Y. Subway Construction-Street Staging and Decking for Open Cut Subway," Vol. 105 (September 4, 1930), pp. 371-375.

"N. Y. Subway Construction-Excavation and Support of Structures in Open-Cut Subway," Vol. 105 (September 18, 1930), pp. 455-458.

"Skyscraper Foundations in Quicksand Area Built within Open Cofferdam," March 26, 1931, pp. 515-519.

"Cofferdamming the Columbia Rock Island," April 30, 1931, pp. 716-719.

"Permanent Cofferdams to be Large Earth-Rock Fills," December 15, 1932, pp. 709-711.

"Deep Excavation for Parker Dam," November 25, 1937, pp. 853-856.

Engineering News-Record (Continued)

"Wrenching out a Cofferdam," May 12, 1938, pp. 677-679.

"Tailor-Made Cofferdam," August 18, 1938, pp. 207-211.

"Air Lift Excavates Cofferdams," Vol. 126, No. 23 (June 5, 1941), p. 83.

"Shipyard Uses Basins Instead of Ways," Vol. 129, No. 9 (August 27, 1942), p. 57.

"Fighting Water in Bridge Foundations," Vol. 130, No. 22 (June 3, 1943), pp. 806-810.

"Cellular Cofferdam Serves as Wall of Ship Construction Basins," October 21, 1943. pp. 70-84.

"Wellpoints in a Pumped-Sand Fill Facilitate Outfall Sewer Construction," August 22, 1946, pp. 92-94.

"Big Cofferdam Built in Turbulent Rapids," Vol. 141, No. 20, (November 11, 1948), pp. 96-99.

"Construction of Concrete Seal in Cofferdam for New Screen Well," Vol. 142, No. 7, (April 28, 1949), p. 62.

"Templet Takes Trouble out of Driving 70 Foot Cofferdam Cell," Vol. 148, No. 3, pp. 34-35, January 17, 1952.

"Three Cofferdams for every Pier," Vol. 140, No. 3, (June 12, 1952), pp. 43-45.

"Contractor Rescues Dredge after 6 Month Mud Bath," Vol. 148, No. 11 (March 13, 1952), pp. 54-55.

Epstein, Harris — "Design of a Cellular Cofferdam," Proceedings, 17th Annual Meeting, Highway Research Board, National Research Council, Vol. 17 (1937), pp. 481-493.

Fellows, C. E. — "Cofferdams and Caissons," Civil Engineering (London), Vol. 38, No. 447-448 (September, 1943), pp. 192-195, 221-224.

Flay, G. F., Jr. — "Unique Cofferdam Foils Old Man River," Civil Engineer, Vol. 20, No. 12, (December, 1950), pp. 42-46.

Follett, G. A. — "The Construction of a Cofferdam," Military Engineer, Vol. 20, No. 109 (January, 1928), pp. 29-31.

Foster, H. A. — "High-Level Highway Bridge...," Civil Engineer, Vol. 14, No. 5 (May, 1944), pp. 195-198.

Fowler, W. H. — "Circular Cell Cofferdam at Deadman," Engineering News-Record, January 9, 1930, pp. 66-68.

Fox, E. N. and McNamee, J. — "Two Dimensional Potential Problem of Seepage into Cofferdam," Philosophical Magazine, Vol. 39, No. 290 (1948).

Froehlich, O. K. — "Bodenmechanische Gesichtspunkte fuer die Berechnung von Fangedaemmen," Bautechnik, Vol. 18, No. 47 (November 1, 1940), pp. 543-547.

Genie Civil — "Le Calcul des Batardeaux Cellulaires Fondes sur Rocher," Vol. 132, No. 11 (June 1, 1955), pp. 213-216.

Goldsmith, E. O. — "Sealing Bridge Cofferdams by Grouting," Engineering News-Record, Vol. 107, No. 10 (October 15, 1931), p. 191.

Gorlinski, J. S. — "Bonneville Dam," Military Engineer, Vol. 27, No. 153 (May-June, 1935), pp. 210-213.

Graves, W. J. — "Cofferdam for New Locks at St. Marys Fall Canal, Sault Sainte Marie, Michigan," Vol. 9, (1917), pp. 265-285, U. S. Corps of Engineers.

Griggs, Julian — "Economy of Steel Sheet Piles for Cofferdam for Bridge Piers," Engineering News-Record, May 5, 1906.

Hager, K. — "Die Berechnung von Fangedammen," Wasserkraft und Wasserwirtschaft, Vol. 26, 1931.

Halmos, E. E. — "Cofferdam Used in Construction of Sharemen Island Dam," Transactions of the American Society of Civil Engineers, Vol. 88, (1925), pp. 1284-1285.

Harding, C. R. — "Pier Construction for the S. P. Railroad Bridge across Suisan Bay," January 30, 1930, pp. 174-180.

Hausen, J. B. — Earth Pressure Calculation, Danish Technical Press, Copenhagen, 1953, p. 271, Engineering Society Library, New York.

Haviland, J. H. — "Earth Cofferdam in Bridge Construction," South African Institution of Engineers Journal, Vol. 26, No. 9 (April, 1920) pp. 202-205, 252-253, and 433-434.

Healey, F. T. — "Cofferdam Built in Swift River on Rock and Boulder Bottom," February 14, 1924, pp. 291-292.

Hedman, A. F. — "Cofferdam Design for Kentucky Dam," Engineering News-Record, Vol. 128 (January 1, 1942), pp. 30-34.

Helmers, N. F. — "Cofferdam for 60 Foot Head with One Line of Sheeting," Engineering News-Record, Vol. 115, No. 1 (July 4, 1935), pp. 14-15.

Hool, G. A. and Kinne, W. S. — Foundations, Abutment and Footings, Second Edition, 1943, pp. 86.

Howard, R. B. — "Single Bridge Pier Built in Cellular Cofferdam," Civil Engineering, Vol. 21, (January, 1951), pp. 41 ff.

Huestes, H. E. — "Building a Sheet-Pile Cofferdam in a 28 Foot Tide," Vol. 87, No. 20 (November 17, 1921) pp. 806-808.

Jacoby, E. — "Grundsaetzliches uber die Berechnung von Doppelten Spindeaeden," Bautechnik, Vol. 19, No. 22 (May 23, 1941), pp. 240-243.

Jacoby H. S. and Davis, R. P. — The Foundation of Bridges and Buildings, Third Edition, 1941, pp. 238-274.

Jansen, C. B. — "Century of Progress Marks Many Improvements in...," Civil Engineering, Vol. 18, No. 10 (October, 1948), pp. 26-31.

Jansen, C. B. — "Constructing the Shipway," Civil Engineering, Vol. 13 (July, 1943), pp. 310-314.

Jenkins, F. L. — "Concrete Cofferdam Wales Give Maximum Work Space," Engineering News-Record, Vol. 144, No. 16 (April 27, 1950), pp. 32-34.

Jennings, R. C. — "West Virginia Highway Bridge Built inside Cellular Cofferdams," Civil Engineering, Vol. 23, No. 6, (June, 1953), pp. 84 ff.

Jervey, H. — "Notes on Construction of Concrete Cofferdam at McGrew Shoals, Alabama," U. S. Corps of Engineers, Vol. 2 (1910), pp. 66-72.

Johnston, H. R. — "Underwater Exploration with Clyx Drills," Engineering News-Record, Vol. 120, No. 12 (March 24, 1938), pp. 436-438.

Jordan, L. J. — "Truss Braced Cofferdam Used in Constructing Intake," Engineering News-Record, Vol. 101, No. 21 (November 22, 1928), pp. 770-771.

Kame, W. B. — "Cheap Little Cofferdam," Engineering News-Record, Vol. 121, No. 23 (July 21, 1938), p. 94.

Keelor, D. P. — "Construction of Montgomery Locks, Ohio River," Military Engineer, Vol. 27, No. 153 (May-June, 1935), pp. 187-190.

Ketchum, E. P. — "Removing a Collapsed Cofferdam," Military Engineer, Vol. 29, No. 165 (May-June, 1937), pp. 203-205.

Koefood, S. M. — "Four Cofferdams for Forty One Foundation," Engineering News-Record, Vol. 123, No. 1 (July 6, 1939), pp. 47-49.

Kozlov, V. S. — "Hydromechanical Design of Sheet Pile Cofferdam," Izvestiya Academiyi Nauk S. S. S. R. Otdellenye Technicheskikh Nauk, No. 6 (1939), pp. 89-100, (in Russian).

Krey, H. — "Erddruck und Erdwiderstand," Fifth Edition, Wilh, Ernst und Sohn, Berlin, 1936.

Laing, R. — "Race Against High Water Features Cofferdam, Construction at McNary," Pacific Builder and Engineer, Vol. 54, No. 6 (June, 1948), pp. 68-70.

McCormick, H. G. Dixon, J. W. — "Mississippi River Cofferdams," Military Engineer, Vol. 28, No. 158 (March-April, 1936), pp. 105-108.

McCormick, H. G. — "Seepage and Pumping in Mississippi River Cofferdams," Engineering News-Record, Vol. 114, No. 10 (March 7, 1935), pp. 339-342.

McCullough, C. B. — "Cofferdam Wrecked by Splitting of Concrete Seal," Engineering News-Record, Vol. 92, No. 11 (March 13, 1924), pp. 460-461.

McManee, J. and Fox, E. N. — "Two Dimensional Potential Problem of Seepage into Cofferdam," Philosophical Magazine, Vol. 39, No. 290 (March, 1948), pp. 165-203.

Maruyasu, T. and Kurosake, T. — "Report on Cement and Chemical Injection Work Applied to Cofferdam Construction and Leakage-Stop of Floating Dam," Japan Society of Civil Engineers, Vol. 38, No. 6 (June, 1953), pp. 21-26.

Meem, J. C. — "Steel Sheet Piling in Cofferdam," Brooklyn Engineers Club Proceedings, Vol. 29, No. 1 (October, 1930), pp. 27-51.

Mulcahy, W. A. and Young, Hugh E. — "Cofferdam Experience at a Bridge," Engineering News-Record, Vol. 83, No. 6 (August 7, 1919), pp. 268-269.

Nisen, E. M. — "Cofferdams on Fox River," Military Engineer, Vol. 18, No. 102 (November-December, 1926), pp. 506-508.

Oakes, J. C. — "Failure of Masonry Cofferdam at Louisville and Portland Canal," U. S. Corps of Engineers, Vol. 8 (1916), pp. 101-109.

Oakes, J. C. — "Ohio River Dam," U. S. Corps of Engineers, Vol. 5 (1913), pp. 177 and 194.

Osler, J. H., Jr. — "Launched Bracing Cuts Cofferdam Cost," Engineering News-Record, Vol. 125, No. 19 (November 7, 1940), pp. 623-625.

Pennoyer, R. P. — "Gravity Bulkheads and Cellular Cofferdams," Civil Engineering, Vol. 4, No. 6 and 10 (June and October, 1934), pp. 301-305 and 547.

Pennoyer, R. P. and Hockingsmith, G. — "Design of Steel Sheet Pile Cofferdam and Design of Wales and Bracing," Civil Engineering, Vol. 5, No. 1 (June, 1935), pp. 19-23.

Potter, C. L. — "An Ice Cofferdam," U. S. Corps of Engineers, Vol. 6 (1914), pp. 439-440.

Pritchard, J. C. — "Underwater Pile Driving and Cofferdam Sealing," Engineering News-Record, June 10, 1926, pp. 930-933.

Pritchard, J. C. — "Building Cellular Wall Cofferdam, St. Louis Intake," Engineering News-Record, Vol. 96 (May 27, 1926), pp. 862-865.

Prugh, B. J. — "How to Avoid Cofferdam Boils," Civil Engineering, Vol. 23, No. 11 (November, 1953), p. 63.

Purcell, C. H. — "Deep Open Caissons for Bay Bridge," Engineering News-Record, August 23, 1934, pp. 227-233.

Quinn, A. D. — "Cofferdam Protects Nearby Foundations," Engineering News-Record, Vol. 140, No. 26 (June, 1948), pp. 1018-1021.

Reigeluth, R. L. — "Cofferdam Sealed in Novel Way...," Vol. 123, No. 5 (August 3, 1939), p. 67.

Reigeluth, R. L. — "Cofferdam Sealed in Novel Way...," Engineering News-Record, Vol. 123, No. 9 (August 31, 1939), pp. 37-38.

Riddle, C. D. — "Constructing a Plant at Grand Coulee Dam," Civil Engineering, Vol. 6, No. 10 (October, 1936), pp. 639-642.

Riedel, C. M. — "Chemicals Stop Cofferdam Leak," Civil Engineering, Vol. 21, No. 4 (April, 1951), pp. 23-24.

Rimsted, I. A. — "Zur Bemessung des Doppelten Spundwand-bauwerken," Ingeniorvidenskabelige Skrifter, No. 4 (1940), 117 pages, (in German).

Ringers, J. A. — "Construction of the New Ijmuiden Lock," Engineering News-Record, May 8, 1930, pp. 769-772.

Ritson, H. — "Cofferdams," Surveyor, Vol. 89, No. 2310 (June 12, 1936), p. 791.

Roads and Streets — "Earth Filled Cofferdam Bored Approach Footings," Vol. 91, No. 6 (June, 1948), pp. 94-96.

Sanger, F. J. — "Vertical Spacing of Cofferdam Bracing," Engineering News-Record, Vol. 145, No. 23 (December 7, 1950), pp. 44-46.

Sauer, M. V. — "St. Lawrence River Control and Remedial Dams," Engineering Journal, Vol. 26, No. 12 (December, 1943), pp. 661-670.

Staniford, C. W. — "Unusual Cofferdam for 1000 Foot Pier, New York City," (April, 1917), pp. 498-542.

Sweeny, F. R. — "Notes on the Design of Single-Wall Cofferdam," Engineering News-Record, Vol. 88, No. 15 (April 10, 1919), pp. 700-711.

Taunton, A. J. S. — "Empleo del Hielo Seco in la Reparacion de Puentes," Ingeniera, (Buenos Aires), Vol. 56, No. 921 (April, 1952), pp. 74-78.

Taunton, A. J. S. — "Ice Cofferdam," Engineering Journal, Vol. 23, No. 7, (July, 1950), pp. 598-601.

Taunton, A. J. S. — "Dry Ice Creates Frozen Cofferdam for Bridge Pier," Civil Engineering, Vol. 20, No. 8 (April, 1950).

Teleford, R. L. "Deep Cofferdam for Hudson River Bridge," Engineering News-Record, August 16, 1928, pp. 232-236.

Terzaghi, K. "Stability and Stiffness of Cellular Cofferdams," Transactions of the American Society of Civil Engineers, Vol. 110 (1945), pp. 1083-1119.

Terzaghi, K. "Shipway with Cellular Cofferdam on Marl Foundation," Transactions of the American Society of Civil Engineers, Vol. 71, No. 9, (November, 1945), pp. 1327-1353.

Terzaghi, K. and Peck Soil Mechanics in Engineering Practice, John Wiley & Sons, Inc., New York, Edition 1948, pp. 230-233.

Thain, T. E. "Cofferdam and River Wall Construction," Practical Engineer, Vol. 59, No. 1672 (March 13, 1919), pp. 124-127.

Thomas, T. C. "Box Cofferdam on the Ouachita and Big Sunflower Rivers," Vol. 9, (1917), pp. 51-71.

Thomson, E. B. "Methods and Cost of Cofferdam Construction at Oregon City Locks, Willametter River, Oregon," U. S. Corps of Engineers, Vol. 10, (1918), pp. 171-191.

Torpen, B. E. and Hartman, O. C. "Third Step Construction at Bonneville Dam," Civil Engineering, Vol. 8, No. 5 (May, 1938), pp. 311-314.

Transactions of the American Society of Civil Engineers

"The Lock 12 Development of the Alabama Power Company, Coosa River, Alabama," Vol. 78, (1915), pp. 1480-1489.

"The Cherry Street Bridge, Toledo, Ohio," Vol. 80 (1916), p. 745.

"Cofferdam for Ohio River Dam #18," Vol. 86 (1923), pp. 114-119, 176-177.

"The Lake Washington Ship Canal, Washington," Vol. 92 (1928), p. 1012.

"The O'Shaughnessy Dam and Reservoir," Vol. 93 (1929), pp. 1428-1492.

Transactions of the American Society of Civil Engineers (Continued)

"George Washington Bridge; Construction of Substructure," Vol. 97 (1933), pp. 206-221.

"Lake Champlain Bridge," Vol. 98 (1933), pp. 639-644.

"Construction Methods on Welland Ship Canal," Vol. 98 (1933), pp. 1189-1199.

Tschbotarloff, G. P. — Soil Mechanics and Foundations, McGraw-Hill Book Co., First Edition, 1951, pp. 522-528.

Warren, Lee — "Cofferdam and Stream Control at Jordan Dam, Alabama," Engineering News-Record, Vol. 106 (May 14, 1931), pp. 804-808.

Wett, D. A. — "Steel Sheet-Pile Cofferdam," Engineering News-Record, Vol. 75 (1916), pp. 533-540.

Weidner, E. L. — "Crib-Sled Nicely Does Trick," Engineering News-Record, Vol. 156, No. 10 (March 8, 1956), pp. 47-48, 50.

Werner, P. W. — "Zur Berechnung der Stauhoehe von Fange daemmen," Baulingenleur, Vol. 21, No. 47/48 (December 20, 1940), pp. 374-375.

Western Construction — "Cofferdam 3000 Feet Long Built at Grand Coulee," Vol. 10, No. 6, (June, 1935), pp. 162-164.

"Grand Coulee Cofferdam," Vol. 11, No. 12 (December, 1936), pp. 386-389.

"Parker Dam Sets a Record for Foundation Depth," March, 1938, pp. 96-101.

"New Los Angeles Sewer Outfall," Vol. 22 (November, 1947), pp. 80-83.

"Different Types of Cofferdam Construction Used at McNary are Mentioned," Vol. 25, No.10 (October, 1950), pp. 75-79.

White, E. E. "Mile Long Cofferdam," Civil Engineering, Vol. 19, No. 6 (June, 1949), pp. 44-47, 87.

White, L. and Prentis, E. A. Cofferdams, Columbia University Press, New York, Second Edition, 1950.

Young, H. E. and Mulcahy, W. A. "Cofferdam Experience at a Bridge," Engineering News-Record, Vol. 83, No. 6 (August 7, 1919), pp. 268-269.